Uncovering cancer immunotherapy resistance: The key role of tumor intrinsic IFNγ response in T cell based therapies

Alex Martinez-Sabadell Aliguer

Universitat Autònoma de Barcelona

Facultat de Medicina

Departament de Bioquímica i Biologia Molecular

Programa de Doctorat en Bioquímica, Biologia Molecular i Biomedicina

Uncovering cancer immunotherapy resistance: The key role of tumor intrinsic IFNγ response in T cell based therapies

Thesis presented by Alex Martinez-Sabadell Aliguer for the degree of Doctor of Philosophy (PhD) in Biochemistry, Molecular Biology and Biomedicine by Universitat Autònoma de Barcelona

Barcelona, 2023

Author:

Alex Martinez-Sabadell Aliguer

Directors:

Dr. Joaquin Arribas Lopez

Dr. Enrique J. Arenas Lahuerta

Tutor:

Dra. Laura Soucek

INDEX

ABSTRACT

Immunotherapy has raised high expectations in the treatment of cancer, particularly in hematological tumors. However, despite promising effects in solid tumors, patients eventually progress due to the emergence of resistance. Therefore, there is an unmet clinical need to identify the mechanisms by which tumors relapse in order to develop new therapeutic strategies to overcome resistances. Built on this evidence, in this thesis we aimed to identify unknown mechanisms of acquired resistance to T cell-based therapies in solid tumors. Using HER2 driven cell lines and PDXs, and a TCB targeting HER2, we generated models of resistance and identified that tumor intrinsic deficient IFNγ response was the driver of resistance. Furthermore, we found that JAK2 downmodulation was the cause of the disrupted IFNγ signaling. By contrast, using CEACAM5 expressing cell lines and PDXs, and a TCB against CEACAM5, we identified the downmodulation of the antigen as a common mechanism of resistance. Therefore, in this thesis we demonstrate that the target antigen is determinant in the acquired resistance mechanism that emerge to redirected lymphocytes, and we found a novel central role of the tumor intrinsic IFNγ signaling in the response to T cell redirection immunotherapy. Finally, using genome wide CRISPR and drug screenings we identified novel targets that open the avenue for the use of treatments to rewire IFNγ signaling in combination with immunotherapies, which can be an efficacious antitumor therapeutic strategy.

RESUMEN

La inmunoterapia ha generado grandes expectativas en el tratamiento del cáncer, particularmente en tumores hematológicos. Sin embargo, a pesar de sus prometedores efectos en tumores sólidos, los pacientes acaban progresando debido a la aparición de resistencias. Por lo tanto, existe una necesidad clínica de identificar los mecanismos por los que los tumores recaen, con el fin de desarrollar nuevas estrategias terapéuticas para superar las resistencias. Partiendo de esta evidencia, en esta tesis se propuso identificar mecanismos desconocidos de resistencia adquirida a terapias basadas en células T en tumores sólidos. Utilizando líneas celulares y PDXs dependientes de HER2, y un TCB dirigido a este antígeno, generamos modelos de resistencia e identificamos que la respuesta deficiente intrínseca al tumor a IFNγ era el impulsor de la resistencia. Además, descubrimos que la pérdida de expresión de JAK2 era la causa de la señalización interrumpida de IFNγ. Por el contrario, utilizando líneas celulares y PDXs que expresan CEACAM5, y un TCB contra CEACAM5, identificamos la pérdida de antígeno como un mecanismo común de resistencia. Por lo tanto, en esta tesis demostramos que el antígeno diana es determinante en el mecanismo predominante de resistencia adquirida que aparece a los linfocitos redirigidos, y encontramos un novedoso papel central de la señalización intrínseca de IFNγ del tumor en la respuesta a la inmunoterapia de redirección de células T. Por último, mediante el uso de cribados de CRISPR en todo el genoma y de fármacos identificamos nuevas dianas que abren la vía para el uso de tratamientos para recuperar la señalización del IFNγ en combinación con inmunoterapias, lo que puede ser una estrategia terapéutica antitumoral eficaz.

ABBREVIATIONS

ACT	Adoptive cell transfer
ADCC	Antibody dependent cytotoxicity
ALL	Acute lymphoblastic leukemia
AML	Acute myeloid leukemia
APC	Antigen presenting cell
B2M	β2 microglobulin
BC	Breast cancer
BsAbs	Bispecific antibody
CAF	Cancer associated fibroblast
CAR	Chimeric antigen receptor
CDK2	Cyclin-dependent kinase 2
cGAS	Cyclic GMP-AMP synthase
ChIP	Chromatin immunoprecipitation
CRC	Colorectal cancer
CRR	Complete response rate
CRS	Cytokine release syndrome
CSF-1	Colony stimulating factor
CTLA-4	Cytotoxic T lymphocyte 4
DAMP	Damage associated molecular partner
DC	Dendritic cell

FAP	Fibroblast activation protein alpha
FRβ	Folate receptor β
GAS	Gamma activated site
GEA	Gastroesophageal carcinoma
GM-CSF	Granulocyte-macrophage colony stimulating factor
GMP	Good manufacturing practice
GrzmB	Granzyme B
GvHD	Graft vs host disease
HCC	Hepatocellular carcinoma
HDAC	Histone deacetylase
HER2	Human epidermal growth factor receptor 2
HIF	Hypoxia inducible factor
HLA	Human leukocyte antigen
HSC	Human stem cell
ICB	Immune checkpoint blockade
ICI	Immune checkpoint inhibitor
IDO	Indoleamine 2,3-dioxygenase
IFN	Interferon
IL	Interleukin
IRF1	Interferon regulatory transcription factor
IS	Immune synapse

ISG	Interferon stimulated gene
ISRE	Interferon-sensitive response element
JAK	Janus kinase
LCOR	Ligand-dependent corepressor
LOH	Loss of heterogeneity
MCL	Mantle cell lymphoma
MDSC	Myeloid derived suppressor cell
MeDIP	Methylated DNA immunoprecipitation
MHC	Major histocompatibility complex
MSI-H	Microsatellite instability-high
NK	Natural killer cell
NSCLC	Non-small cell lung cancer
ORR	Overall response rate
OS	Overall survival
PAP	Prostatic acid phosphatase
PBL	Peripheral blood lymphocytes
PD-1	Programmed cell death 1
PD-L1	Programmed cell death ligand 1
PDX	Patient derived xenograft
PFN	Perforin
PI3K	Phosphatidylinositol-4,5-bisphosphate 3-kinase

PIAS	Protein inhibitors of activated STAT
PTPN2	Protein tyrosine phosphatase non-receptor type 2
RCC	Renal cell carcinoma
RIG-I	retinoic acid-inducible gene I
ScFV	Single chain fragment variable
SOCS	Suppressor of cytokine signaling
STAT	Signal transducer and activator of transcription 1
STING	Stimulator of interferon genes
TAA	Tumor associated antigen
TAM	Tumor associated macrophage
TCR	T cell receptor
TGF-β	Transforming growth factor β
TIL	Tumor infiltrating lymphocytes
TKI	Tyrosine kinase inhibitor
TLR	Toll-like receptor
TMB	Tumor mutational burden
TME	Tumor microenvironment
TNBC	Triple negative breast cancer
TNFα	Tumor necrosis factor α
Tregs	Regulatory T cell
TSA	Tumor specific antigen

TSA Trichostatin A

TYK2 Tyrosine kinase 2

INTRODUCTION

1. Cancer immunology

The immune system is a complex network of cells, tissues, and organs that work together to defend the body against foreign organisms like bacteria, viruses, fungi, or parasites. Additionally, it helps the body recognize and destroy abnormal cells that originate from within the body, such as cancer cells.

The immune system can be divided into two main branches: the innate immune system and the adaptive immune system. The innate system is the body's first line of defense against infection. It includes physical barriers like the skin and mucous membranes, as well as immune cells like neutrophils, macrophages, and natural killer cells (NKs). The innate immune system responds quickly to dangerous insults such as pathogens or aberrant cells, but these responses are not specific. In contrast, the adaptive system components are highly specific to the insult that triggered them, but at the same time are slower to respond. The components of the adaptive system include specialized cells such as B cells, which produce antibodies, and T cells, which can directly attack aberrant cells or help other immune cells respond to the infection. Additionally, lymphocytes have the ability to differentiate into memory cells, so that they can respond more quickly and effectively to subsequent attacks by that specific insult.

Furthermore, it's essential for immune cells to differentiate between "self" and "non-self" to effectively perform their roles. The orchestration of protective immunity requires a sophisticated network of cytokines, chemokines, and receptors. Furthermore, inhibitory receptors contribute to maintaining tissue balance and preventing excessive immune-mediated toxicity.

1.1. The cancer immune cycle

Cancer is characterized by the accumulation of genetic alterations and loss of DNA repair systems. These alterations foment the expression of cancer antigens, which represent an opportunity for the immune system to identify cancer cells as foreign entities. These antigens can be divided into tumor specific antigens (TSA) or neoantigens; and tumor associated antigens (TAA). While TSA are specific of

the tumor due to genomic mutations, TAAs are antigens that are presented when a protein is excessively produced or expressed in the wrong tissue or time. These antigens are presented to immune cells through the major histocompatibility complex (MHC) class I or II. The antigen presentation through the MHC-I by tumor cells is the basis of tumor recognition by T cells, the major component of tumor cytotoxicity and control of the adaptive immune system, as well as the basis of most immunotherapeutic approaches (Boon et al., 1994). Indeed, Chen and Mellman, back in 2013, proposed their cancer-immunity cycle, in which tumor control by the adaptive immune system is proposed in a T cell-based model (Chen & Mellman, 2013).

The first step of the cycle consists in the antigen release by the tumor cells. Once they undergo cell death, antigens are released into the tumor site, where they are processed by dendritic cells (DCs), recognized as foreign, and processed so that they can be presented through the MHC-I and MHC-II, being it the 2nd step. In order for the DCs to process them as immunogenic, certain signals are needed. The proinflammatory cytokines released by the innate and adaptive cells in the tumor microenvironment (TME), such as tumor necrosis factor alpha (TNFα), interferon gamma (IFNγ), and interleukin 1 (IL-1), drive DCs to an immunogenic phenotype. These DCs then travel to the lymph node and act as antigen presenting cells (APCs), priming and activating T cells.

The 3rd step is the prime and activation of T cells by APCs. Before that, T cells originate in the bone marrow from hematopoietic stem cells and then are released into the lymphatic circulation. When arrived in the thymus, the lymphoid progenitor cells mature into T cells, differentiating into $CD8^+$ or cytotoxic, or $CD4^+$ or helper T cells. This process involves the expression of T cell receptors (TCRs) and the selection for T cells that can recognize antigens presented by the body's own cells (positive selection) and the elimination of T cells that react too strongly to the body's own proteins (negative selection) (Germain, 2002). These selected lymphocytes then travel to the lymph nodes, where they encounter DCs coming from the tumor site. The antigen presentation to these naïve T cells results in the priming and activation of $CD4^+$ and $CD8^+$ T cells through the MHC-II and MHC-I respectively. The activated T cells undergo then a clonal expansion and become specific to target a precise antigen (Germain, 2002). For this activation to occur,

apart from the first signal mediated by the MHC-TCR recognition, secondary signals need to happen. For instance, the T cell's CD28 binding to the APC's costimulatory molecules CD80 or CD86, the 4-1BB to the 4-1BB ligand, or the OX40 to OX40L. Moreover, inhibitory signals also regulate T cell activation, such as cytotoxic T lymphocyte 4 (CTLA-4), which bind to the CD80 or CD86 costimulatory domain (Chen & Mellman, 2013).

Once $CD4^+$ and $CD8^+$ T cells are activated, the 4^{th} step consists in the release to circulation, and the 5^{th} the traffic into the tumor, due to attraction chemokines released at the tumor site, such as CXCL9 and CXCL10 (Russo et al., 2020). At the tumor site, T cells exert the 6^{th} step, the recognition of tumor cells through the antigen recognition, and the 7^{th} step, deleting the tumor to complete the cycle, resulting in additional tumor antigen release and sustain of the cancer immune cycle. T cells can attack the tumor through several mechanisms. Probably the most common and effective is through $CD8^+$ T cell recognition of antigens presented by MHC-I on tumor cells. Firstly, recognition needs to happen. To do so, TCR binds to the specific peptide presented by the MHC (pMHC), but inhibitory signals by immune checkpoints, such as programmed cell death ligand 1 (PD-L1) and PD-L2, which bind to the programmed cell death 1 (PD-1) on T cells, can inhibit T cell response. Other immune checkpoints are TIM3 and LAG3 on T cells, which bind to galectin-9 or MHC-II in tumor cells (Marin-Acevedo et al., 2018). However, if correctly activated, T cells release perforin (PFN) and granzyme B (GrzmB), that conclude in caspase activation and apoptosis of tumor cells. Additionally, FasL expressed by T cells can induce apoptosis on target cells through the binding to Fas on cancer cells and subsequent caspase activation (Lowin et al., 1994). Moreover, the release of IFNγ and TNFα, mostly by Th1 $CD4^+$ T cells can exert direct and indirect antitumoral effects (Constant & Bottomly, 1997). They can directly induce apoptosis, as well as cell cycle arrest of tumor cells. Additionally, IFNγ is the major regulator of T cell activity, and its effect on target cells include an increased pMHC-I presentation (Schroder et al., 2004).

However, the cancer immune cycle can be disrupted by the tumor, and current efforts are being made to target every step of the cycle. Most immunotherapeutic strategies are focused to achieve a correct cancer immunity cycle functionality.

Apart from T cells, many other immune and non-immune components have a role in the control and progression of the tumor. Some of them will be further discussed in this introduction. In this thesis, we describe the crucial IFNγ role as a tumor intrinsic resistance mechanism to the immune attack.

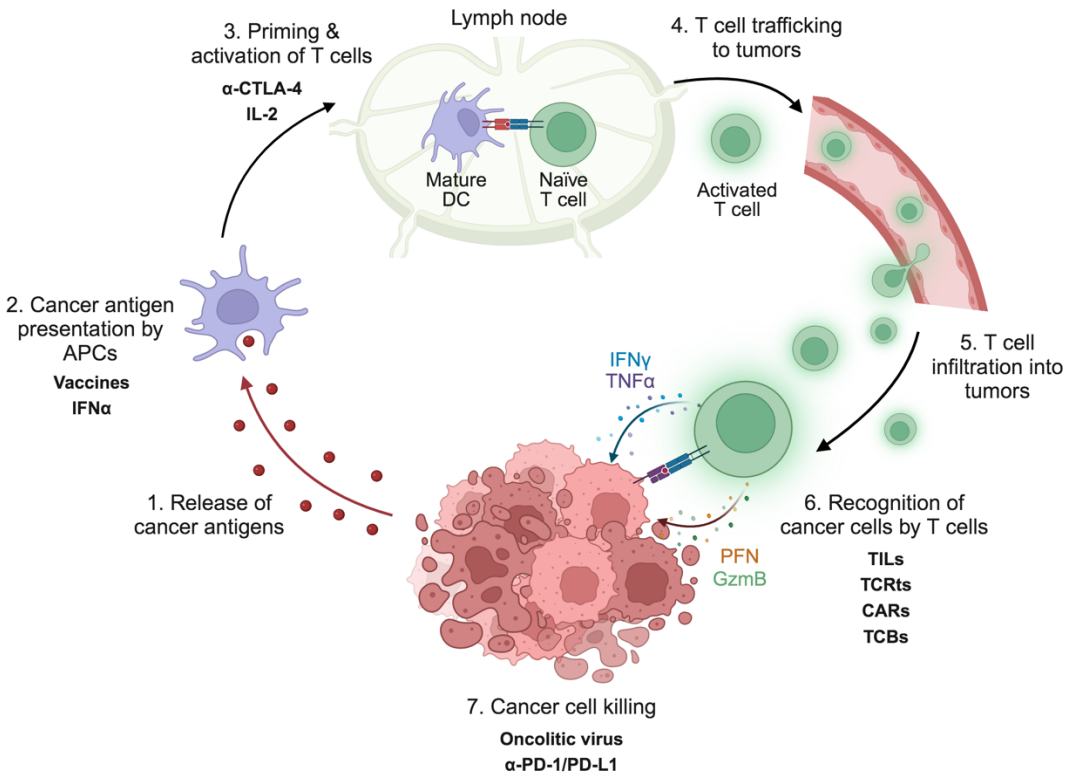

Figure 1: The cancer immunity cycle. T cells are the main mediators of the anticancer immune control. Upon cell death, tumors release antigens (1), which are collected (2) and presented by APCs to naïve T cells in the lymph nodes (3). Activated T cells then traffic (4) and infiltrate (5) into the tumor, where they recognize tumor cells through the TCR-MHC-I interaction (6) and exert their cytotoxic effect to kill cancer cells through PFN, GrzmB, IFNγ and TNFα (7). Tumor cells then undergo apoptosis, releasing tumor antigens, and the cycle continues. Adapted from (Chen & Mellman 2013).

1.2. Immunoediting: From immunosurveillance to tumor escape

The importance of the immune system control in the cancer development has been proposed over the years, now known as cancer immunoediting. The theory suggests that our immune system plays a sentinel role, constantly monitoring the development and progression of cancer. Moreover, it proposes that the immune system not only protects against the development of cancer but also shapes the immunogenicity of tumors. It provides an understanding of the dual role of the

immune system: protecting the host by eradicating cancer cells and shaping the characteristics of tumors to facilitate their survival and growth. It involves complex interactions among various cell types, molecules, and mechanisms that coordinate to eliminate, control, or allow the escape of cancer cells.

The concept of immunoediting emerged as an evolution of the cancer immunosurveillance hypothesis. The original immunosurveillance theory, proposed by Paul Ehrlich in the early 20th century and later refined by Lewis Thomas and Macfarlane Burnet, hypothesized that the immune system constantly monitors and eliminates nascent transformed cells, thereby preventing the development of tumors. However, this theory faced controversy due to lack of empirical evidence and an inability to account for the prevalence of immunogenic tumors (Dunn et al., 2002). In the late 20th century, with advancements in molecular and immunological research, scientists began to observe that the immune system could also unintentionally facilitate tumor growth by selecting for less immunogenic cancer cell variants. This observation led to the development of the immunoediting theory, primarily by Robert Schreiber and colleagues in the early 2000s (Dunn et al., 2002).

The immunoediting theory, encapsulated in the phrase "Elimination, Equilibrium, and Escape" (the three Es), presents a dynamic model of interaction between the immune system and cancer cells. The Elimination phase represents the traditional immunosurveillance process where the immune system identifies and destroys nascent tumor cells. The Equilibrium phase is where the immune system controls but does not eliminate the cancer, leading to a state of immune-mediated dormancy while also selecting for less immunogenic tumor variants. Finally, the Escape phase occurs when the edited tumor evades immune control and progresses to clinically detectable disease.

Elimination phase. In this first phase, once malignant cells appear and start multiplying, immune cells recognize and destroy transformed cells before they develop into tumors. However, it is not fully understood how these malignant cells are recognized. Growing tumors may show themselves by expressing “danger signals”, such as secretion of IFNα and β, expression of stress ligands like MICA/B or release of damage-associated molecular pattern molecules (DAMPs)

from dying tumor cells, thus initiating an anti-tumor innate response, leading to a production of IFNγ (Schreiber, Old & Smyth, 2011). The elimination phase involves innate and adaptive immune cells. From the innate side, NK cells, γδ T cells, macrophages, and DCs play their role. NK cells early detect and eliminate transformed cells independently of antigen recognition. They can detect downregulation of MHC class I molecules on the cell surface, which is a common feature of cancer cells, and release cytotoxic granules to kill these cells (Malmberg et al., 2017), and, alternatively, exert their tumoricidal effect by the engagement of TNF superfamily members such as Fas or TRAIL receptors on tumor cells (Cullen & Martin, 2015). At the same time, γδ T cells, considered an intersection between innate and adaptive immunity, can recognize tumors not only by MHC recognition, but by different ligands (Deseke & Prinz, 2020), and exert it's cytotoxic effect by perforin and granzyme release. Both NK cells and γδ T cells release proinflammatory cytokines when recognize the tumor, such as IFNγ and TNFα, therefore recruiting proinflammatory immune cells to attack the tumor (Park & Lee, 2021). Macrophages are resident in most tissues, and have different receptors that can recognize DAMPs expressed by tumor cells. Once they recognize the cancer cell, they get activated and phagocytize it or release effector molecules including nitric oxide and cytokines (Hume, 2015). Additionally, together with DCs, capture, process, and present tumor antigens to T cells, forming a critical bridge between the innate and adaptive immune responses, as explained above in the cancer immune cycle. Therefore, adaptive immune responses also play a role, with T cells (especially cytotoxic T cells) recognizing specific antigens presented by DCs and initiating an adaptive immune response.

Equilibrium phase*.* If some cancer cells survive the elimination phase, they enter a state of equilibrium with the immune system. This phase is characterized by a dynamic balance between the proliferation of cancer cells and the immune system's ability to control their growth, resulting in a state of tumor dormancy. During equilibrium, the immune system may promote the selection of less immunogenic cancer cell variants, a process known as 'immunoediting'. This phase can persist for years without the formation of clinically detectable cancer. In this phase of the tumor evolution, adaptive immunity is believed to be in charge

of containing tumor progression, specifically $CD8^+$ and $CD4^+$ T cells, together with the production of IL-12 and IFNγ (Schreiber, Old & Smyth, 2011). IL-12, mostly released by APCs, maintains cytotoxic function of T cells (Mirlekar & Pylayeva-Gupta, 2021), while IFNγ, released mainly by Th1 $CD4^+$ cells, maintains functionality of both innate and adaptive immune components, while exerting an anti-tumoral effect (Martinez-Sabadell et al., 2022).

Escape phase. In the escape phase, cancer cell clones that have adapted to evade the immune response begin to proliferate uncontrollably, leading to clinically apparent cancer. Tumor progression can occur due to several mechanisms, including cancer cell intrinsic modifications or an establishment of an immunosuppressive environment. Some examples of intrinsic resistance are loss of antigen expression, down-regulation of MHC molecules, expression of immunosuppressive molecules like PD-L1, or disruption in certain pathways such as IFNγ. Furthermore, secretion of immunosuppressive cytokines by the tumors like transforming growth factor beta (TGF-β) or IL-10 modify the TME, which can lead to the induction of immunosuppressive immune cells, including regulatory T cells (Tregs) and myeloid derived suppressor cells (MDSCs).

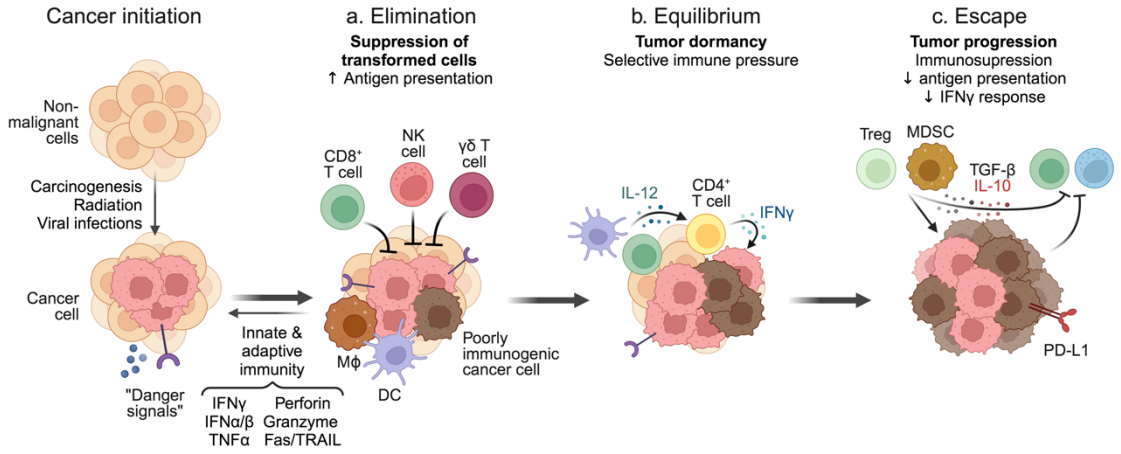

Figure 2: The 3 E's of the immunoediting process. The cancer immunoediting process represents the immune control of the cancer during tumor evolution once intrinsic tumor suppressor mechanisms failed. It consists of three sequential phases: elimination, equilibrium and escape. In the elimination phase, both innate and adaptive immunity collaborate to eradicate developing tumors. If successful, tumor is eradicated. However, if cancer cells escape, they may enter the equilibrium phase, mainly governed by the adaptive immunity, which prevent tumor expansion entering into a tumor dormancy state. In this phase takes place the "immunoediting" process, where poorly immunogenic cell variants emerge due to the immune pressure. Hence, these cell variants are no longer recognized by the adaptive immunity, leading to clinically apparent cancer disease in the escape phase. Adapted from (Schreiber, Old & Smyth, 2011).

This tumor ability to evade the immune destruction was added as a new hallmark of cancer in 2011 by Hanahan and Weinberg, reinforcing its importance in the cancer research field (Hanahan & Weinberg, 2011). The mechanisms by which tumor cells are able to avoid immune destruction will be further discussed in the “Mechanisms of resistance” section, which is the principal aim of this thesis.

However, many aspects of cancer immunosurveillance remain to be elucidated. The understanding of the cancer immunoediting process and tumor evolution has been instrumental in the development of innovative cancer therapies, such as immunotherapies.

2. Immunotherapies

Immunotherapy represents a revolutionary approach to treat cancer that harnesses the power of the body's immune system to combat the disease, instead of directly targeting cancer cells.

Immunotherapy, as a concept of cancer treatment, traces its origins back to the late 19th century when Dr. William B. Coley, often referred to as the "father of immunotherapy," noticed that some cancer patients who developed infections after surgery showed improvement or even remission. He hypothesized that this was due to the immune system's response to the infection, which also affected the cancer. Coley developed a mixture of bacteria known as Coley’s Toxins, which he injected into patients in the hope of stimulating an immune response against cancer (Coley, 1910).

However, it wasn't until the latter part of the 20th century and early 21st century that immunotherapy became a pillar of cancer treatment. In the 1980s, the discovery and development of monoclonal antibodies, which can be designed to recognize specific targets on cancer cells, marked a significant advancement and opened a new scene for posterior immunotherapeutic approaches (Liu, 2014). Then, in 1988, Steven Rosenberg and colleagues reported the first successful use of adoptive cell transfer, using the very same T cells extracted from a patient's tumor to attack the cancer (Rosenberg et al., 1988).

Another critical step came in the early 21st century with the development of immune checkpoint inhibitors (ICI), blocking proteins that prevent immune cells from attacking cancer. Ipilimumab, an anti-CTLA-4, was the first FDA-approved ICI in 2011 (Robert et al., 2011). Since then, several new strategies to treat cancer have emerged, and most of them will be described in this thesis.

The immunotherapeutic approach to treat cancer attempts to directly activate the immune system in order to attack the tumor, but several non-immunotherapeutic approaches have been found to trigger an immune reactivity against the tumor cells. For instance, targeted therapy with monoclonal antibodies are considered "passive" immunotherapies. These are meant to inhibit the target antigen signaling, but it was described long ago another additional effect, to activate immune cells to attack the tumor (Hashimoto et al., 1983). This event is the antibody dependent cellular cytotoxicity (ADCC), which is driven by the recognition of NK cells of the Fc fragment from the antibody through the Fc receptor CD16. This activation prompts a release of granzyme and perforin, as well as the expression of the cytotoxic effector Fas ligand (Yeap et al., 2016). Since the first FDA approval of the first mAb, rituximab, an anti-CD20 antibody used to treat non-Hodgkin's lymphoma, many others have followed, such as trastuzumab (anti-HER2) and cetuximab (anti-EGFR), where the ADCC has been proven to be a major cause of their efficacy (Beano et al., 2008, Latanzio et al., 2017).

Other cancer therapies that can have an anti-tumoral immune effect are the chemotherapy and radiotherapy treatments, mainly due to the killing of tumor cells, which facilitate antigen uptake by APCs, as well as an increased inflammation and proinflammatory signaling in the TME (reviewed respectively in Bracci et al., 2013 and Carvalho & Villar, 2018).

Immunotherapies can be divided in two major groups, that can be combined in order to obtain better results. One approach consists on the therapies that aim to boost a preexisting response, which depend on the classical recognition of the tumor cells by the T cells through the MHC-TCR interaction. The second strategy consists of redirecting the T cells against the tumor, independently of the antigen recognition.

2.1. Antigen presentation dependent therapies

Immunotherapeutic strategies that aim to boost a preexisting response are the ones that depend on the antigen presentation through the MHC class I to the TCR in the T cells (pMHC-TCR). These strategies depend on that recognition, and their aim is to either increase its efficacy or avoid suppressive factors.

2.1.1. Immune checkpoint blockade

Immune checkpoint blockade (ICB) is the most used immunotherapeutic approach in solid malignancies, with 11 FDA approved ICIs (3 vs PD-L1, 5 vs PD-1, 2 vs CTLA-4 and 1 against LAG3), and more than 2000 clinical trials ongoing as of September 2023. The aim of this therapy is to block the inhibitory signals driven by these proteins, the so-called immune checkpoints.

ICIs are approved for several malignancies, including melanoma, NSCLC, head and neck carcinoma, renal cancer, or Hodgkin lymphoma, among others. The main immune checkpoints being targeted in the clinic are the CTLA-4 and the PD-1 and its ligand PD-L1. Both can block immunological antitumor activity, but at different body sites and T cell maturation moments.

CTLA-4 blockade (like ipilimumab) disrupt the interaction between CTLA-4 on T cells and B7 molecules on APCs. In immune escape circumstances, this interaction sends an inhibitory signal that suppress the amplitude of T cell activation. Blocking this interaction, therefore, boosts T cell activation and proliferation, enhancing the immune response against cancer cells (Leach et al., 1994). At the same time, CTLA-4 is constitutively expressed in immunosuppressive Treg cells. Therefore, blocking CTLA-4 prevents T cells from anergy and can cause ADCC in Tregs (Zappasodi et al., 2019).

PD-1 blockade (like pembrolizumab or nivolumab) and PD-L1 blockade (like atezolizumab) disrupt the interaction between PD-1 on T cells and PD-L1 on cancer cells or APCs. Under normal conditions, the binding of PD-1 to PD-L1 transmits an inhibitory signal that reduces T cell function and promotes immune tolerance. However, cancer cells often overexpress PD-L1 to escape immune

attack. Blocking this interaction lifts the inhibition and restores T cell function, enhancing anti-tumor immunity (Zou et al., 2016).

In melanoma, the most immunogenic solid tumor type, ipilimumab plus nivolumab has given patients a great treatment improvement, with an objective response in 58% of the patients and a median overall survival (OS) of 6 years (Larkin et al., 2019). According to the FDA, as of June 2023, ICI treatment is currently approved as a first line of treatment for several malignancies, including ipilimumab plus nivolumab in metastatic melanoma, pembrolizumab plus chemotherapy in PD-L1 amplified non-small cell lung cancer (NSCLC), and different ICI plus tyrosine kinase inhibitors (TKI) in metastatic renal cell carcinoma (RCC).

However, even its remarkable efficacy, some patients suffer from adverse effects, being the most common the cytokine release syndrome (CRS). In this scenario, the direct destruction of target cells and exacerbated activation of T cells induce an excessive release of proinflammatory cytokines such as IFNγ or TNFα. These cytokines then set off a domino effect by activating innate immune cells like macrophages and endothelial cells, which in turn release additional cytokines and lead to a cytokine storm, causing mainly fever and fatigue, or, in the worst-case scenario, multi-organ system failure and death (Shimabukuro-Vornhagen et al., 2018).

Additionally, other immune checkpoints being targeted and currently in clinical trials are TIM3 and B7-H3, among others, and many researchers are trying to identify new ones. Finally, in addition to the inhibition of inhibitory signals, efforts are being put in the activation of costimulatory signals, such as 4-1BB, OX40, or CD40 (Marin-Acevedo et al., 2018).

2.1.2. Immunomodulators

Immune system modulators enhance the body's immune reaction against cancer cells. These can be divided into cytokines, chemokines, and agonists. Cytokines and chemokines can be used to directly boost the immune system to fight against the cancer, or indirectly, by suppressing inhibitory signals. IFNα (Peginterferon alfa-2b) and IL-2 (Aldesleukin) are two FDA approved cytokines that activate immune system through different ways. IFNα, approved for melanoma patients,

enhances antitumor immune functions by activating T cells, as well as inhibiting angiogenesis and promoting cancer cell death in the tumor (Tarhini et al., 2012). Meanwhile, IL-2, approved for RCC and melanoma patients, promotes the activation and multiplication of T and NK cells, with a dual effect, antitumoral due to increased cytotoxicity and Th1 T cell activation, and immunosuppressive due to Treg activation (Jiang et al., 2016). Other potential interleukins to develop as future therapies are IL-15 or IL-12, which activate T and NK cells (Lusty et al., 2017).

Alternatively, blocking immunosuppressive cytokines can also improve anti-cancer immune responses. For instance, blocking TGF-β, a potent inhibitor of T and NK cell cytotoxicity, as well as Treg's and tumor-associated macrophages' (TAM) inductor in the TME (Yang et al., 2010), appears as an interesting strategy. Clinical trials are currently in progress to assess its efficacy in combination with ICI, most of them in solid cancers, by using small molecule receptor kinase inhibitors, blocking antibodies, ligand traps, or vaccines (Kim et al., 2021).

Targeting chemokine receptors is another attractive therapy as well. The antibody drug mogamulizumab, which binds to CCR4, receptor present in immunosuppressive cell types such as Tregs and hematological tumors, is approved for two rare types of non-Hodgkin lymphoma, and it is currently being further investigated in clinical trials to treat solid tumors in combination with ICIs (Yoshie, 2021).

In the immunomodulator agonists side, stimulator of interferon genes (STING) agonists are a promising way to enhance antitumoral activity from T cells. The STING pathway plays a key role in the sensing of tumoral DNA and consequent initiation of immune responses. When activated through an agonist, triggers the production of type I IFNs, leading to an activation of immune cells and effective antitumor response (Xiong et al., 2022). Several clinical trials targeting STING agonists are currently ongoing with promising results, alone or in combination with ICIs (Le Naour et al., 2020).

2.1.3. Cancer vaccines

Cancer vaccines work by delivering a particular tumor or viral antigen to the patient, stimulating the uptake by DCs and subsequent presentation to T cells, which then recognize and attack the cells expressing that particular antigen. Two types of cancer vaccines currently exist, preventive and therapeutic.

Preventive vaccines aim to prevent cancer by targeting viral infections that can lead to cancer, eliciting an immune response against these viral antigens. An example is the gardasil 9 vaccine, directed against the human papillomavirus (HPV), which is associated with various cancers, including cervical, anal, vulvar, and vaginal cancers, as well as oropharyngeal cancer (Cheng et al., 2020).

By contrast, therapeutic vaccines that aim to treat an existing cancer by stimulating an immune response against a particular tumor antigen, leading to the destruction of cancer cells expressing those antigens. These vaccines can be generated to target TAAs or TSAs. For example, the only FDA approved therapeutic vaccine, Sipuleucel-T is directed against the TAA prostatic acid phosphatase (PAP), abnormally produced in prostate cancer (Saxena et al., 2020). Conversely, personalized vaccines against TSAs, being more tumor-specific, have shown encouraging results and are currently a major immunotherapy research focus. Targeting TSAs is not exclusive for cancer vaccine therapy, but for tumor infiltrating lymphocyte (TIL) and TCR engineered T cell (TCRt) therapy as well. In this case, TSA identification is needed, but it is time and cost consuming, due to the fact that a biopsy needs to be taken from the patient, and undergo DNA sequencing, mutation identification, and neoantigen prediction (Lang et al., 2021). Still, responses achieved are stronger and more specific than TAA targeting therapies, and methods and technology are improving rapidly (Janelle et al., 2020).

2.1.4. Oncolytic virus therapy

Using oncolytic viruses represent a pioneering strategy in the treatment of cancer, combining direct tumor cell killing and immune stimulation. These viruses have the great advantage of a good safety and tolerability in patients. Viruses can be modified to increase their capability to infect specifically cancer cells (Liu et al., 2003), and once cancer cells are infected and lysed, viral and tumor antigens are released, infecting surrounding tumor cells and using APCs to prime T cells and attack the tumor. Additionally, oncolytic virus therapy allows to delete genes that suppress immune responses and add others to help stimulate the immune response against cancer. The unique FDA approved T-Vec oncolytic virus is a modified Herpes virus with the gene for Granulocyte-macrophage colony stimulating factor (GM-CSF) incorporated, promoting an immune response by attracting, among others, macrophages to the tumor site (Andtbacka et al., 2015). It is only approved for melanoma patients, but is now being tested in other cancer types, as well as in combination with several additional immunotherapies (Zhang et al., 2023).

2.1.5. TIL therapy

Tumor infiltrating lymphocyte therapy is one of the Adoptive Cell Transfer (ACT) therapies. ACT therapies consist of obtaining cells from the patient, grown in large number in a good manufacturing practice (GMP) laboratory, with or without modifications, and reinfusing them back to the patient. Rosenberg and colleagues demonstrated in 1988 that TILs could be expanded in the laboratory, reinfused in the patient, and mediate cancer regression (Rosenberg et al., 1988). At that time, the whole TIL population was reinfused, but now specific tumor antigens can be targeted. Currently, in order to treat patients with TIL therapy, a biopsy needs to be taken to purify the TILs. Next, the DNA from the tissue sample can be sequenced and compared to healthy tissue to identify the cancer unique mutations. If sequenced, these mutated regions, which constitute neoepitopes, are incorporated into autologous DCs, that are then brought together with TILs from the tumor sample (Lu et al., 2014). The TIL population positive for the recognition of the neoantigen is the one that gets expanded and reinfused to the patient, obtaining a fully personalized treatment.

Melanoma, due to its high prevalence of somatic mutations, is considered the most immunogenic cancer type (Alexandrov et al., 2013). For this reason, it is the most attractive cancer type to test TIL therapy and all the immunotherapies that depend on the antigen presentation through the MHC, called human leukocyte antigen (HLA) in humans. Several clinical trials are ongoing in melanoma and cervical cancer with encouraging results, as well as in colorectal cancer (CRC), cholangiocarcinoma, NSCLC and breast cancer (BC) with preliminary and promising efficacy (Zhao et al., 2022). For instance, a study comparing TIL therapy vs ipilimumab in metastatic melanoma patients, showed a better objective response rate (ORR) in the TIL group, reaching 49% of patients, in comparison to the 21% achieved in the ipilimumab group (Rohaan et al., 2022). Some clinical trials, such as the previous, consist of a simple expansion of the TILs (Rohaan et al., 2022), such as lifileucel, the first TIL product that is going to achieve the FDA approval due to its demonstrated strong efficacy in metastatic melanoma (Sarnaik et al., 2021). Other TIL therapy strategies in preclinical research consist on identifying and expanding reactive TILs populations against the tumor (Besser, 2013), while others are expanded against a specific mutation (Zacharakis et al., 2018, Creelan et al., 2021).

2.1.6. TCR-engineered T cells

Another ACT being developed in the last years is the TCRt therapy, in which autologous T cells from the patient are transduced with a TCR specific for the recognition of a pMHC expressed by the tumor cells. This engineered TCR form a complex with the endogenous CD3, responsible for the signal transduction (Pasetto et al., 2016).

Obtaining a final product with this immunotherapeutic approach is currently challenging, as the obtention of the specific TCR consist in several steps. First, the mutation against which the TCRts are going to be directed needs to be identified. This step is performed as described above in TIL therapy, by the sequencing of the tumor lesion and healthy tissue. Consecutively, the enrichment and isolation of antigen-specific T cells by selectively expanding TILs or peripheral blood lymphocytes (PBL) is performed, and finally, the TCR sequencing of these antigen-specific T cells (Pasetto et al., 2016).

This therapy, therefore, is more complex, personalized, and costly than TIL therapy, with an added advantage, in TCRt therapy T cells are collected by leukapheresis from the blood of the patient, obtaining younger T cells with a less exhausted phenotype and increased proliferative capabilities than TILs (Baulu et al., 2023). Therefore, TCRt therapy is gaining an increasing interest in the search of curing cancer patients through personalized medicine, as new technologies are achieving a more time and cost-effective strategy. More than 200 clinical trials are currently ongoing according to clinicaltrials.gov. Like TIL therapy, this therapy can be directed against TAA or TSA, and most of the clinical trials are targeting CGAs, being NYESO the most targeted so far (Shafer et al., 2022).

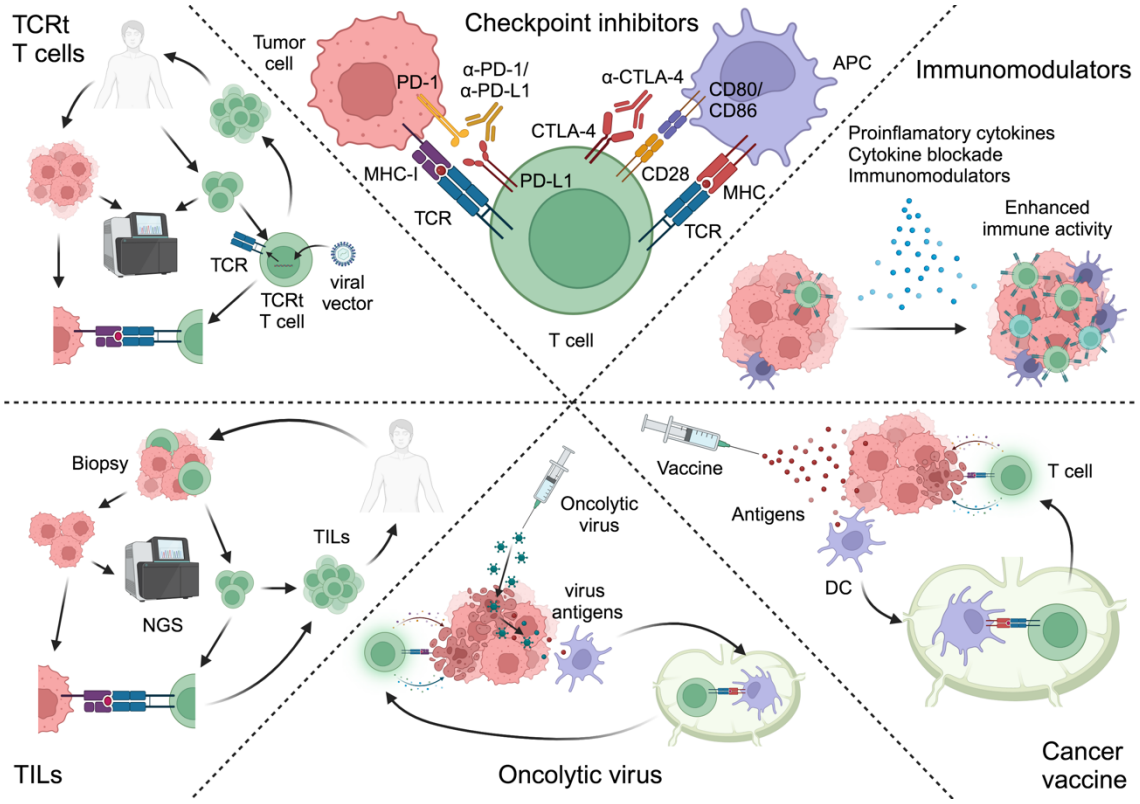

Figure 3: Antigen presentation dependent therapies. Most immunotherapeutic approaches are dependent on the recognition of the tumor cell by the T cell through the pMHC-TCR. These therapies aim to boost a preexisting response using different strategies. ICIs block inhibitory signals impeding T cell functionality and immunomodulators enhance antitumor immune activity by promoting its activation or inhibiting immunosuppressive molecules. Cancer vaccines and oncolytic viruses deliver antigens to improve the recognition of tumor cells by T cells, with the added advantage in oncolytic virus therapy of exerting a cytolytic effect. In TIL and TCRt therapies, T cells are purified from the patient, expanded *ex vivo*, and reinfused in the patient, with the possibility of purifying the tumor-reactive ones in the case of TIL therapy, or transducing T cells with an exogenous TCR to guarantee a specific recognition against a certain antigen in TCRt therapy.

2.2. T cell redirection therapies

In this thesis, we used chimeric antigen receptor (CAR) T cells and bispecific antibodies (bsAbs) to generate models of resistance to immunotherapy. In contrast to the rest of immunotherapeutic approach, their particularity is that are pMHC-TCR recognition independent, and are directed to an antigen expressed in the membrane of the target cells. Their mechanism of action consists on attracting the tumor cell and the T cell, forming an immune synapse through the target antigen and the T cell, activating the latter and triggering the release of granzyme, perforin, and IFNγ to cause cancer cell death (Wei et al., 2022).

2.2.1. CAR T cells

CAR T cell therapy is currently the only FDA-approved ACT approach. Autologous T cells from the patient are engineered to express a CAR construct directed against a certain tumor antigen expressed on the surface of the tumor cells, allowing to recognize and destroy them. CARs consist of a single chain fragment variable (scFv) from an antibody, in charge of recognizing the antigen on tumor cells, fused with intracellular signaling motifs in charge of T cell activation (Gross et al.,1989). CAR constructs have been improved through the years. First generation CARs consisted of only a CD3 intracellular signaling domain, while second generation constructs added an additional costimulatory domain, mainly CD28 or 4-1BB, mimicking the second signal needed for T cell activation. Third generation constructs consisted of two costimulatory domains. Currently, all FDA-approved CAR T therapies are based on second generation constructs, and all six directed against hematological malignancies, CD19 or BCMA on B cells. These therapies have remarkable efficacy, with up to a 91% ORR and 68% complete response rate (CRR) in mantle cell lymphoma (MCL) patients after 3-year follow-up treated with the CAR T against CD19 brexucabtagene autoleucel (Tecartus) (Wang, 2023). Despite that, solid tumor patients cannot benefit from these therapies yet due to the lack of FDA approved CAR constructs, but some preclinical promising candidates are currently in clinical trials. In solid tumors, the low efficacy of CAR T cells is described to be mainly due to: 1) the tumor antigen heterogeneity within a tumor (Dagogo-Jack & Shaw, 2018); 2) difficulties in the trafficking and infiltration into the tumor, which

can be due to fibrosis, dense ECM or decreased chemokine secretion (Salmon et al., 2012); and 3) the immunosuppressive TME. Additionally, with T cell engaging therapies, such as CAR T cells and bsAbs, many patients suffer from CRS driven by an excessive T cell activation and proliferation. Next generation CARs, or “armored” CARs, are being generated to solve these problems using different strategies.

1) In order to surpass the tumor heterogeneity, dual TAAs-targeting CAR T is a strategy that showed great preclinical efficacy *in vivo* (Hirabayashi et al., 2021); as well as BiTEs-secreting CAR T cells, which release a T cell bispecific antibody once the CAR recognizes the tumor cell, with many examples been generated to date with promising preclinical *in vivo* results (Cho et al.i, 2019).

2) In order to solve the difficulties of infiltrating into the tumor, CARs can be “armored” with ECM-degrading agents like heparanase (Caruana et al., 2015), or dual TAA targeting CAR T cells to improve their infiltration, like the dual nectin-4 (expressed in several solid tumors like triple negative breast cancer (TNBC)) and fibroblast activation protein alpha (FAP) CAR T, with increased infiltration and growth remission in *in vivo* models (Li et al., 2022).

3) To overcome an immunosuppressive TME, CAR “constructs” are being armored with cytokines, mainly IL-12. The CAR targeting $MUC16^{ecto}$ constitutively expressing IL-12, showed promising results *in vivo* in ovarian cancer (Koneru et al., 2015), being now in a phase I clinical trial (NCT02498912). Furthermore, CARs can be designed to secrete ICI, such as anti-PD-L1 antibody, which, when activated, block the inhibitory PD-1/PD-L1 axis enhancing antitumor efficacy in *in vivo* models (Suarez et al., 2016).

Furthermore, to avoid toxicities, switchable CAR constructs are a promising strategy, giving the clinician the opportunity to switch off the CAR T cells when needed (Tomasik et al., 2022). In the same direction, CAR NKs appear as a good strategy to avoid toxicities and graft-vs-host disease (GvHD), allowing to use allogenic NKs for the treatment (Xie et al., 2020)

In contrast to TCRs dependent recognition, CAR T cells do not depend on the pMHC recognition and its related resistance mechanisms through lack of antigen

presentation. Despite that, surface antigens represent the 1% of total expressed proteins in a cell, limiting the TAA to which they can be directed. Additionally, CAR Ts exert a stronger activation and cytokine release than TCR activated cells (Poorebrahim et al., 2021). Taking that into account, TCR-like CARs and TCR-CARs are an innovative strategy to target pMHC (Poorebrahim et al., 2021), combining the potent activation driven by the CAR construct and the specificity and broad range of neoepitopes recognition by the TCR. TCR-like CAR consists of a scFV recognizing the pMHC, while the TCR-CAR consists of a TCRv instead of the scFV. These novel strategies need to be further investigated but arouse attention in the cancer immunotherapy field.

2.2.2. Bispecific antibodies

Bispecific antibodies represent a novel class of therapeutic antibodies designed to recognize and bind two different antigens simultaneously. The most common application of bsAbs in cancer therapy involves the design of bsAbs that can bind to a particular antigen on cancer cells and simultaneously bind to immune cells, usually T cells. BsAbs are classified as IgG-like, which have enhanced stability and activity, and non-IgG-like, which are easier to produce and present lower immunogenicity. When referring to T cell directed bsAbs, the IgG-like antibodies are considered as T cell bispecific antibodies, or TCBs; whereas non-IgG-like can broadly differ on its structure, being BiTEs the most common (Wei et al., 2022).

As of September 2023, seven different immunotherapeutic bsAbs are approved to date against cancer. Six of these are approved for hematological malignancies and one against solid tumors. Blinatumomab, a BiTE directed against CD19, was the first FDA-approved bsAb in 2014, against B cell acute lymphoblastic leukemia (B-ALL) (Topp et al., 2014). Additionally, three more TCBs are FDA-approved against CD20 in lymphoma, as well as two more against myeloma, targeting BCMA or GPRC5D. Tebentafusp, a non-IgG-like bsAb targeting the pMHC gp100-HLA-A*02:01, was an important advance of T cell redirection therapies against solid tumors by having remarkable success in uveal melanoma, being FDA-approved in 2021 (Nathan et al., 2021).

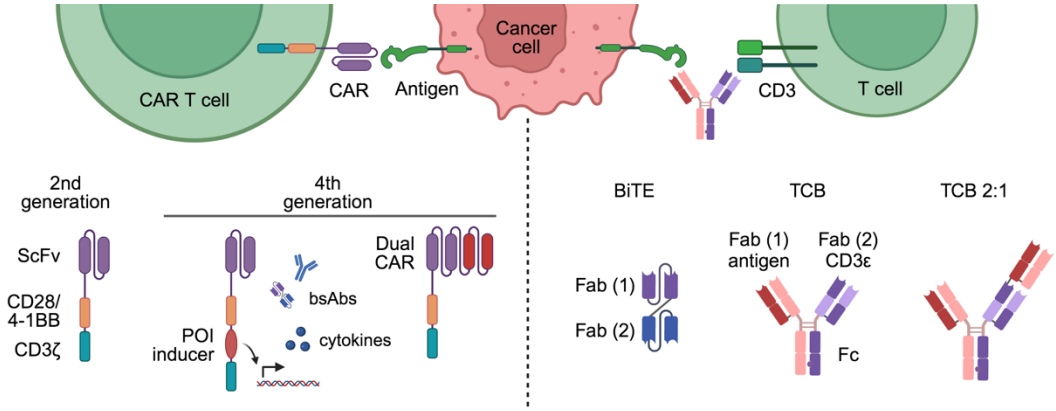

Figure 4: T cell redirection therapies. CAR T cells and bsAbs-driven T cells recognize the tumor cell independently of the antigen presentation through pMHC-TCR, but by recognizing a particular antigen against which are redirected, causing T cell activation and tumor cell attack. CARs consist of a scFV of an antibody that recognize the antigen and intracellular signaling motifs in charge of T cell activation. 2nd generation CARs consist of a motif for "signal 1" and a motif for "signal 2" to activate T cells. 4th generation CARs are "armored" CARs, such as dual antigen recognition constructs or a protein of interest "POI" inducer motif, by which CAR T cells can induce the expression of bsAbs or cytokines, among others. BsAbs are antibody-based molecules and trigger the binding of tumor cells and T cells, activating the latter. BsAbs divide into non-IgG-like, such as BiTE, and IgG-like, the TCBs. In this thesis, the antibodies used (HER2-TCB and CEACAM5-TCB) consist of TCBs with a 2:1 configuration, binding monovalently to CD3 and bivalently to the antigen, being then more tumor-specific and avoiding toxicities.

In this thesis we used TCBs as a tool to generate models of acquired resistance to immunotherapies. Particularly, we focused in the identification of the mechanisms by which solid tumors become resistant, and we identified the tumor intrinsic IFNγ deficient response and the antigen downmodulation as recurrent mechanisms of immune evasion. The specific TCBs used in these studies consist of an advanced strategy developed by Roche, with a configuration of 2:1, meaning that they bind bivalently to the cancer antigen and monovalently to CD3. This configuration gives the advantage of releasing the CD3-binding arm mainly when specifically recognizing the tumor cell with the two antigen-binding arms, avoiding unspecific T cell activation and thus, toxicities. Of note, it has been recently FDA-approved the first TCB with a 2:1 configuration, glofitamab, with two CD20 binding Fab region and one against CD3, for the treatment of lymphoma.

Several other improvements have been made to classical TCBs. These new strategies include targeting immune checkpoints, such as AK104, an anti-PD-1/CTLA-4 bsAb that has been recently approved to treat cervical cancer in China (no reference available), due to its efficacy and its specificity to block TIL's PD-1 rather than circulating lymphocytes, avoiding T cell toxicities. Other strategies

include recruiting NK cells for tumor redirection (Xiao et al., 2023), targeting co-stimulatory molecules such as 4-1BB (Claus et al., 2019), blocking protumorigenic molecules like TGF-β (Yi et al., 2022), or even generating trispecific antibodies, giving the researchers the chance to target two different TAA or activating both the CD3 and a costimulatory domain (Tapia-Gallisteo et al., 2023).

Therefore, during this last decade, huge efforts have been made to develop new strategies to improve patient's outcome. Despite that, resistances arise, and the full understanding of these mechanisms of resistance to current immunotherapies is an unresolved issue. This thesis is focused on the understanding of these escape mechanisms in order to improve the efficacy of immunotherapies.

3. Mechanisms of resistance to immunotherapy

Cancer immunotherapies have yielded remarkable clinical responses, significantly improving the lives of numerous cancer patients. Against hematological tumors, immunotherapy has been proven highly effective, as evidenced by the remarkable success rate of CD19 CAR T cell therapy against acute lymphocytic leukemia, with up to 90% patients with complete remission (Maude et al., 2014).

However, when it comes to solid tumors, the data is less favorable. Although ICI therapy has emerged as the first-line treatment for melanoma, NSCLC, RCC and TNBC, its benefits are experienced by only a subset of patients. Additionally, ICIs are being considered as a viable option for certain advanced and refractory tumor types, including bladder tumors and head and neck tumors. In contrast, other cancers such as pancreatic ductal adenocarcinoma (Timmer et al., 2021), glioblastoma (Rocha Pinheiro et al., 2023) and sarcomas (Birdi et al., 2021) exhibit low response rates to immunotherapy.

In the most favorable scenario for solid tumors, melanoma, where anti-CTLA-4 antibodies (ipilimumab) are combined with PD-1 blockade (nivolumab), which is the first line of treatment for advanced melanoma patients since 2015, the ORR among all patients is 58% (Larkin et al., 2019). Furthermore, in patients with NSCLC harboring high levels of PD-L1, a study comparing PD-L1 blockade

(pembrolizumab) with chemotherapy described an increase in the 5-year overall survival reaching only 32% of patients (Reck et al., 2021). Still, it is the first line of treatment in tumors with PD-L1 ≥50% (Ikezawa et al., 2022). An additional tumor type that has benefitted from immunotherapies but with limited efficacy is TNBC. In PD-L1 overexpressing tumor patients, which represent only one fifth of the patients, pembrolizumab plus chemotherapy has an OS of just 23 months (Cortes et al., 2022), but gained the approval for first line of treatment for these patients.

Although immunotherapy responses are generally considered more durable compared to conventional targeted therapies, a significant number of patients either do not respond to the treatment or experience relapse. This can be attributed to primary resistance mechanisms that arise shortly after initiating treatment or acquired resistance that develops during the course of treatment, leading to a shift from an initially effective response to treatment failure. Nevertheless, in the past decade, there has been substantial progress in the understanding of immunotherapy's effectiveness and mechanisms through extensive preclinical animal studies and clinical trials. This in-depth exploration has revealed remarkable and enduring clinical responses, ushering in a revolutionary treatment approach for various resistant carcinomas. Research is focused on two directions, by the generation of evolving immunotherapeutic strategies in order to increase efficacy, or, at the same time, by trying to elucidate how the tumor evades the immune attack. As a result of this research, the treatment landscape for tumors is gradually evolving.

In terms of response, tumors can be divided, regarding their immunogenicity, into “hot” and “cold” tumors. Low responsive cancer types such as pancreatic cancer (Timmer et al., 2021) or glioblastoma (Rocha Pinheiro et al., 2023) are considered cold, while immunogenic and high responsive types, namely melanoma (Larkin et al., 2019) and NSCLC (Mamdani et al., 2022), are considered hot tumors. This classification is based on tumor immunogenicity and immunotherapy response, and the TME key role in it. Hot tumors are characterized by a high degree of immune cell infiltration, particularly by T cells, which indicates an active immune response against the tumor. Hot tumors also often exhibit a high tumor mutational burden (TMB) and high degree of microsatellite instability (MSI-H), meaning they

have a large number of mutations that create neoantigens that the immune system can recognize. Therefore, these tumors are typically more responsive to immunotherapies. On the contrary, cold tumors, also known as "immune desert" tumors, represent a challenging hurdle, and underscores the importance of identifying the mechanisms by which a tumor becomes cold, and the tumor immune evasion strategies beyond that. These tumors have little to no immune cell infiltration and an often-low mutational burden, which translates into low response rate to immunotherapy (Duan et al., 2020).

Therefore, the sensitivity to immunotherapy of a tumor depends on several factors, and the mechanisms of resistance to immunotherapy can be divided in extrinsic, the ones mediated by other cell populations present in the TME, and intrinsic, mediated by the tumor cells themselves.

3.1. Extrinsic mechanisms

Extrinsic mechanisms of resistance to immunotherapy represent factors outside of the cancer cell itself that can impede the effectiveness of immune-based treatments. Tumor cells interact with several other immune and stromal cell types in the TME, a complex ecosystem composed of various cell types, blood vessels, and signaling molecules, which can foster a suppressive environment that blunts the immune response. This is especially important in solid cancers. For instance, certain cells in the TME, such as Tregs, MDSCs, TAMs or cancer associated fibroblasts (CAFs) can inhibit the activity of anti-tumorigenic immune cells and limit immunotherapy response through immunosuppressive cytokines and receptors expression, or costimulatory molecules repression. The release, composition and balance of cytokines in the TME plays a key role in the immunoediting process and the fate of the immunotherapy treatment. As major players, while high levels of IFNγ and IL-2 would drive a proinflammatory phenotype, high levels of IL-10 and TGF-β cause an immunosuppressive TME.

Moreover, the physical characteristics of the TME, including a dense ECM (desmoplasia), hypoxia and poor nutrient supply, can also compromise immune cell access, function and survival. Lastly, the heterogeneity of the TME, with diverse levels of immune infiltration across different regions of the tumor, can also

contribute to extrinsic resistance. Understanding and overcoming these extrinsic resistance mechanisms is a major focus of current research in cancer immunotherapy.

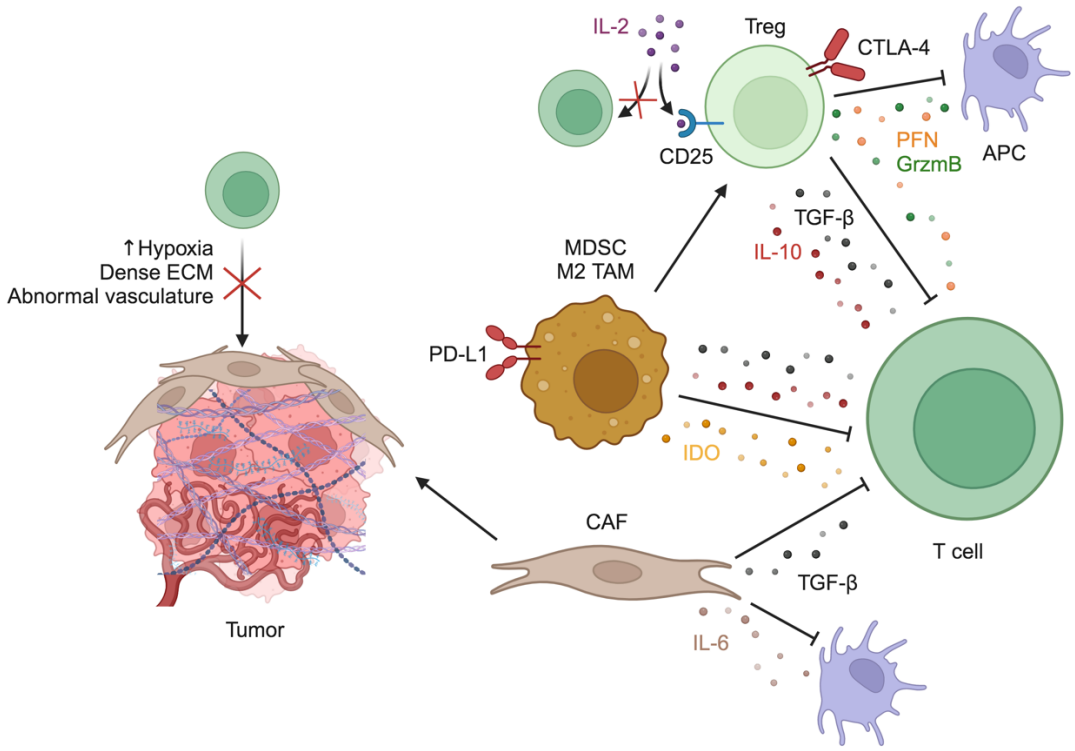

Figure 5: Extrinsic mechanisms of resistance to immunotherapy. Several factors in the TME can elicit an immunosuppressive and protumoral effect. The main cell types involved are Tregs, MDSCs, TAMs, and CAFs, which, by secretion of certain cytokines and metabolites such as TGF-β, IL-10, IL-6, and IDO; or expression of coinhibitory receptors like PD-L1 and CTLA-4, immunosuppress T cell antitumor responses. Moreover, Tregs can dominantly consume IL-2 by the CD25 receptor. Additionally, the TME physical conditions can impede T cell migration and functionality, namely hypoxia, dense ECM, or an abnormal vasculature.

3.1.1. Regulatory T cells (Tregs)

Regulatory T cells are immunosuppressive cells that, in healthy individuals, control autoimmune response. In cancer, though, these cells can exert a negative effect. Tregs, recognized for their $CD4^+$ $CD25^+$ $FoxP3^+$ expression, can inhibit effector T cells by different mechanisms (Ohue & Nishikawa, 2019). The principal mechanism by which they inhibit immunotherapy response is by releasing immunosuppressive cytokines, such as TGF-β or IL-10, inhibiting proliferation and effector functions of T cells (Takahashi et al., 1998). Other methods by which Tregs drive an immunosuppressive TME is by direct cell contact, through CTLA-

4 driven inhibition of DCs by binding to CD80/CD86 (Tekguc et al., 2021); by killing T cells and APCs through granzyme/perforin (Grossman, 2004); or by the dominant consumption of IL-2 in the TME by the CD25 receptor (Chinen et al., 2016). Clinically, Treg abundance in the TME have been associated with poor prognosis in patients in several cancer types, including melanoma, ovarian cancer and NSCLC (Ohue & Nishikawa, 2019). However, although preclinical efforts have been put into targeting this T cell population lately, the difficulty of correctly selecting this population have been a hurdle for its efficacy (Togashi et al., 2019).

3.1.2. Myeloid derived suppressor cells (MDSCs)

Myeloid cells are a critical barrier to protect the host from infections. However, in cancer, they may promote tumor protection and growth. The MDSC are found in the TME and have a role in immunosuppression, as well as in metastasis induction (Condamine et al., 2015). MDSC consist of two differentiated populations, termed granulocytic and monocytic. While having different phenotype and functions, MDSCs suppress T cell function through the production of immunosuppressive metabolites RNI (reactive nitroxide intermediates), cytokines (such as TGF-β and IL-10), enzymes like Indoleamine 2,3-dioxygenase (IDO), and by PD-L1 expression (Lechner et al., 2010). Additionally, they can recruit Tregs to the tumor and monocytic MDSCs can differentiate to TAMs, associated as well with an immunosuppressive TME (Gabrilovich, 2017). MDSC presence is associated with poor prognosis and reduced response to immunotherapies. Clinical studies have shown a decreased response to: ICB in melanoma, prostate cancer and NSCLC; to tumor vaccines in prostate cancer; and to CAR T therapy in B large lymphoma patients with MDSC rich tumors (Hao et al., 2021). Current efforts are made to target this cell population, either by inhibiting them directly or their recruitment to the TME, and in combination with immunotherapies. Promising preclinical results and clinical trials are ongoing (Hao et al., 2021).

3.1.3. Tumor associated macrophages (TAMs)

Tumor associated macrophages are important components of the TME in many solid tumor types. Even the recent awareness of their plasticity and change in the paradigm, they have been historically classified in a conventional binary model, into M1, or proinflammatory state, and M2, or anti-inflammatory state. While M1 state is induced by Th1 cell cytokines, such as IFNγ, the M2 state is induced by Th2 cytokines like IL-4, IL-13, or IL-10, and macrophage colony stimulating factor 1 (CSF-1) (Petty et al., 2021). The conversion from M1 to M2 state is related to a protumorigenic and anti-inflammatory phenotype. M2 TAMs secrete diverse cytokines and chemokines that have an effect on an augmented tumor proliferation, an increased angiogenesis, a promotion of metastasis, and a suppression of immune responses. TAMs can inhibit T cell infiltration, proliferation and activation by chemokines (CCL2, CCL5), cytokines (IL-10, TGF-β), or IDO secretion, as well as expression of PD-L1 and CD80/CD86 (Zhao et al., 2020). TAMs can also induce (by IL-10 or TGF-β secretion) or recruit (by CCL20 or CCL22 production) Tregs to the tumor stroma (Zhao et al., 2020). Higher TAM frequencies are associated with poor prognosis and immunotherapy resistance in glioma, cholangiocarcinoma, ovarian, and breast cancer (Heusinkveld & van der Burg, 2011), thus targeting TAMs is an attractive strategy for solid tumor therapeutic intervention. Some of the therapies being generated are targeting the monocyte recruitment through the disruption of chemokine signaling, depleting TAMs, or by reprogramming TAMs to a M1 proinflammatory phenotype. Clinical trials in different cancer models, in combination with conventional therapies and immunotherapies, have been giving promising results of these TAM targeting therapies (Petty et al., 2021).

3.1.4. Cancer associated fibroblasts (CAFs)

Another layer of complexity in the immunosuppressive environment that can be found in the immune control of the tumor growth are the CAFs. This cell population is one of the most abundant in solid tumor stroma, but it remains poorly understood due to its heterogeneity and lack of specific markers. Despite that, multiple of its protumorigenic functions have been described, such as increased tumor cell invasion, increased tumor growth, and interference with T cell function.

This disruption in T cell functionality is mainly due to the secretion of IL-6, TGF-β, and CXCL12, causing an impairment on DCs function, limiting T cell priming and attraction to the TME, and creating a dense ECM that impedes T cell trafficking and tumor infiltration. Clinically, in CAF-rich tumors like head and neck, esophageal, and colorectal cancers, immunotherapy treated patients display poorer prognosis due to T cell exclusion (Hanley & Thomas, 2020). Therefore, targeting CAF-related signaling is a promising way to tackle cancer, but is particularly challenging due to its heterogeneity (Sahai et al., 2020). Despite that, CAF-associated protumoral biomarker (FAP) is the most encouraging target to inhibit CAFs. In preclinical murine cancer models, FAP targeting through DNA vaccination (Duperret et al., 2018), CAR T cells (Liu et al., 2023), or BiTE-armed oncolytic virus (Sostoa et al., 2019) demonstrated encouraging results, highlighting the possibility of combining CAF-directed therapies with tumor-targeting immunotherapies.

3.1.5. TME physical conditions

Beyond the cell types integrating the TME, the physical conditions a tumor generate have a role in its immunity and response to immunotherapy.

Hypoxia is the oxygen deficiency in a tissue, and is an intrinsic property of most solid tumors. This condition is mainly caused by the fast growth of the tumor and its aberrant vasculature, as well as the increased metabolism by tumor cells and thus, increased oxygen consumption. When oxygen levels decrease, hypoxia-inducible factor (HIF) family of transcription factors get activated, mostly in tumor cells and CAFs, leading to the expression of certain genes involved in tumor growth and survival (Denko, 2008). Among these effects, hypoxia dampens the antitumor immune response by inhibiting effector T and NK cells, as well as DCs, and additionally, activates immunosuppressive components such as MDSCs or Tregs. Targeting hypoxia to enhance the efficacy of immunotherapy is another attractive approach, and several strategies are being developed, including drugs that activate upon hypoxia or anti-HIF signaling drugs in combination with ICIs (Jayaprakash et al., 2022).

Blood vessels within tumors are crucial for tumor expansion and the spread of cancer cells. The process of tumor blood vessel formation, known as tumor angiogenesis, is influenced by several cytokines, being the vascular endothelial growth factor (VEGF) family the main in controlling blood vessel development. In tumors, VEGF-driven angiogenesis leads to an abnormal vasculature that limit T cell infiltration, causes hypoxia and recruits MDSCs (Vetsika et al., 2019). This immunosuppressive phenotype can be reverted by anti-angiogenesis treatments, such as the anti-VEGF antibody bevacizumab, broadly studied in combination with immunotherapies with FDA approved combinations. For instance, in hepatocellular carcinoma (HCC), the first line of treatment is the combination of atezolizumab plus bevacizumab (Tella et al., 2022).

Apart from all the described above, other factors such as the patient's microbiota can determine responses to cancer immunotherapy (reviewed in Pitt, 2016), as well as patient's sex, as seen in a retrospective meta-analysis that indicates that ICB benefit is significantly higher in women (Conforti et al., 2018).

3.2. Intrinsic mechanisms

Intrinsic mechanisms of resistance to immunotherapy involve alterations within the cancer cells that allow them to evade the immune attack. These changes can occur at the genetic, epigenetic, or signaling pathway level, leading to altered protein expression or function that affects how the immune system recognizes and responds to the cancer. Many different mechanisms have been described so far, underlining the remarkable adaptability of the tumors to different scenarios.

As these intrinsic factors are complex and highly variable among different cancers and patients, they present a significant obstacle in the design and application of successful immunotherapeutic strategies. Understanding these resistance mechanisms is therefore a crucial area of ongoing cancer research.

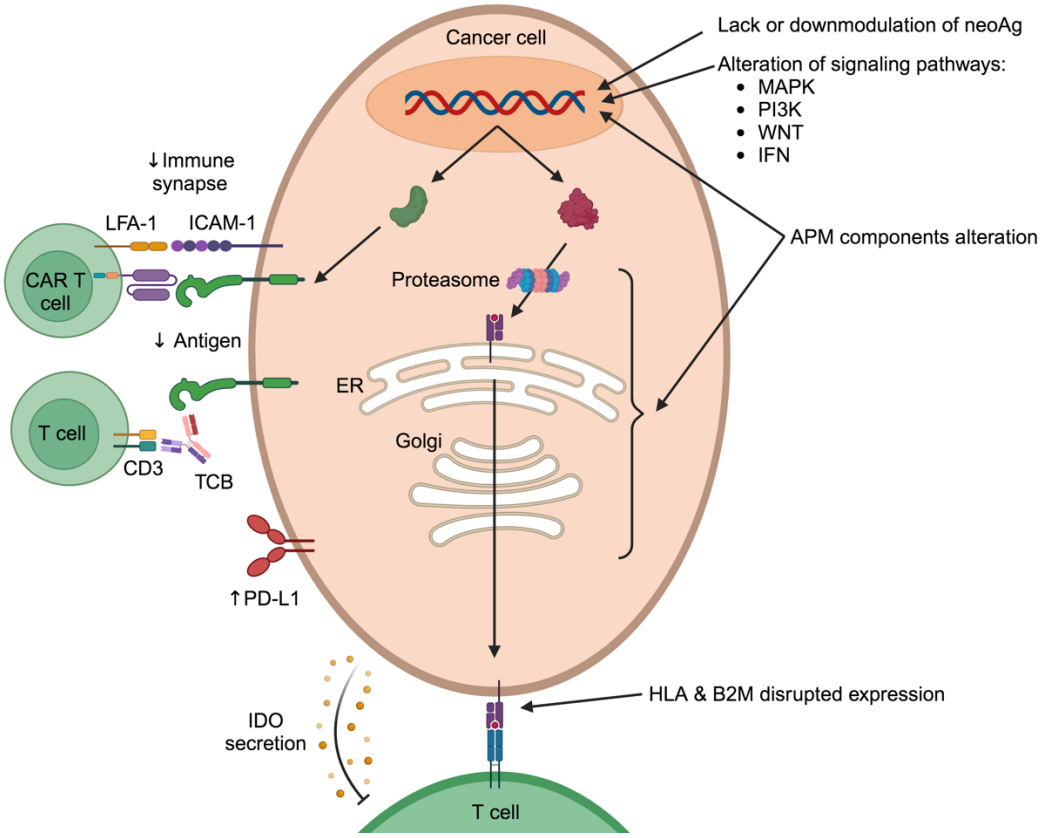

Figure 6: Intrinsic mechanisms of resistance to immunotherapy. Tumor cells can escape the killing mediated by immune cells by several mechanisms, including: lack of antigenic mutations, alterations in the antigen presentation machinery, target antigen downmodulation, impairing the immune synapse with the T cell (by ICAM-1 disrupted binding to LFA-1), impairing T cell function by surface protein expression (i.e. PD-L1) and secretory molecules (i.e. IDO), or alterations of certain signaling pathways, including MAPK, PI3K, WNT, and importantly, IFNγ. Based on (Sharma et al., 2017).

3.2.1. Lack of tumor antigen

When treated with TILs, ICI, or any immunotherapy that needs the TCR recognition of tumor antigens presented by the MHC, lack of tumor antigen may arise as the resistance mechanism.

High TMB, MSI-H, and mismatch repair deficiency are associated with increased antitumor responses and immunotherapy sensitivity (Marabelle et al., 2020, Marabelle et al., 2020). That increase in immunogenicity is due to a remarkable increase in neoantigen expression and presentation (Llosa et al., 2015). Thus, T cell activity and response to immunotherapy can be evaded by tumor cells due to a decrease in neoantigen expression (de Vries et al., 1997, Gubin et al., 2014). Therefore, intrinsic low neoAg expression is often a primary mechanism of resistance. Besides, initially responsive tumors can adapt to the treatment and

experience an “antigenic drift”, in which the antigen is downmodulated and the tumor becomes resistant (Bai et al., 2003, Rosenthal et al., 2019), even though it has been described to be infrequent (Lo, 2021).

Different strategies can be implemented to convert tumors to an antigenic state. Radiation have a strong genotoxic effect, leading to a higher proportion of mutations and neoAg generation, as demonstrated in mice models (Lhuillier et al., 2021). Additionally, in low TMB tumors, oncolytic viruses can bypass the low neoAg generation by the expression of exogenous antigens. In a recent clinical trial with pediatric high-grade glioma patients, considered a “cold” tumor, an oncolytic virus therapy increased T cell infiltration and improved patients’ outcome (Friedman et al., 2021).

3.2.2. Alterations in APM

Alterations in the APM, like the lack of tumor antigen, arises as a mechanism of resistance for antigen presentation dependent immunotherapies. Disruption of the antigen presentation signal pathway leads to a lack of recognition by T cells, and thus, cancer immunotherapy resistance. The disruption of this pathway can occur at several levels, as the antigen presentation machinery involves components in the proteasome, the antigen transporters, and the MHC structural proteins. MHC class I consists of a heterodimer formed by the MHC and the β2 microglobulin (B2M), and both of them can undergo mutations, deletions, and loss of heterozygosity (LOH) (Tran, 2016, Sade-Feldman, 2017), leading to a disrupted expression of the MHC-I. Additionally, genetic alterations can happen in the proteasome components and TAPs (Balasubramanian et al., 2022). Alterations in the APM, though, are not exclusive of genetic alterations, as epigenetic changes can also occur, as described in prostate cancer patients bearing DNA methylation and histone modifications of the HLA I gene (Rodems et al., 2022); as well as transcriptional dysregulation of the components of the pathway (Cho et al., 2021). The APM pathway is tightly controlled by IFNγ response genes, and therefore, if a tumor becomes insensitive to IFNγ, the APM is disrupted (Cho et al., 2021). The loss of HLA expression as an acquired resistance mechanism in patients has been described in different immunotherapeutic treatment strategies, such as ICB, in a lung squamous cell

carcinoma patient who relapsed after initial response to anti-PD-L1/anti-CTLA-4 due to LOH of *B2M* (Gettinger et al., 2017); or TILs, in a melanoma patient with downmodulation of several components of the APM pathway (Donia et al., 2017). Additionally, lack of HLA expression has been demonstrated in several tumor sites, such as melanoma, prostate cancer, or CRC (Hazini et al., 2021). Nevertheless, these MHC-I deficient tumors can be targeted through NK cell recognition and attack, as demonstrated in mice preclinical models (Ni et al., 2012).

3.2.3. Target downmodulation

T cell redirection therapies like BsAbs and CAR T cells, which bypass antigen recognition through the TCR, are independent of these previously described mechanisms. Despite that, these therapies are based on the recognition of a certain antigen in the surface of the tumor cell, and its downmodulation has been described to be a frequent acquired mechanism of resistance. Several studies with CD19 CAR T cells and bispecific antibodies (blinatumomab) reported cases of CD19 negative tumors which escaped treatment due to CD19 loss of expression (Gardner et al., 2017, Mejstríková, 2017). Furthermore, on solid tumors, downmodulation of the antigen as a mechanism of resistance have been described in the clinic in a glioblastoma patient treated with a CAR against IL13Ra2 (Brown et al., 2016). Additionally, in this thesis we describe the antigen downmodulation as a common mechanism of acquired resistance to a TCB targeting CEA in *in vivo* models of patient derived xenografts (PDXs) (Martinez-Sabadell et al., 2022).

Most data regarding the mechanisms of antigen downmodulation are based on CD19 CAR T and blinatumomab clinical experience. These mechanisms include mutations on the target (Maude et al., 2018), alternative splicing (Sotillo et al., 2015) and defects in antigen processing (Braig et al., 2017). Additionally, it has been described the presence of antigen-negative pre-existing clones in tumors relapsing from anti-CD19 therapies (Fischer et al., 2017). These negative tumor cells may evolve then into the dominant clone in the antigen-negative relapse.

3.2.4. Disrupted immune synapse

Recently, several works have been highlighting the importance of a correct binding and immune synapse (IS) formation between a T cell and a tumor cell in the response to immunotherapy. CAR T therapy, importantly, forms a very different IS from a pMHC-TCR mediated synapse, forming a disorganized cytoskeleton and rapid liberation of lytic granules (Davenport et al., 2018). On the contrary, TCB mediated ISs are very similar to the TCR mediated (Carrasco-Padilla et al., 2022). Additionally, CAR constructs have a remarkable lower affinity to the antigen than TCRs, requiring more than 100-fold more antigen to activate T cells (Burton et al., 2023). Furthermore, in order for CARs to elicit a correct synapse and kill tumor cells, the binding of CD2 from T cells and CD58 from tumors, which rearranges the cytoskeleton and costimulates T cells, need to happen, as seen *in vivo* and in patient's samples in hematological tumors (Romain et al., 2022). As a consequence, CD58 aberrations (mutations or lack of expression) correlated with treatment failure in DLBCL patients treated with CD19 CAR (Majzner et al., 2020). Additionally, Maus and colleagues described the importance of a correct immune synapse in the response to CAR T cells, and preliminary data pointed ICAM-1 downmodulation driven by a defective IFNg, as the cause of resistance in solid tumors (Larson et al., 2022). Given all these recent evidences, the study on the correct immune synapse formation is gaining attention in the immunotherapy field.

3.2.5. Cancer immune evasion by surface protein expression and secretory molecules

Tumor cells can express inhibitory immune checkpoints such as PD-L1, PD-L2 or Galectin-9, which inhibit T cells through its ligand TIM-3 (Yang et al., 2021). Among these, PD-L1 appears as the most important. A primary resistance mechanism is the constitutive PD-L1 expression in tumor cells, thus inhibiting T cell responses. This mechanism has been seen in patients of hematological malignancies due to *PDL1* copy number gains (Ansell et al., 2015), or in solid tumor patients due to amplification of the locus containing PD-L1 and PD-L2 (Rooney et al., 2015). The main mechanism by which tumors upregulate PD-L1

is by constitutive IFNγ response (further discussed below), but also by different proinflammatory cytokines such as TNFα and type I IFNs (Cha et al., 2019). Furthermore, mutations in *PTEN,* driving then PI3K/AKT pathway constitutive activation, can elicit a PD-L1 upregulation in an IFNγ dependent or independent manner (Cretella et al., 2019). Furthermore, *EGFR* mutations can constitutively activate *PDL1* transcription through the MAPK pathway (Chen et al., 2015), as well as MYC overexpression by binding to the *PDL1* promoter (Casey et al., 2016). For these reasons, combinatorial strategies with PD-1/PD-L1 blockade plus other therapies such as chemotherapy, radiotherapy or angiogenesis inhibitors, or other immunotherapies such as ipilimumab are currently used in the clinic. Additional strategies being explored in clinical trials include bsAbs or dual CARs targeting PD-1/PD-L1 plus an additional inhibitory immune checkpoint such as CTLA-4, or plus a costimulatory domain agonist, with encouraging results in clinical trials (reviewed in Yi et al., 2022).

Metabolic enzymes represent another layer of immunotherapy resistance. Although IDO is not an immunosupressive chemokine, it is an important resistance mechanism that modulates the TME. This metabolic enzyme is a heme-containing enzyme that catalyzes tryptophan to kynurenine. This tryptophan depletion plays a role in various biological functions, including the immune system regulation (Zhai et al., 2020). In the context of cancer, IDO-mediated tryptophan depletion inhibits T cell proliferation and dampens T cell activity against tumor cells (Zhai et al., 2020). Importantly, increased IDO expression has been associated with hematologic (Corm et al., 2009) and solid tumor malignancies, including BC (Chen et al., 2014) and melanoma (Spekeckaert et al., 2012), and it has been implicated in resistance to ICB therapies in clinical studies, such as anti-PD-1 in sarcoma and NSCLC (Toulmonde et al., 2018, Botticelli et al., 2018). Ongoing clinical trials are combining IDO therapy with checkpoint inhibitors to enhance treatment response. Indeed, a recent follow-up study of ~ 4 years on a phase I/II clinical trial where metastatic melanoma patients have been treated with an IDO/PD-L1 vaccine plus nivolumab have given encouraging results, with an 80% ORR and 50% of CR patients (Lorentzen et al., 2023).

3.2.6. Alterations in oncogenic pathways

Mutation driven dysregulations in several important oncogenic pathway regulators can also have an important role on the tumor immunogenicity and immunotherapy efficacy.

MAPK. For example, a tumor with increased mitogen-activated protein kinase (MAPK) signaling leads to an augmented VEGF and IL-8 secretion, among other proteins, causing an impair in T cell infiltration and activity (Bancroft et al., 2001), and therefore, resistance to immunotherapy. Accordingly, MAPK inhibitors, namely BRAFi dabrafenib and MEKi trametinib, have demonstrated an increased immune response when combined with ICIs, as an increased infiltration, IFNγ signaling, and T cell killing is observed in preclinical *in vivo* models (Liu et al., 2015). In addition, about 50% of melanomas harbor mutated BRAF, mostly V600E, constitutively activating the MAPK pathway (Ascierto et al., 2012). For this reason, combinatorial therapies combining ICIs and targeted therapies are being tested in clinical trials. Despite promising, many combinatorial treatments have been terminated due to serious toxicities like hepatotoxicities or skin complications (Shin et al., 2020). Nevertheless, a phase III clinical trial in $BRAF^{V600}$ mutated melanomas proved the beneficial effect of combining the anti PD-L1 ICI atezolizumab with vemurafenib (BRAFi) and cobimetinib (MEKi), leading to an FDA approval for $BRAF^{V600}$ mutated unresectable or metastatic melanomas (Gutzmer et al., 2020).

PI3K. On the same direction, active phosphatidylinositol-4,5-bisphosphate 3-kinase (PI3K) signaling is associated with decreased antitumor immunity. Lack of tumor suppressor PTEN expression causes an increased PI3K, associated with immunosuppressive molecule release such as VEGF and CCL2. This secretion results in decreased infiltration an effector functions of TILs, as well as chemoattraction of immunosuppressive cells such as Tregs and TAMs, leading to immunotherapy resistance (Peng et al., 2016). Some patient studies have proven the correlation between PTEN loss in resistance to ICIs (anti-CTLA-4 plus anti-PD-1) in several cancer types like melanoma (Roh et al., 2017) and NSCLC (Chen et al., 2019). Several clinical trials are currently ongoing combining PI3K inhibitors and ICI, but few results are published.

WNT. In both a preclinical mouse melanoma model and human metastatic melanoma samples, the persistent activation of the WNT/β-catenin signaling pathway has been observed to result in reduced T cell infiltration and ICB therapy resistance. In murine models, this WNT/β-catenin activation lead to a decrease in CCL4 expression, thus reducing attraction of $CD103^+$ DCs within the tumor microenvironment. This decrease in $CD103^+$ DCs, responsible for $CD8^+$ T cell priming and recruitment, negatively affects the abundance and clonal diversity of cytotoxic $CD8^+$ T cells in the TME (Spranger et al., 2015). Confirming its clinical relevance, a study leaded by Dr. Ribas compared the gene expression profile of biopsies of ICI responder and non-responder patients (treated with ipilimumab plus nivolumab), showing a significant decrease in WNT score in responders. For this reason, targeting the WNT/β-cat pathway may alter the TME from immunologically cold to hot tumors. Recently, clinical trials targeting WNT/β-cat components PORCN and DKK1, positive regulators of the pathway, in combination with ICIs have demonstrated effectivity, such as PORCNi WNT974 plus spartalizumab (anti-PD-1) in several solid tumors (Janku et al., 2020), and DKKi DKN-01 in combination with pembrolizumab (anti-PD-1) in patients with advanced gastroesophageal carcinoma (GEA) (Klempner et al., 2020).

Therefore, we can conclude that tumors employ different intrinsic oncogenic pathways to evade T cell mediated killing and diminish the infiltration of antigen-specific T cells in the tumor microenvironment. Another intrinsic pathway involved in immunotherapy resistance is the IFNγ, which is one of the main focus of this thesis.

4. IFNs

In the last decade, tumor intrinsic IFN response has been described preclinically and clinically as a key player in the sensitivity to immunotherapies. In this thesis, we describe the central role of tumor intrinsic IFNγ response in immunotherapy resistance.

Interferons are key orchestrators of the innate and adaptive immunity, as well as inductors of differentiation, inflammation, and growth arrest. IFN signaling in the TME has been shown to be central to both immune surveillance and escape in

solid tumors. There are three IFN groups, type I IFNs (IFNα and IFNβ), type II (IFNγ) and type III (IFN-lambda) (Negishi et al., 2018). In tumor immunity, the different IFN types' role vary depending on the context, with pleiotropic functions and overlaps between the different IFN signaling cascades and other key oncogenic pathways. This complex system requires a deep understanding to elucidate their role in tumor immunotherapy resistance.

4.1. Biology of IFN

4.1.1. Production and signal transduction

Type I IFNs (IFNIs) can be produced by every nucleated cell in response to an infection or danger signals, and in the cancer context both immune and cancer cells produce and release it (Musella et al., 2017). Despite IFNα/β are very similar in structure and exerted biological activities, the main difference is their origin, IFNα being produced mostly by leukocytes and IFNβ by fibroblasts (Li et al., 2018). In cancer, type I IFNs expression can be activated through different signals, such as the recognition of DAMPs by Toll-like receptors (TLRs), the recognition of damaged RNA (both exogenous and endogenous) by the retinoic acid-inducible gene I (RIG-I), or via damaged DNA recognition (both exogenous and endogenous) by the cyclic GMP-AMP synthase (cGAS) and STING pathway. Type I IFN receptors are expressed in almost every cell type. The binding of IFNα/β to the heterodimeric IFNAR1/IFNAR2 complex drives the signaling through TYK2/JAK1, that can recruit and phosphorylate the STAT1/STAT2/IRF9 complex, called ISGF3, which translocate to the nucleus and bind to interferon-stimulated response elements (ISREs) in certain gene promoters of the called IFN-stimulated genes (ISG). Additionally, TYK2/JAK1 complex can recruit and signal through two STAT1 molecules, as well as through STAT3 and STAT5 homo- or heterodimers (Platanias, 2005).

Type III IFNs, also known as IFNλs, are the least characterized family of interferons. They are structurally similar to type I IFNs and the IL-10 family, and their expression is driven through the same mechanisms as IFNIs. Despite that, IFNλ production is restricted to epithelial cells and DCs (Lauterbach et al., 2010). They interact with a receptor made of the IL-28R-binding chain and IL-10R2,

mostly expressed by epithelial cells, but also in DCs and neutrophils (Lazear et al., 2015). The signaling pathway of type III IFNs is identical to type I IFNs, leading to the activation of JAK1 and TYK2, which then promotes the formation of the ISGF3 transcription factor complex to activate ISGs (Lazear et al., 2015). Despite its similarity to type I IFNs, IFNλ has been mostly related to protection against viral infections as a first barrier, and just recently some preclinical research has been done in the cancer context (Lazear et al., 2019).

IFNγ, in contrast to type I IFNs, is only produced by a restricted number of immune cells (Schoenborn & Wilson, 2007), namely mediators of innate and adaptive immunity such as NKs, $CD8^+$ and $CD4^+$ Th1 cells (Szabo et al., 2002). Activation of cellular receptors or certain cytokines promotes the production of IFNγ, such as the NK cell–activating receptors or the TCR. Regarding the control by cytokines, while IL-12 and IL-18 promote the production of IFNγ, TGF-β and IL-10 inhibit it (Schoenborn & Wilson, 2007). IFNγ binds to IFNGR and triggers the formation of a complex of eight molecules, consisting in two IFNGR1 and two IFNGR2, that associate with two JAK1 and two JAK2. This complex recruit and phosphorylates two STAT1 molecules. Phosphorylated STAT1 dimerizes, translocate to the nucleus and binds to regions of the genome known as IFNγ-activated sites (GAS), present in the promoter of certain ISGs, initiating transcriptional programs that depend on the specific cell type and typically include hundreds of genes. One of the most important GAS genes is *IRF1*, a transcription factor in charge of binding to ISRE regions and transcribing most ISGs, mostly related to host defense and immune regulation, cell cycle, apoptosis, inflammation, and innate and acquired immunity (Schroder et al., 2004, Rettino et al., 2013). IFNγ is therefore considered a pleiotropic cytokine, as it is involved in several different processes. Additionally, IFNγ signal can be transduced through STAT3 homodimers or STAT1-STAT3 heterodimers, by which different ISGs can be transduced in different cell type and context (Gocher et al., 2021)

Moreover, IFNs can activate other non-canonical pathways such as MAPK and PI3K, which have been shown to be needed for the transcription and translation of certain ISGs (Joshi et al., 2009, Joshi et al., 2011, Kaur et al., 2007).

Importantly, IFN pathways, through the transcription of certain ISGs, negatively regulates themselves. In order to avoid an excessive activation of the pathway, which would drive into an exacerbated activation of T cells and autoimmune disease (Yoshimura et al., 2012), IFNs signaling promote the transcription of the negative regulators suppressor of cytokine signaling (SOCS) and protein inhibitors of activated STAT (PIAS) families. SOCS members, being SOCS1 and SOCS3 the most described, exert this inhibition through inhibition of JAK signaling (including TYK2) either by inhibiting their kinase activity or by ubiquitinylating them (Liau et al., 2018). Besides, PIAS members downmodulate IFN signaling by inhibiting STATs phosphorylation and translocation to the nucleus (Niu et al., 2018). Additionally, despite not being regulated by IFNs, the protein tyrosine phosphatase non-receptor type 2 (PTPN2, TCPTP) is a well-known negative regulator of the pathway by dephosphorylating JAKs or STATs (Song et al., 2022).

IFNs, acting on immune and nonimmune cells, protect the organism from transformed cells, despite eventually some of these cells escape (Lawson et al., 2020), and their malignant progression is further shaped by the immune system during the immunoediting process, where particularly IFNγ plays a central role (Dunn et al., 2002).

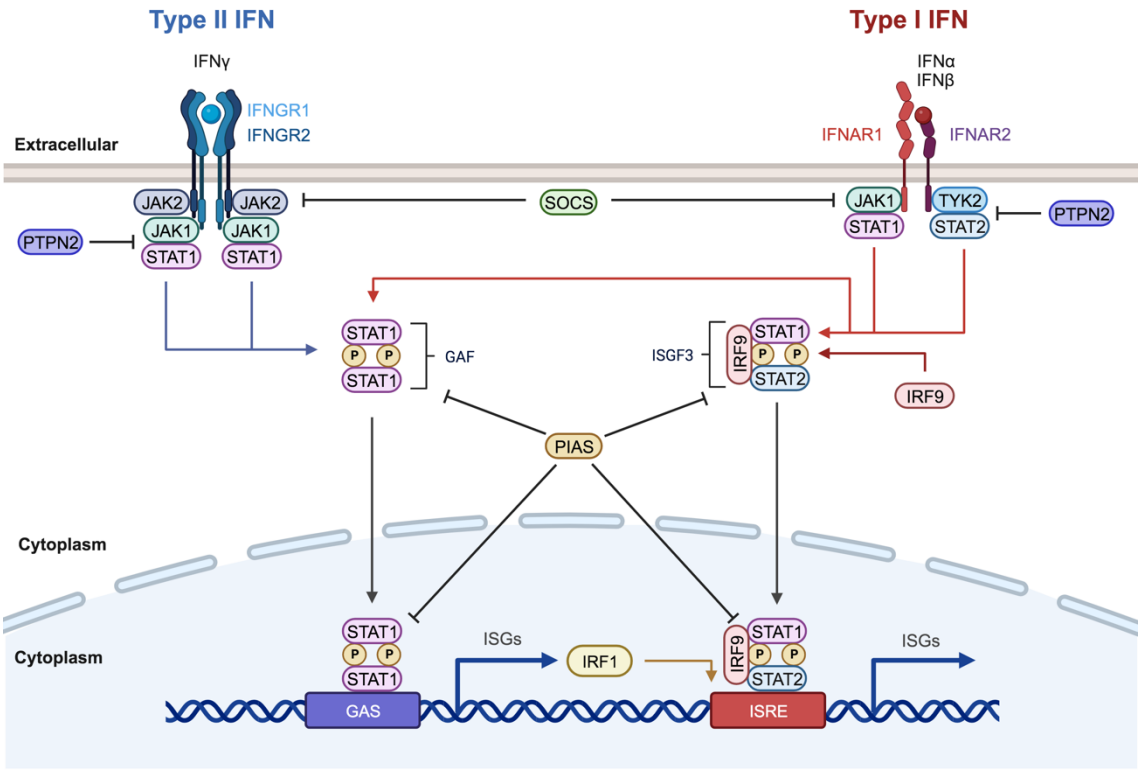

Figure 7: Type I and II IFNs canonical signaling pathways. Type I IFNs (IFNα and β) share a common receptor, the IFNAR, comprised by two subunits, IFNAR1 and IFNAR2, and it associates with TYK2 and JAK1. In contrast, IFNγ binds to IFNGR, composed by two IFNGR1 and two IFNGR2, linked to JAK1 and JAK2. Upon IFNα/β binding, JAKs linked to the IFNAR lead to STAT2 and STAT1 phosphorylation, forming ISGF3 complexes (STAT1, STAT2 and IRF9) that translocate to the nucleus and bind DNA ISRE regions to transcribe ISGs. IFNγ prompt the formation of STAT1 homodimers (GAF) that travel to the nucleus, binding GAS elements in the promoter of specific ISGs, initiating gene transcription, which type I IFNs can also do. The transcription of GAS regions promote IRF1 expression, which then amplifies ISGs transcription by binding to ISRE regions. The negative regulators of the pathway SOCS, PIAS, and PTPN2 can modulate the activation of the pathways by inhibiting them at each step of the pathway.

4.1.2. Effects of IFN on the immune compartment

The IFN canonic role is the coordination of the innate and adaptive branches of the immune system by acting on macrophages, DCs, lymphocytes, and NK cells.

On **macrophages**, IFNγ was the first activating factor described (Schreiber et al., 1985). Both type I and II IFNs are described to promote the differentiation of macrophages to the M1 proinflammatory phenotype, which, consequently, secrete IFNγ and promote cytotoxic activity in $CD8^+$ lymphocytes and enhance antigen presentation (Sica & Mantovani, 2012).

On **DCs**, IFNγ activate antigen presentation by increasing the expression of the MHC class II transactivator CIITA, a transcriptional activator involved in the expression of HLA class II components, and the invariant chain (Ii), a protein necessary for the correct maturation of the HLA class II-antigenic peptide complex (Wolf & Ploegh, 1995). Besides, IFNγ modifies the proteasome so that the antigens are more efficiently processed (Rivett et al., 2001). IFNγ also stimulates the production of IL-12 (Garris et al., 2018), leading to the activation of other immune components of the TME (namely lymphocytes and NK cells). In addition, DCs contact with tumor DNA promote their own activation and IFNI production. This IFNI, in an auto- or paracrine manner, is required for DC maturation, inducing the expression of HLA II molecules and costimulatory factors CD80 and CD86 (Montoya et al., 2002). Furthermore, type I IFNs promote the migratory capabilities of DCs (Parlato et al., 2001).

On **lymphocytes**, IFNs are key in the cancer immunotherapy context. IFNs induce the differentiation of $CD4^+$ T cells to Th1 phenotype, which is characterized by the ability to produce IFNγ, which maintains Th1 lineage and inhibits the differentiation to Tregs and the other main Th cell subsets, establishing a feed-forward mechanism (Bradley et al., 1996). Cytotoxic $CD8^+$ T cells exposure to IFNs is required as well for their full cytolytic activity and differentiation to CD8 effector function and memory, by the upregulation of granzyme, the IL-2 receptor and the transcription factor T-bet, which along with the related transcription factor eomesodermin, induces the production of IFNγ, again establishing a feed-forward loop (Pearce et al., 2003, Agarwal et al., 2009, Lu et al., 2019). Tregs are another subset of T cells influenced by IFNs exposure. In addition to the above mentioned Th1 differentiation, and thus, Treg inhibition, IFNγ has been proven to inhibit Treg proliferation (Cao et al., 2009). Furthermore, IFNγ prompts a 'fragile' Treg cell phenotype, in which Treg cells lose suppressive activity yet maintain FOXP3 expression (Overacre et al., 2018). Moreover, IFNα can reduce Treg infiltration by impairing chemotaxis, as demonstrated by its intratumoral delivery *in vivo* (Hirata et al., 2018). IFNγ and type I IFNs, together with other cytokines like IL-12 or IL-15, are also critical mediators of NK activation and cytotoxic function (Park et al., 2004, Muller et al., 2017). In addition, IFNγ in DCs or tumor cells promote the expression and release of the chemokines

CXCL9 and 10, responsible for the recruitment of T and NK cells into the tumor (Russo et al., 2020).

All the above effects support the consideration of IFNs I and II as proinflammatory cytokines. However, IFNγ is a pleiotropic cytokine that can blunt inflammation by direct apoptosis (Pai et al., 2019) or by inhibition of clonal diversity and proliferation of stem-like T cells (Mazet et al., 2023), and by promoting the production of immunosuppressive factors and the activity of cells that inhibit the T cell antitumoral activity. The pro- and anti-inflammatory activities of IFNγ are probably sequential and the latter avoids deleterious effects when inflammation is no longer needed, which may happen when chronically exposed to IFNγ. Indeed, IFNγ-induced CXCL9/10 expression can have a protumorigenic effect by promoting Treg and M2 macrophages recruitment, tumor growth and increased dissemination (Russo et al., 2020). On the same line, MDSC immunosuppressive activity is enhanced by IFNγ through augmented iNOS expression in the tumors *in vivo* (Shime et al., 2018). Additionally, IFNs induce the expression of inhibitory molecules such as PD-L1 and PD-L2 (Abiko et al., 2015, Garcia-Diaz et al., 2017) and particularly, IFNγ induces production of IDO (Jürgens et al., 2009), generating an immunosuppressive environment. In conclusion, IFNγ plays an essential role in the control of antitumor inflammation, but depending on the context, and more probably, the tumor evolution stage, its role can shift to an immunosuppressive effect.

4.1.3. Effects on cancer cells

In this thesis we identified the tumor intrinsic IFNγ response as a mechanism of resistance to immunotherapy, and therefore, we focus on the cancer cell intrinsic effect of IFNγ.

4.1.3.1. Immunogenicity

IFNγ has a crucial intrinsic role in the control of tumor growth by the immune system. The most important being the control of antigen presentation via MHC-I. This activation occurs at three levels: the generation of peptides, their transport, and their exposure at the cell surface. By triggering the expression of specific

subunits, IFNγ modifies the composition of the proteasome and thereby its proteolytic specificity. Thus, IFNγ changes the repertoire of peptides presented by MHC-I complexes (Gaczynska et al., 1994, Griffin, 1998). IFNγ also promotes the expression of TAP-1, a transmembrane endoplasmic reticulum protein that transports the peptides generated by the proteasome in the cytosol to the lumen of the endoplasmic reticulum (Seliger et al., 1997), and promotes the expression of both MHC class I genes (Chang et al., 1992) and B2M (Hunt & Wood, 1986), another essential component of the MHC class I complex. Additionally, IFNγ upregulates costimulatory molecules such as CD80 and CD86, which bind to CD28 and leads to T-cell activation (Li et al., 1996). Therefore, it is well established that IFNγ increases tumor immunogenicity by globally upregulating the antigen-processing machinery at different levels. Despite that, IFNγ has seemly opposite roles. While the effects on antigen processing result in increased exposure to immune cells, IFNγ also upregulates the inhibitory factor PD-L1, avoiding recognition and attack by T cells (Abiko et al., 2015, Garcia-Diaz et al., 2017). Moreover, IFNIs also have an effect on the cancer cell immunogenicity, as both IFNα and β induce HLA upregulation. For instance, in polycythemia vera, a type of blood cancer, patients treated with the FDA approved IFN-alpha2, HLA I genes were upregulated in treated tumors (Skov et al., 2016), as well as in *in vitro* IFNβ-treated breast cancer cells (Wan et al., 2012).

Furthermore, IFNs also exert intrinsic antiproliferative/cytostatic and cytotoxic effects apparently unrelated to its effects on the immune system or the immunogenicity of cells. Even though these effects explain at least in part the antitumor effect of IFNγ and have been observed by many different researchers in diverse models, the mechanisms underlying them are still being elucidated and they seem to vary with the cellular context.

4.1.3.2. Cell-cycle arrest

IFNγ can induce an antitumoral effect by cell-cycle arrest, as it has been demonstrated in several experimental models. In a human fibrosarcoma cell line, it inhibited cyclin-dependent kinase 2 (CDK2; Bromberg et al., 1996). The mechanism behind was the upregulation of the CDK inhibitor p21 mediated by IRF-1 (Chin et al., 1996). Similarly, in a murine melanoma model, activated $CD8^+$

lymphocytes blocked tumor growth in part because they arrested cancer cells in the G1-phase of the cell cycle through the upregulation of the CDK-inhibitor p27 by the IFNγ secreted by the lymphocytes (Matsushita et al., 2015). Type I IFN also induces cell cycle arrest by CDK1 inhibition as demonstrated *in vitro* in neuroendocrine tumor cell lines (Rosewicz et al., 2004)

The arrest in the cell cycle induced by IFNγ, acting alone or in combination with TNFα, has been described to have the characteristics of cellular senescence in some preclinical models of pancreatic cancer and lymphomas, and in patient's melanoma metastases. It appears that this IFNγ-induced senescence is necessary to restrict the proliferation of cells that resist killing by immune cells (Brenner et al., 2020).

4.1.3.3. Apoptosis

Another effect by which IFNγ exerts its antitumor effect is by apoptosis induction, which has been shown in cells derived from different tumors, including melanoma (Gollob et al., 2005), glioblastoma (Zhang et al., 2007), breast cancer (Arenas et al., 2021), and colon adenocarcinoma (Xu et al., 1998). The mechanisms behind this pro-apoptotic effect are highly diverse, even though there is general coincidence on the central role of IRF-1 in the regulation of apoptosis, upregulating components of the intrinsic apoptotic pathway such as Bak (Kim et al., 2004) or downmodulation of antiapoptotic components like Bcl2A1 (Gollob et al., 2005). In addition, it upregulates components of the extrinsic apoptotic pathway such as the death receptor Fas and its ligand (Xu et al., 1998). Finally, IFNγ, through IRF-1, upregulates initiator (Casp 8,9); executioner (Casp 3,7) (Kim et al., 2004), and pyroptotic caspases (Casp 1,11; Xu, 1998). Type I IFNs also exhibit proapoptotic effects on cancer cells, as demonstrated in *in vitro* studies using IFNα (Scarzello et al., 2007) and IFNβ (Dedoni et al., 2010)

Furthermore, exposure to IFNγ can also trigger apoptosis in tumor cells through autophagy, activated by the production of mitochondrial reactive oxygen species via cytosolic phospholipase A2 (Wang et al., 2018). Additionally, $CD8^+$ T cells' IFNγ can suppress the expression of SLC3A2 and SLC7A11 in cancer cells, promoting tumor ferroptosis (Wang et al., 2019), a nonapoptotic cell death

characterized by the intrinsic impairment of antioxidant defenses (Dixon et al., 2012).

In addition to these direct effects on death receptors or components of the apoptotic machinery, IFNγ have been shown to induce apoptosis indirectly by suppressing the pro-survival signals conveyed by the PI3K pathway (Zhang et al., 2007). Thus, although there is a consensus on the pro-apoptotic effect of IFN on a wide variety of cells, the mechanisms behind seem to be multiple and highly dependent on the cellular context.

In summary, IFNγ effects on tumor cells is pleiotropic, and the mechanisms range from increased immunogenicity to cell-cycle arrest to induction of apoptotic and nonapoptotic cell deaths. In this thesis we identified the tumor intrinsic IFNγ response as a mechanism of resistance to immunotherapy, and therefore, this IFNγ role will be particularly described.

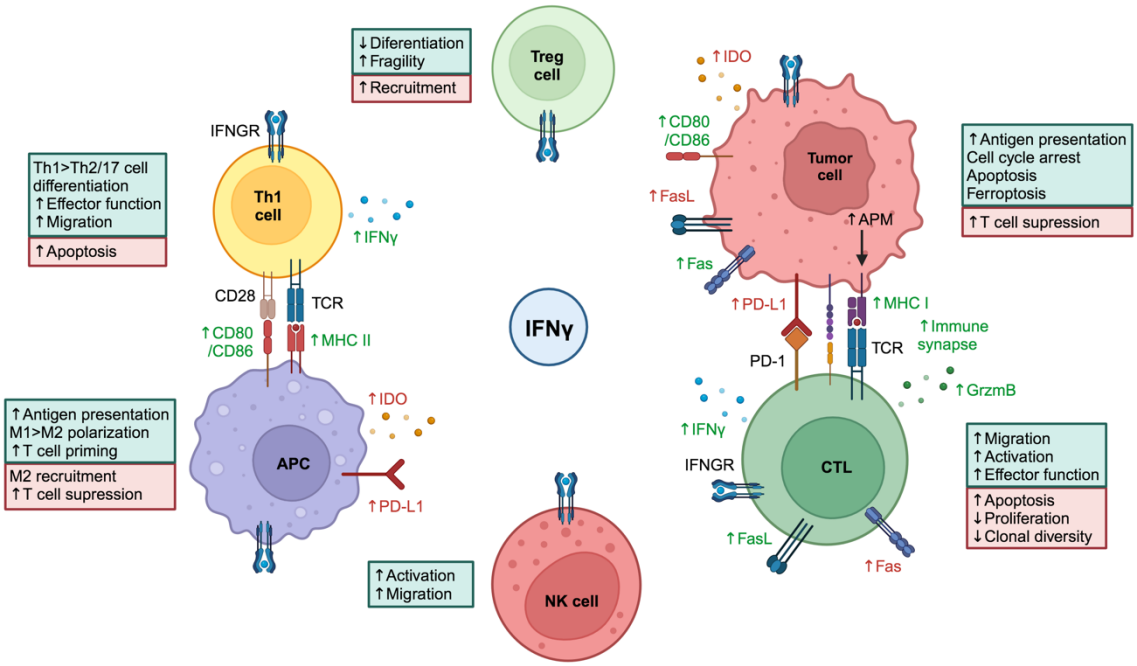

Figure 8: The central role of IFNγ in the TME and the cancer immunogenic response. IFNγ-induced signaling occurs in most cell types, including the ones present in the TME. I each cell type, IFNγ induce different effects, exerting pro and antitumoral effects. Additionally, IFNγ activates the production and release of certain cytokines and chemokines that can have an indirect effect. The biological consequences of these direct and indirect IFNγ-induced signaling in each cell type is summarized in the boxes. The IFNγ responses that make these cell types antitumoral are in green, whereas the responses that make them protumoral are in red. The molecule's word color also identifies them as anti- or protumoral. Adapted from (Gocher et al., 2022).

4.2. Role of tumor intrinsic IFNγ signaling in resistance to immune therapies

To the effects of IFNγ on the non-immune compartment described above, it has been recently acknowledged a key aspect for cancer treatment: the requirement of IFNγ signaling in cancer cells for the efficient killing by T cells targeting them. During the last decade, in contrast with other IFNs and together with supporting preclinical research, several studies have been conducted in clinical trials and patient samples concluding that the tumor intrinsic IFNγ response is crucial for the solid tumor response to immunotherapies.

Regarding antigen presentation dependent immunotherapies such as ICIs and TIL therapy, a remarkable research and advances has been done. Preclinical research studies have identified that IFNγ signaling inactivating mutations confer resistance to T cell–induced cell death in different experimental models resistant to immunotherapies, namely TCRt therapy and ICB (Sucker et al., 2017, Patel et al., 2017). Moreover, IFNGR1 knockout tumors exhibit resistance to anti-CTLA-4 treatment *in vivo* (Gao et al., 2016).

Supporting these preclinical observations, a transcriptomic analysis of baseline and on-therapy tumor biopsies from advanced melanomas treated with nivolumab (anti-PD-1), alone or plus ipilimumab (anti-CTLA-4), revealed an active IFNγ signaling signature, particularly genes involved in antigen processing, as a biomarker of clinical response (Grasso et al., 2020). That is, cancer cells with active IFNγ signaling are more likely to respond to the death mediated by T cells. Moreover, in a group of patients with metastatic melanoma treated with ipilimumab, copy number alterations in IFNγ pathway genes were observed in resistant tumors, namely copy loss of *IFNGR1* and *IFNGR2*, *JAK2* and *IRF1*, as well as amplifications of the negative regulators *SOCS1* and *PIAS4* (Gao et al., 2016). In the same direction, a non-responding epithelial cancer patient treated with TCRt was found to have copy number loss defects in *IFNGR1* and *2*, as well as *TAP1* and *TAP2* (Nagarsheth et al., 2021). Along the same line, melanomas that initially responded to PD-1 blockade (pembrolizumab) became resistant after acquiring genetic lesions that inactivated *JAK1* or *JAK2* (Zaretsky et al., 2016), and loss-of-function mutations in *JAK1/2* lead also to primary resistance to

pembrolizumab in another subset of melanoma patients (Shin et al., 2017). Considering the combined results of these studies, inactivation mutations in components of IFNγ signaling can be found more frequently in non-responders, and the most widespread mechanism of resistance seems to be the inactivation of *B2M*, tightly regulated by IFNγ, as seen in a study with three different cohorts of melanoma patients treated with different ICI, anti-PD-1, and anti-CTLA-4 therapies, respectively (Sade-Feldman et al., 2017).

Therefore, increasing IFNγ sensitivity in the tumor compartment could be a reasonable strategy to overcome cancer immunotherapy resistance. With this aim, researchers are on the search of ways to recover IFNγ functionality. CRISPR screenings aim to discover factors that confer resistance to immunotherapies, or at the same time, molecules that sensitize them. Several studies identified indirect regulators of the IFNγ signaling pathway. The knockout of the protein phosphatase PTPN2, negative regulator of the pathway, in principle a druggable protein, sensitized to anti-PD-1 therapy by enhancing the effect of IFNγ on antigen presentation and growth suppression (Manguso et al., 2017). In the same direction, the knockout of STUB1, an E3 ubiquitin ligase targeting the IFNGR1/JAK1 complex, sensitized to anti-PD-1 therapy and its protein levels correlated with IFNγ response in patient samples *in vivo* (Apriamashvili et al., 2022). Similarly, loss of the RNA-editing enzyme ADAR1 resensitizes cells that have become resistant to a-PD-1 because of impaired antigen presentation (Ishizuka et al., 2019).

It is important to note, however, that in contrast with the previous reports, some patients with tumors bearing inactivating mutations in the IFNγ pathway nonetheless respond to ICIs (Hellmann et al., 2018). An additional level of complexity that may reconcile these contradictory results arises from tumor heterogeneity. An analysis of single-cell RNA sequencing in lung cancer showed that genes encoding components of IFNγ signaling and ISGs, including MHC class II, were heterogeneously expressed (Ma et al., 2019). Thus, under the pressure exerted by immune therapies, tumor cells with low ability to transduce the signal conveyed by IFNγ are expected to be rapidly selected.

Finally, some reports point out that long-term exposure of cancer cells to IFNγ may increase the expression of ligands of multiple inhibitory receptors that block the antitumor effect of T cells, indicating that long-term blockade of IFNγ signaling in cancer cells may improve the destruction of cancer cells by the immune system (Benci et al., 2016). On the same direction, IFNγ signaling has been described to enhance stemness in tumor cells, increasing metastatic capacity and therapy resistance (Beziaud et al., 2023). Thus, according to these reports, IFNγ has a dual anti-tumorigenic and pro-tumorigenic role that needs to be further studied.

Collectively, these evidences indicate that the upregulation of antigen processing induced by IFNγ is critical for the recognition and subsequent activation of T cells directed against tumor specific or associated antigens. One line of resistance deployed by cancer cells is the upregulation of inhibitory factors such as PD-L1, and additional inhibitory factors, which bind to their cognate receptor in T cells inhibiting those that recognize tumor antigens via their TCR. Once these mechanisms of resistance have been disabled by treatment with blocking antibodies, cancer cells use additional lines of resistance, such as the downmodulation of IFNγ signaling that, in turn, downmodulates antigen presentation and, thus, the recognition of cancer cells by T cells via the TCR.

Regarding the role of tumor intrinsic IFNγ signaling pathway in T cell redirection therapies, namely TCBs and CARs, although less studies have been conducted, recent preclinical reports show that impairment of IFNγ signaling also confers resistance to these therapies in different types of solid tumors. Liu and colleagues performed a CRISPR screening in several solid tumor sensitive cell lines to different TCBs, and found out that the knockout of JAK1 was the main driver of resistance to this therapy (Liu et al., 2021). On the same line, in this thesis we demonstrate that a frequent mechanism of acquired resistance to TCB therapy is the downmodulation of the tumor intrinsic IFNγ pathway driven by JAK2 downmodulation (Arenas et al., 2021, Martinez-Sabadell et al., 2022). However, even though the apoptosis can be the plausible mechanism of action of IFNγ, (Liu et al., 2021, Arenas et al., 2021), the precise mechanism by which it is required for the therapy response remains to be elucidated. The recent study led by Dr. Maus shows that in solid cancer, in this case for CAR T treatment, tumor IFNγ response is necessary to express ICAM-1 in order to elicit a correct immune

synapse and therefore, response to therapy (Larson et al., 2022). Therefore, because TCBs or CARs act independently of antigen presentation, these results highlight the importance of the IFNγ response in the death induced by T cells and in an efficient immune synapse formation.

In summary, evidence shows that IFNγ signaling in cancer cells is pivotal for the efficient antitumor effect of T cells and the response to immunotherapies. Under this pressure, malignant cells tend to disrupt IFNγ signaling, which leads to reduced sensitivity to killing by lymphocytes by different mechanisms.

In this thesis, we found two distinct mechanisms of acquired resistance to T cell redirection therapies. We demonstrate the key role of tumor intrinsic IFNγ signaling in the immunotherapy response, as well as the antigen downmodulation as a mechanism to evade antitumor immune response. Additionally, we identified new vulnerabilities that open the avenue for strategies to overcome this resistant phenotype.

HYPOTHESIS AND OBJECTIVES

Hypothesis

Immunotherapy has raised high expectations in the treatment of cancer, but despite remarkable effects, patients eventually progress due to the emergence of resistance, particularly in solid tumors. Therefore, there is a clinical need to identify the mechanisms by which tumors relapse in order to develop new therapeutic strategies to overcome the resistance. Based on the need to identify the reasons behind tumor unresponsiveness, we hypothesized that, by generating acquired resistance models and deciphering their mechanisms, we would unveil new insights into the understanding of immunotherapy resistance, leading to the identification of potential vulnerabilities to overcome it.

Objectives

1. Identification of unknown acquired mechanisms of resistance to T cell redirection immunotherapies in solid tumors.

2. Validation of IFNγ tumor intrinsic response as a mechanism of acquired resistance to immunotherapy in solid tumors.

3. Validation of JAK2 downmodulation as the driver of resistance to T cell redirection immunotherapies.

4. To demonstrate that the target antigen determines the mechanism of resistance to T cell redirection therapies in solid tumors.

5. Identification and validation of antigen downmodulation as a frequent mechanism of resistance in CEACAM5 redirected immunotherapies.

6. Identification and validation of vulnerabilities that overcome a deficient IFNγ response and cancer immunotherapy in solid tumors.

RESULTS

1. Acquired cancer cell resistance to T cell bispecific antibodies and CAR T targeting HER2 through JAK2 down-modulation

nature COMMUNICATIONS

ARTICLE

https://doi.org/10.1038/s41467-021-21445-4 OPEN

Acquired cancer cell resistance to T cell bispecific antibodies and CAR T targeting HER2 through JAK2 down-modulation

Enrique J. Arenas[1,2,8], Alex Martínez-Sabadell[1,8], Irene Rius Ruiz[1,2], Macarena Román Alonso[1], Marta Escorihuela[1], Antonio Luque[1], Carlos Alberto Fajardo[3], Alena Gros[3], Christian Klein[4] & Joaquín Arribas[1,2,5,6,7]✉

Immunotherapy has raised high expectations in the treatment of virtually every cancer. Many current efforts are focused on ensuring the efficient delivery of active cytotoxic cells to tumors. It is assumed that, once these active cytotoxic cells are correctly engaged to cancer cells, they will unfailingly eliminate the latter, provided that inhibitory factors are in check. T cell bispecific antibodies (TCBs) and chimeric antigen receptors (CARs) offer an opportunity to test this assumption. Using TCB and CARs directed against HER2, here we show that disruption of interferon-gamma signaling confers resistance to killing by active T lymphocytes. The kinase JAK2, which transduces the signal initiated by interferon-gamma, is a component repeatedly disrupted in several independently generated resistant models. Our results unveil a seemingly widespread strategy used by cancer cells to resist clearance by redirected lymphocytes. In addition, they open the possibility that long-term inhibition of interferon-gamma signaling may impair the elimination phase of immunoediting and, thus, promote tumor progression.

[1] Preclinical Research Program, Vall d'Hebron Institute of Oncology (VHIO), Vall d'Hebron Barcelona Hospital Campus, Barcelona 08035, Spain. [2] Centro de Investigación Biomédica en Red de Cáncer (CIBERONC), Madrid 28029, Spain. [3] Tumor Immunology & Immunotherapy Group, VHIO, Vall d'Hebron Barcelona Hospital Campus, Barcelona 08035, Spain. [4] Roche Innovation Center Zurich, Roche Pharmaceutical Research and Early Development, Schlieren 8952, Switzerland. [5] Department of Biochemistry and Molecular Biology, Universitat Autónoma de Barcelona (UAB), Bellaterra 08193, Spain. [6] Cancer Research Program, IMIM (Hospital del Mar Medical Research Institute), Barcelona 08003, Spain. [7] Institució Catalana de Recerca i Estudis Avançats (ICREA), Barcelona 08010, Spain. [8] These authors contributed equally: Enrique J. Arenas, Alex Martínez-Sabadell. ✉email: jarribas@vhio.net

T cell-engaging therapies, such as T cell bispecific antibodies (TCBs)—which are functionally similar but structurally different to bispecific T cell engagers, BiTEs—or chimeric antigen receptors (CARs), are raising extraordinary expectations as future treatments for virtually all cancers (for recent reviews on the subject, see refs. [1–11]). Encouraging these expectations, TCBs and CARs have been recently approved to treat some hematologic malignancies[12–14]. In contrast, TCBs and CARs against solid tumors tested to date have failed to show clinical efficacy. This failure prompted intense research and the subsequent identification of mechanisms of primary and acquired resistance, including: (i) defective tumor infiltration of redirected lymphocytes, (ii) immunosuppressive tumor environments, (iii) downmodulation of the antigen against which TCB or CAR are directed and, (iv) upregulation of immune checkpoints (see, the aforementioned reviews). Different strategies are being implemented to overcome these mechanisms of resistance (reviewed in ref. [15]).

All these mechanisms of resistance impinge on the ability of T cells to reach cancer cells and/or on the inhibition of T cells. However, little is known about putative intrinsic mechanisms of resistance of cancer cells. That is, mechanisms deployed by tumor cells to resist killing by fully active and correctly engaged T cells. TCBs and CARs targeting the cell surface receptor HER2 are a useful tool to identify such mechanisms.

HER2 is a tyrosine kinase and, when overexpressed, a driver for breast and gastric cancers[16]. The downregulation of overexpressed HER2 may lead to tumor regression[17]. Thus, in principle, HER2-driven cancer cells are not likely to downmodulate the expression of HER2 to escape TCBs or CARs, making them a suitable experimental system to unveil mechanisms of intrinsic resistance to these therapies.

Using HER2-driven cell lines and patient derived xenografts (PDXs), and a TCB and CAR targeting HER2, here we describe experiments that unveil a mechanism of resistance to redirected T cells. This mechanism should be taken into consideration when designing strategies to increase the efficacy of cancer immunotherapies.

Results

Model of resistance to cell killing by redirected lymphocytes. The structure of the HER2-TCB used in this study has been previously described[18] (see also Supplementary Fig. 1a). Addition of picomolar concentrations of this HER2-TCB to cocultures of peripheral blood mononuclear cells (PBMCs) and the HER2-overexpressing BT474 cells led to the killing of the latter (Supplementary Fig. 1b). It should be noted that the IC50 of HER2-TCB for a given ratio PBMC:BT474 varied depending on the donor of PBMCs. Similar differences have been previously observed[18], and are likely due to alloreactions of different intensities, which parallel different degrees of HLA mismatch, as well as T cell fitness that may depend on the donor. For the 1:1 ratio chosen for subsequent experiments, the IC50 of HER2-TCB varied from ~40 to ~220 pM.

To generate a model of intrinsic resistance to TCB-mediated cell killing, we treated PBMC:BT474 cocultures with HER2-TCB, allowed the cells to recover, and repeated the treatment with a fresh batch of PBMCs and HER2-TCB (Fig. 1a). At every round, we controlled that the alloreaction of PBMCs on target cells was low enough to allow the specific activity of the HER2-TCB. After 6 months, the resulting cells, BT-R, showed an IC50 for the HER2-TCB approximately tenfold higher than that of parental cells (156 pM vs. >1 nM) (Fig. 1b). Resistance was also observed in three dimensional cultures (Supplementary Fig. 1c) and in vivo (Fig. 1c, d). BT-R cells were also resistant to a trastuzumab-based second generation HER2-CAR (described in Supplementary Fig. 1a), in vitro and in vivo (Fig. 1e–h).

As expected, resistance was not due to the downregulation of HER2, as measured by Western blot or flow cytometry (Fig. 1i and Supplementary Fig. 1d). Further, the binding of HER2-TCB to parental and resistant cells was indistinguishable (Fig. 1j).

The sensitivity of resistant cells to different chemotherapeutic agents or to T-DM1, an antibody drug conjugate against HER2, was similar to that of parental BT474 cells (Supplementary Fig. 1e). Thus, BT-R cells are specifically resistant to killing by redirected lymphocytes.

We reasoned that resistance could arise by inhibition of T cells or, alternatively, by intrinsic resistance of target cells. Regarding the first possibility, analysis of a panel of immune checkpoint inhibitors and co-stimulators[19,20], showed no differences between parental and resistant cells, except the downmodulation of B7-H4 (Fig. 1k); however, since this is an inhibitory molecule[21], its downmodulation is not likely a cause of resistance. An array of 80 cytokines, including immunosuppressive cytokines such as TGFβ or IL10, revealed no major differences between cocultures containing parental or resistant cells. The only factor differentially secreted in cocultures with resistant cells was TIMP2 (Fig. 1l and Supplementary Fig. 2a). Quantification of TIMP2 levels confirmed that it is upregulated in BT-R cells (Supplementary Fig. 2b). To functionally characterize this observation, we downregulated the expression of *TIMP2* by means of two specific short hairpin RNAs (shRNAs). The resulting cells, which expressed similar levels of *TIMP2* to those of parental BT474 cells (Supplementary Fig. 2c), showed resistance to HER2-TCB similar to BT-R cells (Supplementary Fig. 2d). Thus, we concluded that the overexpression of TIMP2 by BT-R cells is unrelated to resistance.

Treatment of cocultures of PBMCs and parental BT474 cells with HER2-TCB augmented the secretion of several cytokines characteristic of lymphocyte activation, such as TNF-α, Interferon-gamma (IFN-γ), IL13, or IL5. Supporting that lymphocyte activation is unaffected by resistant cells, the secretion of theses cytokines was similar in assays including BT474 or BT-R cells (Supplementary Fig. 2e). Analysis of PBMC proliferation, or of different makers of activity, namely, CD69 and granzyme B, confirmed that activation of lymphocytes was unaffected in assays with resistant cells (Supplementary Fig. 2f, g). We concluded that lymphocytes are equally activated by resistant cells. Thus, we focused on possible mechanisms of intrinsic resistance of target cells.

Transcriptomic analysis. Analysis by RNA-seq showed that 97 genes were acutely upregulated or downregulated in BT-R cells compared to parental BT474 cells (≥4-fold; $p < 10^{-5}$) (Fig. 2a). Gene set enrichment analysis (GSEA) identified different biological processes that differed between parental and resistant cells (Fig. 2b). We focused in the IFN-γ response (Fig. 2c), because it has been shown that it affects the antitumor response at multiple levels[22]. Analysis of the protein encoded by *IRF1*, a gene specifically regulated by IFN-γ signaling[23], confirmed that this pathway is impaired in resistant cells (Fig. 2d).

IFN-γ signaling is required for efficient killing by redirected lymphocytes. To determine whether the downmodulation of IFN-γ signaling was related to resistance, first we used a blocking antibody. The anti-IFN-γ efficiently impaired killing of parental BT474 cells mediated by the HER2-TCB, in 2D or 3D cultures (Fig. 3a). Similarly, blocking IFN-γ prevented killing of target cells by HER2-CAR T cells (Fig. 3b).

IFN-γ acts on cytotoxic lymphocytes as well as on tumor cells. Maximal cytotoxic activity of T cells requires IFN-γ. On the other hand, IFN-γ impairs the proliferation of tumor cells by inhibiting their progression through the cell cycle and promoting their

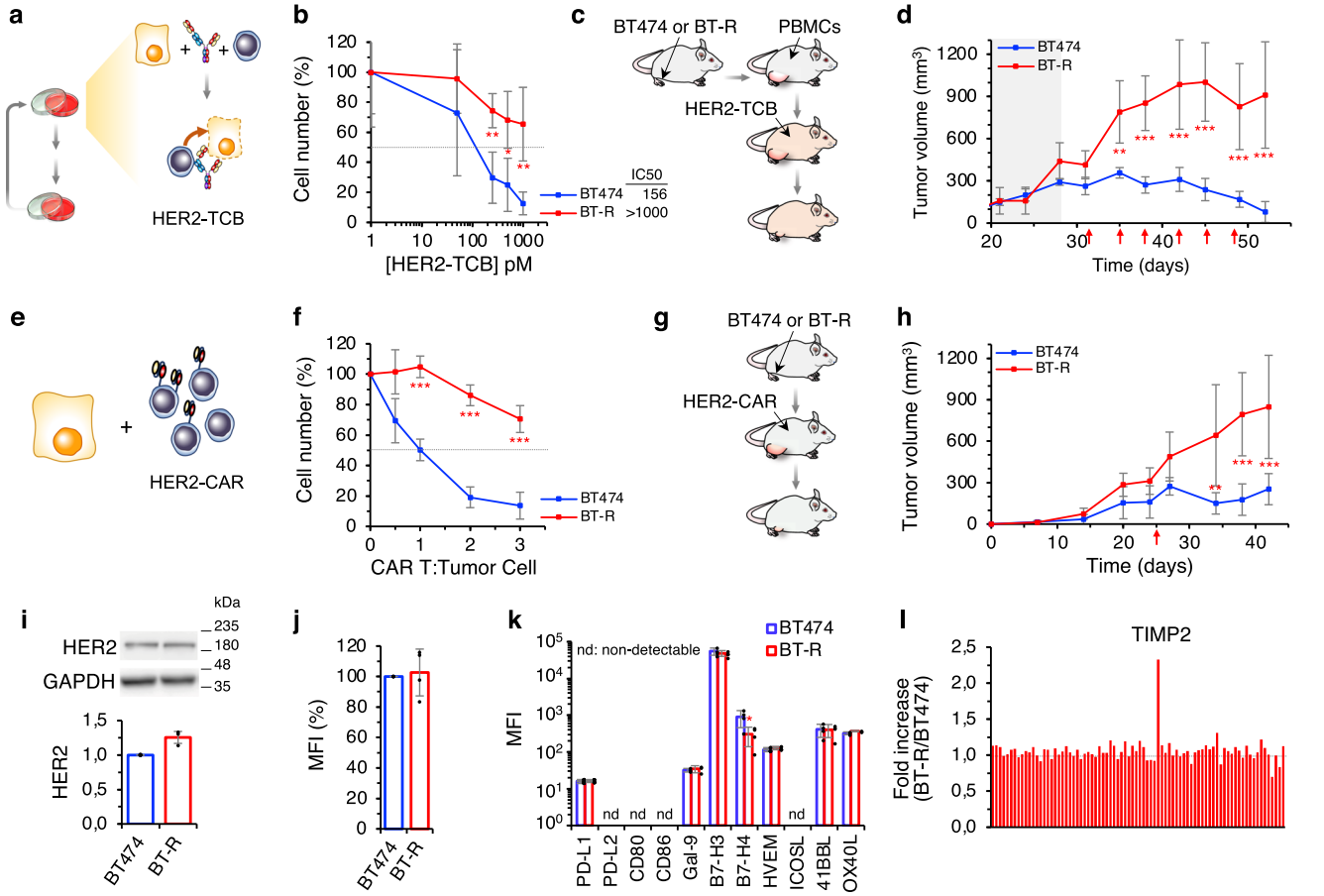

Fig. 1 Generation and characterization of resistant cells. a Schematic showing the assay of HER2-TCB in cocultures. **b** Cocultures of PBMCs with parental BT474 or resistant BT-R cells were treated with different concentrations of HER2-TCB (PBMC:target cell ratio 1:1) for 72 h. Then, viable cells were quantified by flow cytometry using EpCAM as a marker. **c** Schematic showing in vivo treatment with HER2-TCB. Totally, 10^7 BT474 or BT-R cells were injected orthotopically into NSG mice. When tumors reached ~200 mm^3 (dark background), 10^7 PBMCs were injected i.p. Then animals were treated i.v. with 0.125 mg/kg HER2-TCB as indicated (red arrows). **d** Tumor volumes are represented as averages ± SD (standard deviation) ($n = 4$ per arm). **e** Schematic showing the HER2-CAR assay. **f** Parental BT474 cells or resistant BT-R cells were cocultured with different ratios of CAR T cells for 48 h. Cell numbers were calculated and expressed as in (**b**). **g** Schematic showing in vivo treatment with HER2-CAR T cells. Mice were injected with BT474 or BT-R cells as in (**c**). When tumors reached ~200 mm^3, 3×10^6 HER2-CAR T-positive cells were injected i.p. **h** Tumor volumes are represented as averages ± SD (BT474, $n = 6$; BT-R, $n = 8$). **i** Levels of HER2, normalized to BT474 cells, were determined by Western Blot. **j** Cells were stained with HER2-TCB and analyzed by flow cytometry. Results were normalized to BT474 cells. **k** Cells were stained with antibodies against the indicated factors. Results are presented as the MFI of staining in BT474 and BT-R cells. **l**, Levels of 80 cytokines and growth factors were measured using a commercial array in the media conditioned by cocultures of BT474 cells and PBMCs or BT-R cells and PBMCs treated with HER2-TCB. Results are presented as the fold change of BT-R relative to BT474 cells. **b** $^{**}p = 0.005$, $^{*}p = 0.02$, $^{**}p = 0.006$. **f** $^{***}p < 0.001$. **k** $^{*}p = 0.04$, two-tailed t test. **d**, **h** $^{**}p < 0.01$, $^{***}p < 0.001$, two-way analysis of variance (ANOVA) and Bonferroni correction. Data are presented as mean ± SD of four (**b**, **f**, **j**, **k**), or three (**i**) independent experiments. Source data are provided as a Source Data file.

apoptotic death (reviewed in ref. [22]). Thus, the blocking antibody could prevent the killing of target cells by impairing the activation of cytotoxic lymphocytes, blocking the action of IFN-γ on target cells, or a combination of both effects.

To directly test the effect on target cells, we treated BT474 cells with IFN-γ. As shown in Fig. 3c, IFN-γ induced the death of BT474 cells by inducing apoptosis, as shown in the increase of annexin V^+ cells (Fig. 3d). In contrast, resistant cells were unaffected by the same treatment. This result shows that IFN-γ is likely part of the mechanism used by cytotoxic cells to kill target cells, and indicates that BT-R cells became resistant by impairing IFN-γ signaling.

To confirm this hypothesis, we impaired IFN-γ signaling in target cells, by knocking-out the IFNGR1 gene through CRISPR–Cas9 technology, or by downmodulating the expression of IFNGR1 with shRNAs from parental BT474 cells (Fig. 3e). As expected, both methods impaired IFN-γ signaling (Supplementary Fig. 3a, b), and prevented the killing induced by IFN-γ (Fig. 3f). Irrespectively of the method, diminishing the expression of IFNGR1 resulted in resistance to HER2-TCB in coculture assays (Fig. 3g). Consistent results were obtained when we examined the sensitivity to HER2-CAR T cells (Fig. 3h). To validate the results obtained in vitro, we showed that the knock-out of IFNGR1 caused resistance to the HER2-TCB also in vivo (Fig. 3i). The knockdowns of JAK1 or STAT1 from parental BT474 cells also resulted in resistance to the HER2-TCB (Supplementary Fig. 3c, d). Thus, disrupting IFN-γ signaling by different means induces resistance to redirected lymphocytes.

The effects of the IFN-γ-blocking antibodies or of the knock-down of IFNGR1 were not a particularity of BT474 cells, similar effects were observed when assaying different HER2-positive cultures from breast cancer PDXs and an additional cell line (Supplementary Fig. 4a–i). Furthermore, impairment of IFN-γ

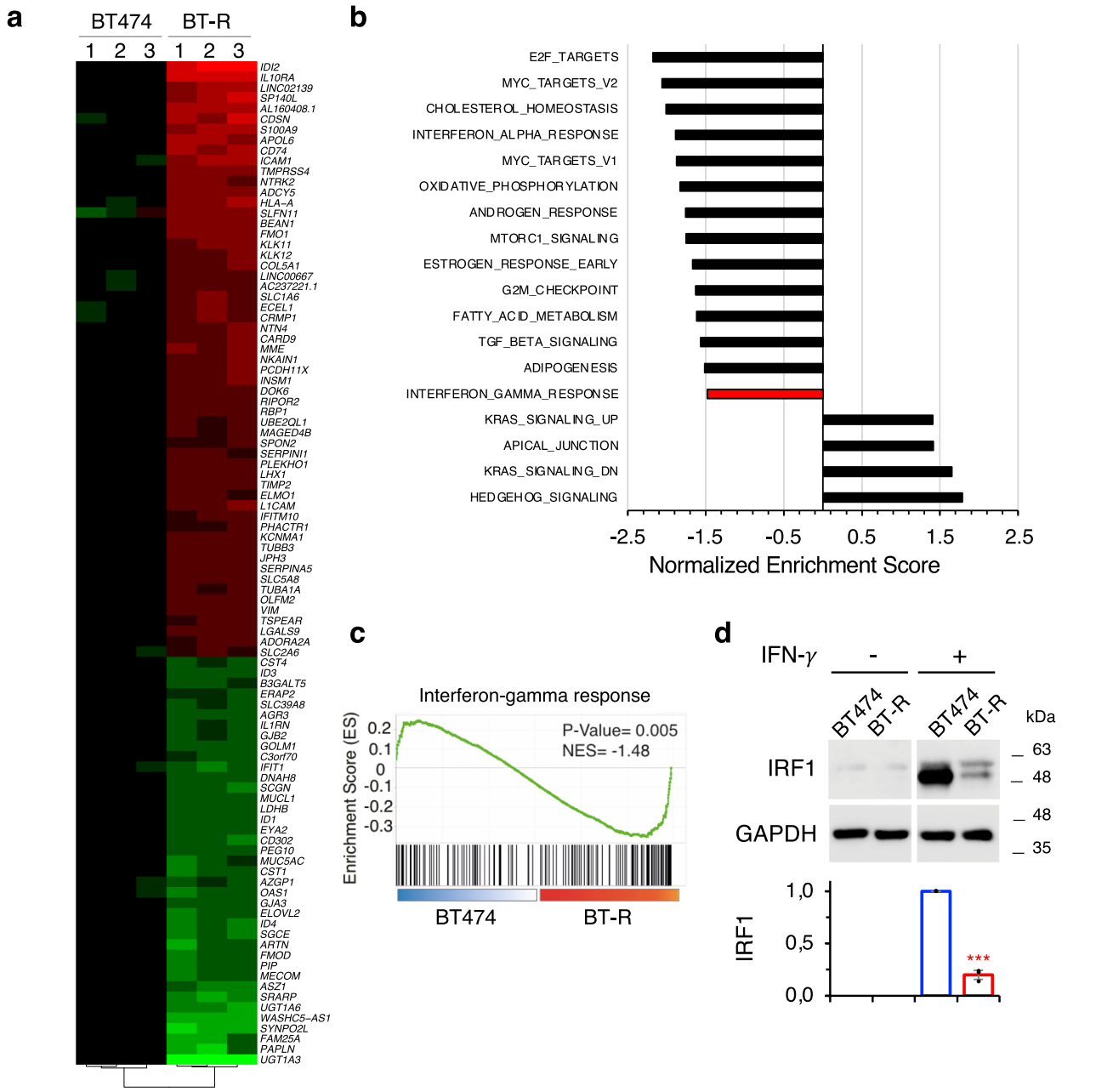

Fig. 2 Transcriptomic analysis. a Heatmap showing the 97 most differentially expressed genes in BT-R cells compared to parental BT474 cells (≥4-fold; $p < 10^{-5}$). *p* Value was obtained from the DESeq2 analysis of the RNA-seq. Genes with FDR < 5% and |shrunken fold change| > 1.5 were considered significant. **b** Pathways showing positive and negative enrichment in BT-R compared with BT474 cells as determined by GSEA. Only statistical gene sets are shown (NOM *p* value < 0.05). **c** IFN-γ response GSEA signature in resistant cells, compared to parental BT474. *p* Value corresponds to the NOM *p* value obtained by GSEA in the HALLMARK database. **d** Levels of IRF1 upon treatment with IFN-γ in BT474 and BT-R cells were determined by Western blot analysis. Results of three independent quantifications, normalized to treated BT474 cells, are presented as mean ± SD. ***$p < 0.001$, two-tailed *t* test. Source data are provided as a Source Data file.

signaling by knocking down IFNGR1, led to resistance to HER2-TCB in cell lines from HER2-positive ovarian and lung cancers (Supplementary Fig. 4j, k).

Components of the IFN-γ signaling pathway in resistant cells. The intracellular signaling pathway activated by IFN-γ is relatively simple. Dimeric IFN-γ triggers the formation of a complex of four receptor molecules (two IFNGR1 and two IFNGR2), four JAK kinases (two JAK1s and two JAK2s) and two molecules of the STAT1 transcription factor. The subsequent phosphorylation of the STAT1s by the JAKs leads to the dimerization and transport to the nucleus of the former, where dimeric pSTAT1 regulates the expression of different genes, including IRF1[22] (Fig. 4a). Analysis of these components in our coculture assays revealed little or no difference in the secretion of IFN-γ or in the expression of IFNGR1 and 2, JAK1 or STAT1 by resistant cells (Fig. 4b–e). In contrast, we observed a marked reduction of JAK2 expression (Fig. 4f), indicating that downmodulation of JAK2 could result in the impairment of IFN-γ signaling. Consistently with this hypothesis, pSTAT1 levels were significantly decreased in resistant cells when treated with IFN-γ (Fig. 4g).

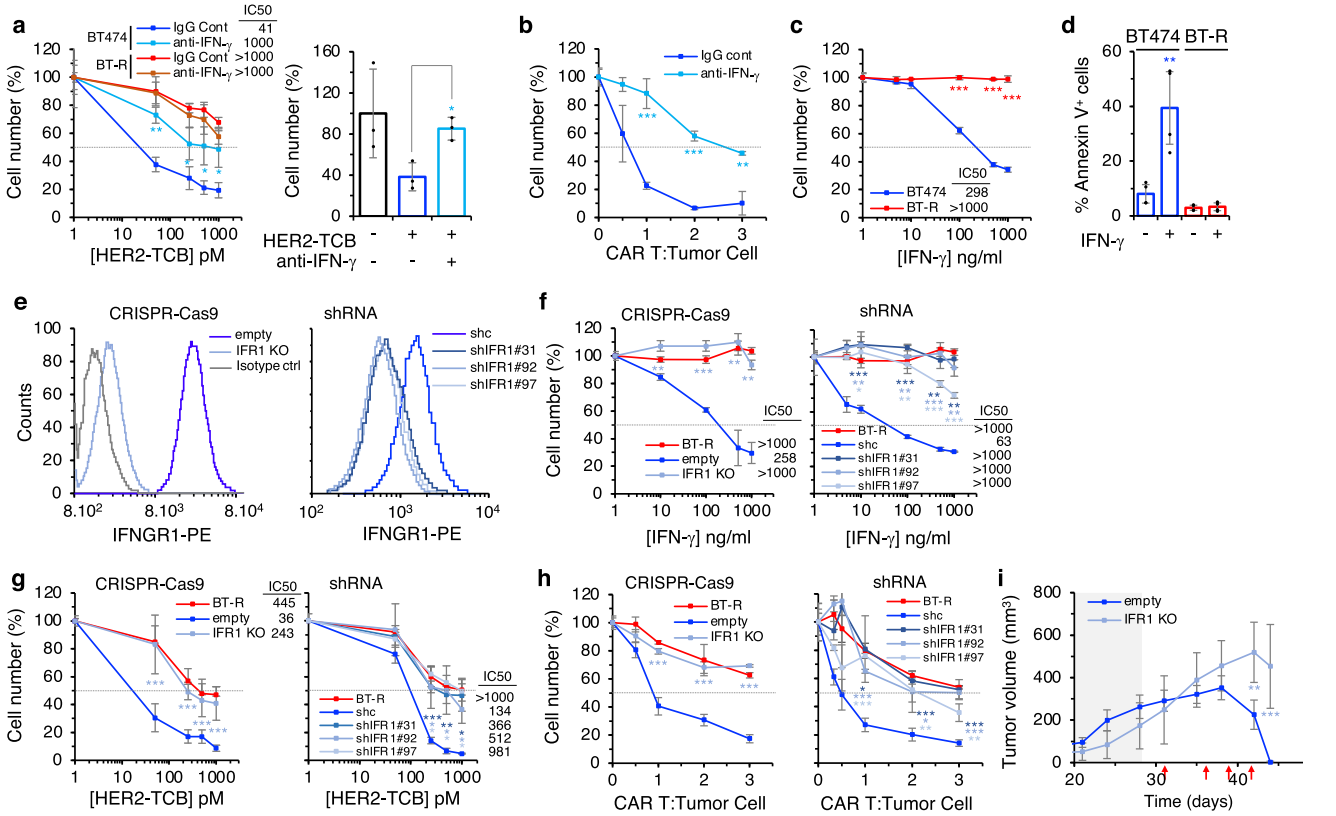

Fig. 3 IFN-γ response is required for efficient killing by redirected lymphocytes. a Left, cocultures of PBMCs with BT474 or BT-R cells were treated with different concentrations of HER2-TCB in presence of an IgG control or an IFN-γ blocking antibody for 72 h. Then, viable cells were quantified by flow cytometry using EpCAM as a marker. Right, BT474 cells were grown in 3D and treated with HER2-TCB in presence of an IgG control (−) or an IFN-γ blocking antibody (+) for 72 h. Viable BT474 cells were quantified by flow cytometry using EpCAM as a marker. Results were normalized to untreated cells. **b** Parental BT474 cells were cocultured with different ratios of CAR T cells for 48 h in the presence of an IgG control or an IFN-γ blocking antibody. Then, cell numbers were calculated and expressed as in (**a**). **c** Parental BT474 or resistant BT-R cells were treated with different concentrations of IFN-γ for 5 days. Cell numbers were estimated with the crystal violet staining assay. **d** Parental BT474 or resistant BT-R cells were treated with 1 μg/ml of IFN-γ and the percentages of apoptotic cells were determined by means of Annexin V^+ cells measured by flow cytometry. **e** Cells were stained with anti-IFNGR1 or isotype antibody and analyzed by flow cytometry. IFR1 stands for IFNGR1. **f** Sensitivity of the indicated cells to IFN-γ was analyzed as in (**c**). **g** The indicated cells were treated with different concentrations of HER2-TCB and analyzed as in (**a**). **h** The indicated cell lines were cocultured with CAR Ts and analyzed as in (**b**). **i** Totally, 6.5×10^7 BT474 cells or the same cells knock-out for IFNGR1 were injected orthotopically into NSG mice. Mice were treated as described in Fig. 1c. Tumor volumes are represented as averages ± SD (empty, $n = 8$; IFR1 KO, $n = 4$). **a** Left, $^{**}p = 0.001$, $^{*}p = 0.05$; right, $^{*}p = 0.01$. **b** $^{***}p < 0.001$, $^{**}p = 0.002$. **c** $^{***}p < 0.001$. **d** $^{**}p = 0.007$. **f** Left, $^{**}p = 0.002$, $^{***}p < 0.001$, $^{**}p = 0.003$, $^{**}p = 0.0013$; right, $^{***}p < 0.001$, $^{**}p = 0.002$ (shIFNGR1 #31); $^{**}p = 0.009$, $^{**}p = 0.006$, $^{***}p < 0.001$, $^{**}p = 0.003$ (shIFNGR1 #92); $^{*}p = 0.02$, $^{**}p = 0.004$, $^{***}p < 0.001$ (shIFNGR1 #97). **g** Left, $^{***}p < 0.001$; right, $^{***}p < 0.001$, $^{**}p = 0.004$, $^{*}p = 0.02$ (shIFNGR1 #31); $^{*}p = 0.046$, $^{*}p = 0.047$, $^{*}p = 0.03$ (shIFNGR1 #92); $^{*}p = 0.05$, $^{*}p = 0.02$, $^{*}p = 0.02$ (shIFNGR1 #97). **h** Left, $^{***}p < 0.001$; right $^{*}p = 0.02$, $^{***}p < 0.001$ (shIFNGR1 #31); $^{***}p < 0.001$, $^{*}p = 0.02$ (shIFNGR1 #92); $^{***}p < 0.001$, $^{**}p = 0.005$, $^{**}p = 0.005$ (shIFNGR1 #97). Two-tailed *t* test. **i** $^{**}p < 0.01$, $^{***}p < 0.001$, two-way ANOVA and Bonferroni correction. Data are presented as mean ± SD of three (**a**–**c**, **f**, **g** right, **h**), four (**d**), or six (**g** left) independent experiments. Source data are provided as a Source Data file.

Resistant cells cultured for up to three months in the absence of any selective pressure showed resistance similar to that of BT-R cells (Supplementary Fig. 5a) and similar levels of JAK2 (Supplementary Fig. 5b). Therefore, resistance is stable and does not require selective pressure. We hypothesized that this stable downmodulation of JAK2 and, thus, resistance could be maintained epigenetically. To test this hypothesis, we treated BT-R cells with different well-characterized drugs that interfere with epigenetic modifications, including the DNA demethylating agent 5-AZA, the histone demethylating agent DZNEP, and the pan-HDAC inhibitor Trichostatin A (TSA). While demethylating agents did not affect *JAK2* transcription, the HDAC inhibitor upregulated *JAK2* expression in BT-R cells (Fig. 4h), indicating that de-acetylation of histone H3 may contribute to the silencing of *JAK2*. Direct analysis of H3K27Me3 and H3K27Ac marks showed reduced levels of the latter in the *JAK2* promoter of BT-R cells (Fig. 4i), confirming that histone acetylation may regulate JAK2 expression. Among the different acetylation marks, H3K27Ac is considered one of the best markers of active promoters and enhancers and it is tightly associated to gene expression[24]. Thus, we concluded that JAK2 is likely down-regulated epigenetically in BT-R cells.

The downmodulation of JAK2 causes resistance to redirected lymphocytes. To establish the functional relevance of the downmodulation observed, we transduced resistant cells with a vector encoding JAK2 (Fig. 5a). As expected, overexpression of JAK2 restored IFN-γ signaling (Supplementary Fig. 5c). Of note, overexpression of JAK2 resulted in re-sensitization to killing by T cells redirected via TCB or CAR and in the re-sensitization to the death induced by IFN-γ (Fig. 5b–d). Confirming the relevance of these in vitro results, overexpression of JAK2 restored sensitivity to the TCB in vivo (Fig. 5e).

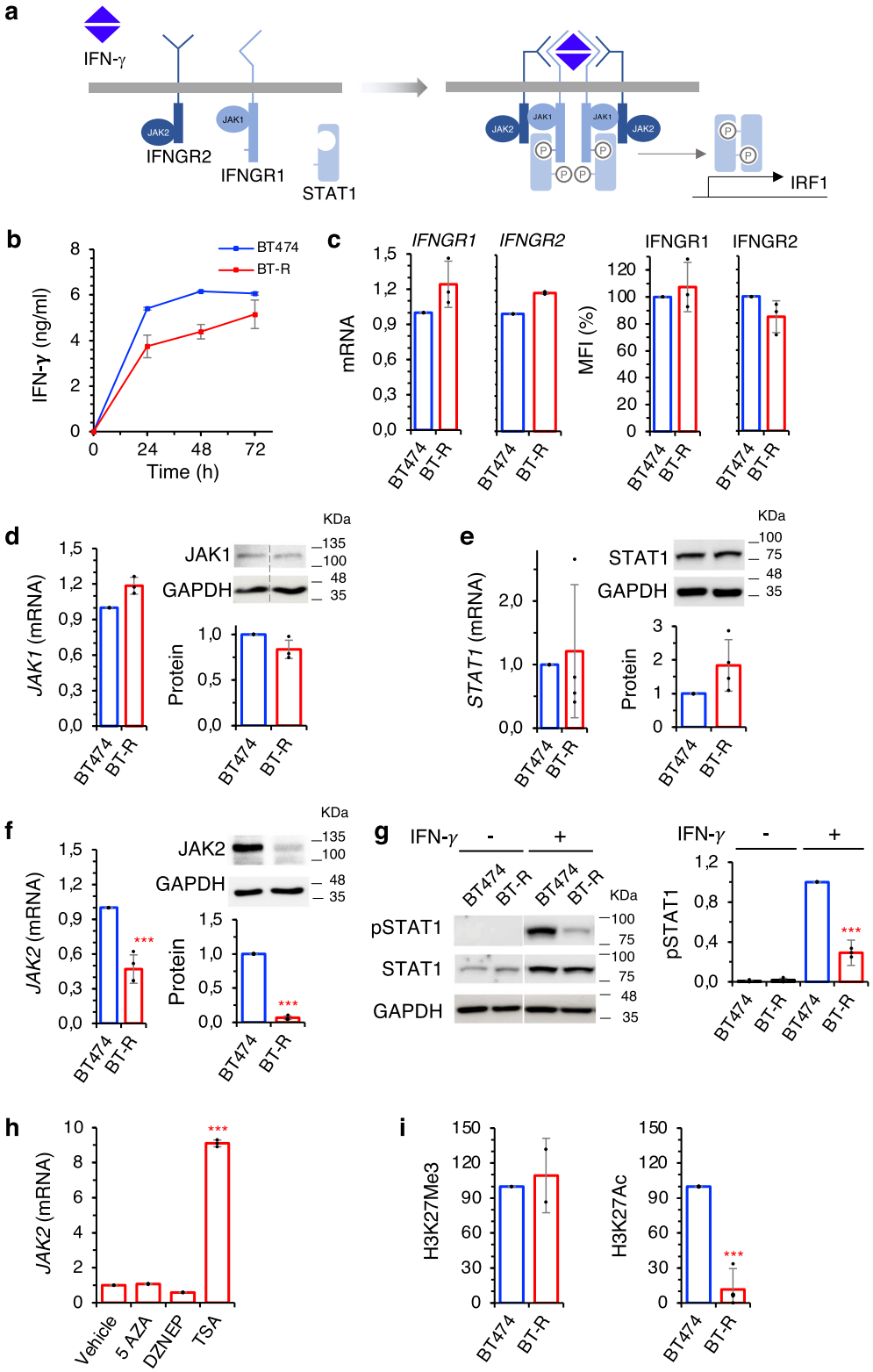

Fig. 4 Components of the IFN-γ signaling pathway in resistant cells. a Schematic showing the IFN-γ signaling pathway. **b** The levels of IFN-γ in the media conditioned by cocultures with BT474 or resistant BT-R in the presence of HER2-TCB was determined by ELISA. **c** The levels of Interferon-gamma receptors 1 and 2, normalized to BT474, were determined by quantitative real-time PCR (left) or flow cytometry with specific antibodies (right). **d**–**f** Levels of JAK1, STAT1, and JAK2 (mRNA and protein), normalized to BT474, as determined by quantitative real-time PCR (left) or Western blot (right). **g** Levels of phosphoSTAT1 in parental and resistant cells were determined by Western Blot. Results were normalized to treated BT474 cells. **h** BT-R cells were treated with indicated compounds for 48 h. Then, the levels of the mRNA encoding *JAK2* were determined by RT-PCR and normalized to the levels in cells treated with vehicle. **i** Levels of H3K27Me3 and H3K27Ac histone marks in the promoter of *JAK2* in BT474 and BT-R cells as measured by ChIP followed by quantitative real-time PCR. Results were normalized to the levels of an IgG control antibody in each sample, and then normalized to the levels in BT474 cells. ***$p < 0.001$, two-tailed *t* test. Data are presented as mean ± SD of two (**b**, **i** left), three (**c**, **d**, **h**, **i** right) or four (**e**–**g**) independent experiments. Source data are provided as a Source Data file.

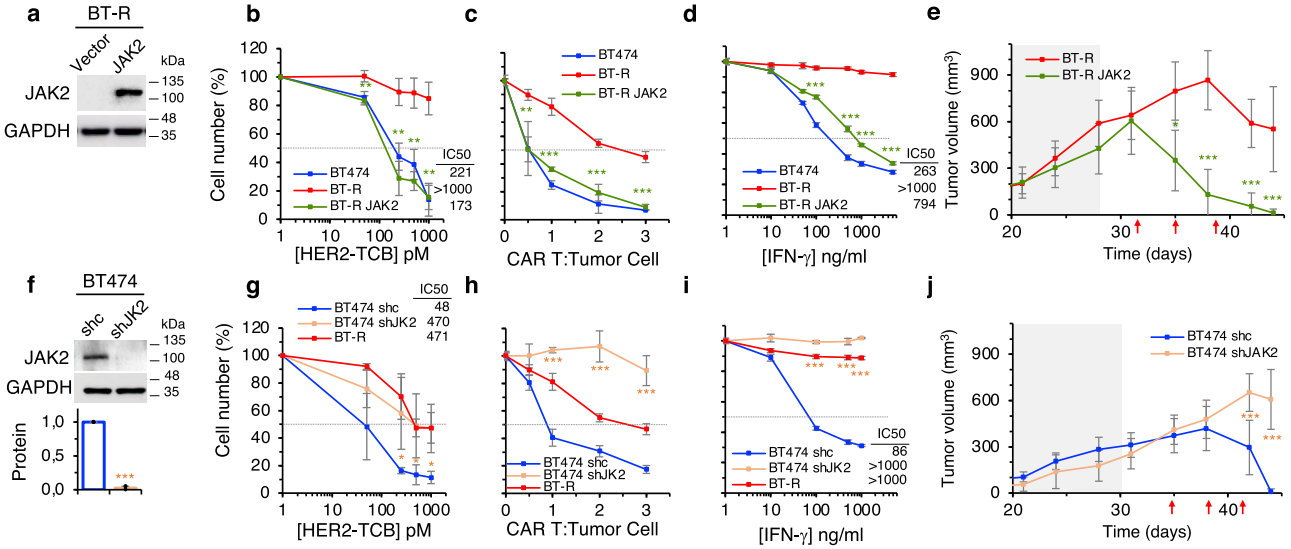

Fig. 5 The downmodulation of JAK2 causes resistance to redirected lymphocytes. a Levels of JAK2 in BT-R cells or the same cells stably transfected with a vector encoding JAK2 were determined by Western blot. Blot shown is representative of four independent experiments. **b** Cocultures of PBMCs with the indicated cells were treated with different concentrations of HER2-TCB for 72 h. Then, viable target cells were quantified by flow cytometry using EpCAM as a marker. **c** The indicated cells were treated with different ratios of CAR T cells. Cell numbers were calculated and expressed as in (**b**). **d** The indicated cells were treated with different concentrations of IFN-γ for 5 days. Cell numbers were estimated with the crystal violet staining assay. **e** Totally, 6.5×10^6 BT-R cells or the same cells expressing JAK2 were injected orthotopically into NSG mice. When tumors reached ~200 mm^3 (dark background), 10^7 PBMCs were injected i.p. Then animals were treated i.v. with 0.125 mg/kg HER2-TCB as indicated (red arrows). Tumor volumes are represented as averages ± SD ($n = 7$ per arm). **f** Levels of JAK2 in BT474 cells stably expressing a non-targeting shRNA (shc) or an shRNA targeting JAK2 (shJK2) were determined by Western blot. Results were normalized to BT474 shc. **g–i** The indicated cells were analyzed as in (**b–d**), respectively. **j** Totally, 6.5×10^6 BT474 cells stably expressing a non-targeting shRNA (shc) or an shRNA targeting JAK2 (shJAK2) were injected into NSG mice and treated as in (**e**). Tumor volumes are represented as averages ± SD (shc, $n = 10$; shJAK2, $n = 5$). **b** $^{**}p = 0.005$, $^{**}p = 0.003$, $^{**}p = 0.002$, $^{**}p = 0.002$. **c** $^{**}p = 0.002$, $^{***}p < 0.001$. **d** $^{***}p < 0.001$. **g** $^{*}p = 0.05$, $^{*}p = 0.05$, $^{*}p = 0.02$. **h**, **i** $^{***}p < 0.001$, two-tailed *t* test. **e**, **j** $^{*}p < 0.05$, $^{***}p < 0.001$, two-way ANOVA and Bonferroni correction. Data are presented as mean ± SD of three (**b–d**, **h**, **i**) or four (**f**, **g**) independent experiments. Source data are provided as a Source Data file.

Conversely, knock-down of JAK2 from parental cells impaired IFN-γ signaling (Fig. 5f and Supplementary Fig. 5d), induced resistance to redirected lymphocytes and to cell death induced by IFN-γ in vitro (Fig. 5g–i), and resistance to the HER2-TCB in vivo (Fig. 5j).

Conceivably, impairment of any of the components that transduce its signal results in defective response to IFN-γ. To determine if different components can be downmodulated in different resistant models, we generated an independent resistant BT474 model following an in vivo approach. We recovered cells from the residual tumor that remained after TCB-treatment, re-grafted them into mice and repeated the process (Supplementary Fig. 6a). After the second round of selection, we obtained cells resistant to HER2-TCB, which were named BT-vR (Supplementary Fig. 6b). The levels of cell surface HER2 in resistant cells were unaltered (Supplementary Fig. 6c), and we observed a downmodulation of JAK2 similar to that in the in vitro selected BT-R cells (Supplementary Fig. 6d). Lymphocyte infiltration, stained with anti-CD3 antibodies, was similar in tumors generated by parental and resistant cells (Supplementary Fig. 6e), showing that deficient infiltration of lymphocytes was not the cause of resistance. Finally, in contrast with parental cells, IRF1 was undetectable in resistant cells (Supplementary Fig. 6e), confirming defective IFN-γ signaling in resistant cells.

To select resistant cells from another source and in different conditions, we implanted a HER2-positive PDXs in mice humanized with $CD34^+$ hematopoietic stem cells as previously described[18]. Once the tumors reached ~200 mm^3, mice were treated with the HER2-TCB, the tumors regressed, were allowed to regrow and the treatment was repeated (Supplementary Fig. 6f). After two rounds of treatment, the tumors were no longer sensitive to the HER2-TCB (Supplementary Fig. 6g). Again, the resistant PDX showed unaltered levels of HER2 but strongly decreased levels of JAK2 (Supplementary Fig. 6h, i). Thus, resistance to HER2-TCB in different contexts results in the same defect: downmodulation of JAK2 and impaired IFN-γ signaling in tumor cells.

Models of resistance to IFN-γ. Treatment of BT474 cells with increasing concentrations of IFN-γ starting at the IC50 during 4 months resulted in resistant cells (designed BT-RG), with an IC50 comparable to that of cells resistant to the HER2-TCB (BT-R) (>1000 ng/ml) (Fig. 6a). As expected, IFN-γ signaling was downmodulated in these resistant cells (Supplementary Fig. 5e). In vitro assays showed that IFN-γ resistant cells were also resistant to the HER2-TCB and to HER2-CAR T cells (Fig. 6b, c). Further, IFN-γ resistant cells were also resistant to the HER2-TCB in vivo (Fig. 6d). Thus, cells selected because of their resistance to IFN-γ showed similar characteristics to those selected for resistance to TCBs, further supporting the relevance of the IFN-γ pathway in resistance to redirected lymphocytes.

Importantly, as was the case with HER2-TCB resistant cells, the levels of JAK2 were significantly reduced in BT-RG cells (Fig. 6e). Next, we performed gain-of-function experiments; that is, analysis of IFN-γ signaling (Supplementary Fig. 5f) and the sensitivity to IFN-γ, HER2-TCB and HER2-CAR of BT-RG cells transfected with JAK2 (Fig. 6f–h). The results confirmed the causal role of JAK2 downmodulation on resistance to killing by redirected lymphocytes, independently of the method to generate cells resistant to IFN-γ signaling.

Similarly to BT-R cells, treatment of BT-RG cells with drugs that interfere with epigenetic modifications showed an effect of the pan-HDAC inhibitor Trichostatin A (TSA) on the expression of *JAK2* (Fig. 6i). In addition, BT-RG showed reduced levels of H3K27Ac in the promoter of *JAK2* (Fig. 6j). Thus, we concluded that JAK2 is also downregulated epigenetically in BT-RG cells.

Chronic treatment with IFN-γ is a convenient way to obtain models of resistance. Thus, to confirm our conclusions, we treated cultures from the two HER2-postive PDXs with IFN-γ to obtain resistant cells. In both cases, resistance to IFN-γ was acquired through downmodulation of JAK2. Consistent with the results obtained with BT474 cells, IFN-γ resistance induced resistance to killing by TCB; further, JAK2 overexpression rescued completely the phenotype (Supplementary Fig. 7). We concluded that breast cancer cells acquire resistance to IFN-γ and, thus, resistance to redirected lymphocytes, by downregulating JAK2 (Fig. 6k).

Discussion

Redirection of lymphocytes, via TCBs or CARs, is already approved to treat some hematological malignancies. This success contrasts with the failures in the treatment of solid tumors. In order to overcome this lack of efficacy, many efforts have focused on counteracting the inhibitory effect that the tumor microenvironment exerts on lymphocytes. Only recently, intrinsic mechanisms or resistance, such as defective death receptor signaling causing resistance to CARs directed against CD19, have been described[25]. The simple approach used in this study allowed to unveil additional mechanisms deployed by cancer cells to resist killing by a fully active lymphocyte with unrestricted access to its target cell.

The impairment of the IFN-γ pathway does not have discernible effects on cell proliferation, as readily shown by the knockdown or knockout of IFNGR1, JAK1, STAT1, or JAK2, but severely affects the sensitivity of cells to the killing by redirected lymphocytes. Thus, alterations conducting to impairment of IFN-γ signaling in tumor cells are likely to arise in patients under the selective pressure imposed by TCBs or CARs.

Activated T cells engage target cells via a cytolytic synapse formed between the TCR and the MHC-antigen complex. These synapses cause the death of the target cells via perforin- and granzyme-induced apoptosis. In addition, FAS-L produced by activated lymphocytes causes death of cells expressing the FAS receptor[26,27]. It is generally assumed that this system suffices to kill target cells and that TCBs and CARs trigger the same mechanism. The results presented here show a previously unnoticed role of the IFN-γ pathway in the killing of HER2-positive cancer cells by lymphocytes, at least those redirected via TCBs or CARs targeting HER2.

Compared with TCR/MHC-antigen synapses, the contacts mediated by TCBs or CARs have some particularities (reviewed in ref. [4]). First, contacts formed via TCR or CARs function independently of MHC[28]. On the other hand, the affinities of TCRs for TCR/MHC-antigen complexes are in the range of 1–100 μM, whereas the affinities of TCBs and CARs are typically below 100–10 nM[29,30]. Finally, few complexes of a given antigen with its cognate MHC are expressed per target cells[31]; in contrast, targets of TCBs and CARs may number in the 1000–10,000 s, or in the 100,000 s in the case of HER2-amplified tumors[32]. In fact, differences between the synapses established by TCR/MHC-antigen and CARs have been directly shown[33]. Probably because of these differences, while the activation of T cells by TCR/MHC–antigen synapses requires additional second signals, TCBs and CARs suffice to activate lymphocytes. Future work should clarify if the dependence of IFN-γ signaling is a particularity of T cell redirected via TCBs or CARs against cells expressing high levels of an antigen, or if it also applies to T cells engaged through TCR/MHC-antigen synapses.

In this regard, loss-of-function mutations in JAK1 or JAK2 have been shown to arise in tumors that progressed to treatment with immune checkpoint inhibitors, showing that IFN-γ pathway may also be critical for the killing of target cells by the TCR/MHC–antigen complex. In addition, recently the downmodulation of genes upregulated by IFN-γ has been correlated with resistance to immune checkpoint blockade[33,34], further supporting the relevance of IFN-γ signaling on the sensitivity of target cells to killing by cytotoxic lymphocytes.

The results presented here, have practical implications, particularly when considering the widespread use of JAK2 inhibitors in the clinic[34]. Our results imply that the systemic use of these inhibitors, currently approved to treat myelofibrosis and hydroxyurea resistant or intolerant polycythemia vera to alleviate the exacerbated activation of the immune system, may impact on cancer immunoediting and, in some contexts, favor tumor progression.

Methods

Study design. This study was designed to identify the mechanisms that trigger the resistance against HER2-TCB and -CAR. In order to generate acquired resistance models and to identify the mechanism described in this work, in vitro and in vivo functional assays were performed, using both tumor cell lines and PDXs. Experiments consisted of combining tumor cells with human lymphocytes and TCBs or CARs targeting HER2. For in vivo models, two sources of human immune cells were used: PBMCs and $CD34^+$ hematopoietic stem cells. All human samples were obtained with informed consent and following institutional guidelines under protocols approved by the Institutional Review Boards (IRBs) at Vall d'Hebron Hospital. Animal work was performed according to protocols approved by the Ethical Committee for the Use of Experimental Animals at the Vall d'Hebron Institute of Oncology. For in vivo experiments, two to five mice were used per group, and they were randomized by tumor size. Mice that died before the end of the experiments for reasons unrelated to treatment or that did not have detectable percentages of human immune cells were excluded. Because of ethical reasons, we ended the experiments before the full development of graft-versus-host disease or when tumor volume surpassed 1500 mm^3. Experiments were performed in a blinded fashion.

Cell lines and primary cultures. BT474 (#HTB-20), SKBR3 (#HTB-30), HEK293T (#CRL-11268), SKOV3 (#HTB-77), and H1781 (#CRL-5894) were obtained from ATCC (Manassas, VA, USA). GP2-293 cells (#631458) were obtained from Clontech. PDX433 ($ER^+/PR^-/HER2^{3+}$) was extracted by core needle biopsy (CNB) from a breast cancer patient's metastasis in the liver. PDX667 ($HER2^+$) was extirpated by CNB from a breast cancer patient's metastasis in the skin. PDX118 ($ER^+/PR^-/HER2^{3+}$) comes from a skin metastasis collected by CNB. All these PDXs have been established at VHIO following institutional guidelines. The IRBs at Vall d'Hebron Hospital provided approval for this study in accordance with the Declaration of Helsinki. Written informed consent was obtained from all patients who provided tissue samples.

Cell lines were cultured under standard conditions in complete medium (DMEM F-12 medium (#21331, Gibco) supplemented with 10% fetal bovine serum (FBS) (#10270, Gibco), 1% L-glutamine (#X0550, Biowest), and 1% penicillin–streptomycin (#P4333, Sigma-Aldrich)). Cells were genetically modified to acquire resistance to certain antibiotics or to downmodulate or overexpress different genes. Cells were routinely tested for the absence of mycoplasma contamination using the MycoAlert™ Mycoplasma detection kit (#LT07-318, Lonza). Cell lines were not authenticated in-house.

PBMC isolation. PBMCs were isolated from fresh buffy coats obtained from healthy donors through the Blood and Issue Bank of Catalonia (BST). Blood was diluted 1:3 with 1× phosphate-buffered saline (PBS) and transferred to a 50 ml falcon tube with Ficoll-Paque PLUS (#70-1440-02, GE Healthcare) at a 1:3 ratio, following the manufacturer's instructions. After obtaining the buffy coat, red blood cells (RBC) were lysed with 1× RBC lysis buffer (#00-4333-57, Invitrogen) for 4 min. Obtained PBMCs were counted and frozen with Cryostor CS10 (#07959, Stemcell Technologies) at −80 °C for in vitro and in vivo experiments.

Generation of resistant cells in vitro. To generate the BT-R model, BT474 cells stably expressing hygromycin resistance were treated with a 3:1 ratio PBMC:Tumor and a concentration of 67.5 pM HER2-TCB in PBMC media (RPMI 1640 (#61870, Gibco), 10% heat-inactivated FBS, 1% L-glutamine, 1% HEPES (#H0887, Sigma-Aldrich), 1% MEM nonessential amino acids solution (#11140, Gibco), and 1% penicillin–streptomycin). After 72 h, media was removed and replaced with complete medium containing 100 μg/ml hygromycin (#10687010, Gibco) during 7 days

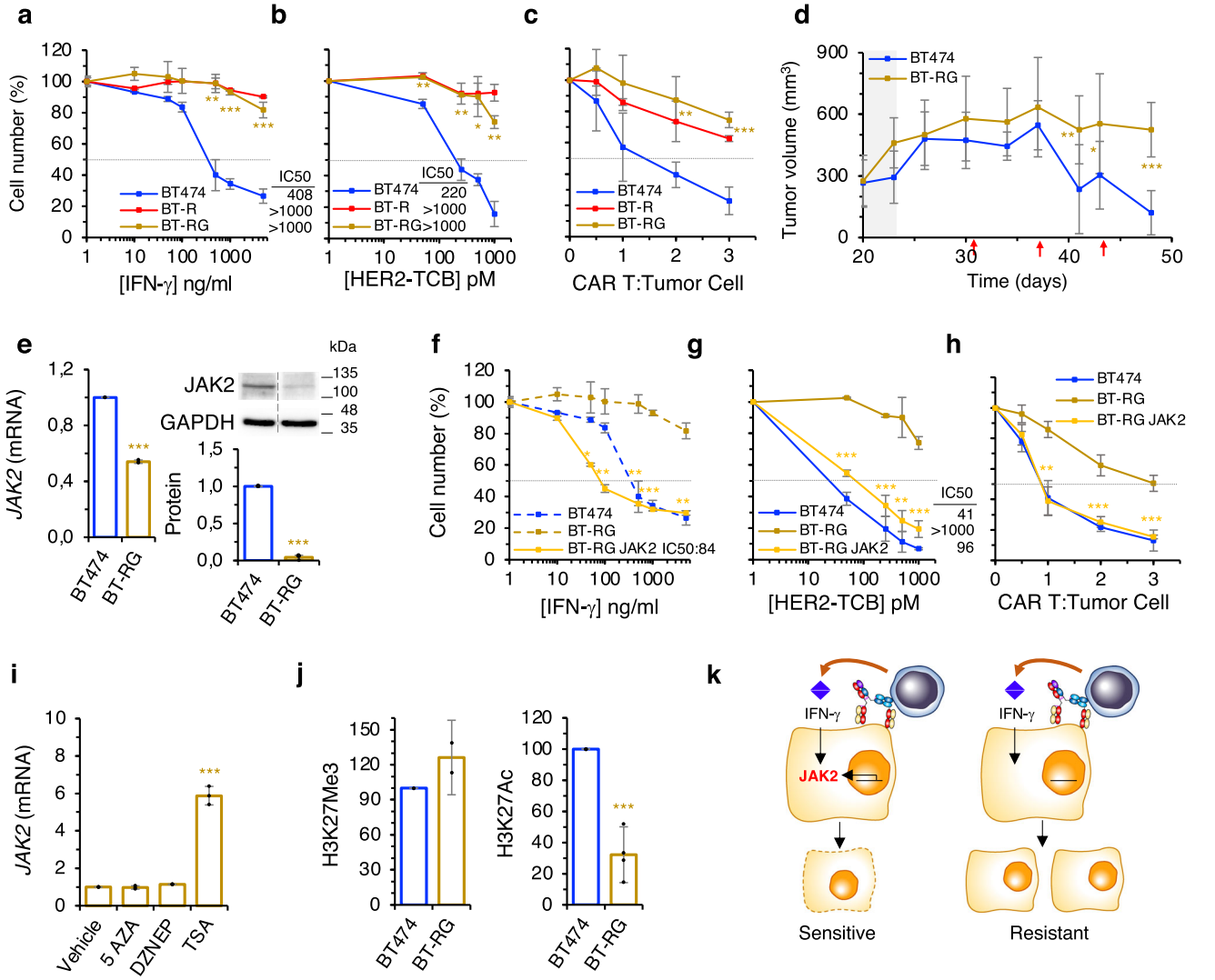

Fig. 6 Model of resistance to IFN-γ. a Parental BT474 cells or resistant BT-R or BT-RG cells were treated with different concentrations of IFN-γ for 5 days. Cell numbers were estimated with the crystal violet staining assay. **b** Cocultures of PBMCs with the indicated cells were treated with different concentrations of HER2-TCB for 72 h. Then, viable target cells were quantified by flow cytometry using EpCAM as a marker. **c** The same cells as in (**a**) were treated with different ratios of CAR T:Tumor cell. Cell numbers were obtained by means of EpCAM counts by flow cytometry. **d** Totally, 10^7 BT474 or resistant BT-RG cells were injected orthotopically into NSG mice. When tumors reached ~300 mm^3 (dark background), 10^7 PBMCs were injected i.p. Then animals were treated i.v. with 0.125 mg/kg HER2-TCB as indicated (red arrows). Tumor volumes are represented as averages ± SD (BT474, $n = 8$; BT-RG, $n = 6$). **e** The levels of JAK2 (mRNA and protein) as determined by quantitative real-time PCR (left) or Western blot (right). Results were normalized to BT474 cells. **f**–**h** The indicated cells were analyzed as in (**a**–**c**), respectively. **i** BT-RG cells were treated with indicated compounds for 48 h. Then, the levels of the mRNA encoding *JAK2* were determined by RT-PCR and normalized to the levels in cells treated with vehicle. **j** Levels of H3K27Me3 and H3K27Ac histone marks in the promoter of *JAK2* in BT474 and BT-RG cells as measured by ChIP followed by quantitative real-time PCR. Results were normalized to the levels of an IgG control antibody in each sample, and then normalized to the levels in BT474 cells. **k** Schematic drawing summarizing our findings. **a** $^{**}p = 0.002$, $^{***}p < 0.001$. **b** $^{**}p = 0.009$, $^{**}p = 0.006$, $^{*}p = 0.013$, $^{**}p = 0.002$. **c** $^{**}p = 0.008$, $^{***}p < 0.001$. **e** $^{***}p < 0.001$. **f** $^{*}p = 0.02$, $^{**}p = 0.004$, $^{**}p = 0.002$, $^{***}p < 0.001$, $^{**}p = 0.002$. **g** $^{**}p = 0.005$, $^{***}p < 0.001$. **h** $^{**}p = 0.0015$, $^{***}p < 0.001$. **i**, **j** $^{***}p < 0.001$. Two-tailed *t* test. **d** $^{*}p < 0.05$, $^{**}p < 0.01$, $^{***}p < 0.001$, two-way ANOVA and Bonferroni correction. Data are presented as mean ± SD of three (**a**–**c**, **e**–**i**), two (**j** left) or four (**j** right) independent experiments. Source data are provided as a Source Data file.

to specifically kill remaining PBMCs. The process was repeated several times. Resistant population was obtained after 6 months.

Interferon-gamma resistant models were established by culturing cells in presence of increasing IFN-γ (#300-02, Peprotech) concentrations, starting at 100 ng/ml and reaching 1 µg/ml. In the three models (BT474-RG, PDX667-RG, and PDX433-RG) resistance was obtained after 4 months of treatment.

T cell cytotoxicity assays. All target cells were seeded in 96-well flat bottom plates (0.01×10^6 cells/well) (#353075, Corning Life Sciences). Effector PBMCs were added to each well at the indicated ratio in PBMC medium. Different concentrations of HER2-TCB were added to the wells. The plates were incubated for 72 h.

At the endpoint cells were harvested with trypsin–EDTA (#25300096, Gibco) and resuspended in fluorescence-activated cell sorting (FACS) buffer (PBS 1×, 2.5 mM EDTA, 1% bovine serum albumin (BSA) (#A9647, Sigma-Aldrich), 5% horse serum (#26050, Gibco)) in polypropylene V-bottom 96-well plates (#651201, Greiner Bio-One). Twenty minutes later, samples were centrifuged and cells were stained with the epithelial cell marker anti-human EpCAM (#324212, BioLegend) at 1:300 concentration in FACS buffer in ice for 30 min. After a wash with 1× PBS, samples were resuspended in the viability marker Zombie Aqua at 1:1000 (#423101, BioLegend) in 1x PBS and acquired on LSR Fortessa, using BD FACSDiva software (BD Biosciences). Number of alive cells was analyzed with FlowJo software (BD Life Sciences) by means of EpCAM counts. Gating strategy for tumor $EpCAM^+$ counts is shown in Supplementary Fig. 8.

When treated with CAR Ts, target cells were seeded as described above. After 24 h, effector CAR Ts targeting HER2 were added to each well at the indicated

ratios in PBMC medium. The plates were incubated for 48 h. Endpoint was assayed as previously explained.

For the IFN-γ blocking experiments, tumor cells were seeded as explained before, and in addition to the PBMCs and HER2-TCB/CAR Ts, either 20 μg/ml of anti-human IFN-γ (#506512, Biolegend) or mouse IgG control (#400123, Biolegend) was added in the coculture. Experiment lasted 72 or 48 h respectively and endpoint was assayed as previously explained.

3D organoid assay. Tumor cells were seeded in 48-well plates (10^3 cells/well) in a drop of 20 μl of matrigel (#356235, Corning). Each drop was dispensed in the center of the well and incubated for 15 min at RT. After matrigel was solidified, 250 μl of 3D breast tumor organoid media[35], were added to each well. Media was replaced twice a week and 3D formation was assessed after 15 days. Organoids per well were counted and assumed that each of them consisted of approximately 50 cells. Organoid media was removed and 3D structures were cocultured with PBMCs at a 2:1 ratio in PBMC media and treated with HER2-TCB at 1 nM for 72 h.

For the IFN-γ blockade experiment, same assay was followed but adding either 20 μg/ml of anti-human IFN-γ or mouse IgG control to the coculture with PBMCs.

At the endpoint, organoids were disaggregated by adding 500 μl of trypsin for 30 min at 37 °C. Then, cells were collected and incubated for 30 min on ice to liquify matrigel. Fully disaggregated organoids were washed and stained as previously explained. Number of alive cells was analyzed with FlowJo software by means of EpCAM counts. Gating strategy for tumor $EpCAM^+$ counts is shown in Supplementary Fig. 8.

Flow cytometry. Cells were harvested with StemPro Accutase (#A1110501, Gibco) and resuspended in FACS buffer. Twenty minute later, samples were centrifuged and cells were incubated for 30 min with the specified antibody. After a wash and Zombie Aqua staining, samples were acquired on LSR Fortessa. The following antibodies were used: hPDL1 (#329736), hCD80 (#305221), hCD86 (#305425), hGalectin-9 (#348905), hB7-H3 (#351003), hB7-H4 (#358103), hHVEM (#318805), hICOS-L (#309403), h41BB-L (#311503), hOX40-L (#316307), hIFNGR1 (#308606), hIFNGR2 (#308504), all from Biolegend at 1:100 dilution. As an isotype control, PE mouse IgG Isotype Ctrl (#400114, Biolegend) was used at 1:100.

In the case of HER2 staining, cells were incubated in FACS buffer for 30 min with Trastuzumab (#180288-69-1, Herceptin, Roche) at 2.5 μg/ml. After two washes with PBS, a secondary conjugated antibody Anti-human Alexa-488 (#A-11013, Invitrogen) was incubated with the cells at a concentration of 1:500 for 30 min. Cells were then washed with 1× PBS and resuspended in Zombie Aqua viability marker and acquired on LSR Fortessa. HER2-TCB binding assay was performed by incubation of cells with 10 nM HER2-TCB for 30 min, followed by the procedure described above.

PD-L2 staining consisted of a primary and secondary antibodies incubation. The incubation with the primary antibody, anti-PD-L2 (#130098525, Miltenyi Biotec), lasted 30 min at 1:11 concentration, and after a wash with 1× PBS, samples were incubated with the secondary antibody anti-biotin (#130113292, Miltenyi Biotec) at 1:50 for 30 min. After a wash and Zombie Aqua staining, samples were acquired on LSR Fortessa using BD FACSDiva software.

The activation marker CD69 (#310914, Biolegend) in $CD8^+$ cells (#344712, Biolegend) was used in order to assess T-cell activation after 72 h of coculture with tumoral cells and 67.5 pM HER2-TCB (both at 1:300 concentration).

Ki-67 intracellular staining was performed in PBMCs after 72 h of coculture with BT474 cells using different concentrations of HER2-TCB. First, cells were incubated with zombie aqua for 25 min at 1:500 concentration at room temperature (RT). Then, cells were washed and stained with a CD8 antibody as previously explained. After a wash with 1× PBS, cells were fixed with 200 μl of fresh prepared (1 part of concentrate with 3 parts of diluent) fixation/permeabilization working solution (#00-5523-00, Invitrogen) for 25 min on ice in dark. Supernatant was removed after a centrifugation and cells were permeabilized with 1× permeabilization buffer for 25 min on ice in dark. After supernatant was removed, cells were stained with anti-Ki-67 antibody (#563756, BD Biosciences) in 1× permeabilization buffer at 1:300 concentration for 1 h at RT, washed with 1× PBS and acquired on LSR Fortessa. Flow cytometry data was analyzed with FlowJo software (BD Life Sciences). Gating strategy for T-cell proliferation, activation marker analysis, and for median fluorescence intensity (MFI) measures is shown in Supplementary Fig. 8.

IFN-γ cytotoxicity assays. Tumor cells were seeded in flat bottom 96-well plates (0.01×10^6 cells/well). After 24 h cells were treated with different concentrations of IFN-γ. Treatment lasted for 5 days and cell death was assayed by crystal violet staining of alive cells. Cells were fixed for 30 min with 10% glutaraldehyde, washed, and stained for other 30 min with 0.1% crystal violet (#548-62-9, Sigma-Aldrich). After three washes with water, plates were let dry overnight. For the readout, 100 μl of 10% acetic acid were added to each well and absorbance was read at 560 nm using an Infinite M200 Pro Multimode Microplate Reader (TECAN).

Antitumor drugs cytotoxic assays. Tumor cells were seeded as described above. After 24 h cells were treated with different concentrations of paclitaxel (#33069-62-4, Paclitaxel Hospira, Pfizer), doxorubicin (#23214-92-8, Farmiblastina, Pfizer), or T-DM1 (#1018448-65-1, Kadcyla, Roche). Treatment lasted for 3 days in the case of the chemotherapeutic agents paclitaxel and doxorubicin, and 6 days when treated with T-DM1. Cell death was assayed by crystal violet staining of alive cells and read at the Infinite M200 Pro Multimode Microplate Reader (TECAN).

Western blot. For Western blot, protein extracts were isolated by lysing the cells in homemade lysis buffer (130 mM NaCl, 0.01% NP-40, 1% glycerol, 2 mM EDTA pH 8 and 20 mM Tris-HCl pH 7.4), supplemented with phosphatase inhibitors 5 μM β-glycerolphosphate, 5 μM sodium fluoride, 1 μM sodium orthovanadate and cOmplete™, EDTA-free protease inhibitor cocktail (#COEDTAF-RO, Sigma-Aldrich, 1 tablet per 10 ml lysis buffer). Protein extracts were sonicated for 10 s at 4.5 V to break the cell apart. Tubes were centrifuged 19,000 ×*g* 10 min and supernatant was collected.

Protein lysates were resolved by sodium dodecyl sulfate polyacrylamide gel electrophoresis and then transferred to a 0.45 μm nitrocellulose membrane (#10600002, GE Healthcare Biosciences). Totally, 20–30 μg of protein lysate was loaded per experiment. Membranes were incubated with 5% BSA or 5% non-fat milk in TBS-T (1× tris-buffered saline with 0.1% tween 20 (#P7949, Sigma-Aldrich)). After blocking, membranes were incubated overnight with primary antibodies.

After washing, membranes were incubated with horseradish peroxidase-conjugates antibodies (GE Healthcare) for 1 h. Membranes were developed with Immobilon Western Chemiluminescent HRP Substrate (#WBKLS0500, Millipore) and protein bands were visualized in Amersham™ Imager 600 (GE Life Sciences).

Antibodies used were: HER2 (#AM134, Biogenex), JAK1 (#3344, Cell Signaling Technology (CST)), JAK2 (#3230, CST), pSTAT1 (#9167, CST), STAT1 (#9172, CST), IRF1 (#sc-497, Santa Cruz Biotechnology (SC)), and GAPDH (#ab128915, Abcam). All antibodies were used at 1:1000 concentration in 5% BSA except GAPDH (1:5000). Quantification of protein levels was done with ImageJ (National Institutes of Health). Quantifications are the result of ≥3 independent biological replicates. All original Western blots are provided in the Source data file.

RNA isolation and qRT-PCR. Total RNA was isolated from adherent cells by using RNeasy Mini Kit (#74106, Qiagen) according to the manufacturer's protocol. RNA was eluted in RNase-free water and quantified using NanoDrop™ 2000 spectrophotometer (Thermo Fisher Scientific).

cDNA was prepared from 1 μg template RNA using the high capacity cDNA reverse transcription Kit (#4368813, Applied Biosystems) according to the manufacturer's protocol.

Real-time quantification of transcript abundance was determined by qRT-PCR using the TaqMan Gene Expression probes (Applied Biosystems) and TaqMan Universal Master Mix II (#4440039, Applied Biosystems), in 384-well plates in 7900HT Fast Real-Time PCR System (Applied Biosystems), following the manufacturer's protocol.

The following TaqMan probes were used: *TIMP2* (Hs00234278_m1), *IFNGR1* (Hs00988304_m1), *IFNGR2* (Hs00194264_m1), *JAK1* (Hs01026983_m1), *JAK2* (Hs01078136_m1), *STAT1* (Hs01013996_m1), *GAPDH* (Hs02758991_g1). Data was analyzed with sodium dodecyl sulfate (SDS) software, RQ Manager, and DataAssist software (Applied Biosystems), using the $2^{-\Delta CT}$ method. *GAPDH* was used as an endogenous control.

Drugs targeting epigenetic modifications. Cells were treated with 5 μM of different drugs for 48 h: 5-Azacytidine (#A2385, Sigma-Aldrich), 3-Deazaneplanocin A (DZNEP, #HY-10442, MedChemExpress) or Trichostatin A (TSA, #HY-15144, MedChemExpress). Then, RNA was isolated and subjected for *JAK2* expression by RT-qPCR.

Chromatin immunoprecipitation (ChIP). Indicated cells were grown to 70% confluence, collected, and subsequently cross-linked with 1% formaldehyde shaking at 37 °C temperature for 10 min. Reaction was quenched by incubating the samples with 125 mM Glycine (#BP381, Fisher Scientific) for 5 min. Cells were pellet at 5×10^6 cells/vial and stored at −80 °C.

Cell pellets were resuspended in SDS lysis buffer (1% SDS, 10 mM EDTA, 50 mM Tris pH 8) with 1:200 Protease Inhibitor Cocktail Set III (#535140, Merck Millipore) for 30 min on ice. Samples were then sonicated to generate fragments of DNA between 100 and 600 bp with the Bioruptor (Diagenode). After 20 min on ice, samples were centrifuged at 19,000 × *g* and supernatant was diluted 1/10 with Dilution buffer (0.01% SDS, 1.1% Triton X-100, 1.2 mM EDTA, 16.7 mM Tris pH 8, 167 mM NaCl), in order to decrease concentration of SDS. Samples were incubated with 10 μl of Dynabeads protein A (#10002D, Invitrogen) and 1 μg of irrelevant antibody Rabbit IgG (#I8140, Sigma-Aldrich) per IP in that sample, as a preclearing. Incubations lasted for 3 h rotating at 4 °C. Magnets were used to discard the beads, and the samples were separated per IP, saving 10% for the input. Totally, 3 μg of corresponding antibody was added at each tube and samples were incubated overnight rotating end over end at 4 °C. The antibodies used were: Rabbit IgG, anti-H3K27Me3 (#07-449, Merck Millipore) and anti-H3K27Ac (#ab4729, Abcam).

Samples were incubated with 50 µl of prewashed dynabeads and incubated 3 h rotating at 4 °C. Dynabeads were then washed 3 times with low salt and 3 times with high salt buffer (0.1% SDS, 1% Triton X-100, 2 mM EDTA, 20 mM Tris pH 8, and 150 or 500 mM NaCl respectively) and 2 times with LiCl buffer (250 mM LiCl, 1% NP-40, 1% NaDOC, 1 mM EDTA, 10 mM Tris pH 8). Samples were then incubated with 48 µl of elution buffer (0.4% SDS, 5 mM EDTA, 10 mM Tris pH 8, 300 mM NaCl) supplemented with 2 µl proteinase K (#RPTOTKSOL, Roche). Then, samples were incubated shaking 1 h at 55 °C and subsequently overnight at 65 °C. Input samples were treated the same way. DNA was purified from the eluted samples with the MinElute PCR Purification Kit (#28006, Qiagen) following the manufacturer's instructions.

Finally, qPCR was performed with the ChIP samples using SYBR green reagent (#733-1390, Quantabio). A 179-bp segment of the *JAK2* promoter was amplified with the following primers: 5′-GGATGTGAGTGGGAGCTGAG-3′ (sense) and 5′-GAGATAACACCCACCGGCTA-3′ (antisense). Data shown is the result of normalizing the specific signal of each antibody (normalized to the IgG control signal) of BT-R or BT-RG to the parental BT474 cells.

Humanized xenograft models. In the PBMCs humanized xenograft models, NSG mice were injected orthotopically in two flanks with 6.5×10^6 or 10^7 tumor cells in 100 µl of 1:1 PBS:matrigel. Once tumor size reached a specified volume, animals were intraperitoneally injected with 10^7 PBMCs obtained from healthy donors. After 24 h, animals started treatment and were treated biweekly with HER2-TCB (0.125 mg/kg) or vehicle intravenously.

In the HER2-CAR in vivo experiment, NSG mice were injected orthotopically with 10^7 tumor cells. Once tumors were around 200-300 mm^3, animals were intraperitoneally treated once with 3×10^6 HER2-CAR T-positive cells.

To obtain immunodeficient mice with a reconstituted human immune system, $CD34^+$ cells were purified from human cord blood obtained through the Blood and Tissue Bank of Catalonia. Blood was diluted 1:2 with 1× PBS + 2 mM EDTA and transferred to a 50 ml falcon tube with 15 ml of Ficoll–Paque PREMIUM (#70-1440-02, GE Healthcare), following the manufacturer's manual. After obtaining the mononuclear cells, resting RBC were lysed with 1× RBC lysis buffer for 4 min. $CD34^+$ cells were purified by negative selection by incubating the mononuclear cells with EasySep Human Progenitor Cell Enrichment Cocktail with Platelet Depletion (#19356, StemCell Technologies), following manufacturer's protocol. Purity of the remaining cell mix was checked with anti-human CD34 (#60013, StemCell) and anti-human CD45 (#304008, Biolegend) staining at 1:300 concentration in FACS buffer. Samples were acquired in LSR Fortessa and percentage of CD34 and CD45 cells were analyzed in FlowJo. Obtained cells were frozen with Cryostor CS10 at −80 °C.

$CD34^+$ cells were injected intravenously in 5-week-old female NSG mice previously treated with busulfan (15 mg/kg) to remove the hematopoietic system of the mice. After 4–5 months, levels of humanization were checked by flow cytometry and mice with more than 30% of human $CD45^+$ cells in blood were used for in vivo experiments. Totally, 10^7 tumor cells were orthotopically implanted per flank, and once these reached ~200 mm^3, animals were randomized and treated biweekly with HER2-TCB (0.25 mg/kg) or vehicle (intravenously).

At the end of the experiments, tumors were analyzed. Tumors were cut into small pieces and divided into samples for IHC, protein, flow cytometry, or reinjection. Samples for IHC were fixed and embedded in paraffin. Samples for western blot were incubated with lysis buffer, supplemented with phosphatase and protease inhibitors, in BashingBead lysis tubes (#S6003, Zymo Research) and homogenized in Precellys Evolution Homogenizer (Bertin Technologies).

Samples for flow cytometry and reinjection were digested in 300 U/ml collagenase IA (#C2674, Sigmsa-Aldrich) and 100 U/ml hialuronidase IS (#H3506, Sigma-Aldrich) in DMEM F-12 medium. After 1 h of incubation at 37 °C with shaking at 10 × *g*, the mixture was filtered through 100 µm strainers. RBC were lysed with 1× RBC for 5 min RT. After a wash with 1× PBS, samples were counted and either reinjected or stained for HER2 and EpCAM as previously explained and acquired on LSR Fortessa. Data were analyzed with FlowJo software (BD Life Sciences). Gating strategy for MFI measures is shown in Supplementary Fig. 8.

All mice in this study were kept within Home Office limits of 22 °C ± 2 °C, 55–65% humidity and run on a 12 h light/dark cycle that runs from 8 a.m. to 8 p.m.

Generation of in vivo resistant cells. In the generation of BT474 resistant to HER2-TCB, the humanized PBMCs xenograft model was used. NSG mice were injected orthotopically with 10^7 tumor cells. Once tumor size reached 300 mm^3, animals were intraperitoneally injected with 10^7 PBMCs obtained from healthy donors. After 24 h, animals started the treatment and were treated biweekly with an increasing concentration of HER2-TCB or vehicle intravenously. HER2-TCB treatments started from 0.0325 mg/kg, and concentration was gradually increased until reaching 0.25 mg/kg. After two passages, resistant tumors (termed as BT-vR) were obtained.

In the case of the generation of PDX118 resistant model to HER2-TCB, $CD34^+$ humanized xenograft model was used. Humanized mice containing >30% $hCD45^+$ in peripheral blood were orthotopically implanted with 10^7 tumor cells. Once tumors reached 300 mm^3, animals started biweekly treatment with an increasing concentration of HER2-TCB or vehicle intravenously. HER2-TCB treatments started from 0.0325 mg/kg, and concentration was gradually increased until reaching 0.25 mg/kg. After two passages, resistant tumors (termed as 118-vR) were obtained.

Immunohistochemistry. The following primary monoclonal antibodies were used: anti-IRF1 (#HPA063131, Atlas Antibodies) and anti-CD3 (#790-4341, Ventana Medical Systems (Ventana)). For immunohistochemistry, fixed tissue samples embedded in paraffin were sectioned at 4 µm thickness. Sections were heated at 60 °C, deparaffinized with xylene and hydrated with two steps of incubation with different dilutions of ethanol.

When stained with anti-IRF1, antigen retrieval was performed by boiling the samples for 20 min in citrate buffer pH 6 (#S2369, Agilent). Endogenous peroxidase was blocked by incubating the samples with 3% peroxide hydrogen (#108597, Merck Millipore) diluted in absolute methanol for 20 min. Slides were also blocked with 3% BSA in 1× PBS for 10 min. Samples were then incubated overnight with the primary antibody anti-IRF1 diluted 1:650 in EnVision FLEX Antibody Diluent (#K8006, Agilent). Next, the slides were incubated with EnVision System-HRP labeled polymer anti-rabbit secondary antibody (#K4003, Agilent). Samples were then stained with DAB substrate chromogen (#K3468, Agilent) for 1–4 min and counterstained with harris hematoxylin (#H3404, Vector Laboratories) for 2 min, followed by dehydration with ethanol and xylene, and finally mounted in DPX.

Immunohistochemical staining of CD3 was performed using a Discovery ULTRA autostainer (Ventana). Heat-induced antigen retrieval was executed using Cell Conditioning 1 (#950-124 Ventana) for 40 min at 95 °C. Endogenous peroxidase block was performed with the CM inhibitor from the ChromoMap DAB kit (#760-159, Ventana) for 8 min. Then, the anti-CD3 primary antibody, ready to use, was applied 32 min at 36 °C. Next, samples were incubated for 8 min with detection kit UltraMap anti-Rabbit HRP (#760-4315, Ventana). Reactions were detected using the ChromoMap DAB Kit. Finally, the slides were counterstained with Haematoxylin II (#790-2208, Ventana) 8 min and Bluing Reagent (#760-2037, Ventana) 4 min, followed by dehydration with ethanol and xylene, and mounted in DPX.

Slides were scanned in the NanoZoomer 2.0-HT slide scanner (Hamamatsu Photonics) and visualized in the NDP.view2 software (Hamamatsu Photonics).

Cytokine array. Detection of 80 cytokines (ENA-78, G-CSF, GM-CSF, Gro a/b/g, CXCL1, CCL1, IL-1 alpha, IL-1 beta, IL-2, IL-3, IL-4, IL-5, IL-6, IL-7, IL-8, IL-10, IL-12, IL-13, IL-15, IFN-gamma, MCP-1, MCP-2, MCP-3, M-CSF, CCL22, MIG, MIP-1 beta, MIP-1 delta, RANTES, SCF, SDF-1 alpha, CCL17, TGF beta, TNF alpha, TNF beta, EGF, IGF-1, Angiogenin, OSM, TPO, VEGF-A, PDGF-BB, Leptin, BDNF, CXCL13, CCL23, CCL11, CCL24, CCL26, FGF-4, FGF-6, FGF-7, FGF-9, FLT-3 ligand, Fractalkine, GCP-2, GDNF, HGF, IGFBP-1, IGFBP-2, IGFBP-3, IGFBP-4, IL-16, CXCL10, LIF, LIGHT, MCP-4, MIF, MIP-3 alpha, NAP-2, NT-3, NT-4, OPN, OPG, PARC, PLGF, TGF beta 2, TGF beta 3, TIMP-1, and TIMP-2) was conducted in culture supernatants of untreated and treated BT474 and BT-R cells. Cells were seeded at 1×10^6 cells per 6 mL of PBMC medium alone or in coculture with a ratio 3:1 of PBMCs and 67.5 pM of HER2-TCB. After 48 h of coculture, supernatant was harvested and frozen. In order to detect differences in parental and resistant cells cytokine secretomes, a human cytokine array (#AAH-CYT-5, RayBiotech) was used with these supernatants following the manufacturer's recommendations. Quantification of cytokine levels was done with ImageJ following manufacturer's instructions.

ELISA. In order to assay TIMP2 release, a TIMP2 ELISA (#DY971, R&DSystems) was used with the same supernatants as specified above, following the manufacturer's manual.

In the case of IFN-γ ELISA, supernatants from treated BT474 and BT-R were obtained at the conditions described above, with different timepoints (24, 48, and 72 h). The culture supernatants were used to perform a human interferon-gamma ELISA (#31673539, Immunotools), following manufacturer's instructions.

Granzyme B activity. Target cells (BT474 or BT-R) were seeded, 0.25×10^6 in 60 mm plates (#430166, Corning), cocultured with PBMCs at a PBMC:Target cell ratio of 3:1 and treated with HER2-TCB at a concentration of 67.5 pM for 72 h. After 72 h, tumor cells and PBMCs were harvested and lysed with 100 µl of lysis buffer. Lysed cells were centrifuged at 21,000×*g* for 10 min at 4 °C to pellet cell nuclei and other cell debris. Supernatants were harvested and assayed for protease activity. Reaction was performed in a non-treated 96-well-plate (#442404, Thermo Fisher Scientific). Each well contained 25 µl of lysis supernatant, granzyme B substrate Ac-IEPD-pNA (#368057, Sigma-Aldrich) at a final concentration of 300 µM and reaction buffer (0.1 M HEPES pH 7.0, 0.3 M NaCl, 1 mM EDTA) in a total volume of 250 µl/well. Mixtures were incubated at 37 °C overnight and color reaction generated by the cleavage of the pNA substrate was measured at a wavelength of 405 nm with the Infinite M200 PRO (Tecan) plate reader[36].

Annexin V assay. Cells were treated with 1 µg/ml of IFN-γ for 5 days. In order to assay the number of apoptotic cells, cells were harvested, washed, and stained with APC-Annexin V (1:20 from stock, #550475, BD Pharmigen) for 15 min RT. After a

wash with 1× PBS, samples were resuspended in 1:500 Propidium Iodine (PI) (#81845, Sigma-Aldrich) viability marker and acquired on LSR Fortessa. Data was analyzed with FlowJo software (BD Life Sciences). Annexin V^+ cells were considered as apoptotic cells. Gating strategy is shown in Supplementary Fig. 8.

Viral tumor cells infections. For lentivirus production, HEK293T cells were first incubated for 2 h with 25 µM chloroquine (#C6628, Sigma-Aldrich) to increase transfection rate. Cells were then transfected with 1 µg/ml of pMD2.G (#12259, Addgene) envelope expressing plasmid, 1.2 µg/ml of psPAX2 (#12260, Addgene) lentiviral packaging vector, and 1.2 µg/ml of the specific lentiviral vector, using 10 µg/ml of polyethylenimine (PEI) (#24765, Polysciences) as transfection agent. Twenty-four hour after transfection, growth medium was replaced with complete medium. After 48 h, viral particles-containing supernatant was harvested and filtered with 0.45 µm PVDF filters (#SLHV033RS, Millipore).

For infections, target cells were seeded in 6-well plates (0.5×10^6 cells/well). After 24 h, being the confluence around 75%, tumor cells were incubated with the viral supernatants and 8 µg/ml polybrene (#H9268, Sigma-Aldrich), and centrifuged 45 min at 1000 × *g*. After 24 h, medium was replaced with complete medium. Twenty-four hour later, infected cells were selected with either 100 µg/ml hygromicin in BT474 cells, 20 µg/ml blasticidin (#ant-bl, Invivogen) in the case of Lenti-Cas9-2A-Blast (#73310, Addgene) BT474 infected cells, or 1 µg/ml puromycin (#P8833, Sigma-Aldrich) in the rest of infections. Selection was subsequently maintained for one week.

In order to generate resistance to HER2-TCB, BT474 were infected with pBABE-hygro (#1765, Addgene), conferring them resistance to hygromicin.

For silencing, the plasmids were obtained from the lentiviral MISSION shRNA Library: TIMP2 (Clones TRCN0000052433, TRCN0000052434), IFNGR1 (TRCN0000300831, TRCN0000058792, TRCN0000304197), JAK2 (TRCN0000003180), JAK1 (TRCN0000121215, TRCN0000121275), and STAT1 silencing (TRCN0000280021, TRCN0000280024), all from Sigma-Aldrich. As a control, tumor cells were infected with scramble shRNA (#1864, Addgene). To overexpress JAK2 in BT-R cells, JAK2 (V617F)-pcw107v5 was used (#64610, Addgene), and empty vector pcw107 (#62511, Addgene) was used as control.

To generate the BT474 KO IFNGR1 cell line, cells were infected with Lenti-Cas9-2A-Blast (#73310, Addgene). After selected with blasticidin, cells were infected with either a CRISPR gRNA targeting IFNGR1 (#HS5000021477, Sigma) or the LV04 control universal gRNA vector (#CRISPR18, Sigma). These gRNAs confer puromycin resistance and BFP expression, and cells were selected with 1 µg/ml puromycin. To obtain KO IFNGR1 cells, these were stained with hIFNGR1 as explained before, and BFP^{high}/IFNGR1 negative expressing cells were sorted in FACSAria I Digital Cell Sorter (BD Biosciences), obtaining a pool of cells. Validation of KO IFNGR1 cells was done by IFNGR1 staining.

RNASeq. Total RNA was isolated from adherent cells as explained before. Extractions of three independent biological replicas were performed. To determine the total RNA quality and quantity was used Qubit® RNA HS Assay (Life Technologies) and RNA 6000 Nano Assay on a Bioanalyzer 2100 (Agilent). The RNASeq libraries were prepared following the TruSeq®Stranded mRNA LT Sample Prep Kit protocol (Illumina, October 2017). Briefly, total RNA (500 ng) was enriched for the polyA mRNA fraction and fragmented by divalent metal cations at high temperature. In order to achieve the directionality, the second strand cDNA synthesis was performed in the presence of dUTP. The blunt-ended double stranded cDNA was 3′ adenylated and Illumina platform compatible adaptors with unique dual indexes and unique molecular identifiers (Integrated DNA Technologies) were ligated. The ligation product was enriched with 15 PCR cycles and the final library was validated on an Agilent 2100 Bioanalyzer with the DNA 7500 assay (Agilent).

The RNASeq libraries were sequenced on HiSeq 4000 (Illumina) with a read length of 2× 76 bp using HiSeq 4000 SBS kit in a fraction of a HiSeq 4000 PE Cluster kit sequencing flow cell lane. Image analysis, base calling and quality scoring of the run were processed using the manufacturer's software Real Time Analysis (RTA 2.7.7).

RNA-seq reads were mapped against the human reference genome (GRCh38) using STAR/2.5.3a with ENCODE parameters for long RNA. Genes were quantified with RSEM/1.3.0 using the gencode.v29 human annotation. Quality control of the mapping and quantification was performed with 'gtfstats' from GEMtools 1.7.0 (https://gemtools.github.io/). Differential expression analysis was performed with DESeq2/1.18[37] with default parameters. Genes with false-discovery rate < 5% and |shrunken fold change| > 1.5 were considered significant. GSEA was performed with fgsea[38]. PCA was performed with the top 500 most variable genes and the rlog transformed counts. Heatmaps with the top 50 differentially expressed genes (DEGs) were done with the pheatmap R package (https://cran.rproject.org/web/packages/pheatmap/index.html).

Pathway enrichment was assessed through the pre-ranked version of GSEA, and we used gene sets derived from the HALLMARK database[39].

The biological pathways associated with DEGs were explored by using the two GSEA gene sets of Hallmarks. The *p* values indicate whether DEGs were significantly enriched in a biological pathway compared with the background. Shown are pathways with *p* values < 0.01.

HER2-CAR T production. To produce CAR Ts against HER2, a vector plasmid coding for HER2-CAR was synthesized and cloned into pMSGV-1 retroviral vector (Genscript, Netherlands). Then, stocks of HER2-CAR (pMSGV1-HER2-VL-VH-H8) retrovirus were produced as follows. Firstly, culture plates were coated with Poly-D-Lysine 0.001% w/v in 1× PBS for 1 h at RT, to increase cell attachment. After 1 h, PBS was removed and GP2-293 cells seeded. The day after, cells were transfected with 0.3 µg/ml of envelope plasmid RD-114 (a gift from Alena Gros' Lab, VHIO) and 0.7 µg/ml of transfer plasmid (HER2), with 4.6 µl/ml of Lipofectamine 2000 transfection reagent (#11668, Invitrogen), in DMEM F-12 without supplements. After 8 h, media was changed with complete medium. Three days later, cell supernatant containing retrovirus particles was collected and filtered with 0.45 µm polyvinylidene fluoride (PVDF) filters.

PBMCs were stimulated with 50 ng/ml of α-CD3 (OKT3) (#16-0037-85, Thermo-Fisher) and 300 IU/ml IL-2 (#703892-4, Novartis) in PBMC media for 48 h before transduction. The day before transduction, 6-well plates were coated with 2 ml of 10 µg/ml retronectin (#T100A, Takara) in 1× PBS overnight at 4 °C. The day of transduction, cell supernatant containing retroviral particles was centrifuged in the retronectin-precoated 6-well plates for 2 h at 2000 × *g* at 32 °C. Next, viral supernatant was removed and stimulated PBMCs were added on top in PBMC media with 300 IU/ml IL-2 at a concentration of 2×10^6 PBMCs in 4 ml/transduction well. Plates were centrifuged for 10 min at 500 × *g* at 32 °C. After 48 h, CAR Ts were transferred to cell culture flasks (#156367 and #156499, ThermoFisher Scientific) to continue its expansion. Five days after transduction, CAR expression levels were checked. A minimum of 20% CAR positive cells was used for experiments. After 13 days of expansion, CAR Ts were frozen down in Cryostor CS10 at −80 °C and later used for coculture and in vivo experiments.

Statistics. For animal experiments, two-way analysis of variance (ANOVA) with Bonferroni correction posttest was used using Graphpad. In the rest of the cases, unpaired parametric *t* test was used using Excel. Data were considered significative when $p < 0.05$.

Reporting summary. Further information on research design is available in the Nature Research Reporting Summary linked to this article.

Data availability

The RNAseq data in this study have been deposited in Sequence Read Archive (SRA) database and are accessible through the SRA Bioproject accession code PRJNA674313 (https://www.ncbi.nlm.nih.gov/bioproject/?term=PRJNA674313). Source data are available as a Source Data file. The remaining data are available within the Article, Supplementary Information or available from the authors upon request.

Received: 28 October 2020; Accepted: 24 January 2021;
Published online: 23 February 2021

References

1. Goebeler, M.-E. & Bargou, R. C. T cell-engaging therapies—BiTEs and beyond. *Nat. Rev. Clin. Oncol.* **16**, 2825–434 (2020).
2. Singh, A. K. & McGuirk, J. P. CAR T cells: continuation in a revolution of immunotherapy. *Lancet Oncol.* **21**, e168–e178 (2020).
3. Rader, C. Bispecific antibodies in cancer immunotherapy. *Curr. Opin. Biotechnol.* **65**, 9–16 (2019).
4. Strohl & Naso. Bispecific T-cell redirection versus chimeric antigen receptor (CAR)-T cells as approaches to kill cancer cells. *Antibodies* **8**, 41–68 (2019).
5. Labrijn, A. F., Janmaat, M. L., Reichert, J. M. & Parren, P. W. H. I. Bispecific antibodies: a mechanistic review of the pipeline. *Nat. Rev. Drug Discov.* **18**, 585–608 (2019).
6. Schultz, L., Mackall, C. & Driving, C. A. R. T cell translation forward. *Sci. Transl. Med.* **11**, eaaw2127 (2019).
7. Clynes, R. A. & Desjarlais, J. R. Redirected T cell cytotoxicity in cancer therapy. *Annu. Rev. Med.* **70**, 437–450 (2019).
8. Slaney, C. Y., Wang, P., Darcy, P. K. & Kershaw, M. H. CARs versus BiTEs: a comparison between T cell-redirection strategies for cancer treatment. *Cancer Discov.* **8**, 924–934 (2018).
9. June, C. H. & Sadelain, M. Chimeric antigen receptor therapy. *N. Engl. J. Med.* **379**, 64–73 (2018).
10. Thakur, A., Huang, M. & Lum, L. G. Bispecific antibody based therapeutics: strengths and challenges. *Blood Rev.* **32**, 339–347 (2018).
11. Shah, N. N. & Fry, T. J. Mechanisms of resistance to CAR T cell therapy. *Nat. Rev. Clin. Oncol.* **16**, 372–385 (2019).
12. Kantarjian, H. et al. Blinatumomab versus chemotherapy for advanced acute lymphoblastic leukemia. *N. Engl. J. Med.* **376**, 836–847 (2017).
13. Locke, F. L. et al. Long-term safety and activity of axicabtagene ciloleucel in refractory large B-cell lymphoma (ZUMA-1): a single-arm, multicentre, phase 1-2 trial. *Lancet Oncol.* **20**, 31–42 (2019).

14. Bouchkouj, N. et al. FDA approval summary: axicabtagene ciloleucel for relapsed or refractory large B-cell lymphoma. *Clin. Cancer Res.* **25**, 1702–1708 (2019).
15. Rafiq, S., Hackett, C. S. & Brentjens, R. J. Engineering strategies to overcome the current roadblocks in CAR T cell therapy. *Nat. Rev. Clin. Oncol.* **17**, 147–167 (2020).
16. Arteaga, C. L. & Engelman, J. A. ERBB receptors: from oncogene discovery to basic science to mechanism-based cancer therapeutics. *Cancer Cell* **25**, 282–303 (2014).
17. Moody, S. E. et al. Conditional activation of Neu in the mammary epithelium of transgenic mice results in reversible pulmonary metastasis. *Cancer Cell* **2**, 11–11 (2002).
18. Rius Ruiz, I. et al. p95HER2-T cell bispecific antibody for breast cancer treatment. *Sci. Transl. Med.* **10**, eaat1445 (2018).
19. Thomas, D. A. & Massagué, J. TGF-beta directly targets cytotoxic T cell functions during tumor evasion of immune surveillance. *Cancer Cell* **8**, 369–380 (2005).
20. Smith, L. K. et al. Interleukin-10 directly inhibits CD8+ T cell function by enhancing N-glycan branching to decrease antigen sensitivity. *Immunity* **48**, 299–312 (2018). e5.
21. Kryczek, I. et al. B7-H4 expression identifies a novel suppressive macrophage population in human ovarian carcinoma. *J. Exp. Med.* **203**, 871–881 (2006).
22. Alspach, E., Lussier, D. M. & Schreiber, R. D. Interferon γ and its important roles in promoting and inhibiting spontaneous and therapeutic cancer immunity. *Cold Spring Harb. Perspect. Biol.* **11**, a028480 (2019).
23. Der, S. D., Zhou, A., Williams, B. R. & Silverman, R. H. Identification of genes differentially regulated by interferon alpha, beta, or gamma using oligonucleotide arrays. *Proc. Natl Acad. Sci. USA* **95**, 15623–15628 (1998).
24. Heintzman, N. D. et al. Histone modifications at human enhancers reflect global cell-type-specific gene expression. *Nature* **459**, 108–112 (2009).
25. Singh, N. et al. Impaired death receptor signaling in leukemia causes antigen-independent resistance by inducing CAR T-cell dysfunction. *Cancer Discov.* **10**, 552–567 (2020).
26. Löffler, A. et al. A recombinant bispecific single-chain antibody, CD19 x CD3, induces rapid and high lymphoma-directed cytotoxicity by unstimulated T lymphocytes. *Blood* **95**, 2098–2103 (2000).
27. Benmebarek, M.-R. et al. Killing mechanisms of chimeric antigen receptor (CAR) T cells. *Int. J. Mol. Sci.* **20**, 1283 (2019).
28. Offner, S., Hofmeister, R., Romaniuk, A., Kufer, P. & Baeuerle, P. A. Induction of regular cytolytic T cell synapses by bispecific single-chain antibody constructs on MHC class I-negative tumor cells. *Mol. Immunol.* **43**, 763–771 (2006).
29. Purbhoo, M. A., Irvine, D. J., Huppa, J. B. & Davis, M. M. T cell killing does not require the formation of a stable mature immunological synapse. *Nat. Immunol.* **5**, 524–530 (2004).
30. Kammertoens, T. & Blankenstein, T. It's the peptide-MHC affinity, stupid. *Cancer Cell* **23**, 429–431 (2013).
31. Purbhoo, M. A. et al. Quantifying and imaging NY-ESO-1/LAGE-1-derived epitopes on tumor cells using high affinity T cell receptors. *J. Immunol.* **176**, 7308–7316 (2006).
32. Kallioniemi, O. P. et al. ERBB2 amplification in breast cancer analyzed by fluorescence in situ hybridization. *Proc. Natl Acad. Sci. USA* **89**, 5321–5325 (1992).
33. Davenport, A. J. et al. Chimeric antigen receptor T cells form nonclassical and potent immune synapses driving rapid cytotoxicity. *Proc. Natl Acad. Sci. USA* **115**, E2068–E2076 (2018).
34. Bose, P. & Verstovsek, S. JAK2 inhibitors for myeloproliferative neoplasms: what is next? *Blood* **130**, 115–125 (2017).
35. Sachs, N. et al. A living biobank of breast cancer organoids captures disease heterogeneity. *Cell* **172**, 373–382 (2018). e10.
36. Yang, J., Pemberton, A., Morrison, W. I., Connelley, T. & Granzyme, B. Is an essential mediator in CD8+ T Cell Killing of *Theileria parva*-infected cells. *Infect. Immun.* **87**, 397 (2019).
37. Love, M. I., Huber, W. & Anders, S. Moderated estimation of fold change and dispersion for RNA-seq data with DESeq2. *Genome Biol.* **15**, 550 (2014).
38. Korotkevich, G., Sukhov, V. & Sergushichev, A. Fast gene set enrichment analysis. *bioRxiv* https://doi.org/10.1101/060012 (2019).
39. Liberzon, A. et al. The molecular signatures database hallmark gene set collection. *Cell Syst.* **1**, 417–425 (2015).

Acknowledgements

This work was supported by Breast Cancer Research Foundation (BCRF-20-08), Instituto de Salud Carlos III Project Reference number AC15/00062 and the EC under the framework of the ERA-NET TRANSCAN-2 initiative co-financed by FEDER, Instituto de Salud Carlos III (CB16/12/00449 and PI19/01181), and Asociación Española Contra el Cáncer (AECC). E.J.A. was funded by the Spanish Government (Juan de la Cierva Formación FJCI-2017-34900). Acknowledgements to the Cellex Foundation for providing research facilities and equipment. This research has been funded by the Comprehensive Program of Cancer Immunotherapy & Immunology (CAIMI) supported by the BBVA Foundation (grant 89/2017).

Author contributions

E.J.A. and A.M.S. designed and performed most experiments, interpreted, and analyzed the data, and revised the paper. I.R.R. and M.R. produced HER2-CAR T cells and revised the paper. M.E. and A.L. performed in vivo experiments. C.A.F. and A.G. designed the HER2-CAR T. C.K. provided the HER2-TCB, and corrected the paper. J. Arribas designed the study, interpreted the data, and wrote the paper.

Competing interests

C.K. declares employment, stock ownership, and patents with Roche. A.G. reports receiving funding from Novartis, VCNBiosciences and Merck KGaA, has received speaker honoraria from Roche, and has consulted for Achilles Therapeutics, Neon Therapeutics, Genentech, PACT Pharma and Oxford Immunotherapy. J.A. has received research funds from Roche, Synthon, Menarini, and Molecular Partners and consultancy honoraria from Menarini. The remaining authors declare no competing interests.

Additional information

Supplementary information The online version contains supplementary material available at https://doi.org/10.1038/s41467-021-21445-4.

Correspondence and requests for materials should be addressed to J.A.

Peer review information *Nature Communications* thanks the anonymous reviewers for their contribution to the peer review of this work. Peer review reports are available.

Reprints and permission information is available at http://www.nature.com/reprints

Publisher's note Springer Nature remains neutral with regard to jurisdictional claims in published maps and institutional affiliations.

Supplementary information

Acquired cancer cell resistance to T cell bispecific antibodies and CAR T targeting HER2 through JAK2 down-modulation

Enrique J. Arenas[1, 2, #], Alex Martínez-Sabadell[1, #], Irene Rius Ruiz[1,2], Macarena Román Alonso[1], Marta Escorihuela[1], Antonio Luque[1], Carlos Alberto Fajardo[3], Alena Gros[3], Christian Klein[4], Joaquín Arribas[1, 2, 5, 6, 7]

[1] Preclinical Research Program Vall d'Hebron Institute of Oncology (VHIO), Barcelona, 08035, Spain.

[2] Centro de Investigación Biomédica en Red de Cáncer, Monforte de Lemos, Madrid, 28029, Spain.

[3] Cancer Immunotherapy & Immunology CAIMI Program, VHIO, Barcelona, 08035, Spain.

[4] Roche Innovation Center Zurich, Roche Pharmaceutical Research and Early Development, Wagistrasse 18, 8952 Schlieren, Switzerland.

[5] Department of Biochemistry and Molecular Biology, Universitat Autónoma de Barcelona, Campus de la UAB, 08193, Bellaterra, Spain.

[6] Cancer Research Program, IMIM (Hospital del Mar Medical Research Institute), Barcelona, Spain.

[7] Institució Catalana de Recerca i Estudis Avançats (ICREA), 08010, Barcelona, Spain.

[#] These authors contributed equally

Corresponding Author:

Joaquín Arribas PhD

Vall d'Hebron Institute of Oncology (VHIO)

C/Natzaret, 115-117

Barcelona 08035, Spain

Phone: +34 93 274 6026

E-mail: jarribas@vhio.net

Supplementary Fig. 1: Co-culture assays to determine the activity of TCBs and CARs, expression of HER2 in parental BT474 cells and BT-R resistant cells and sensitivity to different antitumor treatments.

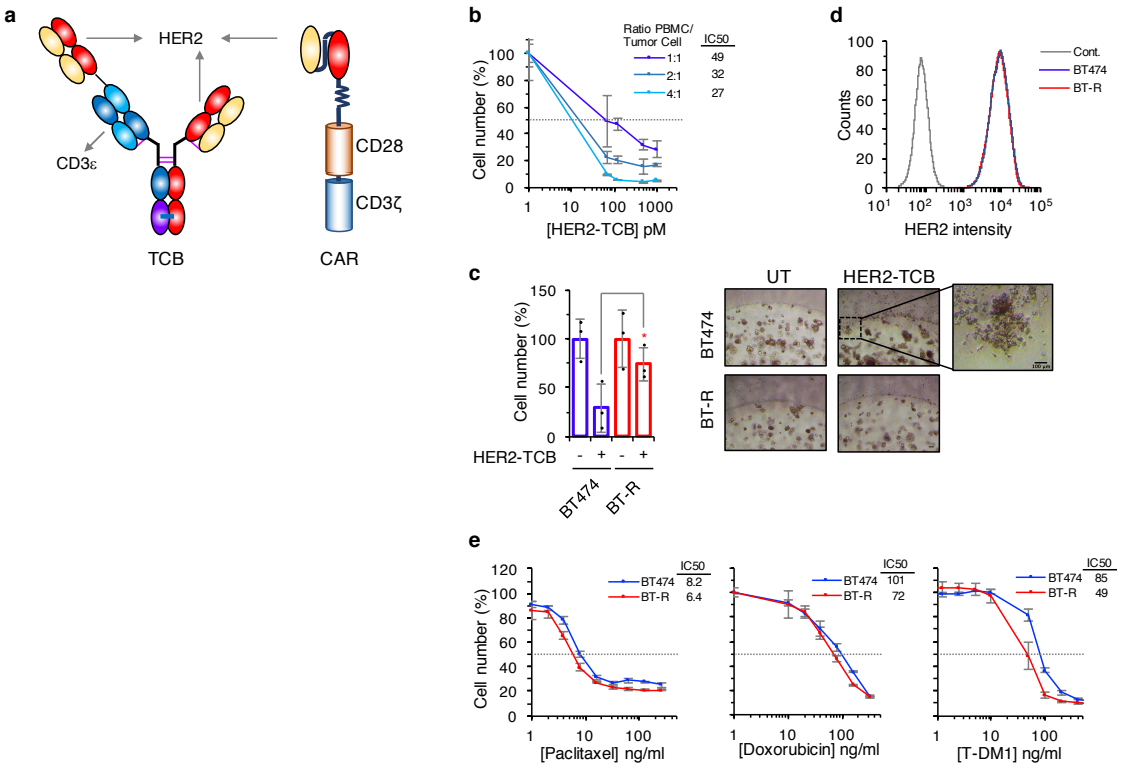

a, Schematic drawings of the HER2-TCB and HER2-CAR used in this study.

b, Co-cultures of PBMCs with BT474 cells at different ratios were treated with different concentrations of HER2-TCB for 72 h. Then, viable BT474 cells were quantified by flow cytometry using EpCAM as a marker.

c, Left, co-cultures of PBMCs with BT474 and resistant BT-R were grown in 3D and treated with 1 nM HER2-TCB for 72 h. Viable target cells were quantified as in **b** and normalized to untreated condition. *p=0.04, two-tailed t test.

Right, representative microphotographs of the 3D cultures.

d, Cells were stained with anti-HER2 and analyzed by flow cytometry. As control BT474 cells were stained with an irrelevant primary antibody.

e, Parental BT474 or resistant BT-R cells were treated with different concentrations of the indicated drugs. Treatment lasted 72 h in the chemotherapies treatments and 6 days in the T-DM1 experiment. Then, viable cells were quantified by the crystal violet assay.

Data are presented as mean ± SD of two (**b**) or three (**c**, **e**) independent experiments. Source data are provided as a Source Data file.

Supplementary Fig. 2: Cytokines and growth factors secreted and status of lymphocyte activation in co-cultures of parental BT474 cells and BT-R resistant cells.

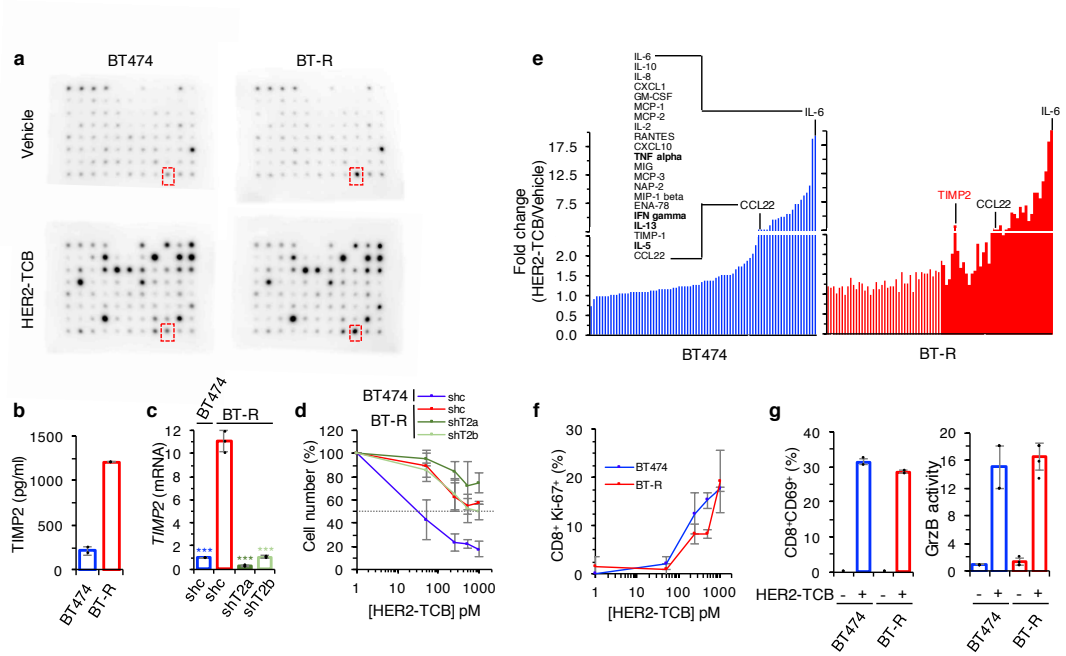

a, Analysis of a panel of cytokines and growth factors in the media conditioned by co-cultures of PBMCS with BT474 or BT-R cells treated with vehicle or HER2-TCB.

b, Expression of TIMP2 as determined by ELISA.

c, Expression of *TIMP2*, normalized to BT474, as determined by quantitative real-time PCR. ***p<0.001, two-tailed t test.

d, Co-cultures of PBMCs with the indicated cells were treated with different concentrations of HER2-TCB for 72 h. Then, viable target cells were quantified by flow cytometry using EpCAM as a marker.

e, Quantification of array showed in **a**. Data is shown as a fold change of co-cultures treated with HER2-TCB relative to co-cultures treated with vehicle. On the left and right, data on parental BT474 and BT-R, respectively.

f, The proliferation of lymphocytes was determined by Ki67 staining of $CD8^+$ cells in co-cultures treated with HER2-TCB for 72 h.

g, The percentage of $CD8^+CD69^+$ lymphocytes or Granzyme B activity were determined in co-cultures of PBMCs with parental BT474 or BT-R cells treated with 67.5 pM of the HER2-TCB for 72 h. $CD8^+CD69^+$ positivity was determined by flow cytometry. Granzyme B was measured by using the granzyme B substrate Ac-IEPD-pNA. Color reaction generated by the cleavage of the pNA substrate was measured. Results were normalized to untreated BT474 cells.

Data are presented as mean ± SD of two (**b**, **f**, **g** left), three (**c**, **d**), or four (**g** right) independent experiments. Source data are provided as a Source Data file.

Supplementary Fig. 3: IFN-γ signaling in cells knock-down or KO for IFNGR1 and knock-down of JAK1 and STAT1.

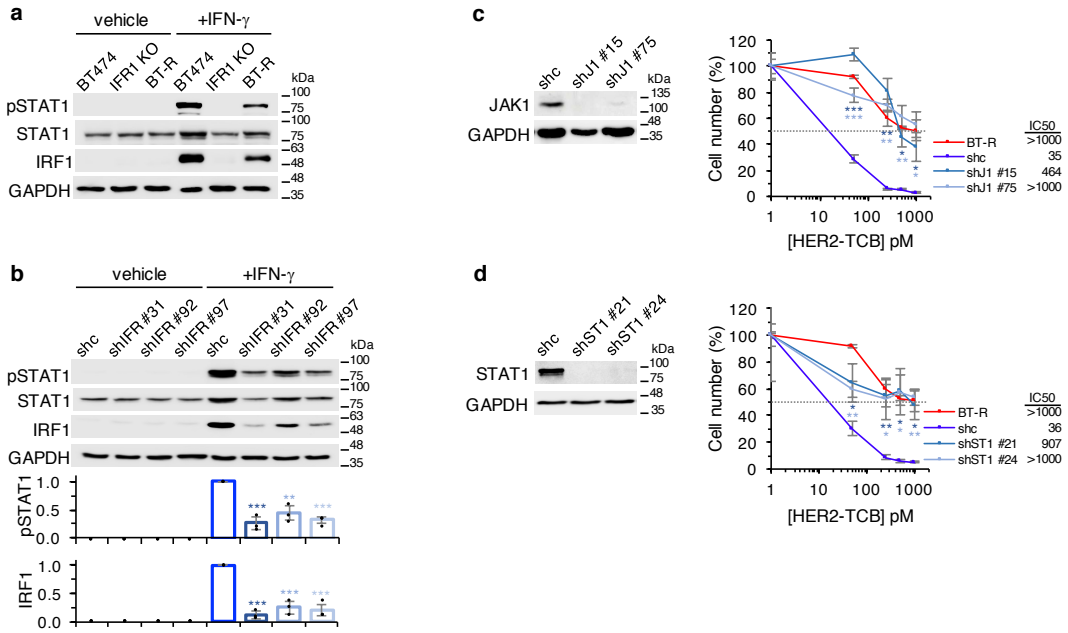

a, **b**, Western blot analysis of the expression of components of the IFN-γ intracellular signaling pathway components. Results were normalized to treated BT474 cells. **p=0.03, ***p<0.001, two-tailed t test.

c, d, Left, BT474 cells expressing control shRNA (shc) or shRNAs targeting JAK1 (shJ1) or STAT1 (shST1) were lysed and analyzed by Western blot with the indicated antibodies. Right, Co-cultures of PBMCs with BT-R cells or BT474 expressing the indicated shRNAs were treated with different concentrations of HER2-TCB for 72 h. Then, viable cells were quantified by flow cytometry using EpCAM as a marker. ***p<0.001, **p=0.005, *p=0.01, *p=0.03 (shJ1 #15), ***p<0.001, **p=0.002, **p=0.009, *p=0.01 (shJ1 #75); *p=0.03, **p=0.007, *p=0.01, *p=0.02 (shST1 #21); **p=0.003, *p=0.04, *p=0.04, **p=0.0042 (shST1 #24), two-tailed t test.

Data are presented as mean ± SD of three independent experiments. Source data are provided as a Source Data file.

Supplementary Fig.4: Role of IFN-γ signaling in the response of different HER2-positive cancer models to HER2-TCB.

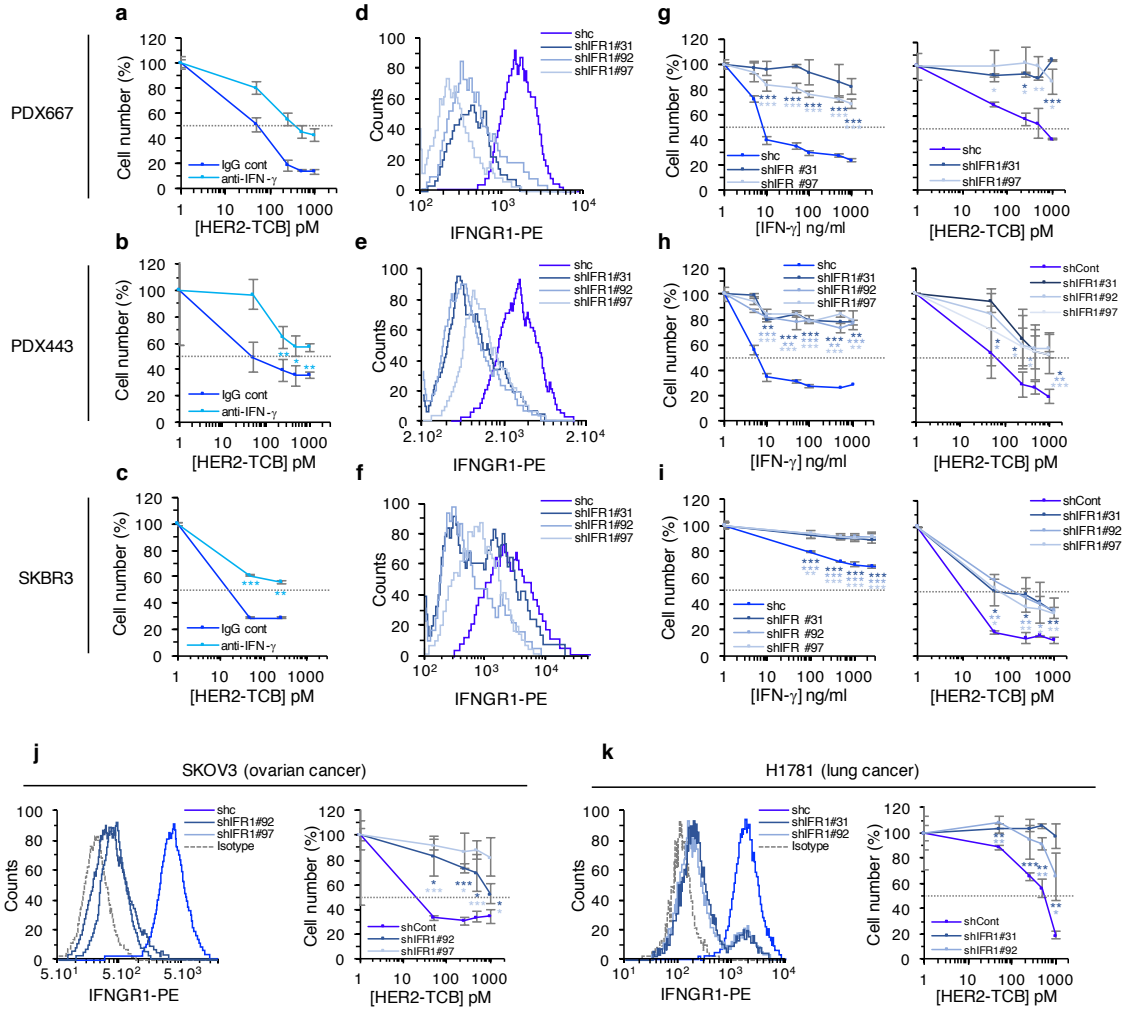

a, **b**, **c**, Co-cultures of PBMCs with the indicated breast cancer-derived cells were treated with different concentrations of HER2-TCB in presence of an IgG control or an IFN-γ blocking antibody for 72 h. Then, viable target cells were quantified by flow cytometry using EpCAM as a marker. Results are expressed as averages ± SD of two, four and three independent experiments, respectively.

d, **e**, **f**, Cells were stained with anti-IFNGR1 and analyzed by flow cytometry.

g, **h**, **i**, Left, the indicated cells were treated with different concentrations of IFN-γ for 5 days. Cell numbers were estimated with the crystal violet staining assay. The results of three independent experiments are expressed as averages ± SD.

Right, the indicated cells were treated with different concentrations of HER2-TCB and analyzed as in **a**, **b**, **c**.

j, k, Left, cells were analyzed as in **d**, **e**, **f**.

Right, cultures from the cell lines SKOV3 and H1781 derived from ovary and lung cancers respectively, were treated and analyzed as in **g**, **h**, **i**. Results are expressed as averages ± SD of three independent experiments.

(**b**) **p=0.008, *p=0.018, **p=0.007. (**c**) ***p<0.001, **p=0.002. (**g**) left, ***p<0.001; right, *p=0.04, ***p<0.001 (shIFNGR1 #31); *p=0.049, *p=0.013. **p=0.003, *p=0.012 (shIFNGR1 #97). (**h**) left, **p=0.002, ***p<0.001, **p=0.002 (shIFNGR1 #31); ***p<0.001, **p=0.002, **p=0.001 (shIFNGR1 #92); ***p<0.001, **p=0.007 (shIFNR1 #97); right, *p=0.02, *p=0.046, *p=0.01 (shIFNGR1 #31); *p=0.04, *p=0.014, **p=0.003 (shIFNGR1 #92); *p=0.02, *p=0.02, ***p<0.001 (shIFNGR1 #97). (**i**) left, **p=0.002, ***p<0.001; right, *p=0.04, *p=0.04, **p=0.005 (shIFNGR1 #31); **p=0.004, **p=0.005, *p=0.02 (shIFNGR1 #92); *p=0.012, **p=0.008, *p=0.013, **p=0.0014 (shIFNGR1 #97). (**j**) *p=0.03, ***p<0.001, *p=0.04, *p=0.04 (shIFNGR1 #92); ***p<0.001, *p=0.02, *p=0.02 (shIFNGR1 #97). (**k**) **p=0.005, ***p<0.001, **p=0.004, **p=0.002 (shIFNGR1 #31); **p=0.008, **p=0.007, *p=0.046 (shIFNGR1 #92). Two-tailed t test. Source data are provided as a Source Data file.

Supplementary Fig. 5: Resistance stability of BT-R cells and IFN-γ signaling in BT-R, BT474 or BT-RG cells engineered to gain or silence the expression of JAK2.

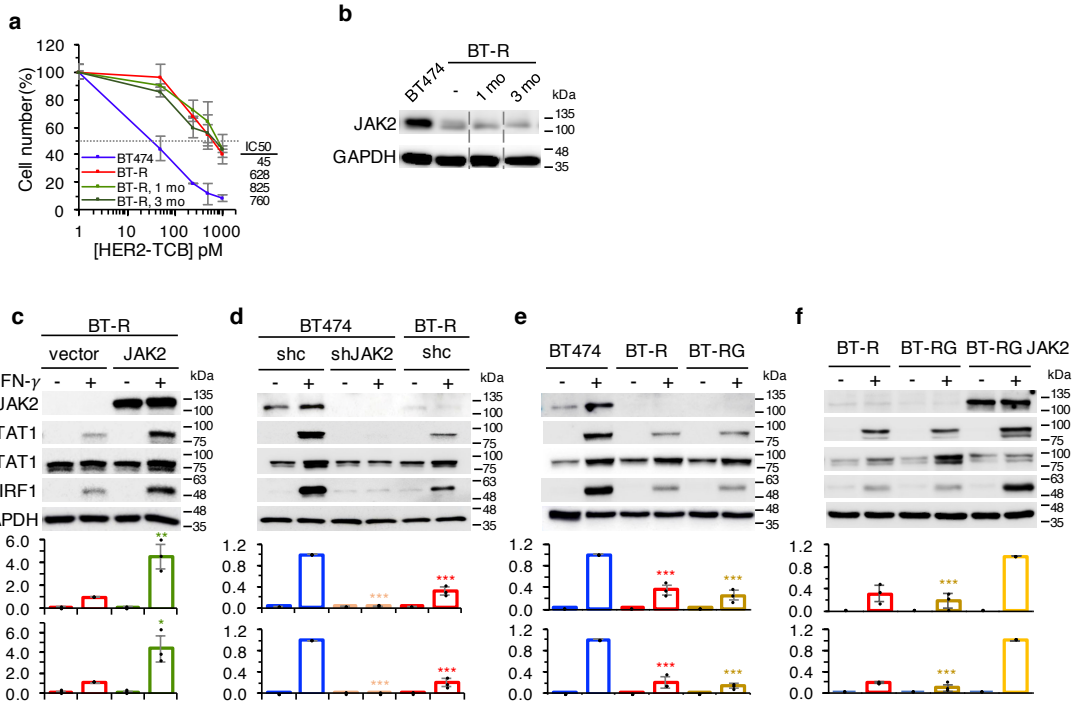

a, Co-cultures of PBMCs with parental BT474 or resistant BT-R cells kept under selective pressure or cultured in normal medium during 1 or 3 months were treated with different concentrations of HER2-TCB for 72 h. Then, viable cells were quantified by flow cytometry using EpCAM as a marker.

b, Levels of JAK2 as determined by Western blot on the same cells as in **a**.

c-f, Western blot analysis of the expression of components of the IFN-γ intracellular signaling pathway components.

(**c**) **p=0.009, *p=0.02. (**d**, **e**, **f**) ***p<0.001, two-tailed t test. Data are presented as mean ± SD of two (**a**) or three (**c**, **d**, **e**, **f**) independent experiments. Source data are provided as a Source Data file.

Supplementary Fig. 6: Generation of additional models of resistance to HER2-TCB in vivo.

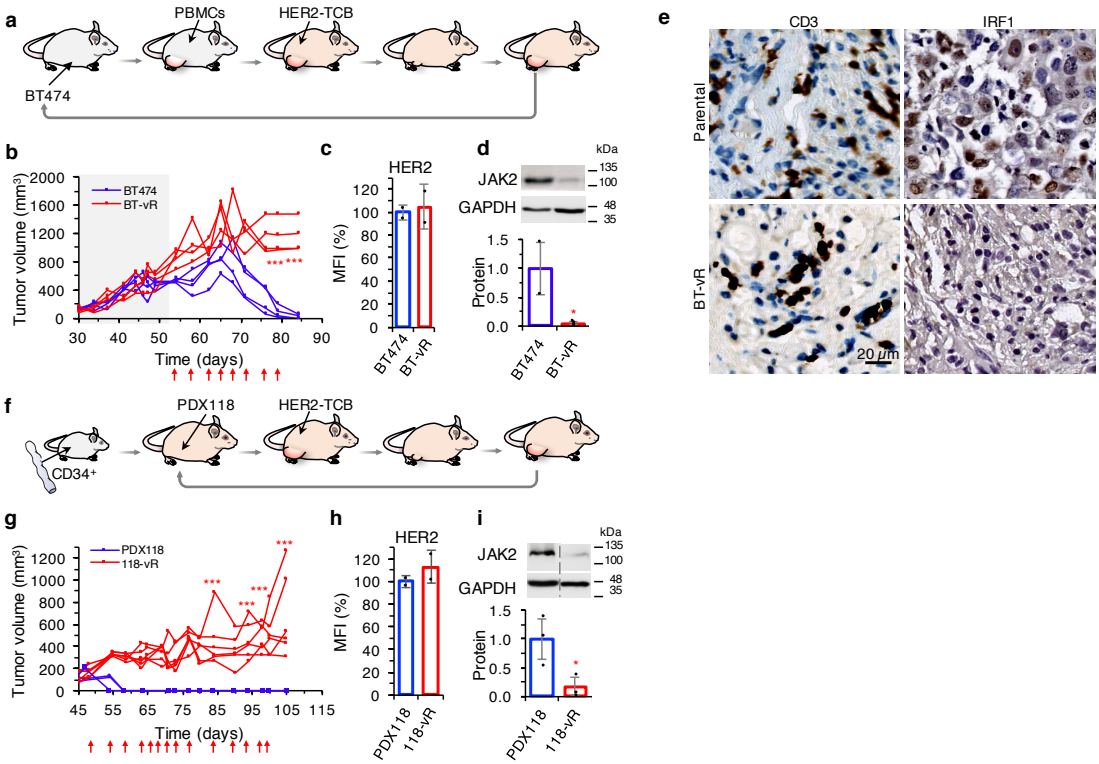

a, Schematic showing the generation of additional models. 10^7 BT474 cells were injected orthotopically into NSG mice. When tumors reached ~200 mm^3, 10^7 PBMCs were injected i.p. Then animals were treated i.v. with an increasing concentration of HER2-TCB. Tumors were allowed to regrow, excised, and injected again into NSG mice.

b, Mice were injected with 10^7 BT474 or BT-vR cells and treated with 0.25 mg/kg HER2-TCB. Treatments are indicated by red arrows. Tumor volumes of individual mice are represented (n=4 per group).

c, Cells were stained with anti-HER2 and analyzed by flow cytometry. Quantitative data, normalized to BT474, corresponds to averages ± SD of two determinations.

d, Levels of JAK2 as determined by Western blot. Quantitative data, normalized to BT474, corresponds to averages ± SD of two different parental and four different resistant tumor determinations.

e, Representative immunohistochemical staining of hCD3 and hIRF1 in tumor sections. Images are representative of all tumors in **b**.

f, Schematic showing the generation of additional models. PDX118 was grafted in mice humanized with $CD34^+$ cells. When tumors reached ~200 mm^3, animals were treated i.v. with an increasing concentration of HER2-TCB. Tumors were allowed to regrow and treatment was repeated.

g, Mice humanized with $CD34^+$ cells were grafted with PDX118, or 118-vR tumors. Mice were treated i.v. with 0.25 mg/kg HER2-TCB. Tumor volumes of individual mice are represented (PDX118, n=3; 118-vR, n=6).

h, **i**, Levels of HER2 or JAK2 were determined as in **c**, **d**. Quantitative data corresponds to averages ± SD of two (**h**) and three (**i**) determinations.

(**d**) *p=0.02. (**i**) *p=0.04, two-tailed t test. (**b** and **g**) ***p<0.001, two-way ANOVA and Bonferroni correction. Source data are provided as a Source Data file.

Supplementary Fig. 7: Models of resistance to IFN-γ are also resistant to HER2-TCB because of JAK2 downmodulation.

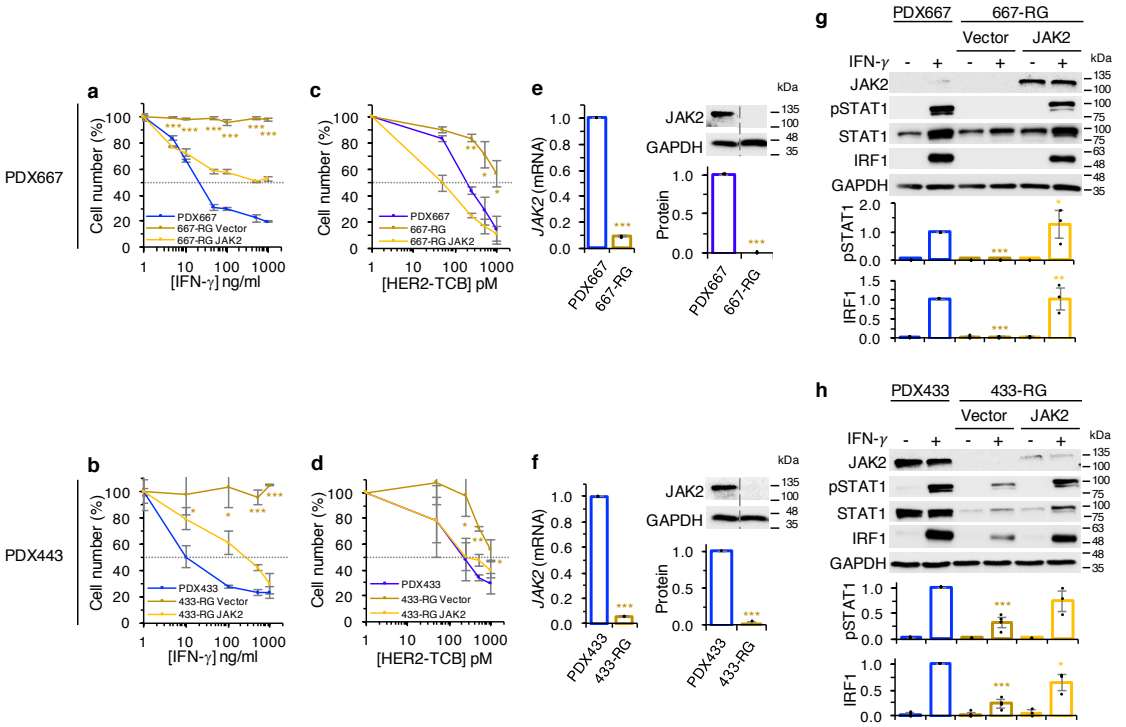

a, **b**, The indicated cells were treated with different concentrations of IFN-γ for 5 days. Cell numbers were estimated with the crystal violet staining assay.

c, **d**, Co-cultures of the indicated cells were treated with different concentrations of HER2-TCB for 72 h. Then, viable cells were quantified by flow cytometry using EpCAM as a marker.

e, **f**, The levels of JAK2 (mRNA and protein) as determined by quantitative real-time PCR (left) or Western blot (right). Results were normalized to parental cells.

g, **h**, Western blot analysis of the expression of components of the IFN-γ intracellular signaling pathway components. Results were normalized to treated parental cells.

(**a**) ***p<0.001. (**c**) **p= 0.004, *p=0.012, p*=0.02. (**e**) ***p<0.001. (**g**) *p=0.02, **p=0.008, ***p<0.001. (**b**) *p=0.018, *p=0.014, ***p<0.001. (**d**) *p=0.02, **p=0.002, *p=0.013. (**f**) ***p<0.001. (**h**) *p=0.04, ***p<0.001, two-tailed t test. Data are presented as mean ± SD of three independent experiments. Source data are provided as a Source Data file.

Supplementary Fig. 8: Gating strategies used for functional assays, protein expression and cell sorting.

Gating strategy I

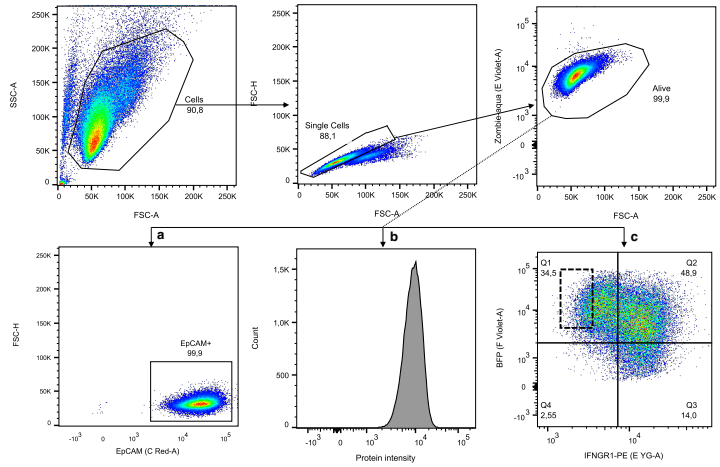

Gating strategy II

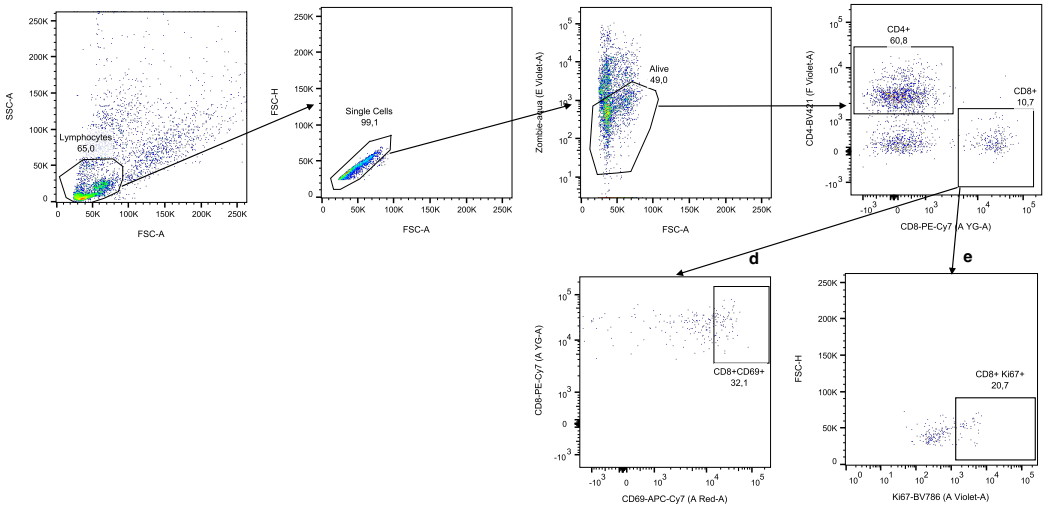

a, Gating strategy to obtain EpCAM^{+} cell counts in functional T cell cytotoxicity assays presented on **Fig. 1b,1f, Fig. 3a, b,g,h, Fig. 5b,c,g,h, Fig. 6b,c,g,h, Supplementary Fig. 1b,c, Supplementary Fig. 2d, Supplementary Fig. 3c,d, Supplementary Fig. 4a-c,g-k, Supplementary Fig. 5a, Supplementary Fig 7c,d**.

b, Gating strategy to measure MFI for a particular surface protein: HER2 (presented on **Supplementary Fig. 1d, Supplementary Fig. 6c**,**h**), HER2-TCB binding (presented on **Fig 1j**), IFNGR1 (presented on **Fig. 3e, Fig. 4c, Supplementary Fig. 4d-f,j,k**), IFNGR2 (presented on **Fig. 4c**), PDL1, PDL2, CD80, CD86, Galectin-9, B7-H3, B7-H4, HVEM, ICOS-L, 41BB-L, OX40-L (presented on **Fig. 1k**). Same strategy was used for Annexin V^{+} analysis presented on **Fig. 3d**, but in this case the viability marker used was PI.

c, Gating strategy to sort BFP^{high}/IFNGR1 (square dashes) negative expressing cells from BT474 cells expressing Cas9 and a CRISPR gRNA targeting IFNGR1, used for in vitro cytotoxic assays (presented on **Fig. 3f-h**) and in vivo (presented on **Fig. 3i**).

d, e, Gating strategy to obtain the % of CD69^{+} (**d**) and Ki67^{+} cells (**e**) from CD8^{+} cells used in functional in vitro T cell cytotoxicity assays, presented on **Supplementary Fig. 2f** and **g**.

2. The target antigen determines the mechanism of acquired resistance to T cell-based therapies

Cell Reports

Article

The target antigen determines the mechanism of acquired resistance to T cell-based therapies

Graphical abstract

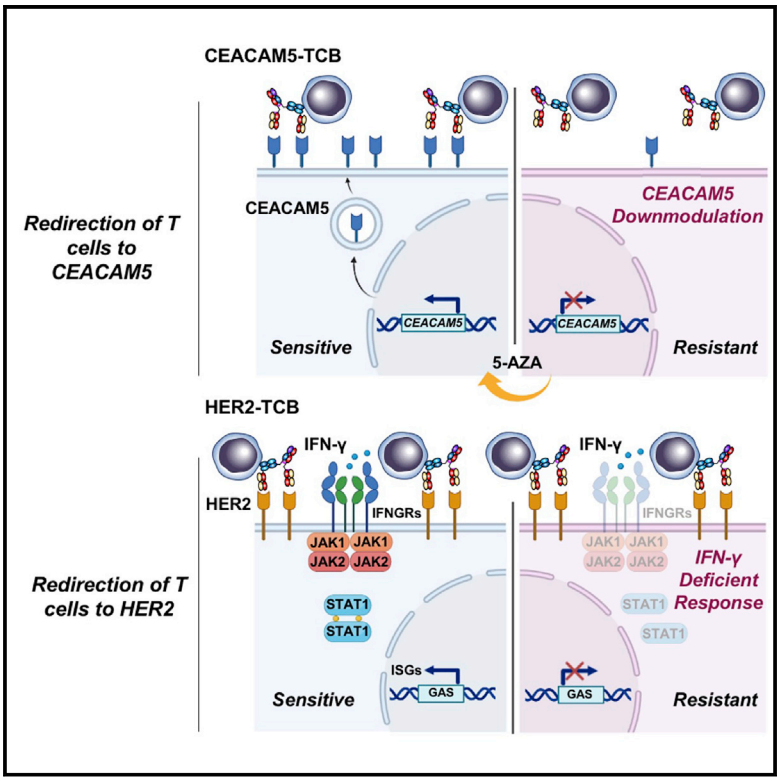

Authors

Alex Martínez-Sabadell, Beatriz Morancho, Irene Rius Ruiz, ..., Marina Bacac, Joaquín Arribas, Enrique J. Arenas

Correspondence

earenas@vhio.net (E.J.A.), jarribas@imim.es (J.A.)

In brief

Despite the success of immunotherapy, cancer patients eventually progress due to the emergence of resistance. Martínez-Sabadell et al. show that different mechanisms of acquired resistance to T cell engaging bispecific antibodies emerge depending on the selected tumor antigen. These data will help to anticipate mechanisms and approaches to tackle resistances.

Highlights

- Different mechanisms of resistance to TCBs emerge depending on the targeted tumor antigen
- Acquired resistant cells to a TCB targeting CEACAM5 exhibit reduced antigen expression
- 5-AZA overcomes resistance to CEACAM5-TCB by recovering the expression of CEACAM5
- Resistance to HER2-TCB in contrast is mediated by downmodulation of IFN-γ signaling

Martínez-Sabadell et al., 2022, Cell Reports *41*, 111430
October 18, 2022
https://doi.org/10.1016/j.celrep.2022.111430

CellPress

Cell Reports

CellPress
OPEN ACCESS

Article

The target antigen determines the mechanism of acquired resistance to T cell-based therapies

Alex Martínez-Sabadell,[1,2,3,4,10] Beatriz Morancho,[1] Irene Rius Ruiz,[1,2] Macarena Román Alonso,[1] Pablo Ovejero Romero,[1] Marta Escorihuela,[1] Irene Chicote,[5] Hector G. Palmer,[5] Lara Nonell,[6] Mercè Alemany-Chavarria,[6] Christian Klein,[7] Marina Bacac,[7] Joaquín Arribas,[1,2,3,8,9,*] and Enrique J. Arenas[1,2,10,11,*]

[1]Preclinical Research Program, Vall d'Hebron Institute of Oncology (VHIO), 08035 Barcelona, Spain
[2]Centro de Investigación Biomédica en Red de Cáncer, Monforte de Lemos, 08029 Madrid, Spain
[3]Cancer Research Program, Institut Hospital del Mar d'Investigacions Mèdiques (IMIM), 08003 Barcelona, Spain
[4]Department of Biochemistry and Molecular Biology, Universitat Autónoma de Barcelona, 08193 Bellaterra, Spain
[5]Translational Program, Stem Cells and Cancer Laboratory (VHIO), 08035 Barcelona, Spain
[6]Bioinformatic Unit (VHIO), 08035 Barcelona, Spain
[7]Roche Innovation Center Zurich, Roche Pharma Research and Early Development, pRED, Zurich, Switzerland
[8]Department of Medicine and Life Sciences, Universitat Pompeu Fabra, 08003 Barcelona, Spain
[9]Institució Catalana de Recerca i Estudis Avançats (ICREA), 08010 Barcelona, Spain
[10]These authors contributed equally
[11]Lead contact
*Correspondence: earenas@vhio.net (E.J.A.), jarribas@imim.es (J.A.)
https://doi.org/10.1016/j.celrep.2022.111430

SUMMARY

Despite the revolution of immunotherapy in cancer treatment, patients eventually progress due to the emergence of resistance. In this scenario, the selection of the tumor antigen can be decisive in the success of the clinical response. T cell bispecific antibodies (TCBs) are engineered molecules that include binding sites to the T cell receptor and to a tumor antigen. Using gastric CEA$^+$/HER2$^+$ MKN45 cells and TCBs directed against CEA or HER2, we show that the mechanism of resistance to a TCB is dependent on the tumor antigen. Acquired resistant models to a high-affinity-CEA-targeted TCB exhibit a reduction of CEA levels due to transcriptional silencing, which is reversible upon 5-AZA treatment. In contrast, a HER2-TCB resistant model maintains HER2 levels and exhibit a disruption of the interferon-gamma signaling. These results will help in the design of combinatorial strategies to increase the efficacy of cancer immunotherapies and to anticipate and overcome resistances.

INTRODUCTION

Immunotherapeutic agents have revolutionized anticancer therapy, providing a potentially curative option for patients who are refractory to standard treatments (Mellman et al., 2011). Bispecific antibodies (TCBs) or chimeric antigen receptors (CARs) are promising immunotherapies that have been recently approved for the treatment of some hematologic malignancies (Kantarjian et al., 2017; Locke et al., 2019; Bouchkouj et al., 2019; Velasquez et al., 2018).

In contrast to conventional targeted therapies (Sabnis and Bivona, 2019; Ellis and Hicklin, 2009), TCBs and CARs targeting different antigens have the same mechanism of action, namely activating T cells to kill tumor cells (Cohen et al., 2020; Slaney et al., 2018). As a consequence, independently of the TCB/CAR-targeted antigen, the same mechanism of resistance may be expected, particularly when it comes to parameters related to T cell functionality. Several studies and clinical evidence point out that antigen loss is one of the most frequent mechanisms of resistance to the redirection of CAR T therapies in hematological diseases (Shah and Fry, 2019; Song et al., 2019). However, there is no evidence that this also applies to TCBs and whether this is a random event, or if the biology of the antigen plays an important role in the mechanism of resistance.

Carcinoembryonic antigen (CEA) is a tumor-associated antigen that is upregulated in several types of cancer, including colorectal cancer (CRC). Patients who harbor microsatellite stability (MSS) subtype CRC have a poor response to immunotherapeutic agents, such as anti-PD1 or CTLA-4 blockade (Le et al., 2017). Therefore, CEA is an attractive target for the treatment of these patients. Previously, it has been pre-clinically reported that CEA expression is a major determinant of efficacy of CEA-TCB, independent of the tumor-driving gene, such as APC, TP53, KRAS, or BRAF (Bacac et al., 2016a,b) and a CEA-TCB is currently being evaluated in clinical trials. Differently from hematological malignancies, the development of TCBs in solid tumors has been more challenging. In this regard, as for most of therapies, the occurrence of primary or acquired resistance is a limiting factor

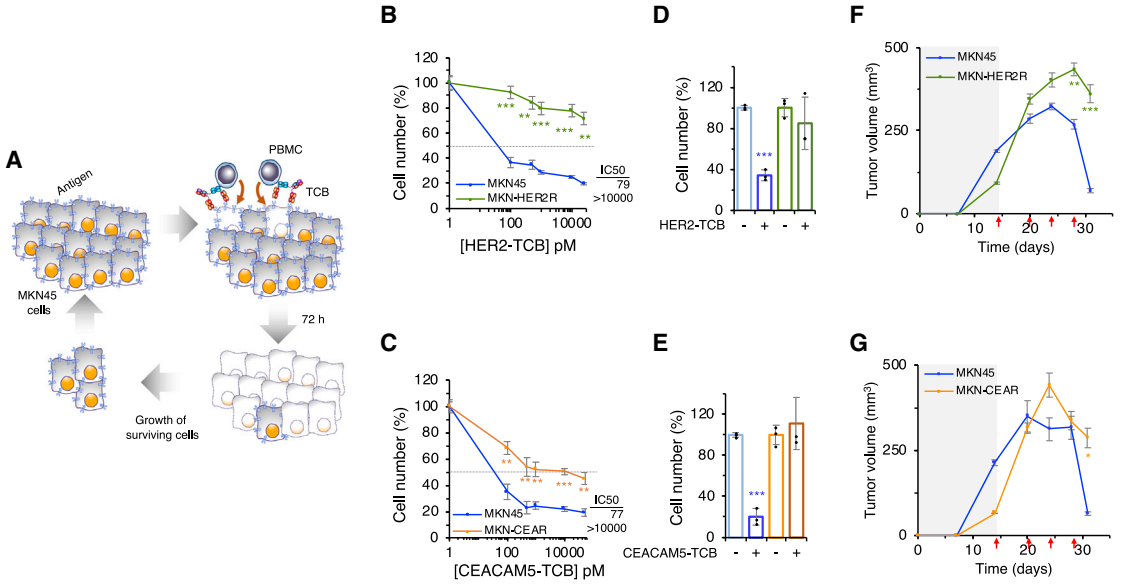

Figure 1. Generation and characterization of MKN45 resistant cells

(A) Schematic showing the generation of resistant cells to TCB targeting CEA or HER2 in the MKN45 cell line model.

(B and C) Co-cultures of PBMCs with parental MKN45 or resistants MKN-HER2R or MKN-CEAR cells were treated with different concentrations of HER2-TCB or CEACAM5-TCB (PBMC:target cell ratio 1:1) for 72 h. Then, viable cells were quantified by flow cytometry using EpCAM as a marker.

(D and E) MKN45 and MKN-HER2R or MKN-CEAR cells were grown in 3D and treated in co-culture with PBMCs at a 2:1 ratio with 1 nM HER2-TCB (D) or 5:1 ratio with 500 pM CEACAM5-TCB (E) for 72 h. Viable target cells were quantified as in (B).

(F and G) 10^6 MKN45 and MKN-HER2R or MKN-CEAR cells were injected subcutaneously into NSG mice. When tumors reached ~150 mm^3 (dark background), 10^7 PBMCs were injected intraperitoneally. Then animals were treated intravenously with 0.125 mg/kg HER2-TCB or 1 mg/kg CEACAM5-TCB as indicated (red arrows). Tumor volumes are represented as averages ± SEM. (F) MKN45, n = 11; MKN-HER2R, n = 7, (G) n = 5 per arm. (B–E) **p < 0.01, ***p < 0.001, two-tailed t test. (F and G) *p < 0.05, **p < 0.01, ***p < 0.001, two-way analysis of variance (ANOVA) and Bonferroni correction. (B–E) Data are presented as mean ± SD of three independent experiments.

and remains biologically one of the most important elements to study. As a consequence, intense research led to the identification of different mechanisms of resistance (Rafiq et al., 2020).

Human epidermal growth factor 2 (HER2) is a receptor tyrosine kinase overexpressed in 25% of breast and gastric cancers (Arteaga and Engelman, 2014), and its downregulation may lead to tumor regression (Moody et al., 2002). Despite the success of anti-HER2 therapies such as the monoclonal antibodies trastuzumab, pertuzumab, T-DM1 and DS-9201 (trastuzumab-deruxtecan), or the inhibitors Lapatinib and Neratinib, a high proportion (40%) of advanced breast cancer cases progress (Arteaga and Engelman, 2014). Therefore, there is a clinical need to develop more effective treatments against HER2-driven tumors. Previously, a highly efficacious HER2-TCB demonstrated robust potency in HER2-overexpressing tumor models (Junttila et al., 2014; Slaga et al., 2018), and currently there is a phase I clinical trial using the HER2 T cell dependent bispecific antibody in patients with locally advanced or metastatic HER2-expressing cancers (NCT03448042). However, little is known about the mechanisms of resistance against TCBs, and there is a need to anticipate them.

Using as a model the gastric $HER2^+/CEA^+$ MKN45 cell line, and TCBs targeting CEA or HER2, here we describe different mechanisms of resistance of redirected T cells depending on the selected antigen. We further confirm this evidence by generating different cell lines and patient-derived xenograft (PDX) models with acquired resistance. These results should be taken into consideration when designing combinatorial strategies to increase the efficacy of cancer immunotherapies.

RESULTS

Characterization of models of acquired resistance to cell killing by redirected lymphocytes

To generate an experimental model of resistance to cell killing mediated by different TCBs, we chronically treated *in vitro* the gastric cancer $CEA^+/HER2^+$ MKN45 cell line in co-culture either with a high-affinity CEA-targeting TCB (CEACAM5-TCB) (Teijeira et al., 2022) or HER2-TCB (Arenas et al., 2021) for 6 months with increasing concentrations of TCBs at a 3:1 ratio of PBMCs:MKN45 cells (Figures 1A and S1A). As a result, we generated two cell lines, MKN-HER2R, resistant to HER2-TCB, and MKN-CEAR, with lower sensitivity to CEACAM5-TCB, both with a half maximal inhibitory concentration (IC50) for the respective TCB more than 100-fold higher than that of parental cells (79 pM versus > 10 nM in MKN-HER2R and 77 pM versus > 10 nM in MKN-CEAR) (Figures 1B and 1C). This decrease in sensitivity (hereafter resistance) was also observed in both models in three-dimensional cultures (Figures 1D and 1E) and *in vivo* (Figures 1F, 1G, and S1B).

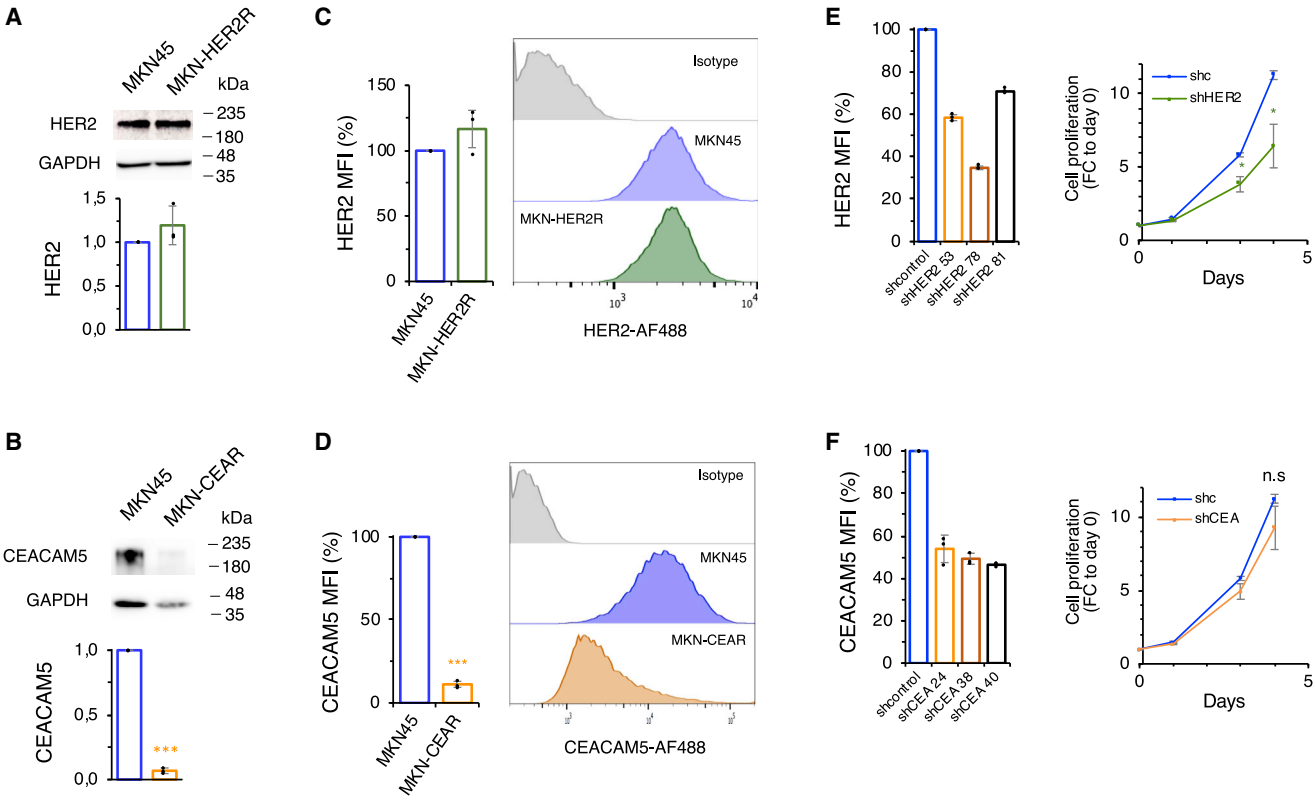

Figure 2. The target antigen determines the mechanism of resistance to TCBs

(A and B) The levels of HER2 or CEA were determined by western blot and normalized to MKN45 cells.

(C and D) The levels of HER2 or CEA were determined by flow cytometry and normalized to MKN45 cells.

(E and F) Left, MKN45 cells downmodulating HER2 or CEACAM5 were stained with anti-HER2 or anti-CEACAM5 and analyzed by flow cytometry. Quantification is normalized to short hairpin RNA control (shcontrol). Right, the same cells were cultured and its proliferation was assayed by crystal violet staining assay. The results of the three independent downmodulating cell lines (shHER2 #53, #78, #81 and shCEA #24, #38, and #40) are shown. (A–F) *p < 0.05, ***p < 0.001, two-tailed *t* test. (A-D) Data are presented as mean ± SD of three independent experiments.

Analysis by RNA sequencing showed more than 500 genes acutely up- or downregulated in resistant cells compared with parental MKN45 (adjusted p value < 0.05 and |logFC| > 1). Gene set enrichment analysis identified a significant number of processes differentially expressed between the conditions (Figure S2), showing the differences between resistant and sensitive cells.

Therefore, these models were used to study whether the mechanism of resistance is dependent on the tumor antigen.

CEA expression is reduced in CEACAM5-TCB acquired resistant cells

We analyzed protein levels of both, HER2 and CEA, in acquired resistant cells (Figures 2A–2D). CEACAM5-TCB resistant cells exhibit lower CEA protein expression level. In addition, analysis of 24 clones showed that there is no heterogeneity in MKN-CEAR cells (Figure S3A). In contrast, HER2-TCB resistant cells maintain levels of HER2.

To further characterize these models, we assessed lymphocyte activation and functionality. Analysis of different markers of T cell activation such as CD25 and CD69, and functionality by means of IFN-γ release and granzyme B activity, showed that the activation of lymphocytes by MKN45 and the MKN-HER2R is very similar, as the levels of the antigen are equal between parental and resistant cells. In contrast, the activation of lymphocytes by the acquired resistant model MKN-CEAR is significantly reduced, because these cells decrease the levels of the antigen and therefore lymphocytes cannot be properly activated (Figure S3B). In addition, this disruption in the activation of lymphocytes in the MKN-CEAR resistance model, but not in the MKN-HER2R, was observed by means of CD25 immunohistochemical staining in *in vivo* tumors from Figures 1F and 1G (Figure S3C).

We reasoned that this difference can be due to the dependence of HER2 in tumor progression. In order to demonstrate this hypothesis, we modified MKN45 cells with short hairpin RNA (shRNA) against HER2 and CEA. Results showed that, in contrast to CEA, cells modified with shHER2 proliferated less (Figures 2E and 2F). This evidence suggests that HER2-TCB-resistant cells do not downmodulate HER2 because its proliferation depends on its expression, even though MKN45 cells are not amplified for HER2. Of note, we previously described that resistance to HER2-TCB does not lead to the downregulation of HER2 levels in another tumor type such as HER2-amplified breast cancer (Arenas et al., 2021).

Interestingly, in order to reproduce a more heterogeneous and realistic scenario, which is what happens in the clinic, we performed bystander experiments by mixing parental and resistant cells stably expressing different fluorescent protein reporters, and comparing the cytotoxic effect of the TCBs in pure and mixed populations *in vitro* and *in vivo*. The results clearly showed that there is no bystander effect in any of the two resistant models *in vitro* and *in vivo* (Figure S4).

Collectively, these results demonstrate that depending on the tumor antigen, the mechanism of resistance differs.

Reduction of CEA antigen expression is a common mechanism across different acquired resistant models

To demonstrate that the downregulation of CEA expression may be a mechanism of resistance common to many tumors, we generated an additional *in vitro* acquired resistance model in a low CEA-expressing CRC cell line, the SW1222 (Figure S5). The CEACAM5-TCB-resistant model SW-CEAR showed downregulation of CEA (Figure S6A). Furthermore, overexpression of CEA in the MKN-CEAR and SW-CEAR models restores sensitivity, showing the causal role of CEA levels in affecting the activity of CEACAM5-TCB (Figures 3A and S6B). To further explore why CEACAM5-TCB-resistant cells downregulate CEA, we hypothesized that this regulation was at the transcriptional level. Confirming this hypothesis, both SW-CEAR and MKN-CEAR models downregulate *CEA* mRNA expression. In addition, when we treated resistant cells with the DNA demethylating agent 5-Azacytidine (5-AZA), cells recovered *CEA* expression at the level of parental cells (Figures 3B and S6C). In addition, this *CEA* recovery was paralleled to the expression at the surface and with a sensitivity to CEACAM5-TCB upon 5-AZA treatment (Figures 3C, 3D, S6D, and S6E). Interestingly, we observed that cells treated with 5-AZA for 48 h and then kept without the drug for up to 1 month did not recover the downmodulation of CEA protein levels, demonstrating that the upregulation of CEA due to the 5-AZA effects is irreversible (Figure S6F). Confirming the relevance of these *in vitro* results, strikingly, combination effect of 5-AZA with the CEACAM5-TCB led to a significant tumor reduction of resistant tumors (Figure 3E). In concordance, treatment with 5-AZA *in vivo* recovered partially CEA expression at the transcription and protein level (Figures 3F and 3G). To elucidate the mechanistic insight on the epigenetic silencing of *CEACAM5*, first we studied the *CEACAM5* loci on the genome browser, in which we found few CpG sites, suggesting that in principle, the *CEACAM5* loci is not likely to be methylated. Confirming this observation, Methylated DNA immunoprecipitation (MeDIP) showed no significant differences in the methylation status of the *CEACAM5* loci between resistant and sensitive cells. In addition, we did not see biological differences that could explain the recovery of CEACAM5 by 5-AZA treatment in resistant cells (Figure S7A). Furthermore, direct analysis of H3K27Ac and H3K27Me3 histone marks by chromatin immunoprecipitation (ChIP) using specific antibodies, and primers specific for the *CEACAM5* promoter, showed no significant differences between sensitive and resistant cells, and either with the treatment of 5-AZA, demonstrating that the transcriptional levels of *CEACAM5* are not correlated with the levels of these two epigenetic marks (Figure S7B). Therefore, the epigenetic silencing of *CEACAM5* and the effect of 5-AZA seems to be an indirect methylation effect on the *CEACAM5* locus, suggesting that there is another layer of regulation. We hypothesized that there is a transcription factor that regulates the transcription of the *CEACAM5* gene. In concordance with this hypothesis, enrichment of annotated transcription factor signatures showed significant differences between sensitive MKN45- and MKN-CEAR-resistant cells (Figure S7C). We concluded that CEA is transcriptionally silenced in resistant cells and that combination with 5-AZA overcomes resistance to CEACAM5-TCB.

In addition, we generated a panel of CRC PDXs derived from metastatic biopsies of patients enrolled in a phase I clinical trial using cibisatamab (CEA-TCB) (NCT02324257) at Vall d' Hebron Hospital. Four PDXs expressing high CEA levels were generated from four different patients (Figure S8A).

In order to analyze the sensitivity of these PDXs to the high-affinity CEA-targeting TCB (CEACAM5-TCB), these were implanted in fully CD34$^+$ stem cell humanized mice and treated, showing that only one was sensitive to the CEACAM5-TCB treatment *in vivo*, as well as the MKN45 cell line (Figure S8B). It is important to note that these results show that the activity of CEACAM5-TCB is not exclusively dependent on the CEA expression levels, as sensitive and primary resistant PDXs express comparable CEA levels at the surface (Figure S8A). Staining with CD3 antibodies showed that response to CEACAM5-TCB was not due to different levels of lymphocyte infiltration (Figure S8C). Therefore, these results suggest that, particularly in primary refractory patients, different mechanisms beyond the CEA expression levels and intra-tumor T cell infiltration contribute to the efficient activity of CEACAM5-TCB *in vivo*.

We took advantage of the sensitive PDX model to generate an *in vivo* CEACAM5-TCB-acquired resistant PDX. For that, we chronically treated the PDX63 with CEACAM5-TCB and serially transplanted it for three rounds, until it did not respond to the treatment (Figure 4A). This acquired resistance model (PDX63-R) presented lower CEA expression levels while infiltration by T cells was maintained (Figures 4B and 4C). Collectively, these data support our *in vitro* results using the MKN45 and SW1222 acquired resistant models to CEACAM5-TCB.

In conclusion, our pre-clinical findings indicate that downregulation of CEA expression or selection of tumor clones with lower CEA expression (as consequence of efficient killing of high-CEA-expressing tumor clones by CEACAM5-TCB) but not HER2, may be one of the mechanisms of acquired resistance to TCBs.

Resistance to HER2 targeting is mediated by downmodulation of IFN-γ signaling

In the case of the HER2-TCB-resistant model, we explored alternative mechanisms of acquired resistance. Given our previous study describing intrinsic interferon-gamma (IFN-γ) response is essential for the response to the redirection of T lymphocytes (Arenas et al., 2021), we explored this possibility in the MKN-HER2R model showed in Figure 1B. The MKN-HER2R cells were clearly resistant to IFN-γ and exhibit a deficient signaling pathway by means of p-STAT1 and IRF1 (Figures 5A and 5B). Supporting the relevance of the model, analysis of the sensitivity to IFN-γ in 18 clones showed that there is no heterogeneity in MKN-HER2R cells (Figure S9A). Of note, the role of

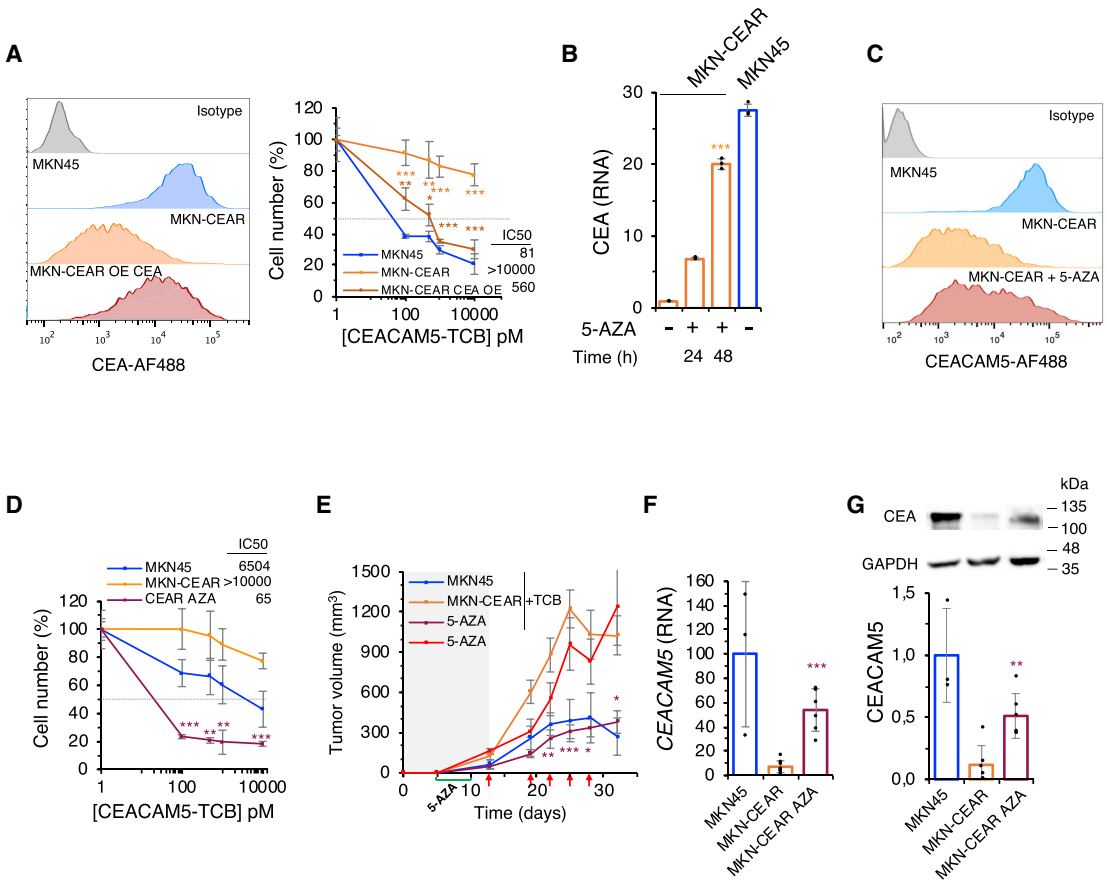

Figure 3. DNA demethylating agent 5-Azacitadine treatment recovers CEA expression and overcomes resistance to CEACAM5-TCB

(A) Left, levels of CEA in parental or MKN45, CEAR, and CEAR cells stably transfected with a vector encoding CEACAM5 (CEAR CEA OE) were determined by flow cytometry. Right, same cells were co-cultured with PBMCs at a 1:1 ratio and treated with different concentrations of CEACAM5-TCB for 72 h. Then, viable cells were quantified by flow cytometry using EpCAM as a marker.

(B) Indicated cells were treated with 1 μM 5-AZA for 48 h. Then, the levels of the mRNA encoding CEACAM5 were determined by RT-qPCR and normalized to the levels of CEAR cells treated with vehicle.

(C) Levels of CEA in parental MKN45, CEAR, and CEAR cells treated for 72 h with 1 μM 5-AZA were determined by flow cytometry.

(D) Same cells were co-cultured with PBMCs at a 1:1 ratio and treated with different concentrations of CEACAM5-TCB for 72 h. CEAR cells were pretreated for 72 h with 1 μM 5-AZA before adding PBMCs and CEACAM5-TCB. Then, viable cells were quantified by flow cytometry using EpCAM as a marker.

(E) 10^6 MKN45 or MKN-CEAR cells were injected subcutaneously into NSG mice. From day 5–10 post injection, MKN-CEAR AZA and MKN-CEAR AZA-TCB groups were treated daily with 2 mg/kg 5-Azacitadine. When tumors reached ~150 mm^3 (dark background), 10^7 PBMCs were injected intraperitoneally. Then animals were treated intravenously with 1 mg/kg CEACAM5-TCB as indicated (red arrows). Tumor volumes are represented as averages ± SEM (MKN45, n = 8, CEAR, n = 12, AZA, n = 4, AZA + TCB, n = 5).

(F) Tumors from (E) were assayed for CEACAM5 mRNA expression by RT-qPCR. Quantitative data corresponds to mean ± SD of three different parental, five different resistant, and five different 5-AZA treated resistant tumors. Results were normalized to MKN45 tumors.

(G) Tumors from (E) were assayed for CEACAM5 protein expression by western blot. Quantitative data corresponds to mean ± SD of three different parental, five different resistant, and four different 5-AZA treated resistant tumors. Results were normalized to MKN45 tumors. (A-D, F, G) *p < 0.05, **p < 0.01, ***p < 0.001, two-tailed *t* test. (E) *p < 0.05, **p < 0.01, ***p < 0.001, two-way ANOVA and Bonferroni correction. (A-D) Data are presented as mean ± SD of three independent experiments.

IFN-γ in this scenario is independent on the antigen presentation, as MKN45-HER2R cells were also resistant to the CEACAM5-TCB (Figure S9B). As a proof of principle, we impaired IFN-γ signaling in parental cells, by knocking-out the receptor of interferon-gamma 1 (IFNGR1) through CRISPR-Cas9 technology (Figure 5C). Confirming our previous findings, KO-IFNGR1 cells were resistant to both HER2-TCB and IFN-γ (Figures 5D and 5E). As expected, KO-IFNGR1 cells exhibit deficient signaling pathway upon the treatment of IFN-γ by means of p-STAT1 and IRF1 (Figure S9C), and overexpressing IFNGR1 in KO cells rescued the phenotype (Figures S9D–S9F). Analysis of the components of the IFN-γ pathway in the acquired resistant model showed little or no difference in the expression of IFNGR2, JAK1, or STAT1 in resistant cells (Figure S9G). In contrast, we observed a significant reduction of both JAK2 and IFNGR1 levels (Figures 5F and 5G). In addition, treatment with 5-AZA did not

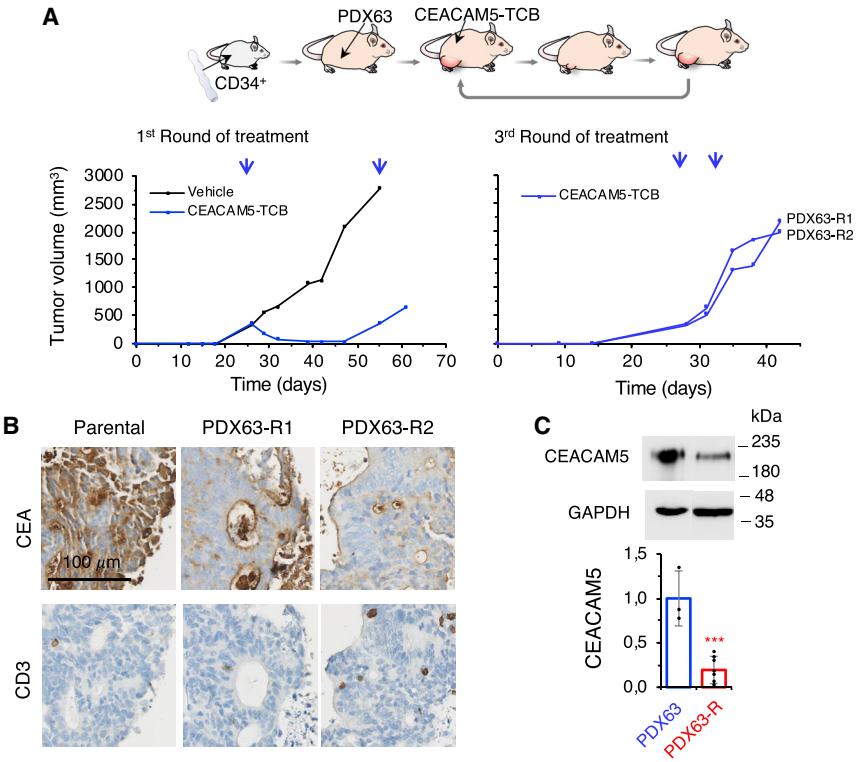

Figure 4. An *in vivo* resistant model corroborates CEACAM5-TCB downregulation resistance mechanism

(A) Schematic showing the generation of PDX63-R tumors. PDX63 was grafted in mice humanized with $CD34^+$ cells. When tumors reached ~400 mm^3 animals were treated intravenously with vehicle or 5 mg/kg of CEACAM5-TCB and tumor volumes were monitored (left). At the end of the experiment, the tumor of the CEACAM5-TCB arm was implanted into new humanized mice, and they were treated and monitored as in left. After two rounds of treatment with CEACAM5-TCB, tumors were implanted into new humanized mice (right), treated with CEACAM5-TCB and monitored as in left. Tumors were allowed to regrow and treatment was repeated. Tumor volumes of individual mice at the first (left) and the third (right) round of treatment are represented. Representative tumors out of seven are shown in right.

(B) Representative immunohistochemical stainings of hCEACAM5 and hCD3 in tumor sections are presented.

(C) Levels of CEACAM5 as determined by western blot. Quantitative data correspond to mean ± SD of three different parental and seven different resistant tumor determinations. ***$p < 0.001$, two-tailed *t* test.

alter the levels of these two proteins (Figures S9H and S9I), demonstrating that the effect of 5-AZA is specific for the MKN-CEAR model, supporting our previous hypothesis.

In addition, we generated models of acquired resistance to IFN-γ. Treatment of MKN45 cells with increasing concentration of IFN-γ starting at the IC50, during 4 months resulted in resistant cells (designed MKN45-RG) (Figures S10A and S10B). *In vitro* assays showed that IFN-γ resistant cells were also resistant to the HER2-TCB and CEACAM5-TCB (Figures S10C and S10D). As expected, IFN-γ signaling was downmodulated in these resistant cells (Figure S10E). Thus, cells selected because of their resistance to IFN-γ showed similar characteristics to those selected for resistance to TCBs, further supporting the relevance of the IFN-γ pathway in resistance to TCBs.

We concluded that the gastric $HER2^+$ model used in this study acquired resistance to IFN-γ and, thus, resistance to TCBs.

DISCUSSION

Redirection of lymphocytes, via TCBs or CARs, has been approved for the treatment of some B and plasma cell malignancies. This success contrasts with the challenges observed in the treatment of solid tumors. As a consequence, intense efforts have been focused on the identification of mechanisms of resistance (Sharma et al., 2017; O'Donnell et al., 2019). Antigen loss is a well-established mechanism of resistance to CAR T therapies. Patients who progressed to a CAR T targeting CD19 showed loss of CD19 expression at the surface, due to alternative splicing, interruption in the transport of antigen to the cell surface, or due to the emergence of an antigen negative clone within a heterogeneity population (Fischer et al., 2017; Sotillo et al., 2015). In contrast to conventional targeted therapies, this event may happen randomly in therapies based on the redirection of T lymphocytes, as TCBs and CARs targeting different antigens behave with the same mechanism of action (Cohen et al., 2020; Slaney et al., 2018). Using the MKN45 cell line, which expresses two different tumor antigens (CEA and HER2), and two different TCBs targeting CEA or HER2, in this study we show that different mechanisms of resistance arise depending on the antigen targeted (Figure 6).

Several CEA-targeting immunotherapies beyond TCBs are currently in preclinical or clinical development, including TCBs, CAR T cells, TCR engineered T cells, or CEA vaccines (Parkhurst et al., 2011). However, despite the promising results obtained in preclinical studies, targeting CEA in the clinic has been challenging. Previous reports showed that heterogeneity and plasticity of CEA expression appear to confer low sensitivity to cibisatamab (CEA-TCB) in patient-derived organoids (PDOs) (Bacac et al., 2016a; Gonzalez-Exposito et al., 2019). Here, by using the CEACAM5-TCB, a different CEA-targeting TCB with significantly higher affinity and potency, we unveil one of the potential mechanisms of acquired resistance and suggest that strategies to recover CEA expression in combination with immunotherapies could be promising to increase the benefits of CEA-targeting immunotherapies. Particularly, in this study we unveil that CEA was downregulated at the transcriptional level, and we imply the potential use of DNA demethylating agents such as 5-AZA to overcome resistance and to

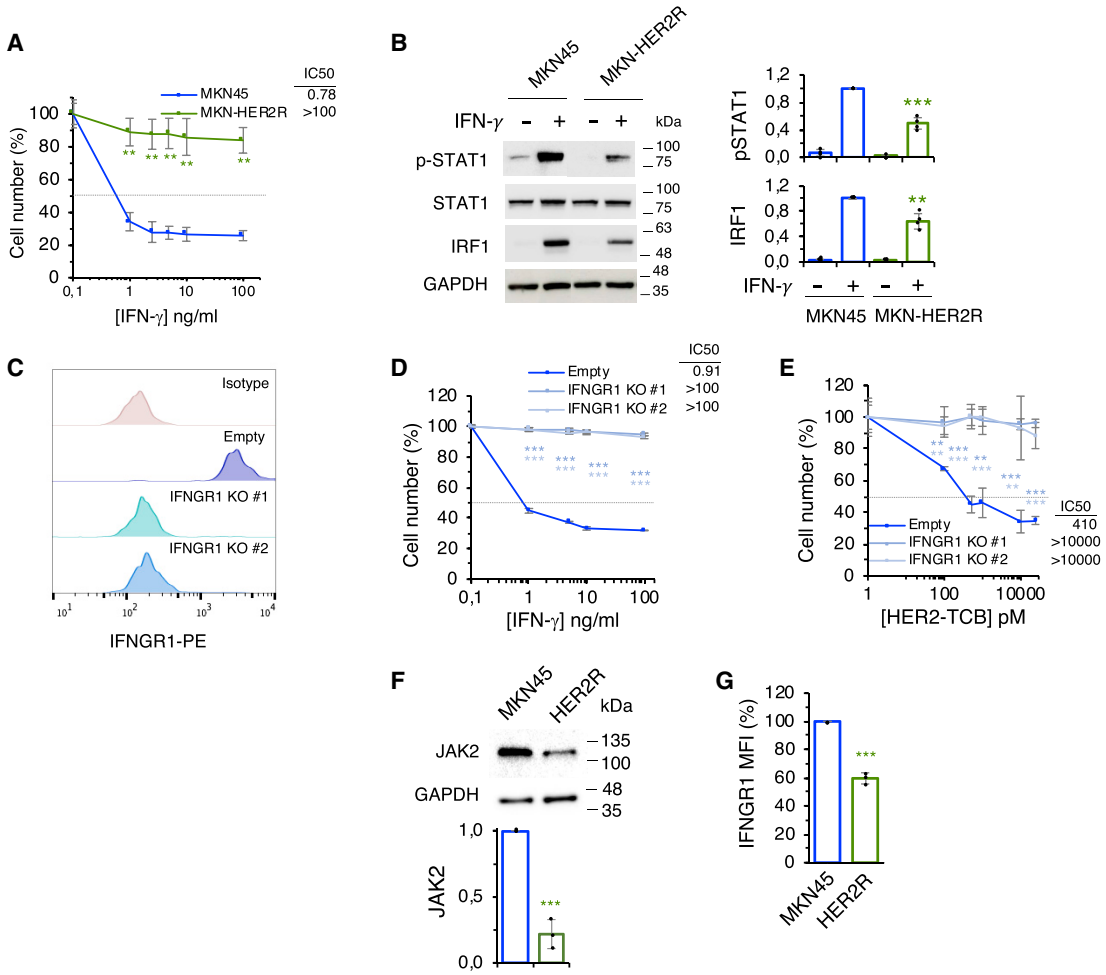

Figure 5. Resistance to TCBs targeting HER2 is mediated by downmodulation of IFN-γ signaling

(A) Parental MKN45 or MKN-HER2R cells were treated with different concentrations of IFN-γ for 3 days. Cell numbers were estimated with the crystal violet staining assay.

(B) Levels of phospho-STAT1, STAT1, and IRF1 upon 4 h treatment with 10 ng/mL IFN-γ were determined by western blot. Results were normalized to treated MKN45 cells.

(C) MKN45 cells or same cells stably transfected with a CRISPR targeting IFNGR1 (KO) were stained with anti-IFNGR1 or isotype antibody and analyzed by flow cytometry.

(D) Sensitivity of the indicated cells to IFN-γ was analyzed as in (A).

(E) Co-cultures of PBMCs with the same cells were treated with different concentrations of HER2-TCB for 72 h. Then, viable cells were quantified by flow cytometry using EpCAM as a marker.

(F) Levels of JAK2 in MKN45 and MKN-HER2R cells were determined by western blot.

(G) Levels of IFNGR1 in MKN45 and MKN-HER2R cells were determined by flow cytometry. $^{**}p < 0.01$, $^{***}p < 0.001$, two-tailed *t* test. Data are presented as mean ± SD of three independent experiments.

increase the efficacy of CEA-TCB. Indeed, 5-AZA is a widely used DNA demethylating agent (Christman, 2002; Santini et al., 2001) and demonstrate promising results in different clinical trials for cancer treatment (Huls et al., 2019; van der Helm et al., 2013). In addition, the demethylation effects of 5-AZA on CEA expression are irreversible, in principle because 5-AZA demethylates the DNA and therefore the enzyme engaged to catalyze DNA methylation (DNMT1) is not able to transfer the methyl groups to specific CpG structures in the following DNA daughter molecules. In addition, according to our results, the effect of 5-AZA was specific for the CEA-resistant model, as 5-AZA did not have effect on the expression of the two components downmodulated in the acquired resistant model to HER2-TCB (MKN-HER2R).

Our mechanistic studies using MeDIP and ChIP on the CEACAM5 loci showed no differences between sensitive MKN45 and resistant MKN-CEAR cells, and no biological differences that could explain the recovery with the treatment of 5-AZA, suggesting that the epigenetic silencing of CEACAM5 is likely due to an indirect methylation effect on the antigen-encoding locus. We hypothesize that there is a transcription factor that regulates the transcription of the *CEACAM5* gene. We

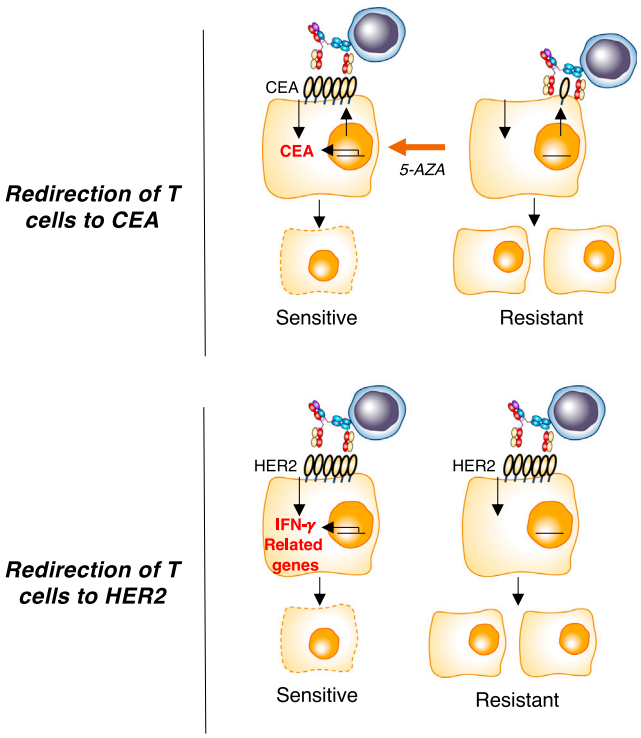

Figure 6. Schematic drawing summarizing our findings

performed enrichment analysis of annotated transcription factor signatures and observed significant different transcription families differentially enriched between sensitive MKN45 and resistant MKN-CEAR. Further studies should be performed to identify those transcription factors.

In this regard, in future TCB studies and CAR constructs, the identification of mechanisms leading to disrupted target expression will be needed in order to optimize responses. It is important to note that CEA expression level is not the only factor contributing the activity of CEACAM5-TCB, as in our panel of CRC PDXs derived from metastatic biopsies with comparable levels of CEA expression, only one was sensitive to CEACAM5-TCB. Consequently, these data suggest that different mechanisms of primary resistance, such as stromal barriers, an immunosuppressive tumor environment, or other factors affect the activity of CEACAM5-TCB.

The main mechanisms of resistance to immunotherapy described so far are focused on the ability of T cells to reach cancer cells and/or on the inhibition of T cells (Sharma et al., 2017; O'Donnell et al., 2019). Our results show that, in contrast to the acquired resistant models to a TCB targeting the CEA antigen, an acquired resistant model to an HER2-TCB, even using HER2 non-amplified tumor cells, maintains antigen levels. Instead, these resistant cells exhibit an intrinsic deficient IFN-γ signaling, which is the cause of resistance to active T lymphocytes. Several pivotal studies, including the one performed by our group (Arenas et al., 2021), point out the key contribution of altered IFN-γ signaling to immunotherapy response and resistance: (1) melanoma patients' resistance to immune checkpoints inhibitors revealed alteration of IFN-γ genes (Zaretsky et al., 2016); (2) an *in vivo* CRISPR screening revealed the activation of the negative regulator PTPN2 as a resistance inductor (Manguso et al., 2017); (3) ARAD1 can block IFN-γ signaling pathway and lead to immunotherapy resistance (Ishizuka et al., 2019); (4) downregulation of genes upregulated by IFN-γ correlates with resistance to immune checkpoint blockade (Grasso et al., 2020); and (5) JAK2 downmodulation leads to IFN-γ deficient response and acquired resistance to T cell bispecific antibodies and CAR T targeting HER2 (Arenas et al., 2021). Of note, the role of IFN-γ in our model is independent on the antigen presentation, as MKN45-HER2R was also resistant to the CEACAM5-TCB. This result is expected, as in theory, antigen presentation is not required for tumor recognition and killing by T cells for TCB activity. T cell engagers work independently of the MHC/TCR complex, a known fact given that they engage CD3e and thus bypass the classical T cell activation via peptides presented on MHC. This was published several years ago using BiTEs (Nagorsen and Baeuerle, 2011). In addition, studies using tumor cells knocked-out for MHC class I showed killing via BiTEs supports this evidence. Further studies should be performed to elucidate the role of IFN-γ in resistance to redirected lymphocytes, a mechanism beyond antigen presentation. In summary, the results showed in this study unveil a mechanism of resistance to T cell-based therapies, and imply the potential use of IFN-γ as a surrogate biomarker of response to immunotherapies. In addition, they open the avenue for the screening of therapies that could overcome deficient IFN-γ response.

The results presented here have practical implications, particularly in the design of combinatorial strategies to overcome resistance or low sensitivity to a TCB or CAR. Our results imply that the selection of a particular antigen may have an impact on the type of mechanism of acquired resistance that emerge in patients refractory to T cell redirected therapies. Although intrinsic IFN-γ response and heterogeneity of CEA expression have been reported as mechanisms of resistance, in this study we describe that depending on the target antigen to which T lymphocytes are redirected, the mechanism of acquired resistance that emerge is different. In the case of CEA-targeting TCB resistant models, we observed that reduction of CEA antigen expression is one of the acquired resistance mechanisms. For other antigens, such as HER2, this event would probably not be as frequent due to its oncogenic role. These results should be taken into consideration when designing combinatorial strategies to overcome resistance and to increase the efficacy of cancer immunotherapies.

Limitations of the study

We clearly demonstrated that the mechanism of acquired resistance to TCBs that emerges is different depending on the target antigen to which T lymphocytes are redirected. However, this current study has several limitations. First, the mechanistic insight of CEA downmodulation is not fully demonstrated, and further studies should address why CEA is downmodulated and the cause of its recovery upon 5-AZA treatment. Second, the intrinsic mechanism of resistance of CEA^{+} CRC PDX tumors is not evaluated given the scarce number of PDXs, and further studies should increase the number of PDXs to have a robust

conclusion of why CEA-positive tumors are resistant. Third, the mechanisms of resistance explained in this study were not assessed in clinical samples, in principle due to the lack of access to patient samples that were treated with T cell bispecific antibodies. When available, the mechanisms of resistance described in these preclinical models will have to be validated in clinical samples.

STAR★METHODS

Detailed methods are provided in the online version of this paper and include the following:

- KEY RESOURCES TABLE
- RESOURCE AVAILABILITY
  - Lead contact
  - Materials and availability
  - Data and code availability
- EXPERIMENTAL MODEL AND SUBJECT DETAILS
  - Immune cells
  - Mice
  - Cell lines and primary cultures
  - Patient-derived xenograft establishment
- METHOD DETAILS
  - PBMC isolation
  - TCB constructs generation
  - Generation of resistant cells *in vitro*
  - T cell cytotoxicity assays
  - 3D organoid assay
  - Flow cytometry
  - 5-Azacytadine treatments *in vitro*
  - RNA isolation and qRT-PCR
  - RNASeq
  - Metilated DNA immunoprecipitation (MeDIP)
  - Chromatin Immunoprecipitation (ChIP)
  - Interferon-gamma cytotoxicity assays
  - Cell proliferation assays
  - Western blot
  - Humanized xenograft models
  - Generation of patient-derived xenografts and acquired *in vivo* resistant model
  - Immunohistochemistry
  - Viral tumor cells infections
  - ELISA
  - Granzyme B activity
- QUANTIFICATION AND STATISTICAL ANALYSIS
- ADDITIONAL RESOURCES

SUPPLEMENTAL INFORMATION

Supplemental information can be found online at https://doi.org/10.1016/j.celrep.2022.111430.

ACKNOWLEDGMENTS

This work was supported by Asociación Española Contra el Cancer (AECC), Breast Cancer Research Foundation (BCRF-21-008), and Instituto de Salud Carlos III (PI19/01181). A.M.S. was funded by the Spanish Government (PFIS FI20/00188). B.M. was funded by a fellowship from PERIS (Departament de Salut, Generalitat de Catalunya). M.R.A. was funded by Agency for Management of University and Research Grants (AGAUR, 2022 FI_B2 00080). P.O.R. was funded by the BBVA. E.J.A. was funded by the AECC (POSTD211413A-REN). VHIO acknowledges the Cellex Foundation for providing research facilities and equipment, the Centro de Investigación Biomédica en Red de Cáncer (CIBERONC) from the Institute of Health Carlos III (ISCIII), and the Department of Health (Generalitat de Catalunya, SLT008/18/00198 SLT008/18/00205) for their support on this research. The authors acknowledge financial support from the State Agency for Research (Agencia Estatal de Investigación) (CEX2020-001024-S/AEI/10.13039/501100011033) and for the Cancer Immunology and Immunotherapy (CAIMI-2) program funded by BBVA Foundation. We would like to remark the funding from B.M PERIS (Spain). The authors thank Dr. Anne Freimoser-Grundschober and Roche for helping provide the TCBs. The graphical abstract was created with BioRender.com.

AUTHOR CONTRIBUTIONS

E.J.A. and A.M.S. designed and performed most experiments, interpreted and analyzed the data, and revised the manuscript. B.M., I.R.R., M.R.A., and P.O.R. performed experiments and revised the manuscript. M.E. performed *in vivo* experiments. I.C. and H.G.P. performed *in vivo* experiments. L.N. and M.A.C. analyzed the transcriptomic data. M.B. provided the CEACAM5-TCB and reviewed the manuscript. C.K. provided the HER2-TCB and reviewed the manuscript. E.J.A. and J.A. designed the study, interpreted the data, and wrote the manuscript.

DECLARATION OF INTERESTS

M.B. declares employment, stock ownership, and patents with Roche. C.K. declares employment, stock ownership, and patents with Roche. J.A. has received research funds from Roche, Synthon, Menarini, and Molecular Partners, and consultancy honoraria from Menarini.

Received: November 2, 2021
Revised: June 20, 2022
Accepted: September 8, 2022
Published: October 18, 2022

REFERENCES

Arenas, E.J., Martinez-Sabadell, A., Rius Ruiz, I., Román Alonso, M., Escorihuela, M., Luque, A., Fajardo, C.A., Gros, A., Klein, C., and Arribas, J. (2021). Acquired cancer cell resistance to T cell bispecific antibodies and CAR T targeting HER2 through JAK2 down-modulation. Nat. Commun. *12*, 1237. https://doi.org/10.1038/s41467-021-21445-4.

Arteaga, C.L., and Engelman, J.A. (2014). ERBB receptors: from oncogene discovery to basic science to mechanism-based cancer therapeutics. Cancer Cell *25*, 282–303. https://doi.org/10.1016/j.ccr.2014.02.025.

Bacac, M., Fauti, T., Sam, J., Colombetti, S., Weinzierl, T., Ouaret, D., Bodmer, W., Lehman, S., Hofr, T., Hosse, R.J., et al. (2016a). A novel carcinoembryonic antigen T-cell bispecific antibody (CEA TCB) for the treatment of solid tumors. Clin. Cancer Res. *22*, 3286–3297. https://doi.org/10.1158/1078-0432.CCR-15-1696.

Bacac, M., Klein, C., and Umana, P. (2016b). Cea TCB: a novel head-to-tail 2:1 T cell bispecific antibody for treatment of CEA-positive solid tumors. OncoImmunology *5*, e1203498. https://doi.org/10.1080/2162402X.2016.1203498.

Bacac, M., Colombetti, S., Herter, S., Sam, J., Perro, M., Chen, S., Bianchi, R., Richard, M., Schoenle, A., Nicolini, V., et al. (2018). CD20-TCB Obinutuzumab pretreatment as next-generation treatment of hematologic malignancies. Clin. Cancer Res. *24*, 4785–4797. https://doi.org/10.1158/1078-0432.CCR-18-0455.

Bouchkouj, N., Kasamon, Y.L., Angelo de Claro, R., George, B., Lin, X., Lee, S., Blumenthal, G.M., Bryan, W., McKee, A.E., and Pazdur, R. (2019). FDA approval summary: axicabtagene ciloleucel for Relapsed or refractory large

B-cell lymphoma. Clin. Cancer Res. *25*, 1702–1708. https://doi.org/10.1158/1078-0432.CCR-18-2743.

Christman, J.K. (2002). 5-Azacytidine and 5-aza-2′-deoxycytidine as inhibitors of DNA methylation: mechanistic studies and their implications for cancer therapy. Oncogene *21*, 5483–5495. https://doi.org/10.1038/sj.onc.1205699.

Cohen, A.D., Raje, N., Fowler, J.A., Mezzi, K., Scott, E.C., and Dhodapkar, M.V. (2020). How to Train Your T cells: Overcoming immune Dysfunction in multiple Myeloma. Clin. Cancer Res. *26*, 1541–1554. https://doi.org/10.1158/1078-0432.CCR-19-2111.

Ellis, L.M., and Hicklin, D.J. (2009). Resistance to targeted therapies: Refining anticancer therapy in the Era of molecular Oncology. Clin. Cancer Res. *15*, 7471–7478. https://doi.org/10.1158/1078-0432.CCR-09-1070.

Fischer, J., Paret, C., Malki, K.E., Alt, F., Wingerter, A., Neu, M.A., Kron, B., Russo, A., Lehmann, N., Roth, L., et al. (2017). CD19 Isoforms Enabling resistance to CART-19 immunotherapy are expressed in B-ALL patients at Initial Diagnosis. J. Immunother. *40*, 187–195. https://doi.org/10.1097/CJI.0000000000000169.

Gonzalez-Exposito, R., Semiannikova, M., Griffiths, B., Khan, K., Barber, L.J., Woolston, A., Spain, G., von Loga, K., Challoner, B., Patel, R., et al. (2019). CEA expression heterogeneity and plasticity confer resistance to the CEA-targeting bispecific immunotherapy antibody cibisatamab (CEA-TCB) in patient-derived colorectal cancer organoids. J. Immunother. Cancer *7*, 101. https://doi.org/10.1186/s40425-019-0575-3.

Grasso, C.S., Tsoi, J., Onyshchenko, M., Abril-Rodriguez, G., Ross-Macdonald, P., Wind-Rotolo, M., Champhekar, A., Medina, E., Torrejon, D.Y., Sanghoon Shin, D., et al. (2020). Conserved interferon-gamma signaling Drives clinical response to immune checkpoint blockade therapy in Melanoma. Cancer Cell *38*, 500–515. https://doi.org/10.1016/j.ccell.2020.08.005.

Huls, G., Chitu, D.A., Havelange, V., Jongen-Lavrencic, M., van de Loosdrecht, A., Biemond, B.J., Sinnige, H., Hodossy, B., Graux, C., van Marwijk Kooy, R., et al. (2019). Azacitidine maintenance after intensive chemotherapy improves DFS in older AML patients. Blood *133*, 1457–1464. https://doi.org/10.1182/blood-2018-10-879866.

Ishizuka, J.J., Manguso, R.T., Cheruiyot, C.K., Bi, K., Panda, A., Iracheta-Vellve, A., Miller, B.C., Du, P.P., Yates, K.B., Dubrot, J., et al. (2019). Loss of ADAR1 in tumours overcomes resistance to immune checkpoint blockade. Nature *565*, 43–48. https://doi.org/10.1038/s41586-018-0768-9.

Junttila, T.T., Li, J., Johnston, J., Hristopoulos, M., Clark, R., Ellerman, D., Wang, B., Li, Y., Mathieu, M., Li, G., et al. (2014). Antitumor efficacy of a bispecific antibody that targets HER2 and activates T cells. Cancer Res. *74*, 5561–5571. https://doi.org/10.1158/0008-5472.CAN-13-3622-T.

Kantarjian, H., Stein, A., Gökbuget, N., Fielding, A.K., Schuh, A.C., Ribera, J., Wei, A., Dombret, H., Foà, R., Bassan, R., et al. (2017). Blinatumomab versus chemotherapy for advanced Acute Lymphoblastic Leukemia. N. Engl. J. Med. *376*, 836–847. https://doi.org/10.1056/NEJMoa1609783.

Le, D.T., Durham, J.N., Smith, K.N., Wang, H., Bartlett, B.R., Aulakh, L.K., Lu, S., Kemberling, H., Wilt, C., Luber, B.S., et al. (2017). Mismatch repair deficiency predicts response of solid tumors to PD-1 blockade. Science *357*, 409–413. https://doi.org/10.1126/science.aan6733.

Locke, F.L., Ghobadi, A., Jacobson, C.A., Miklos, D.B., Lekakis, L.J., Oluwole, O.O., Lin, Y., Braunschweig, I., Hill, B.T., Timmerman, J.M., et al. (2019). Long-term safety and activity of axicabtagene ciloleucel in refractory large B-cell lymphoma (ZUMA-1): a single-arm, multicentre, phase 1-2 trial. Lancet Oncol. *20*, 31–42. https://doi.org/10.1016/S1470-2045(18)30864-7.

Manguso, R.T., Pope, H.W., Zimmer, M.D., Brown, F.D., Yates, K.B., Miller, B.C., Collins, N.B., Bi, K., LaFleur, M.W., Juneja, V.R., et al. (2017). In vivo CRISPR screening identifies Ptpn2 as a cancer immunotherapy target. Nature *547*, 413–418. https://doi.org/10.1038/nature23270.

Mellman, I., Coukos, G., and Dranoff, G. (2011). Cancer immunotherapy comes of age. Nature *480*, 480–489. https://doi.org/10.1038/nature10673.

Moody, S.E., Sarkisian, C.J., Hahn, K.T., Gunther, E.J., Pickup, S., Dugan, K.D., Innocent, N., Cardiff, R.D., Schnall, M., and Chodosh, L.A. (2002). Conditional activation of Neu in the mammary epithelium of transgenic mice results in reversible pulmonary metastasis. Cancer Cell *2*, 451–461. https://doi.org/10.1016/s1535-6108(02)00212-x.

Nagorsen, D., and Baeuerle, P.A. (2011). Immunomodulatory therapy of cancer with T cell-engaging BiTE antibody blinatumomab. Exp. Cell Res. *317*, 1255–1260. https://doi.org/10.1016/j.yexcr.2011.03.010.

O'Donnell, J.S., Teng, M.W.L., and Smyth, M.J. (2019). Cancer immunoediting and resistance to T cell-based immunotherapy. Nat. Rev. Clin. Oncol. *16*, 151–167. https://doi.org/10.1038/s41571-018-0142-8.

Parkhurst, M.R., Yang, J.C., Langan, R.C., Dudley, M.E., Nathan, D.N., Feldman, S.A., Davis, J.L., Morgan, R.A., Merino, M.J., Sherry, R.M., et al. (2011). T cells targeting carcinoembryonic antigen can mediate regression of metastatic colorectal cancer but induce severe transient colitis. Mol. Ther. *19*, 620–626. https://doi.org/10.1038/mt.2010.272.

Puig, I., Chicote, I., Tenbaum, S.P., Arqués, O., Herance, J.R., Gispert, J.D., Jimenez, J., Landolfi, S., Caci, K., Allende, H., et al. (2013). A personalized preclinical model to evaluate the metastatic potential of patient-derived colon cancer initiating cells. Clin. Cancer Res. *19*, 6787–6801. https://doi.org/10.1158/1078-0432.CCR-12-1740.

Rafiq, S., Hackett, C.S., and Brentjens, R.J. (2020). Engineering strategies to overcome the current roadblocks in CAR T cell therapy. Nat. Rev. Clin. Oncol. *17*, 147–167. https://doi.org/10.1038/s41571-019-0297-y.

Sabnis, A.J., and Bivona, T.G. (2019). Principles of resistance to targeted cancer therapy: Lessons from basic and Translational cancer biology. Trends Mol. Med. *25*, 185–197. https://doi.org/10.1016/j.molmed.2018.12.009.

Santini, V., Kantarjian, H.M., and Issa, J.P. (2001). Changes in DNA methylation in Neoplasia: Pathophysiology and Therapeutic implications. Ann. Intern. Med. *134*, 573–586. https://doi.org/10.7326/0003-4819-134-7-200104030-00011.

Schaefer, W., Regula, J.T., Bähner, M., Schanzer, J., Croasdale, R., Dürr, H., Gassner, C., Georges, G., Kettenberger, H., Imhof-Jung, S., et al. (2011). Immunoglobulin domain crossover as a generic approach for the production of bispecific IgG antibodies. Proc. Natl. Acad. Sci. USA *108*, 11187–11192. https://doi.org/10.1073/pnas.1019002108.

Shah, N.N., and Fry, T.J. (2019). Mechanisms of resistance to CAR T cell therapy. Nat. Rev. Clin. Oncol. *16*, 372–385. https://doi.org/10.1038/s41571-019-0184-6.

Sharma, P., Hu-Lieskovan, S., Wargo, J.A., and Ribas, A. (2017). Primary, Adaptive, and acquired resistance to cancer immunotherapy. Cell *168*, 707–723. https://doi.org/10.1016/j.cell.2017.01.017.

Slaga, D., Ellerman, D., Lombana, T.N., Vij, R., Li, J., Hristopoulos, M., Clark, R., Johnston, J., Shelton, A., Mai, E., et al. (2018). Avidity-based binding to HER2 results in selective killing of HER2-overexpressing cells by anti-HER2/CD3. Sci. Transl. Med. *10*, eaat5775. https://doi.org/10.1126/scitranslmed.aat5775.

Slaney, C.Y., Wang, P., Darcy, P.K., and Kershaw, M.H. (2018). CARs versus BiTEs: a comparison between T cell-redirection strategies for cancer treatment. Cancer Discov. *8*, 924–934. https://doi.org/10.1158/2159-8290.CD-18-0297.

Song, M.K., Park, B.B., and Uhm, J.E. (2019). Resistance mechanisms to CAR T-cell therapy and overcoming strategy in B-cell hematologic malignancies. Int. J. Mol. Sci. *20*, 5010. https://doi.org/10.3390/ijms20205010.

Sotillo, E., Barrett, D.M., Black, K.L., Bagashev, A., Oldridge, D., Wu, G., Sussman, R., Lanauze, C., Ruella, M., Gazzara, M.R., et al. (2015). Convergence of acquired Mutations and alternative splicing of CD19 Enables resistance to CART-19 immunotherapy. Cancer Discov. *5*, 1282–1295. https://doi.org/10.1158/2159-8290.CD-15-1020.

Teijeira, A., Migueliz, I., Garasa, S., Karanikas, V., Luri, C., Cirella, A., Oliveira, I., Cañamero, M., Alvarez, M., Ochoa, M.C., et al. (2022). Three-dimensional colon cancer organoids model the response to CEA-CD3 T-cell engagers. Theranostics *12*, 1373–1387. https://doi.org/10.7150/thno.63359.

van de Wetering, M., Francies, H.E., Francis, J.M., Bounova, G., Iorio, F., Pronk, A., van Houdt, W., van Gorp, J., Taylor-Weiner, A., Kester, L., et al. (2015). Prospective derivation of a living organoid biobank of colorectal cancer patients. Cell *161*, 933–945. https://doi.org/10.1016/j.cell.2015.03.053.

van der Helm, L.H., Veeger, N.J.G., van Marwijk Kooy, M., Beeker, A., de Weerdt, O., de Groot, M., Alhan, C., Hoogendorn, M., Laterveer, L., van de Loosdrecht, A.A., et al. (2013). Azacitidine results in comparable outcome in newly diagnosed AML patients with more or less than 30% bone marrow blasts. Leuk. Res. *37*, 877–882. https://doi.org/10.1016/j.leukres.2013.03.022.

Velasquez, M.P., Bonifant, C.L., and Gottschalk, S. (2018). Redirecting T cells to hematological malignancies with bispecific antibodies. Blood *131*, 30–38. https://doi.org/10.1182/blood-2017-06-741058.

Zaretsky, J.M., Garcia-Diaz, A., Shin, D.S., Escuin-Ordinas, H., Hugo, W., Hu-Lieskovan, S., Torrejon, D.Y., Abril-Rodriguez, G., Sandoval, S., Barthly, L., et al. (2016). Mutations associated with acquired resistance to PD-1 blockade in Melanoma. N. Engl. J. Med. *375*, 819–829. https://doi.org/10.1056/NEJMoa1604958.

STAR★METHODS

KEY RESOURCES TABLE

REAGENT or RESOURCE	SOURCE	IDENTIFIER
Antibodies		
HER2-TCB	Roche	N/A
CEACAM5-TCB	Roche	N/A
DP47-TCB	Roche	N/A
hIFNGR1 antibody	Biolegend	Cat#308606 RRID:AB_314726
hIFNGR2 antibody	Biolegend	Cat#308504 RRID:AB_314718
PE Mouse IgG1, κ Isotype Ctrl (FC) Antibody	Biolegend	Cat#400114 RRID:AB_314718
Trastuzumab	Roche	Cat#180288-69-1
Goat anti-Human IgG (H + L) Cross-Adsorbed Secondary Antibody, Alexa Fluor™ 488	Invitrogen	Cat#A-11013 RRID:AB_141360
APC/Cyanine7 anti-human CD69 Antibody	Biolegend	Cat#310914 RRID:AB_314849
APC anti-human CD25 Antibody	Biolegend	Cat#302610 RRID:AB_314280
PE/Cyanine7 anti-human CD8 Antibody	Biolegend	Cat#344712 RRID:AB_2044008
Rabbit IgG Control Antibody	Sigma-Aldrich	Cat# I8140, RRID:AB_1163661
Histone H3 (acetyl K27) Antibody	Abcam	Cat# ab4729, RRID:AB_2118291
Histone H3 trimethyl (Lys27) Antibody	Millipore	Cat# 07-449, RRID:AB_310624
Anti-c-erbB-2 (Her-2/neu)	Biogenex	Cat#AM134GP
CEA/CD66e (CB30) Mouse mAb	Cell Signaling Technology	Cat#2383 RRID:AB_2077488
Jak1 (6G4) Rabbit mAb	Cell Signaling Technology	Cat#3344 RRID:AB_2265054
Jak2 (D2E12) XP® Rabbit mAb	Cell Signaling Technology	Cat#3230 RRID:AB_2128522
Phospho-Stat1 (Tyr701) (58D6) Rabbit mAb	Cell Signaling Technology	Cat#9167 RRID:AB_561284
Stat1 Antibody	Cell Signaling Technology	Cat#9172 RRID:AB_2198300
IRF1 Antibody (C-20)	Santa Cruz Biotechnology	Cat#sc-497 RRID:AB_631838
Recombinant Anti-GAPDH antibody [EPR6256] - Loading Control	Abcam	Cat#ab128915 RRID:AB_11143050
Rabbit IgG HRP Linked Whole Ab	Cytiva	Cat# NA934 RRID:AB_772206
Mouse IgG HRP Linked Whole Ab	Cytiva	Cat# NA931 RRID:AB_772210
Anti-Human CD34 Antibody, Clone 581	StemCell	Cat#60013 RRID:AB_2783003
PE anti-human CD45 Antibody	Biolegend	Cat#304008 RRID:AB_314396
Anti-CD25	Atlas Antibodies	Cat#HPA054622 RRID:AB_2682546
Anti-CEA	Ventana Medical Systems	Cat#760-4594
Anti-CD3	Ventana Medical Systems	Cat#760-4341

(*Continued on next page*)

Continued

REAGENT or RESOURCE	SOURCE	IDENTIFIER
Biological samples		
Umbilical cord blood	Blood and Tissue Bank of Catalonia (BST)	N/A
Buffy Coats (PBMCs)	Blood and Tissue Bank of Catalonia (BST)	N/A
Patient Derived Xenografts (PDXs)	Biopsies from clinical trial NCT02650713	N/A
Chemicals, peptides, and recombinant proteins		
PBS	Biowest	Cat#L0615
Ficoll-Paque PLUS	GE Healthcare	Cat#70-1440-02
Red Blood Cell (RBC) Lysis Buffer	Invitrogen	Cat#00-4333-57
Bovine Serum Albumin (BSA)	Sigma-Aldrich	Cat#A9647
CryoStor CS10	StemCell Technologies	Cat#07959
Horse Serum	Gibco	Cat#26050
DMEM:F12 Medium	Gibco	Cat#21331
RPMI 1640	Gibco	Cat#61870
HEPES	Sigma-Aldrich	Cat#H0887
MEM Non-Essential Amino Acids Solution	Gibco	Cat#11140
Penicillin-Streptomycin	Sigma-Aldrich	Cat#P4333
Blasticidin	Invivogen	Cat#ant-bl-1
Trypsin-EDTA	Gibco	Cat#25300096
Bovine Serum Albumin (BSA)	Sigma-Aldrich	Cat#A9647
Busulfan	Tillomed	N/A
Fetal Bovine Serum (FBS)	Gibco	Cat#10270106
L-Glutamine	Biowest	Cat#X0550
Collagenase IA	Sigma-Aldrich	Cat#C2674
Hyaluronidase	Sigma-Aldrich	Cat#H3506
StemPro Accutase	Gibco	Cat#A1110501
5-Azacytidine	Sigma-Aldrich	Cat#A2385
TaqMan Universal Master Mix II	Applied Biosystems	Cat#4440039
Recombinant Human IFN-γ	Prepotech	Cat#300-02
Crystal Violet	Sigma-Aldrich	Cat#548-62-9
Formaldehyde	Sigma-Aldrich	Cat#47608
Glycine	Fisher Scientific	Cat#BP381
Protease Inhibitor Cocktail Set III	Merck Millipore	Cat#535140
Proteinase K	Roche	Cat#RPTOTKSOL
cOmplete™, EDTA-free Protease I nhibitor Cocktail	Sigma-Aldrich	Cat#COEDTAF_RO
Tween 20	Sigma-Aldrich	Cat#P7949
Cell conditioning 1	Ventana Medical Systems	Cat#950-124
CM inhibitor (ChromoMap DAB kit)	Ventana Medical Systems	Cat#760-159
Haematoxylin II	Ventana Medical Systems	Cat#790-2208
Bluing Reagent	Ventana Medical Systems	Cat#760-2037
Polyethylenimine (PEI)	Polysciences	Cat#24765
Polybrene	Sigma-Aldrich	Cat#H9268
Puromycin	Sigma-Aldrich	Cat#P8833
Granzyme B substrate Ac-IEPD-pNA	Sigma-Aldrich	Cat#368057
Critical commercial assays		
EasySep Human Progenitor Cell Enrichment Kit with Platelet depletion	StemCell Technologies	Cat#19356
CryoStor CS10	StemCell Technologies	Cat#07930

(*Continued on next page*)

Continued

REAGENT or RESOURCE	SOURCE	IDENTIFIER
Matrigel	Corning	Cat#356235
Rneasy Mini Kit	Qiagen	Cat#74106
cDNA reverse transcription Kit	Applied Biosystems	Cat#4368813
Qubit® RNA BR Assay kit	ThermoFischer Scientific	Cat#Q10210
RNA 6000 Nano Bioanalyzer 2100 Assay	Agilent	Cat#5067-1511
MagMeDIP qPCR Kit	Diagenode	Cat#C02010021
QIAamp DNA Mini Kit	Qiagen	Cat#51304
SYBR green reagent	Quantabio	Cat#733-1390
Dynabeads protein A	Invitrogen	Cat#10002D
MinElute PCR Purification Kit	Qiagen	Cat#28006
Immobilon Western Chemiluminescent HRP Substrate	Milipore	Cat#WBKLS0500
Ultramap anti-rabbit HRP kit	Ventana Medical Systems	Cat#760-4315
Human IFNgamma ELISA	Immunotools	Cat#31673539
Deposited data		
Raw RNA sequencing data	This paper	GEO: GSE210592
Experimental models: Cell lines		
MKN45	Dr. Hector Palmer (VHIO)	N/A
SW1222	Dr. Hector Palmer (VHIO)	N/A
COLO201	Dr. María Cascante (UB)	N/A
HEK293T	ATCC	Cat#CRL-3216
Experimental models: Organisms/strains		
NSG (NOD.Cg-Prkdcscid Il2rgtm1Wjl/SzJ)	Charles River	Cat#614
Oligonucleotides		
CEACAM5 TaqMan probe	ThermoFischer Scientific	Cat#Hs00944025_m1
GAPDH TaqMan probe	ThermoFischer Scientific	Cat#Hs02758991_g1
CEACAM5 f: 5′-GAGGCAGAAATGAGAG GGGA-3′	Sigma-Aldrich	N/A
CEACAM5 r: 5′-AACGTTTTGTCAAGGC TGCT-3′	Sigma-Aldrich	N/A
Recombinant DNA		
Lenti CMV V5-LUC Blast (w567-1)	Addgene	Cat#21474
Lenti-Cas9-2A-Blast	Addgene	Cat#73310
pMD2.G	Addgene	Cat#12259
psPAX2	Addgene	Cat#12260
CMV-RFP	Dr. Joaquin Arribas (VHIO)	N/A
HER2 shRNA TRCN0000332953	Sigma-Aldrich	N/A
HER2 shRNA TRCN0000039878	Sigma-Aldrich	N/A
HER2 shRNA TRCN0000039881	Sigma-Aldrich	N/A
CEA shRNA TRCN0000427824	Sigma-Aldrich	N/A
CEA shRNA TRCN0000119238	Sigma-Aldrich	N/A
CEA shRNA TRCN0000119240	Sigma-Aldrich	N/A
Scramble shRNA	Addgene	Cat#1864
pLV[Exp]-Puro-EFS > hCEACAM5[NM_004363.5]	VectorBuilder	N/A
pLV[Exp]-Puro-EF1A > hIFNGR1[NM_000416.3]	VectorBuilder	N/A
Pbabe puro EGFP	Addgene	Cat#128041
IFNGR1 CRISPR gRNA	Sigma-Aldrich	Cat##HS5000021477
IFNGR1 CRISPR gRNA	Sigma-Aldrich	Cat##HS5000021478
LV04 control universal gRNA vector	Sigma-Aldrich	Cat#CRISPR18

(*Continued on next page*)

Continued

REAGENT or RESOURCE	SOURCE	IDENTIFIER
Software and algorithms		
BD FACSDiva software	BD Biosciences	N/A
FlowJo	BD Biosciences	N/A
7900HT Fast Real-Time PCR System	Applied Biosystems	N/A
SDS RQ Manager	Applied Biosystems	N/A
DataAssist software	Applied Biosystems	N/A
Real Time Analysis	Illumina	N/A
R Software	R Software	N/A
ImageJ	National Institutes of Health	N/A
NDP.view2 software	Hamamatsu Photonics	N/A
Prism8	Graphpad	N/A
Other		
EasySep magnet	StemCell Technologies	Cat#18001
Mr. Frosty	Thermo Scientific	Cat#5100-0001
BD LRSFortessa	BD Biosciences	N/A
BD FACSAria I Digital Celll Sorter	BD Biosciences	N/A
Polypropylene V-bottom 96 well-plates	Greiner Bio-One	Cat#651201
V-bottom shape 96-well-plates	Corning Life Sciences	Cat#353075
NanoDrop 2000	Thermo Fischer Scientific	N/A
Infinite M200 Pro Multimode Microplate Reader	TECAN	N/A
NovaSeq 6000	Illumina	N/A
Covaris M220 Focused ultrasonicator	Covaris	N/A
Microtubes AFA Fiber Pre-Slit Snap-Cap 130 μL	Covaris	Cat#520045
Bioruptor	Diagenode	N/A
Nitrocellulose membranes	GE Healthcare Biosciences	Cat#10600002
Amersham Imager 600	GE Lie Sciences	
BashingBead lysis tubes	Zymo Research	Cat#S6003
Precellys Evolution Homogenizer	Bertin Technologies	N/A
NanoZoomer 2.0-HT slide scanner	Hamamatsu Photonics	N/A
0.45 μm PVDF filters	Milipore	Cat#SLHV033RS
Discovery ULTRA autostainer	Ventana Medical Systems	N/A
Non-treated 96 well-plate	Thermo Fischer Scientific	Cat#442404

RESOURCE AVAILABILITY

Lead contact

Further information and requests for resources and reagents should be directed to and will be fulfilled by the lead contact, Enrique J. Arenas (earenas@vhio.net).

Materials and availability

Cell lines generated in this study are available from the lead contact upon request.

Data and code availability

- RNA-seq data has been deposited at GEO database and is publicly available as of the date of publication. Accession number is listed in the key resources table.
- This paper does not report original code.
- Any additional information required to reanalyze the data reported in this paper is available from the lead contact upon request.

EXPERIMENTAL MODEL AND SUBJECT DETAILS

Immune cells

In this study we used two sources of immune cells: PBMCs and $CD34^+$ hematopoietic stem cells. PBMCs and cord blood units for $CD34^+$ cell isolation were obtained from anonymous healthy donors through the Blood and Tissue Bank of Catalonia (BST). All human samples were obtained following institutional guidelines under protocols approved by the institutional review boards (IRBs) at Vall d'Hebron Hospital.

Mice

For *in vivo* experiments, 5-week-old female NSG (NOD.Cg-Prkdcscid Il2rgtm1Wjl/SzJ) (#614) mice were purchased from Charles River. Mice were randomized by tumor size, and those that died before the end of the experiments for reasons unrelated to treatment or that did not have detectable percentages of human immune cells were excluded. Because of ethical reasons, we ended the experiments before the full development of graft-versus-host disease or when tumor volume surpassed 1500 mm^3. Experiments were not performed in a blinded fashion. Animal work was performed according to protocols approved by the Ethical Committee for the Use of Experimental Animals at the Vall d'Hebron Institute of Oncology.

Cell lines and primary cultures

MKN45 and SW1222 were obtained as a gift from Dr. Hector Palmer (VHIO), and COLO201 were a gift from Dr. Marta Cascante (Universitat de Barcelona). HEK293T (#CRL-3216) were obtained from ATCC.

Cell lines were cultured under standard conditions in complete medium (DMEM F-12 medium (#21331, Gibco) supplemented with 10% fetal bovine serum (FBS) (#10270, Gibco), 1% L−Glutamine (#X0550, Biowest), and 1% Penicillin-Streptomycin (#P4333, Sigma-Aldrich)). Cells were genetically modified to acquire resistance to certain antibiotics or to downmodulate or overexpress different genes.

Patient-derived xenograft establishment

The patient-derived xenografts (PDXs) were obtained from liver biopsies of patients enrolled in the clinical trial NCT02650713. PDXs used in this study derive from patients of both sexes and 18 years and older. All PDXs have been established at VHIO following institutional guidelines. The IRBs at Vall d'Hebron Hospital provided approval for this study in accordance with the Declaration of Helsinki. Written informed consent was obtained from all patients who provided tissue samples.

METHOD DETAILS

PBMC isolation

PBMCs were isolated from fresh buffy coats obtained from healthy donors. Blood was diluted 1:3 with 1x PBS and transferred to a 50mL falcon tube with Ficoll-Paque PLUS (#70-1440-02, GE Healthcare) at a 1:3 ratio, following the manufacturer's instructions. After obtaining the buffy coat, red blood cells were lysed with 1x RBC lysis buffer (#00-4333-57, Invitrogen) for 4 min. Obtained PBMCs were counted and frozen with Cryostor CS10 (#07959, Stemcell Technologies) at −80°C for co-culture and *in vivo* experiments.

TCB constructs generation

HER2-TCB was designed as a 2 + 1 CrossMabCH1-CL based on trastuzumab and CH2525 variable domains as described in (Bacac et al., 2016a) and (Schaefer et al., 2011), and CEACAM5-TCB was designed as a charged 2 + 1 CrossMAb VH-VL based on T84.66 and CH2527 variable domains as described in (Bacac et al., 2018). As a control, DP47-TCB in the analogous 2 + 1 CrossMabCH1-CL format based on a germline non-binding variable domain was applied. TCBs were purified using standard methods: Protein A affinity chromatography (MabSelect SuRe) followed by catione exchange chromatography (Butyl-Sepharose 4FF/POROS XS) and size exclusion chromatography (Superdex 200) and formulation in 20 mM histidine/histidine-HCl, 140 mM sodium chloride buffer at pH 6.0. All TCBs were analyzed for absence of aggregates by analytical size exclusion chromatography and absence of endotoxins.

Generation of resistant cells *in vitro*

To generate the resistant models, parental cells (MKN45, SW1222) were transfected with Lenti CMV V5-LUC Blast (w567-1) (#21474, Addgene) in order to obtain blasticidin resistance. Cells were treated with a 3:1 ratio PBMC:Tumor and an increasing concentration of HER2 or CEACAM5-TCB in PBMC media (RPMI 1640 (#61870, Gibco), 10% Heat-Inactivated FBS, 1% L−Glutamine, 1% HEPES (#H0887, Sigma-Aldrich), 1% MEM Non-Essential Amino Acids Solution (#11140, Gibco) and 1% Penicillin-Streptomycin). After 72 h, media was removed and replaced with complete medium containing 20 μg/mL blasticidin (#ant-bl-1, Invivogen) during 7 days to specifically kill remaining PBMCs. The process was repeated several times. In the three models (MKN45-HER2R, MKN45-CEAR, SW-CEAR) resistance was obtained after 6 months and around 20 rounds of treatment.

Interferon-gamma resistant model (MKN45-RG) was established by culturing cells in presence of increasing IFN-γ concentrations, starting at 100 ng/mL and reaching 1 μg/mL. Resistant population was obtained after 4 months.

T cell cytotoxicity assays

All target cells were seeded in 96-well flat bottom plates (0.01 x 10^6 cells/well) (#353075, Corning Life Sciences). Effector PBMCs were added to each well at the indicated ratio in PBMC medium. Different concentrations of the respective TCB were added to the wells. The plates were incubated for 72 h.

At the endpoint cells were harvested with Trypsin-EDTA (#25300096, Gibco) and resuspended in FACS buffer (PBS 1x, 2.5 mM EDTA, 1% BSA (#A9647, Sigma-Aldrich), 5% horse serum (#26050, Gibco)) in polypropylene V-bottom 96 well-plates (#651201, Greiner Bio-One). Twenty minutes later, samples were centrifuged and cells were stained with the epithelial cell marker anti-human EpCAM (#324212, BioLegend) at 1:300 concentration in FACS buffer in ice for 30 min. After a wash with 1× PBS, samples were re-suspended in the viability marker Zombie Aqua at 1:1000 (#423101, BioLegend) in 1x PBS and acquired on LSR Fortessa (BD Biosciences). Number of alive cells was analyzed with FlowJo software (BD Life Sciences) by means of EpCAM counts.

3D organoid assay

Tumor cells were seeded in 48 well-plates (10^3 cells/well) in a drop of 20 μL of matrigel (#356235, Corning). Each drop was dispensed in the center of the well and incubated for 15 min at room temperature. After matrigel was solidified, 250 μL of 3D colorectal cancer organoid media (van de Wetering et al., 2015), were added to each well. Media was replaced twice a week and 3D formation was assessed after 15 days. Organoids per well were counted and assumed that each of them consisted of approximately 50 cells. Organoid media was removed and 3D structures were co-cultured with PBMCs for 72h at a 2:1 ratio in PBMC media and treated with 1 nM HER2-TCB or at a 5:1 ratio with 500 pM CEACAM5-TCB.

At the endpoint, organoids were disaggregated by adding 500 μL of trypsin for 30 min at 37°C. Then, cells were collected and incubated for 30 min on ice to liquefy matrigel. Fully disaggregated organoids were washed and stained as previously described. Number of alive cells was analyzed with FlowJo software by means of EpCAM counts.

Flow cytometry

Cells were harvested with StemPro Accutase (#A1110501, Gibco) and resuspended in FACS buffer. Twenty minutes later, samples were centrifuged and cells were incubated for 30 min with the specified conjugated or primary antibody. Conjugated antibodies hIFNGR1 (#308606), hIFNGR2 (#308504) and the isotype control PE mouse IgG Isotype Ctrl (#400114), all from Biolegend, were used at 1:100. After a wash and Zombie Aqua staining, samples were acquired on LSR Fortessa.

In the case of HER2 and CEACAM5 staining, cells were incubated in FACS buffer for 30 min with Trastuzumab (#180288-69-1, Herceptin, Roche) at 2.5 mg/mL, or 10 nM CEACAM5-TCB. Primary antibodies were then bound to its antigen, and after a PBS wash, a secondary conjugated antibody Anti-human Alexa 488 (#A-11013, Invitrogen) was incubated with the cells at a concentration of 1:500 for 30 min. Cells were then washed with 1x PBS, resuspended in Zombie Aqua viability marker and acquired on LSR Fortessa.

The activation markers CD69 (#310914) and CD25 (#302610) in $CD8^+$ cells (#344712), all from Biolegend at 1:300 concentration, were used in order to assess T cell activation after 72 h of co-culture with tumoral cells and the corresponding TCB.

Flow cytometry data was analyzed with FlowJo software (BD Life Sciences).

5-Azacytadine treatments *in vitro*

To assess the recovery of CEA expression in resistant cells, these were treated with 1 μM of 5-Azacytidine (#A2385, Sigma-Aldrich) for 24h and 48h when assayed the RNA expression, 48h for MeDIP and ChIP assays, and 72h when assayed the surface protein expression by flow cytometry. To assess MKN-HER2R cells response to 5-AZA, 48h treatment with 1 μM drug was used.

For T cell cytotoxicity assays, 5000 cells were seeded per well and pretreated for 72h with 1 μM of 5-AZA. On the day of treatment with CEACAM5-TCB and PBMCs, wells were cleaned with PBS 1x and then co-cultured as previously described. Treatments with 5-AZA consisted of media renewal every 24h.

RNA isolation and qRT-PCR

Total RNA was isolated from adherent cells by using RNeasy Mini Kit (#74106, Qiagen) according to the manufacturer's protocol. RNA was eluted in RNase-free water and quantified using NanoDrop™ 2000 spectrophotometer (Thermo Fisher Scientific).

cDNA was prepared from 1 μg template RNA using the high capacity cDNA reverse transcription Kit (#4368813, Applied Biosystems) according to the manufacturer's protocol.

Real-time quantification of transcript abundance was determined by qRT-PCR using the TaqMan Gene Expression probes (Applied Biosystems) and TaqMan Universal Master Mix II (#4440039, Applied Biosystems), in 384- well plates in 7900HT Fast Real-Time PCR System (Applied Biosystems), following the manufacturer's protocol.

The TaqMan probes against *CEACAM5* (Hs00944025_m1) *and GAPDH* (Hs02758991_g1)were used. Data was analyzed with SDS RQ Manager and DataAssist software (Applied Biosystems), using the $2^{-\Delta CT}$ method. *GAPDH* was used as an endogenous control.

RNASeq

Total RNA was quantified by Qubit RNA BR Assay kit (#Q10210, Thermo Fisher Scientific) and the integrity was checked by using RNA 6000 Nano Bioanalyzer 2100 Assay (#5067-1511, Agilent).

The RNASeq libraries were prepared using the Stranded Total RNA Prep with Ribo-Zero Plus (Illumina) following the manufacturer's recommendations and the final library was validated on an Agilent 2100 Bioanalyzer with the DNA 7500 assay (Agilent).

The libraries were sequenced on NovaSeq 6000 (Illumina) with a read length of 2 × 51bp following the manufacturer's protocol for dual indexing. Image analysis, base calling and quality scoring of the run were processed using the manufacturer's software Real Time Analysis (RTA v3.4.4) and followed by generation of FASTQ sequence files.

Bioinformatic analyses were performed in R (version 4.0.3) on the counts table obtained using the nf-core/rnaseq pipeline (version 3.5) with GRCh38 and default parameters.

Differential gene expression was assessed with the voom + limma strategy in the limma package (version 3.48.3). Genes having less than 10 counts in at least 2 samples were excluded from the analysis. Correction for multiple comparisons was performed using false discovery rate (FDR), obtaining the adjusted p values. Genes were considered to be differentially expressed between studied conditions if the adjusted p value was <0.05 and the $|logFC| > 1$.Functional analysis was performed using the ranked Gene Set Enrichment Analysis (GSEApreranked) as implemented in clusterProfiler R package (version 4.0.5). Functional annotation was obtained from the following, gene set collections in the Molecular Signatures Database (MSigDB, version 7.5.1): 1) C5.GO.BP: gene sets derived from the Biological Process Gene Ontology (GO); 2) C2.CP.KEGG: gene sets derived from the KEGG PATHWAY database; 3) C2.CP.Reactome: gene sets derived from Reactome database; 4) C3.TFT: gene sets predicted to contain transcription factor binding sites in their promoter regions.

Data have been deposited to the Gene Expression Omnibus (GEO) under Series accession number GSE210592.

Metilated DNA immunoprecipitation (MeDIP)

MeDIP was performed using MagMeDIP qPCR Kit (#C02010021, Diagenode) following manufacturer's instructions, with modifications at the DNA extraction and purification and the DNA shearing steps.

Cell collection and lysis was performed following kit's instructions, and nucleic acid extraction and purification was performed using the DNA extraction kit QIAamp DNA Mini Kit (#51304, Qiagen). Samples were then sonicated to generate fragments of DNA between 300 and 500 bp with the Covaris M220 Focused ultrasonicator (Covaris). In particular, 5 μg of DNA in 100 μL were added to microtubes AFA Fiber Pre-Slit Snap-Cap 130 μL (#520045, Covaris) and the following ultrasonicator program was used: 7°C temperature, 50W peak incident power, 10% duty factor, 200 cycles per burst (cpb), and 180 s treatment time. Methylated DNA immunoprecipitation and isolation was performed following manufacturer's protocol.

Finally, qPCR was performed with the MeDIP samples using SYBR green reagent (#733-1390, Quantabio). A 159-bp segment of the *CEACAM5* promoter was amplified with the following primers: 5′-GAGGCAGAAATGAGAGGGGA-3′ (sense) and 5′-AACGTT TTGTCAAGGCTGCT-3′ (antisense). Data shown is the result of normalizing the specific signal of the MeDIP antibody of MKN45 or 5-AZA treated MKN-CEAR to the resistant MKN-CEAR cells.

Chromatin Immunoprecipitation (ChIP)

Indicated cells were grown to 70% confluence, collected, and subsequently cross-linked with 1% formaldehyde (#47608, Sigma-Aldrich) shaking at 37°C temperature for 10 min. Reaction was quenched by incubating the samples with 125 mM Glycine (#BP381, Fisher Scientific) for 5 min. Cells were pellet at 5 x 10^6 cells/vial and stored at −80°C.

Cell pellets were resuspended in SDS lysis buffer (1% SDS, 10 mM EDTA, 50 mM Tris pH 8) with 1:200 Protease Inhibitor Cocktail Set III (#535140, Merck Millipore) for 30 min on ice. Samples were then sonicated to generate fragments of DNA between 100 and 600 bp with the Bioruptor (Diagenode). After 20 min on ice, samples were centrifuged at 19,000 x g and supernatant was diluted 1/10 with Dilution buffer (0.01% SDS, 1.1% Triton X-100, 1.2 mM EDTA, 16.7 mM Tris pH 8, 167 mM NaCl), in order to decrease concentration of SDS. Samples were incubated with 10 μL of Dynabeads protein A (#10002D, Invitrogen) and 1 μg of irrelevant antibody Rabbit IgG (#I8140, Sigma-Aldrich) per IP in that sample, as a preclearing. Incubations lasted for 3 h rotating at 4°C. Magnets were used to discard the beads, and the samples were separated per IP, saving 10% for the input. 3 μg of corresponding antibody was added at each tube and samples were incubated overnight rotating end over end at 4°C. The antibodies used were: Rabbit IgG, anti-H3K27Ac (#ab4729, Abcam) and anti-H3K27Me3 (#07-449, Merck Millipore).

Samples were incubated with 50 μL of pre-washed dynabeads and incubated 3 h rotating at 4°C. Dynabeads were then washed 3 times with low salt and 3 times with high salt buffer (0.1% SDS, 1% Triton X-100, 2mM EDTA, 20 mM Tris pH 8, and 150 or 500 mM NaCl respectively) and 2 times with LiCl buffer (250 mM LiCl, 1% NP-40, 1% NaDOC, 1 mM EDTA, 10 mM Tris pH 8). Samples were then incubated with 48 μL of elution buffer (0.4% SDS, 5 mM EDTA, 10 mM Tris pH 8, 300 mM NaCl) supplemented with 2 μL proteinase K (#RPTOTKSOL, Roche). Then, samples were incubated shaking 1 h at 55°C and subsequently overnight at 65°C. Input samples were treated the same way. DNA was purified from the eluted samples with the MinElute PCR Purification Kit (#28006, Qiagen) following the manufacturer's instructions.

Finally, qPCR was performed with the ChIP samples using SYBR green reagent. The *CEACAM5* promoter region was amplified with the same primers as the MeDIP. Data shown is the result of normalizing the specific signal of each antibody (normalized to the IgG control signal) of MKN45 or 5-AZA treated MKN-CEAR to the resistant MKN-CEAR cells.

Interferon-gamma cytotoxicity assays

MKN45 cells were seeded in flat bottom 96-well plates (5 x 10^3 cells/well). After 24 h cells were treated with different concentrations of Interferon-gamma (#300-02, Peprotech). Treatment lasted for 3 days and cell death was assayed by crystal violet staining of alive

cells. Cells were fixed for 30 min with 10% Glutaraldehyde, washed, and stained for other 30 min with 0.1% Crystal violet (#548-62-9, Sigma-Aldrich). After three washes with water, plates were let dry overnight. For the readout, 100 μL of 10% Acetic acid were added to each well and absorbance was read at 560 nm using an Infinite M200 Pro Multimode Microplate Reader (TECAN).

Cell proliferation assays

MKN45 cells were seeded in flat bottom 96-well plates (5 x 10^3 cells/well). At day 0, 1, 3 and 4 cell proliferation was assayed by crystal violet staining of alive cells.

Western blot

For Western blot, protein extracts were isolated by lysing the cells in homemade lysis buffer (130 mM NaCl, 0.01% NP-40, 1% glycerol, 2 mM EDTA pH 8 and 20 mM Tris-HCl pH 7.4), supplemented with phosphatase inhibitors 5 μM β−Glycerolphosphate, 5 μM sodium fluoride, 1 μM sodium orthovanadate and cOmplete™, EDTA-free Protease Inhibitor Cocktail (#COEDTAF-RO, Sigma-Aldrich, 1 tablet per 10 mL lysis buffer). Protein extracts were sonicated for 10 s at 4.5 V to break the cell apart. Tubes were centrifuged 14,000 rpm 10 min and supernatant was collected.

Protein lysates were resolved by SDS PAGE and then transferred to a 0.45 μm nitrocellulose membrane (#10600002, GE Healthcare Biosciences). 20-30 μg of protein lysate was loaded per experiment. Membranes were incubated with 5% BSA or 5% non-fat milk in TBS-T (1x Tris-Buffered Saline with 0.1% tween 20 (#P7949, Sigma-Aldrich)). After blocking, membranes were incubated overnight with primary antibodies.

After washing, membranes were incubated with horseradish peroxidase-conjugated antibodies (Cytiva) for 1 h.Membranes were developed with Immobilon Western Chemiluminescent HRP Substrate (#WBKLS0500, Millipore) and protein bands were visualized in Amersham™ Imager 600 (GE Life Sciences).

Antibodies used were: HER2 (#AM134, Biogenex), CEACAM5 (#2383, Cell Signaling Technology (CST)), JAK1 (#3344, CST), JAK2 (#3230, CST), p-STAT1 (#9167, CST), STAT1 (#9172, CST), IRF1 (#sc-497, Santa Cruz Biotechnology (SC)), and GAPDH (#ab128915, Abcam). Secondary antibodies used were purchased from Cytiva, anti-rabbit (NA934) for all primary antibodies except CEACAM5, for which anti-mouse (NA931) was used. All antibodies were used at 1:1000 concentration in 5% BSA except GAPDH and secondary antibodies (1:5000). Quantification of protein levels was done with ImageJ (National Institutes of Health). Quantifications are the result of $\geq$3 independent biological replicates.

Humanized xenograft models

In the PBMCs humanized xenograft models, NSG mice were injected orthotopically with 10^6 tumor cells in 100 μL of 1:1 PBS:matrigel. Once tumor size reached a specified volume, animals were intraperitoneally injected with 10^7 PBMCs obtained from healthy donors. After 24 h, animals started treatment and were treated biweekly with HER2-TCB (0.125 mg/kg), CEACAM5-TCB (1 mg/kg) or vehicle intravenously.

For the 5-Azacitadine *in vivo* experiment, before humanization, mice were treated intraperitoneally daily with 5-Azacitadine 2 mg/kg from day 5 to day 10 post-injection.

At the end of the experiments, tumors were analyzed. Tumors were cut into small pieces and divided into samples for IHC, protein, RNA analysis, or flow cytometry. Samples for IHC were fixed and embedded in paraffin. Samples for RNA analysis were incubated with lysis buffer from RNAeasy Mini Kit. Samples for Western blot were incubated with lysis buffer supplemented with phosphatase and protease inhibitors. RNA and protein samples were put in BashingBead lysis tubes (#S6003, Zymo Research) and homogenized in Precellys Evolution Homogenizer (Bertin Technologies).

Samples for flow cytometry were digested in 300 U/ml collagenase IA (#C2674, Sigma-Aldrich) and 100 U/ml hialuronidase IS (#H3506, Sigma-Aldrich) in DMEM F-12 medium. After 1 h of incubation at 37°C with shaking at 10 x g, the mixture was filtered through 100 μm strainers. Red blood cells were lysed with 1x RBC for 5 min RT. After a wash with 1x PBS, samples were counted and acquired on LSR Fortessa for RFP or GFP positive cells detection. Data was analyzed with FlowJo software (BD Life Sciences).

To obtain immunodeficient mice with a reconstituted human immune system, $CD34^+$ cells were purified from human cord blood obtained through the Blood and Tissue Bank of Catalonia. Blood was diluted 1:2 with 1xPBS + 2mM EDTA and transferred to a 50mL falcon tube with 15 mL of Ficoll-Paque PREMIUM (#70-1440-02, GE Healthcare), following the manufacturer's manual. After obtaining the mononuclear cells, resting red blood cells were lysed with 1x RBC lysis buffer for 4 min. $CD34^+$ cells were purified by negative selection by incubating the mononuclear cells with EasySep Human Progenitor Cell Enrichment Cocktail with Platelet Depletion (#19356, StemCell Technologies), following manufacturer's protocol. Purity of the remaining cell mix was checked with anti-human CD34 (#60013, StemCell) and anti-human CD45 (#304008, Biolegend) staining at 1:300 concentration in FACS buffer. Samples were acquired in LSR Fortessa and percentage of CD34 and CD45 cells were analyzed in FlowJo. Obtained cells were frozen with Cryostor CS10 at −80°C. Four/five-week-old NSG mice were treated intraperitoneally with busulfan (15 mg/kg) to ablate the hematopoietic system of the mouse. The next day, 100.000 $CD34^+$ cells were intravenously injected. After 4 to 5 months, the percentages of circulating human $CD45^+$ cells were determined, and mice containing >30% $hCD45^+$ in peripheral blood were orthotopically implanted with 10^5 tumor cells. Once tumors reached ~150 mm^3, animals were randomized and treated biweekly with CEACAM5-TCB (1 mg/kg) or vehicle (intravenously).

Generation of patient-derived xenografts and acquired *in vivo* resistant model

Human tumors used in this study were from biopsies at Vall d'Hebron University Hospital enrolled at NCT02650713 clinical trial. Clinical samples were processed and implanted subcutaneously in NOD SCID mice to generate PDX. When tumors reached 800-1000 mm^3, they were excised, digested and 10^5 cells were implanted subcutaneously in new CD34+ humanized NSG mice (Puig et al., 2013). Efficacy was tested by treating the PDXs biweeekly i.v. with CEACAM5-TCB (1 mg/kg) or vehicle. Acquired resistant PDX63 tumors (PDX63-Rs) were generated by treating humanized mice bearing the PDX63 with CEACAM5-TCB (1 mg/kg) as described previously. Once tumor size reached a specified volume, ~400 mm^3, mice were treated, and when tumors regressed, treatment was stopped. Resistant PDX63 tumors were obtained after 3 passages in different humanized treated mice.

Immunohistochemistry

The following primary monoclonal antibodies were used: anti-CEA (#760-4594) and anti-CD3 (#790-4341), both from Ventana Medical Systems (Ventana), and anti-CD25 (#HPA054622, Human Protein Atlas). For immunohistochemistry, fixed tissue samples embedded in paraffin were sectioned at 4 μm thickness. Sections were heated at 60°C, deparaffinized with xylene and hydrated with two steps of incubation with different dilutions of ethanol.

Immunohistochemical staining of CD3 was performed using a Discovery ULTRA autostainer (Ventana). Heat-induced antigen retrieval was executed using Cell Conditioning 1 (#950-124, Ventana) for 40 min at 95°C. Endogenous peroxidase block was performed with the CM Inhibitor from the ChromoMap DAB kit (#760-159, Ventana) for 8 min. Then, the anti-CD3 primary antibody, ready to use, was applied 32 min at 36°C. Next, samples were incubated for 8 min with detection kit UltraMap anti-Rabbit HRP (#760-4315, Ventana). Reactions were detected using the ChromoMap DAB Kit. Finally, the slides were counterstained with Haematoxylin II (#790-2208, Ventana) 8 min and Bluing Reagent (#760-2037, Ventana) 4 min, followed by dehydration with ethanol and xylene, and mounted in DPX.

CD25 immunohistochemical staining was performed using the HPA054622 antibody from Human Protein Atlas and following manufacturer's protocol.

Immunohistochemical staining of CEA was performed using a Benchmark ULTRA autostainer (Ventana). Heat-induced antigen retrieval was executed using Cell Conditioning 1 (#950-224 Ventana) for 20 min at 95°C. Endogenous peroxidase block was performed with the UV Inhibitor from the UltraView DAB kit (#760-500, Ventana) for 4 min. Then, the CEA primary antibody, ready to use, was applied 32 min at 36°C. Next, samples were incubated for 8 min with detection kit UltraView universal HRP Multimer. Reactions were detected using the Ultraview DAB Kit. Finally, the slides were counterstained with Hematoxylin (#790-2021, Ventana) 8 min and Bluing Reagent 4 min, followed by dehydration with ethanol and xylene, and mounted in DPX.

Slides were scanned in the NanoZoomer 2.0-HT slide scanner (Hamamatsu Photonics) and visualized in the NDP.view2 software (Hamamatsu Photonics).

Viral tumor cells infections

For lentivirus production, HEK293T cells were first incubated for 2 h with 25 μM chloroquine to increase transfection rate. Cells were then transfected with 1 μg/mL of pMD2.G (#12259, Addgene) envelope expressing plasmid, 1.2 μg/mL of psPAX2 (#12260, Addgene) lentiviral packaging vector, and 1.2 μg/mL of the specific lentiviral vector, using 10 μg/mL of polyethylenimine (PEI) (#24765, Polysciences) as transfection agent. 24 h after transfection, growth medium was replaced with complete medium. After 48 h, viral particles-containing supernatant was harvested and filtered with 0.45 μm PVDF filters (#SLHV033RS, Millipore).

For infections, target cells were seeded in 6 well-plates (0.5 x 10^6 cells/well). After 24 h, being the confluence around 75%, tumor cells were incubated with the viral supernatants and 8 μg/mL polybrene (#H9268, Sigma-Aldrich), and centrifuged 45 min at 2250 rpm. After 24 h, medium was replaced with complete medium. 24 h later, infected cells were selected with 20 μg/mL blasticidin (#ant-bl, Invivogen) in the case of Lenti CMV V5-LUC Blast (#21474, Addgene), Lenti-Cas9-2A-Blast (#73310, Addgene), and CMV-RFP (J. Arribas' lab) infected cells, or 1 μg/mL puromycin (#P8833, Sigma-Aldrich) in the rest of infections. Selection was subsequently maintained for one week.

For silencing, the plasmids were obtained from the lentiviral MISSION shRNA Library: HER2 (Clones TRCN0000332953, TRCN0000039878, TRCN0000039881), and CEA (TRCN0000427824, TRCN0000119238, TRCN0000119240), all from Sigma-Aldrich. As a control, tumor cells were infected with Scramble shRNA (#1864, Addgene). To overexpress CEA in MKN-CEAR cells and IFNGR1 in MKN45 cells, the plasmids generated by Vector Builder pLV[Exp]-Puro-EFS > hCEACAM5[NM_004363.5] and pLV [Exp]-Puro-EF1A > hIFNGR1[NM_000416.3] were used, as well as empty vector as control. For the expression of GFP in MKN-HER2R and MKN-CEAR cell lines, pbabe puro EGFP (#128041, Addgene) was used. For the expression of RFP in MKN45 cell line, a CMV-RFP plasmid was used.

To generate the MKN45 KO IFNGR1 cell line, cells were infected with Lenti-Cas9-2A-Blast. After selected with blasticidin, cells were infected with either a CRISPR gRNA targeting IFNGR1 (#HS5000021477, #HS5000021478 Sigma) or the LV04 control universal gRNA vector (#CRISPR18, Sigma). These gRNAs confer puromycin resistance and BFP expression, and cells were selected with 1 μg/mL puromycin. To obtain pure KO IFNGR1 cells, these were stained with hIFNGR1 as explained before, and BFP^{high}/IFNGR1 negative expressing cells were sorted in FACSAria I Digital Cell Sorter (BD Biosciences), obtaining a pool of cells. Validation of KO IFNGR1 cells was done by IFNGR1 staining.

ELISA

Supernatants from the coculture of MKN45, MKN-HER2R or MKN-CEAR with the corresponding TCB at 100pM and 1:3 ratio of tumor cells:PBMCs for 72h were assayed for an IFN-γ ELISA (#31673539, Immunotools) following manufacturer's instructions.

Granzyme B activity

Tumor cells and PBMCs from the coculture specified above were harvested and lysed with 100 μL of lysis buffer. Lysed cells were centrifuged at 21,000 x g for 10 min at 4°C to pellet cell nuclei and other cell debris. Supernatants were harvested and assayed for protease activity. Reaction was performed in a non-treated 96 well-plate (#442404, Thermo Fisher Scientific). Each well contained 25 μL of lysis supernatant, granzyme B substrate Ac-IEPD-pNA (#368057, Sigma-Aldrich) at a final concentration of 300 μM and reaction buffer (0.1M HEPES pH 7.0, 0.3M NaCl, 1mM EDTA) in a total volume of 250 μL/well. Mixtures were incubated at 37°C overnight and color reaction generated by the cleavage of the pNA substrate was measured at a wavelength of 405 nm with the Infinite M200 PRO (Tecan) plate reader.

QUANTIFICATION AND STATISTICAL ANALYSIS

For animal experiments, data is presented as the mean ± standard error of the mean (SEM). The statistical significance of differences was assessed by two-way ANOVA with Bonferroni correction post-test by using Prism 8. In the rest of the cases, data is presented as the mean ± standard deviation (SD), and statistical significance was assessed by unpaired parametric t test using Excel. Data was considered statistically significative when $p < 0.05$. Statistical details can be found in the figure legends.

ADDITIONAL RESOURCES

The PDXs used in this study were obtained from liver biopsies of patients enrolled in a clinical trial using a TCB targeting CEA (CEA-TCB) (NCT02650713, https://clinicaltrials.gov/ct2/show/NCT02324257).

Cell Reports, Volume *41*

Supplemental information

The target antigen determines the mechanism of acquired resistance to T cell-based therapies

Alex Martínez-Sabadell, Beatriz Morancho, Irene Rius Ruiz, Macarena Román Alonso, Pablo Ovejero Romero, Marta Escorihuela, Irene Chicote, Hector G. Palmer, Lara Nonell, Mercè Alemany-Chavarria, Christian Klein, Marina Bacac, Joaquín Arribas, and Enrique J. Arenas

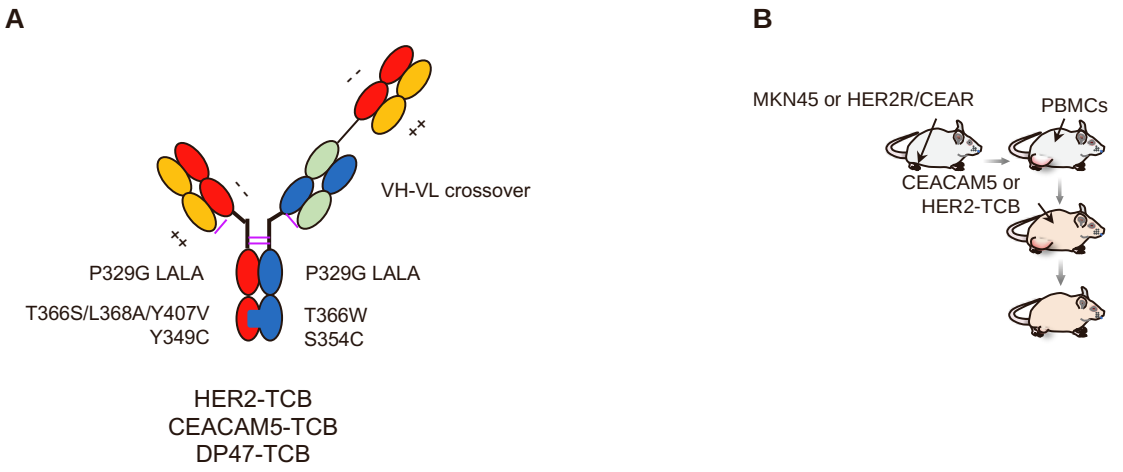

Supplementary Fig. 1 Schematic showing the TCBs structure and *in vivo* assay approaches used in the study. Related to Figure 1.

A, Schematic drawing of the HER2-TCB or CEACAM5-TCB used in this study.

B, Schematic showing the assay of TCB treatment in a PBMC humanized model.

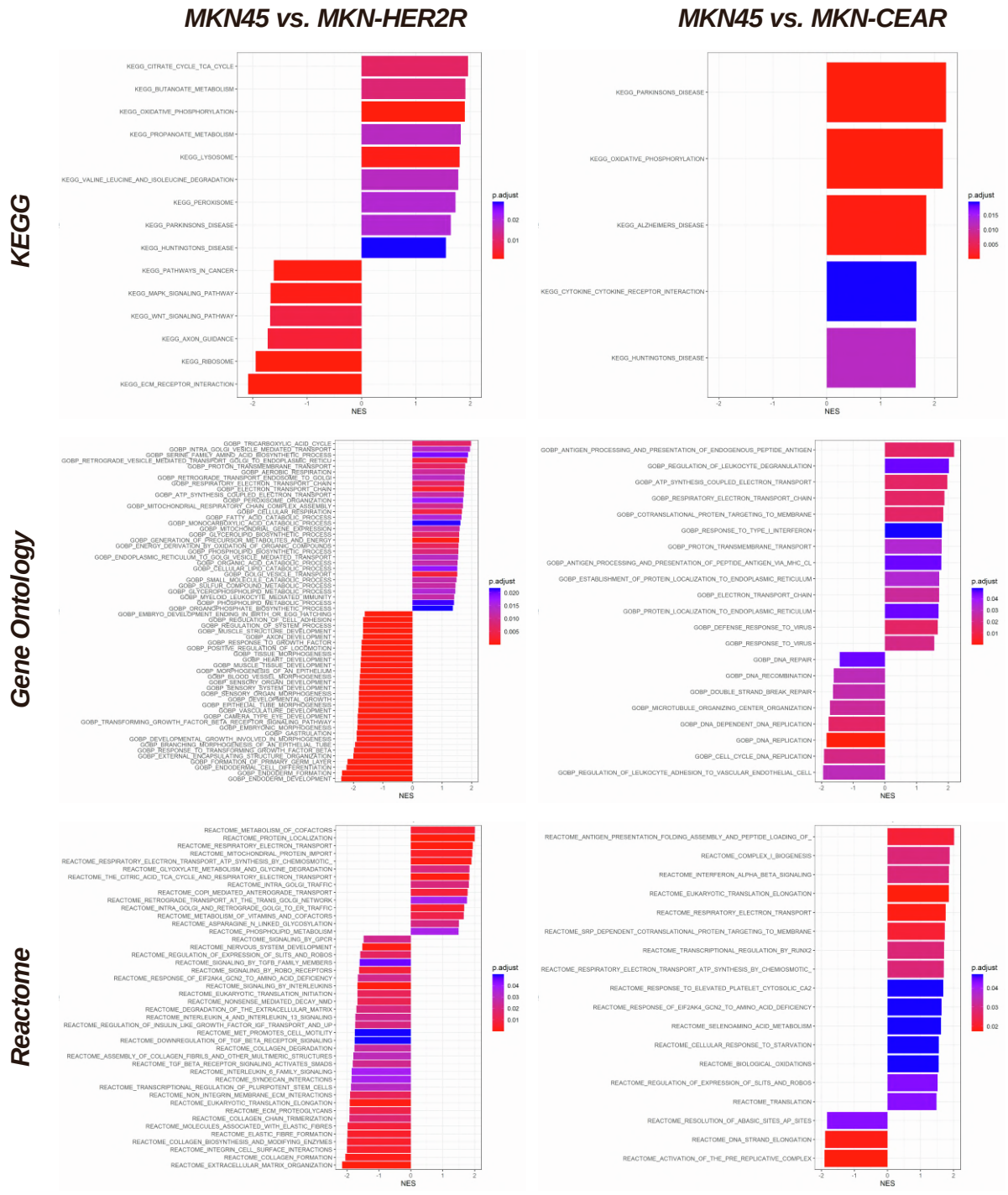

Supplementary Fig. 2 Transcriptomic analysis in MKN-HER2R and MKN-CEAR cell lines. Related to Figure 2.

A, Pathways showing positive and negative enrichment in MKN45 cells compared to MKN-HER2R (above) or MKN-CEAR (below) resistant cells as determined by KEGG, GO, or REACTOME. Only statistically significant gene sets are shown (adjusted p-value<0.05).

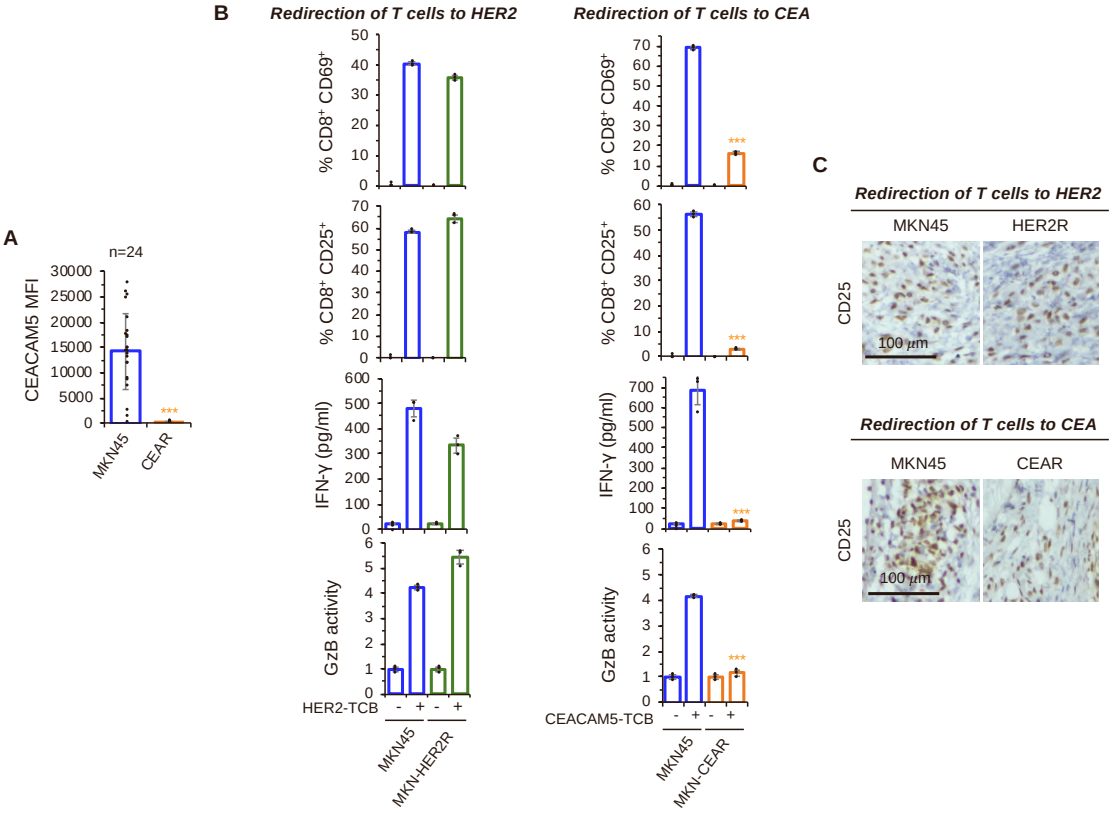

Supplementary Fig. 3 Heterogeneity and T cell activation and T cell functionality in acquired resistant models. Related to Figures 1 and 2.

A, MKN45 and MKN-CEAR cells were subcloned by sorting single cells. Single clones' CEACAM5 expression was assayed by flow cytometry (n=24). Results are normalized to MKN45 clones. Data is presented as mean ± SD of single clones' expression.

B, MKN45, MKN-HER2R and MKN-CEAR were co-cultured with 3:1 ratio of PBMCs and treated with 100 pM HER2-TCB (left) or 100 pM CEACAM5-TCB (right). Activation markers CD69 and CD25 in $CD8^+$ cells were assayed by flow cytometry. An ELISA of IFN-γ was performed in the same supernatants. Granzyme B activity was assayed using the granzyme B substrate Ac-IEPD-pNA. Results were normalized to untreated MKN45 cells. Data are presented as mean ± SD of three independent experiments.

C, Representative images of the CD25 immunohistochemical staining in tumors from the *in vivo* experiment in Fig. 1 F and G are shown.

***p < 0.001, two-tailed *t* test.

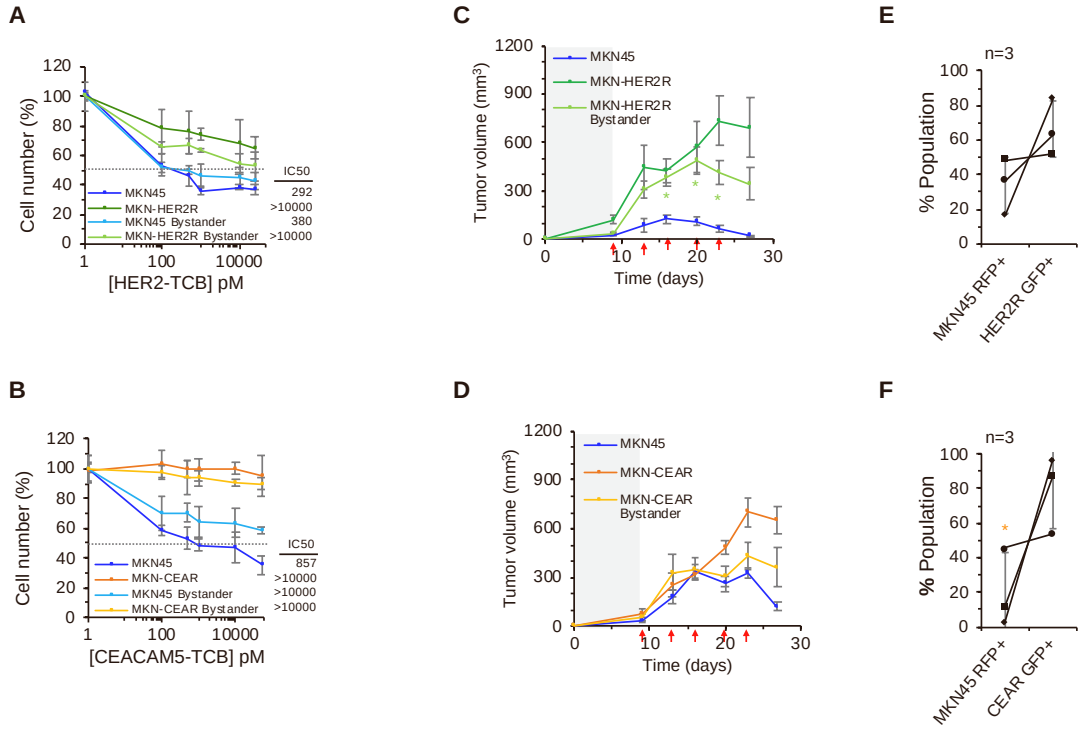

Supplementary Fig. 4 Bystander effect studies *in vitro* and *in vivo*. Related to Figures 1 and 2.

A, **B**, Parental cells were infected with a vector encoding RFP and resistants MKN-HER2R and MKN-CEAR with a vector encoding GFP. Co-cultures of PBMCs with parental MKN45, resistants MKN-HER2R (**A**) or MKN-CEAR (**B**) or a 1:1 mixture of parental and resistant cells were treated with different concentrations of HER2-TCB or CEACAM5-TCB (PBMC:target cell ratio 1:1) for 72 h. Then, viable cells were quantified by flow cytometry using EpCAM, RFP, and GFP as markers. Data are presented as mean ± SD of three independent experiments.

C, **D**, 10^6 MKN45, MKN-HER2R (**C**) or MKN-CEAR cells (**D**), or a 1:1 mixture of parental and resistant cells were injected subcutaneously into NSG mice. When tumors reached ~100 mm^3 (dark background), 10^7 PBMCs were injected i.p. Then animals were treated i.v. with 0.125 mg/kg HER2-TCB or 1 mg/kg CEACAM5-TCB as indicated (red arrows). Tumor volumes are represented as averages ± SEM. (n=5 per arm).

E, **F**, Resistant bystander tumors from **C** and **D** were disaggregated and surviving population was assayed by flow cytometry, by means of MKN45 RFP^+ and resistant GFP^+ cells (**E**=HER2R GFP^+ and **F**=CEAR GFP^+) (n=3 tumors).

*$p < 0.05$, two-tailed *t* test.

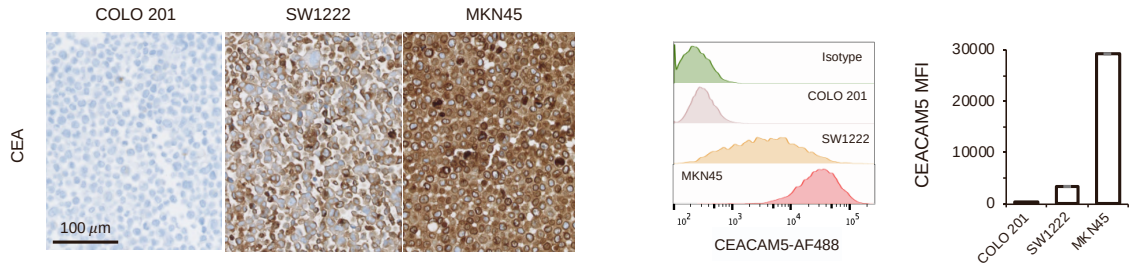

Supplementary Fig. 5 Selection of *in vitro* models expressing CEA. Related to Figures 2 and 3.

CEACAM5 expression in the respective cell lines determined by immunohistochemical stainings (left) or flow cytometry (right).

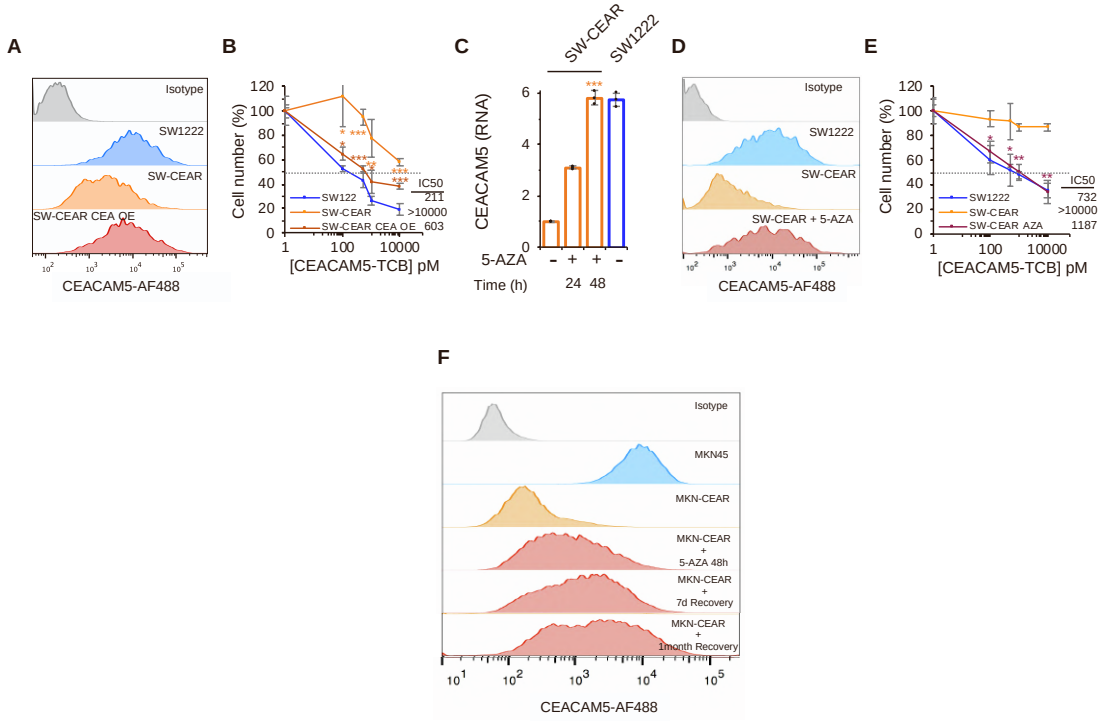

Supplementary Fig. 6 Additional *in vitro* acquired resistant models corroborate CEACAM5 downregulation resistance mechanism and show that demethylating agents recover CEA expression and resensitize resistant cells. Related to Figure 3.

A, Levels of CEA in parental SW1222), CEAR, and CEAR cells stably transfected with a vector encoding CEACAM5 (CEAR CEA OE) were determined by flow cytometry.

B, Same cells were co-cultured with PBMCs at a 2:1 (A) or 1:1 ratio (B) and treated with different concentrations of CEACAM5-TCB for 72 h. Then, viable cells were quantified by flow cytometry using EpCAM as a marker.

C, Indicated cells were treated with 1µM 5-AZA for 48 h. Then, the levels of the mRNA encoding CEACAM5 were determined by RT-PCR and normalized to the levels of CEAR cells treated with vehicle.

D, Levels of CEA in parental SW1222 (A) or MKN45 (B), CEAR, and CEAR cells treated for 72 h with 1 µM 5-AZA were determined by flow cytometry.

E, Same cells were co-cultured with PBMCs at a 2:1 (A) or 1:1 ratio (B) and treated with different concentrations of CEACAM5-TCB for 72 h. CEAR cells were pretreated for 72 h of 1µM 5-AZA before adding PBMCs and CEACAM5-TCB. Then, viable cells were quantified by flow cytometry using EpCAM as a marker.

F, CEACAM5 expression after 5-AZA treatment and removal. MKN-CEAR cells were treated with 1µM 5-AZA for 48 h. After removal of 5-AZA, expression of CEACAM5 was assayed by flow cytometry at the determined timepoints.

*p < 0.05, **p < 0.01, ***p < 0.001, two-tailed *t* test. Data are presented as mean ± SD of three independent experiments.

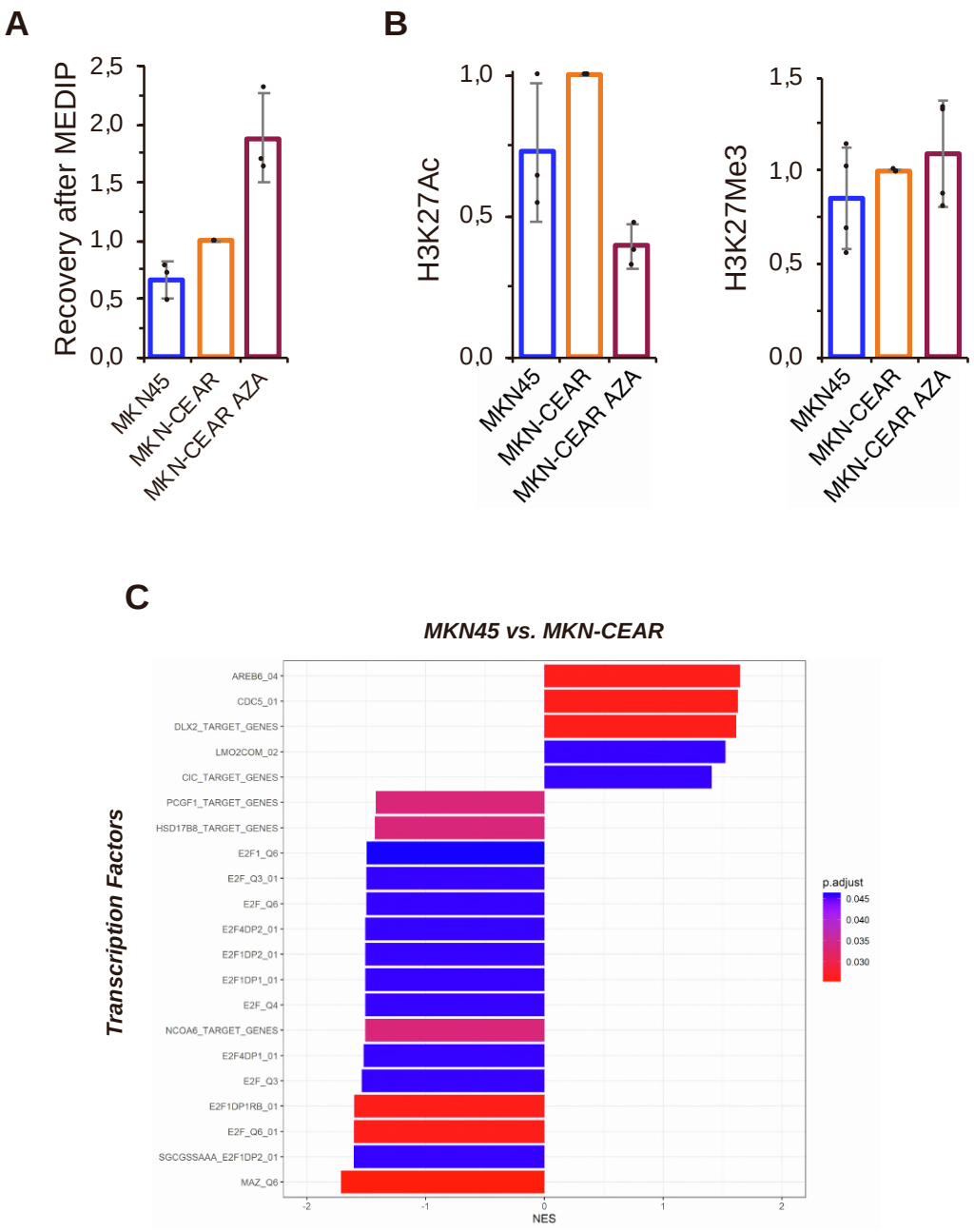

Supplementary Fig. 7 Characterization of *CEACAM5* loci and transcription factor enrichment analysis in MKN-CEAR resistant cells. Related to Figure 3.

A, Recovery of the *CEACAM5* promoter region after Methylated DNA Immunoprecipitation (MeDIP) in MKN45, MKN-CEAR cells and MKN-CEAR treated cells with 1 μM 5-AZA for 48 h. Methylation status of the promoter was measured by MeDIP followed by quantitative real-time PCR. Results were normalized to the input in each sample, and then normalized to the levels in MKN-CEAR cells.

B, Levels of H3K27Ac and H3K27Me3 histone marks in the promoter of *CEACAM5* in same cells as in A. Chromatin status was measured by ChIP followed by quantitative real-time PCR. Results were normalized to the levels of an IgG control antibody in each sample, and then normalized to the levels in MKN-CEAR cells.

C, Transcription factor target genes showing positive and negative enrichment of MKN45 compared to MKN-CEAR cells as determined by TF Enrichment Analysis. Only statistically significant gene sets are shown (adjusted p-value<0.05).

Data are presented as mean ± SD of three independent experiments.

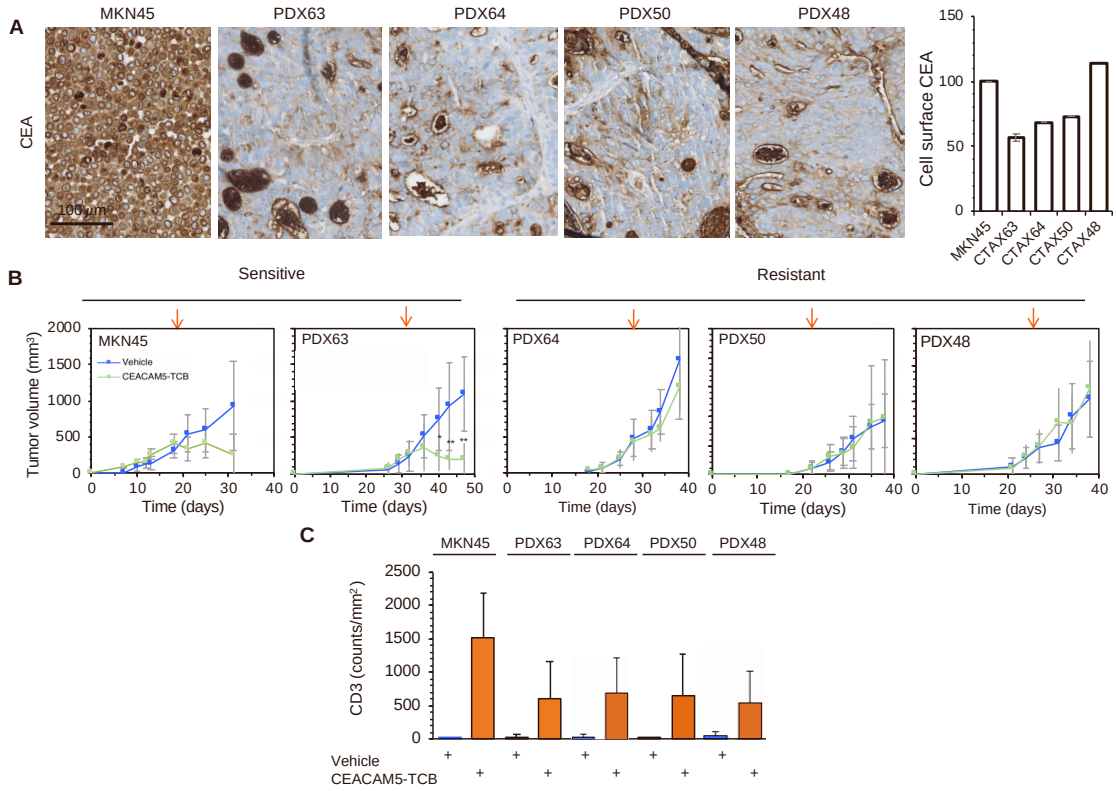

Supplementary Fig. 8 Screening of sensitivity to CEACAM5-TCB in different CEA$^+$ CRC PDXs models. Related to Figure 4.

A, CEACAM5 expression of the studied PDXs determined by immunohistochemical stainings (left) or flow cytometry (right).

B, Sensitivity to CEACAM5-TCB in different CEA$^+$ PDXs models implanted in humanized CD34$^+$ mice. Treatment start is shown by orange arrows. Tumor volumes are represented as averages ± SD.

C, CD3 counts per mm^2 of tumor determined by immunohistochemical stainings.

*p < 0.05, **p < 0.01, two-way ANOVA and Bonferroni correction.

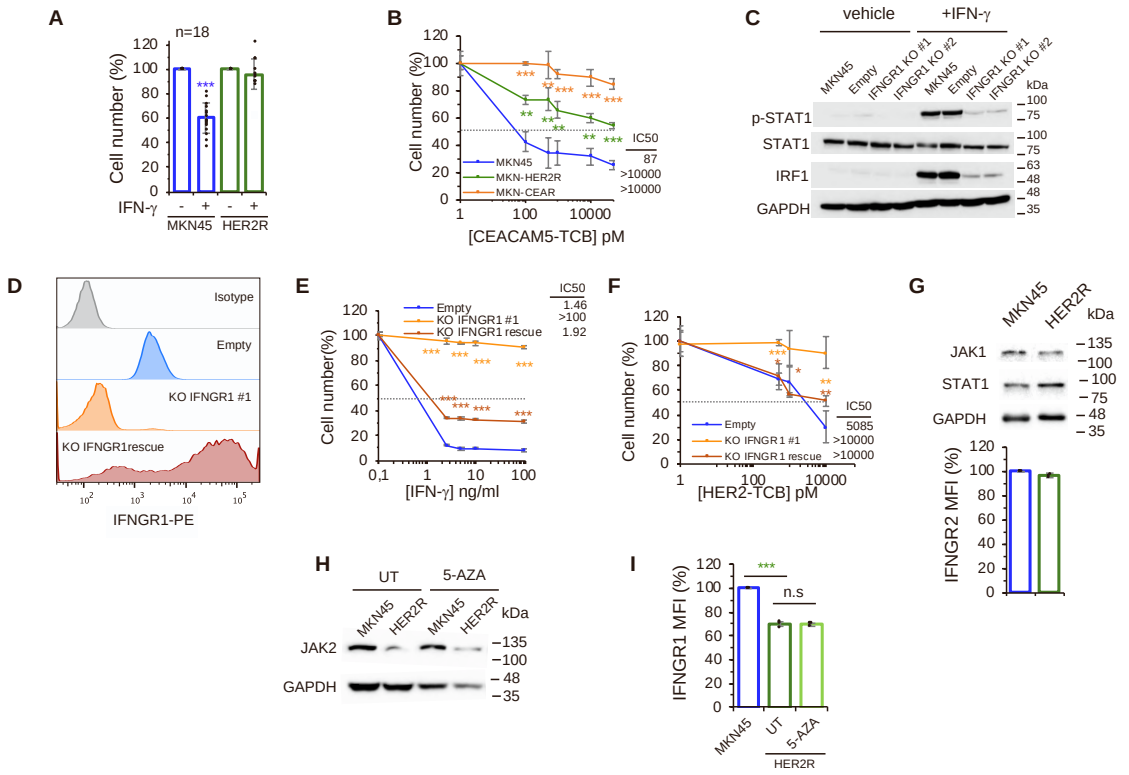

Supplementary Fig. 9 IFN-γ is required for the efficient killing of T cell redirected lymphocytes. Related to Figure 5.

A, MKN45 and MKN-HER2R cells were subcloned by sorting single cells. Single clones' sensitivity to IFN-γ was assayed by treating cells for 72 h with 100 ng/ml IFN-γ and cell number was estimated by crystal violet assay (n=18). Data is presented as mean ± SD of single clones' sensitivity.

B, Co-cultures of PBMCs with parental MKN45, MKN-HER2R or MKN-CEAR cells were treated with different concentrations of CEACAM5-TCB for 72 h. Then, viable cells were quantified by flow cytometry suing EpCAM as a marker.

C, Levels of STAT1, phospho-STAT1 and IRF1 upon 4 h treatment with 10 ng/ml IFN-γ were determined by Western blot in the indicated cell lines.

D, MKN45 empty cells, KO IFNGR1 cells, or KO cells stably transfected with a vector encoding IFNGR1 were stained with anti-IFNGR1 or isotype antibody and analyzed by flow cytometry.

E, Same cells were treated with different concentrations of IFN-γ for 3 days. Cell numbers were estimated with the crystal violet staining assay.

F, Co-cultures of PBMCs with the same cells were treated with different concentrations of HER2-TCB for 72 h. Then, viable cells were quantified by flow cytometry using EpCAM as a marker.

G, Levels of JAK1 and STAT1 in MKN45 and MKN-HER2R cells were determined by Western blot. Levels of IFNGR2 were determined by flow cytometry.

H, Levels of JAK2 in MKN45 and MKN-HER2R cells with and without the treatment with 1μM 5-AZA for 48 h were determined Western blot.

I, Levels of IFNGR1 in MKN45 and MKN-HER2R cells with and without the treatment with 1μM 5-AZA for 48 h were determined by flow cytometry.

*p < 0.05, **p < 0.01, ***p < 0.001, two-tailed *t* test. (B-I) Data are presented as mean ± SD of three independent experiments.

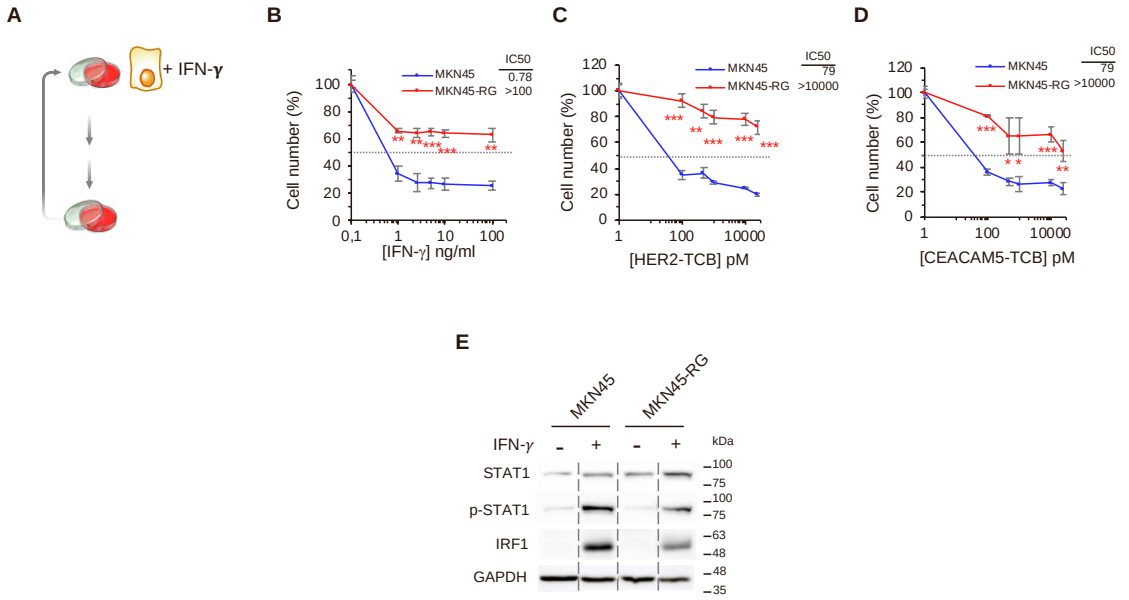

Supplementary Fig. 10 Resistance to IFN-γ leads to resistance to both HER2 and CEACAM5-TCBs. Related to Figure 5.

A, Schematic showing the generation of resistant cells to IFN-γ in the MKN45 cell line model.

B, Parental MKN45 or MKN45-RG cells were treated with different concentrations of IFN-γ for 3 days. Cell numbers were estimated with the crystal violet staining assay. Vertical dashed lines indicate the positions where lanes that were not contiguous on the blot were juxtaposed to remove unused lanes.

C, **D**, Co-cultures of PBMCs with the same cells were treated with different concentrations of HER2-TCB (**C**) or CEACAM5-TCB (**D**) for 72 h. Then, viable cells were quantified by flow cytometry using EpCAM as a marker.

E, Levels of STAT1, phosphoSTAT1 and IRF1 upon 4 h treatment with 10 ng/ml IFN-γ were determined by Western blot.

**p < 0.01, ***p < 0.001, two-tailed *t* test. Data are presented as mean ± SD of three independent experiments.

3. Deciphering the mechanism of action of IFNγ in cancer immunotherapy resistance and strategies to rewire tumor intrinsic IFNγ deficient response

3.1 Tumor intrinsic IFNγ response is required for an efficient immune synapse in T cell redirection therapies

In this thesis, we identified a central role of the tumor intrinsic IFNγ signaling in the response to T cell redirection immunotherapy via TCBs and CAR T cells. We hypothesized that the mechanism of action of IFNγ was an antitumor apoptotic effect (**Figure 3d, Results 1 (R1)**). However, it has been recently described that a deficient tumor intrinsic IFNγ response impinge on the capability of solid tumor cells to form a correct immune synapse with CAR T cells directed against them (Larson et al., 2022). By knocking out the *IFNGR1* gene in glioblastoma cell lines, researchers found that, even correctly activated, EGFR-CAR T cells were not able to exert the cytotoxic effect against tumor cells, due to loss of avidity between the tumor cell and cancer cell, driven by ICAM-1 loss of IFNγ-dependent induction after CAR T treatment (Larson et al., 2022). However, this study use CAR T cells, and no studies reported to date demonstrate if a disrupted immune synapse driven by IFNγ defective response is the cause of resistance to redirected lymphocytes via TCBs. Importantly, it is described that TCBs form a more "TCR-like", a more organized immune synapse, than CAR T cells (Roda-Navarro et al., 2020), and therefore, interactions could differ. Therefore, we hypothesized that the disruption of the immune synapse due to a deficient IFNγ signaling response could be the cause of resistance in our models of acquired resistance to TCB therapies.

To address this question, we used our model of acquired resistance BT-R (**Figure 1, R1**), in which the *JAK2* downmodulation drives IFNγ deficient response, and thus, T cell redirection therapy resistance (**Figure 5, R1**). We performed imaging experiments at Roche Innovation Center Zurich (RICZ), in Dr. Kunz laboratory. To test if IFNγ deficient response drives a deficient immune synapse, we used the parental BT474 cell line, the counterpart resistant BT-R, and the BT-R overexpressing JAK2, in cocultures either with the HER2-TCB and preactivated

$CD8^+$ T cells or with CAR T cells targeting HER2. The pipeline used for these experiments is depicted in **Figure 9A**. Briefly, purified $CD8^+$ T cells were activated with IL-2 and the CD3/CD28 antibody (#10971, Stemcell) overnight, and additional 48h more with only IL-2. Simultaneously, tumor cells were stained with the cell tracker CMAC blue (#C2110, ThermoFisher) and seeded overnight in microscopy plates. On the day of the experiment, activated $CD8^+$ T cells, or freshly thawed CAR-HER2 were stained with the deep red cell tracker (#C34565, ThermoFisher), and cocultured with tumor cells and the caspase 3/7 marker green (#4440, Sartorius) in order to trace apoptosis in the cocultures. After 30 minutes of incubation, slides were imaged with a confocal microscope (inverted LSM 700, Zeiss) with a temperature and CO_2-controlled stage for 4 hours. Live acquisition was performed with a 20x objective. Movies were collected using Zen software (Zeiss) coupled to the microscope, and analyzed with the Imaris 9.9 software.

Strikingly, the BT-R resistant cells exhibited a decrease in the average contact area of the contacts with both T cell redirection therapies, demonstrating that, even a recognition is happening, the area of contact significantly decreases when T cells are cocultured with resistant cells (**Figure 9B** and **9C**). Supporting the results that this deficiency is driven by IFNγ deficient response, when JAK2 was overexpressed in resistant cells, the immune synapse was recovered at the levels of the parental cells (**Figure 9B**).

Therefore, these results indicate that an efficient immune synapse regulated by tumor intrinsic IFNγ signaling can be required for the cytotoxic effect of T cell redirection therapies. Therefore, IFNγ, in addition to the pro-apoptotic effect, also regulates the correct binding of T cells and tumor cells in CAR T and TCB therapy, and its deficient signaling impairs both antitumor effects.

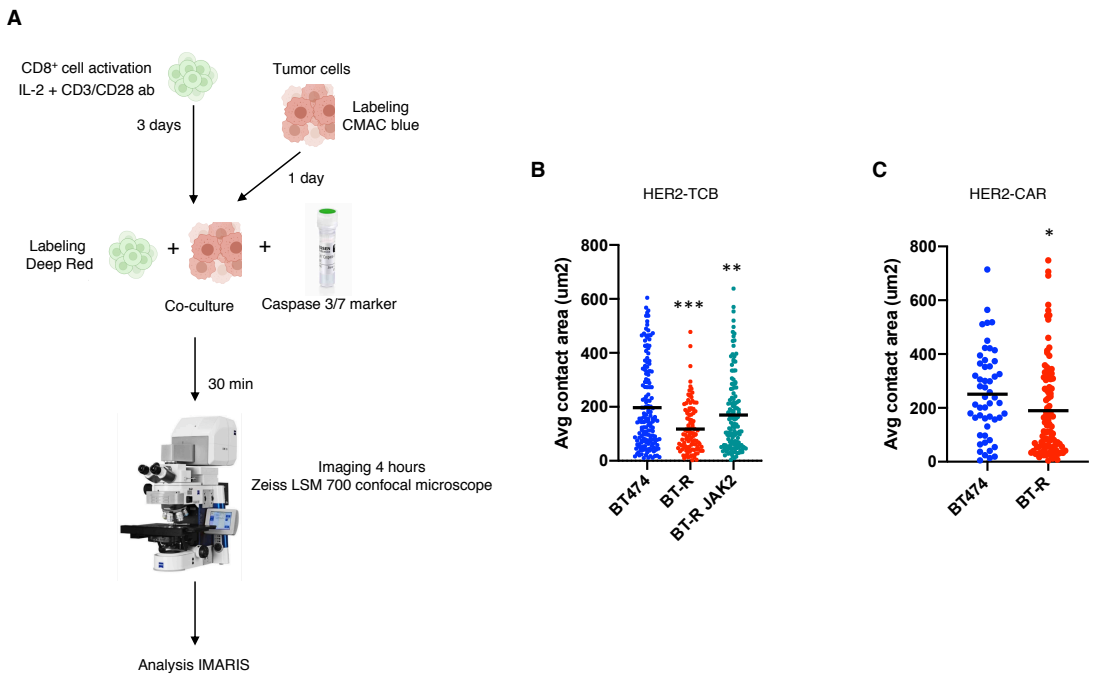

Figure 9: BT-R cells exhibit a deficient immune synapse in both TCB and CAR T cell redirection coculture. A) Schematic drawing of the imaging protocol performed at RICZ. **B**) Parental BT474, BT-R resistant, or BT-R JAK2 overexpressing cells were cocultured with $CD8^+$ T cells at 1:1 ratio and 1nM HER2-TCB and coculture was imaged for 4 hours. The individual interactions between a single tumor cell and a single T cell is represented as an average of the contact area of these unique interactions, as determined with the IMARIS imaging analysis software. **C**) BT474 and BT-R cells were cocultured with HER2-CAR T cells at 1:1 ratio and the cocultures were imaged for 4 hours, and analyzed as in **B**).
*p<0.05, **p<0.01, ***p<0.001, two-tailed t test.

3.2 Identification of new combinatorial strategies to improve T cell redirected therapies

Taking into account all previous findings, we conclusively established that deficient IFNγ is a mechanism of resistance to immunotherapy, including redirected lymphocytes via TCBs and CARs. Therefore, we hypothesized that using unbiased approaches such as a genome wide CRISPR screening and a drug screening will unveil novel vulnerabilities and new combinatorial therapies superior to current immune therapies.

3.2.1 A genome wide CRISPR screening identifies SOCS1 as a target that overcome resistance to IFNγ and immunotherapy

In order to expand our previous analysis of resistance to redirected lymphocytes, we performed a genome-wide screening by CRISPR on parental BT474 and BT-R resistant cells (**Figure 10A**). To do so, cells were infected with a lentiviral genome-scale CRISPR library (#73179-LV, Addgene) at low multiplicity of infection to tag each cell with one unique gRNA. Then, we treated cells with IFNγ, as we have previously demonstrated that sensitivity to IFNγ correlates with sensitivity to redirected lymphocytes. Thus, we hypothesized that genes whose deletion promotes or inhibits death mediated by IFNγ in BT474 or BT-R cells, will also determine the sensitivity to redirected lymphocytes. In particular, we analyzed the comparison of conditions under the pressure of IFNγ by the MAGeCK pipeline (in collaboration with Dr. Levy, Dr. Gros' laboratory, VHIO), as we were interested in genes whose loss recovered IFNγ response, thus, gRNAs negatively enriched after the treatment (**Figure 10A**).

Interestingly, we identified SOCS1, a negative regulator of the IFNγ pathway (Liau et al., 2018), whose knockout recover sensitivity to IFNγ sensitivity (**Figure 10B**). We further validated this result with two independent gRNAs, and the deletion of *SOCS1* not only reactivated the IFNγ signaling pathway by means of pSTAT1 and IRF1 (**Figure 10C**), but also overcame resistance to IFNγ and redirected lymphocytes via HER2-TCB (**Figure 10D** and **10E**). Importantly, these observations were further validated *in vivo* in PBMC humanized mice, where BT-R SOCS1 KO tumors exhibited a similar sensitivity to the HER2-TCB as the parental BT474 cells (**Figure 10F**). Furthermore, in order to expand the importance of targeting SOCS1, SOCS1 knockout was further validated in additional models of acquired resistance established in the laboratory including a gastric and BC PDXs (data not shown).

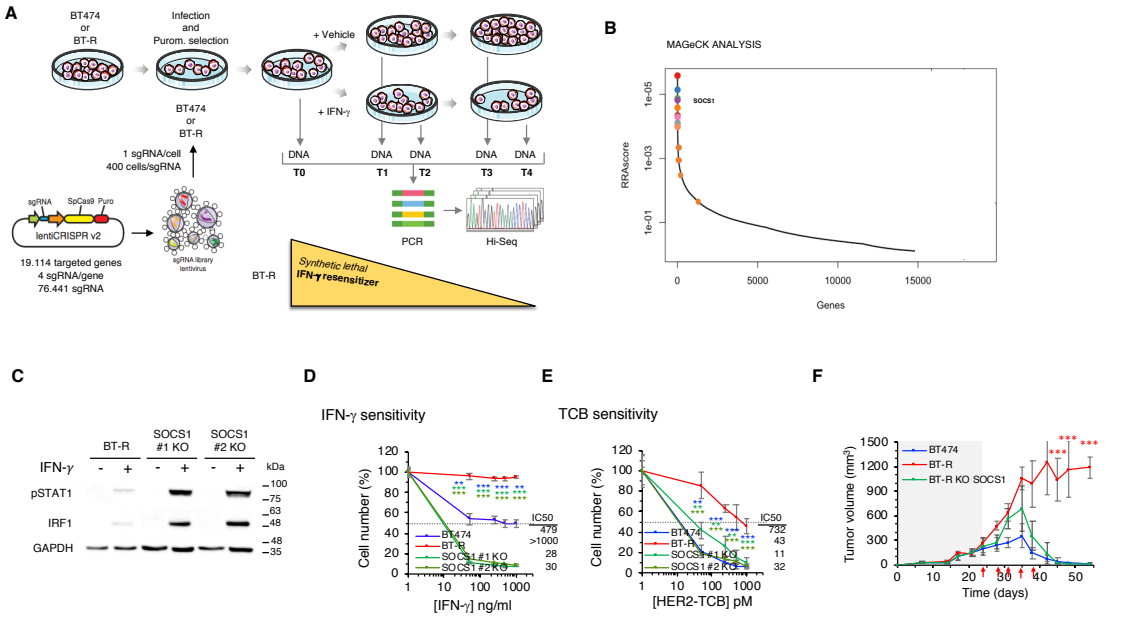

Figure 10: Identification of a novel candidate gene which disruption overcomes sensitivity to immunotherapies. A) Schematic drawing showing the genome-wide CRISPR screening on parental BT474 and BT-R cells; **B**) MAGeCK analysis performed comparing the sequence of BT-R after the treatment of IFNγ. Genes negatively enriched, meaning that were loss after the treatment, are shown; **C**) Western blot analysis of the expression of the IFNγ intracellular signaling pathway components pSTAT1 and IRF1 in BT-R cells or BT-R cells modified with two independent CRISPR gRNA of *SOCS1*. **D**) Parental, BT-R cells, or BT-R SOCS1 KO cells were treated with different concentrations of IFNγ for 7 days. Cell numbers were estimated with the crystal violet staining assay; **E**) Same cells as D) were co-cultured with PBMCs and treated with different concentrations of HER2-TCB for 3 days. Cell numbers were estimated by flow cytometry using EpCAM as a marker; **F**) 10^7 BT474, BT-R, and BT-R KO SOCS1 were injected into the mammary fat pad of NSG mice. When tumors reached ~250 mm^3, $2x10^6$ PBMCs were injected i.p. Then animals were treated i.v. with 0,125 mg/kg HER2-TCB as indicated (red arrows). Tumor volumes are represented as averages ± SD.
p<0.01, ***p<0.001, (D-E**) two-tailed t test. (**F**) two-way ANOVA and Bonferroni correction. Data are presented as mean ± SD of three (**D-E**) independent experiments.

Currently, there is no inhibitor or strategy to abolish the activity of SOCS1. Therefore, we hypothesize that the generation of a novel drug that targets this SOCS1 will be an effective strategy to overcome resistance to immunotherapies by rewiring the IFNγ signaling pathway.

In summary, we identified a novel gene and mediator of response to immunotherapies, a key vulnerability in resistant cells which mediate the re-sensitization to IFNγ and therefore to TCBs and CAR T cells.

3.2.2 A drug screening identifies several FDA approvd candidates that can rewire IFNγ signaling and overcome cancer immunotherapy resistance

In addition to the CRISPR screening, in this thesis, we used a custom repurposing FDA approved library in order to find new vulnerabilities that overcome resistance to IFNγ and redirected lymphocytes. This library, designed at the group of Silvestre Vicent (CIMA), consists of 300 compounds and covers the majority of targetable proteins and pathways involved in cancer. Using the same conditions as conventional cytotoxic assays, we performed the drug screening in the acquired resistant model BT-R cells to both IFNγ and redirected lymphocytes with the HER2-TCB. BT-R cells were seeded in 96 well plates and pre-treated for 24h with the compounds at 1μM, and after 24 hours, media was removed, and cells were then treated with the HER2-TCB or IFNγ for 3 and 7 days, respectively. Several candidates resensitized BT-R cells to either only IFNγ, only HER2-TCB or both IFNγ and HER2-TCB.

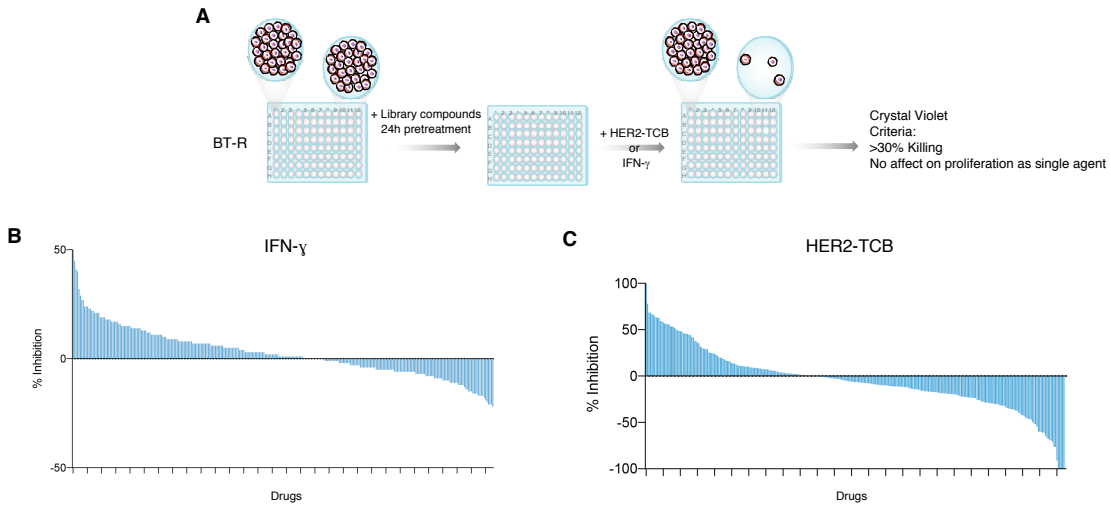

Figure 11: Identification of drugs as promising strategies to overcome resistance to immunotherapies. A) Schematic drawing showing the performed screening. BT-R cells were treated with IFNγ or HER2-TCB with a custom library of 300 compounds. Criteria to select the drugs are shown. **B**) & **C**) Waterfall plot showing the % of growth inhibition of the 300 drugs used in both screenings. % of inhibition was determined by normalizing the value to vehicle treated cells.

Several promising candidates have been identified, some being FDA-approved and broadly used in the clinic, which can therefore be rapidly implemented in the

clinical practice. Further studies will elucidate the potential of combining T cell therapies and the dugs identified in this study.

In conclusion, in this thesis we uncover a novel mechanism of resistance to immunotherapies, which is a deficiency in the IFNγ signaling pathway, and identified promising novel candidates that reactivate the IFNγ pathway recovering sensitivity.

DISCUSSION

Tumor immunotherapy has shown promising clinical benefit against several cancers, with the greatest effect in hematological cancers and the most immunogenic solid tumors such as melanoma or NSCLC (Alexandrov et al., 2013). However, many patients are unresponsive to the treatment, exhibiting primary resistance; or experience relapse after a period of remission, acquiring resistance to the treatment. On top of that, some cancer types, mostly solid tumors, remain completely unresponsive to current immunotherapies. To this end, research is conducted to identify those mechanisms of resistance in order to find vulnerabilities and overcome them. While initially unresponsive tumors may exhibit unresolvable hurdles that make them inadequate for immunotherapy treatment, patients who initially responded to treatment bore tumors that displayed specific traits that made them sensitive to T cell killing, and we hypothesize that these traits can be recovered. Therefore, in this thesis we aimed to identify unknown mechanisms of acquired resistance. To remark the importance of this line of research, in advanced melanoma, the most responsive solid tumor to immunotherapy, the 5-year follow up study of patients treated with nivolumab plus ipilimumab revealed a 62% of patients with ongoing responses, meaning that approximately one third of the tumors became resistant to the treatment after initially responding (Larkin et al., 2019). Accordingly, identifying how tumors become resistant is an urgent clinical need, to then identify combinatorial therapies to overcome it, as well as finding biomarkers of response to better select patients that will benefit from the specific therapy.

To address this challenge, in this thesis we developed models of acquired resistance to immunotherapies, and we found three major findings. First, the tumor intrinsic IFNγ key role in the response to T cell redirection immunotherapies, namely TCBs and CAR T cells. Secondly, the importance of the selected targeted antigen in the mechanism of resistance that may develop when tumors are treated with T cell redirection therapies. Third, we identified strategies and promising combinatorial treatments to revert the deficient IFNγ response, and thus, recover immunotherapy response.

1. Tumor intrinsic deficient IFNγ response is a driver of resistance to immunotherapy

In this thesis we demonstrated the importance of an active IFNγ tumor intrinsic signaling in order to respond to the T cell attack. By generating different cancer models of acquired resistance to TCBs, both *in vitro* and *in vivo*, we demonstrated that a disruption in the IFNγ signaling, mostly driven by *JAK2* downmodulation, impairs the T cell cytotoxic effect on cancer cells (**Figure 4f, Results 1 (R1); Figure 5F, Results 2 (R2)**). This role of IFNγ as a mechanism of immune escape is broadly supported in clinical studies in the case of solid tumors treated with ICIs or TCRt. Given the fact that IFNγ is a major regulator of the APM, the most plausible mechanism by which IFNγ deficient response leads to immunotherapy resistance in antigen presentation dependent therapies such as ICIs or TCRt is a deficient tumor recognition by the T cells (Grasso et al., 2020, Nagarsheth et al., 2021). By contrast, in T cell redirection immunotherapies such as TCBs and CAR T cells, being independent of antigen presentation, the mechanisms by which IFNγ drives immunotherapy resistance remain to be fully understood.

In antigen presentation dependent immunotherapies, mainly ICIs, extensive research has been done on the IFNγ role in solid tumor resistance. In a study with ipilimumab treated melanoma patients, non-responder tumors (both primary and acquired resistant) displayed copy number loss in IFNγ pathway genes, as well as copy number gain in negative regulators of the pathway like *SOCS1* and *PIAS4* (Gao et al., 2016). IFNγ signaling defects have been also recently correlated with resistance to TCRt T cell therapy, as seen in a study with metastatic HPV-associated epithelial cancer patients treated with HPV E7 antigen targeting TCRt T cells, where two resistant patients' tumors bore copy number loss in interferon response genes (Nagarsheth et al., 2021). Moreover, some studies point out mutations in *JAK1/2* as the cause of primary (Shin et al., 2017) or acquired resistance (Zaretsky et al., 2016) to ICIs in melanoma. Consequently, genetic alterations in different components of the IFNγ signaling pathway, including *JAK1* and *JAK2*, are associated with immunotherapy resistance. However, it is important to note that all our HER2-TCB and IFNγ acquired resistance models displayed a transcriptomic downmodulation of *JAK2*

(**Figure 4f, Figure 6e, Figure S6e-f, R1; Figure 5F, R2**), and importantly, in the acquired resistant models to HER2-TCB (BT-R) and IFNγ (PDX667-RG), we performed an exome sequencing and no mutations or copy number variants were found in any of the components of the IFNγ signaling (data not shown). On the contrary, the BT-R and BT-RG acquired resistance models derived from the BT474 HER2^{+} BC cell line exhibited a defective response to IFNγ due to *JAK2* transcriptomic downmodulation, probably driven by the observed decrease in the epigenetic mark of activation H3K27Ac in the promoter of *JAK2* (**Figure 4i, R1**). Accordingly, treatment with the histone deacetylase (HDAC) inhibitor trichostatin A (TSA) was sufficient to upregulate transcriptomic levels of *JAK2*, indicating that the de-acetylation of histone H3 may contribute to the silencing of *JAK2* (**Figure 4h, R1**). Therefore, these results open the avenue to test HDAC inhibitors treatment in *JAK2* low tumors to recover IFNγ response and overcome resistance to immunotherapies. It is important to remark that not much is known about the biological transcriptional regulation of *JAK2* (Hubbard, 2018), and even though it has been previously demonstrated that IFNγ upregulates *JAK2* (Grasso et al., 2020), probably due to feedback loop mechanisms, this has been the first time a *JAK2* transcriptome modulation mechanism has been described. Therefore, our results indicate that the disruption of the IFNγ pathway may arise due to other mechanisms beyond mutations. Importantly, supporting our findings, other clinical studies show this correlation between a defective IFNγ signature and resistance to ICIs (nivolumab and ipilimumab), in which resistant melanomas display transcriptomic defects of IFNγ genes (Rodig et al., 2018, Grasso et al., 2020).

However, although we demonstrated that *JAK2* transcriptional downmodulation leads to immunotherapy resistance, if the H3K27Ac mark is the cause of *JAK2* downmodulation remains to be elucidated. To address this question, BT-R cells could be transduced with the Cas9-p300 activator expression plasmid (Hilton et al., 2015), by which a particular gRNA would target the *JAK2* promoter, attract the Cas9 to the specific genome site, and the histone acetyltransferase p300 would acetylate the histone mark present there. If the H3K27Ac mark and *JAK2* transcription are recovered, that would indicate that *JAK2* is directly epigenetically regulated by the H3K27Ac mark. Nonetheless, this epigenetic

regulation was only found in the BT-R and BT-RG cells, and could be a particularity, so further studies should be performed in other models of *JAK2* downmodulation, as little is known about its regulation (Hubbard, 2018).

Supporting our findings, recent preclinical research besides us describe the tumor IFNγ deficient signaling as a mechanism of resistance to T cell redirection therapies in solid tumors, namely TCBs (Liu et al., 2021) and CAR T cells (Larson et al., 2022). Despite several clinical trials are ongoing in solid tumors, no data is currently accessible (i.e. RNA-seq), which poses a challenge for researchers studying the mechanisms of response of patient's tumors to these therapies. However, preclinical studies show that, by knocking out either *IFNGR1* or *JAK1* in NSCLC or glioblastoma solid tumor cells, respectively, the IFNγ pathway gets inactivated and cancer cells develop resistance to the T cell attack. On the same line, by knocking out *IFNGR1*, in this thesis we show that the IFNγ signal transduction is required for the response to the HER2-targeting TCB and CAR *in vitro,* and to the HER2-TCB *in vivo* (**Figure 3, R1**). The disruption of this pathway, therefore, also promotes lack of sensitivity to immunotherapies independent of the antigen presentation, such as redirected T cells via TCB or CAR T cell treatments. Of note, the IFNγ role in immunotherapy resistance is not cancer type dependent, as downmodulation of *IFNGR1* has been shown to protect from T cell attack in glioblastoma and pancreatic cancer (Larson et al., 2022), and we expanded these results in BC, ovarian cancer and NSCLC (**Figure S4, R1**), and gastric cancer (**Figure S9D-F, R2**). Importantly, in this scenario, T cells are correctly activated as observed by means of the CD25 activation marker and granzyme B release (**Figure S2g, R1; Figure S3B-C, R2**), indicating that the resistance is tumor intrinsic. These results were also observed in the study by Larson, in which *IFNGR1* KO tumors were able to equally activate CAR T cells, as seen in terms of activation, proliferation, and exhaustion, among other evidences (Larson et al., 2022). Therefore, we hypothesize that among the diverse antitumoral actions of IFNγ (Martinez-Sabadell et al., 2021), the role of the IFNγ deficiency as a mechanism of resistance to T cell redirection is due to its apoptotic effect, as seen by means of Annexin V upon IFNγ treatment (**Figure 3d, R1**). Nonetheless, this assay was only performed in the BT-R model and this mechanism should be verified in the rest of acquired resistant models generated.

Additionally, the apoptosis effect of IFNγ as a possible cause of resistance to ICB was proposed in the study by Gao and colleagues, in which they observed that murine melanoma cells genetically knocked down for *IFNGR1* exhibited less apoptosis by means of Annexin V *in vitro,* which was paralleled to resistance to anti-CTLA-4 *in vivo* (Gao et al., 2016).

By contrast, Larson and colleagues demonstrate in glioblastoma preclinical models that *IFNGR1* knockout tumor cells exhibited a disrupted immune synapse with EGFR-CAR T cells (Larson et al., 2022). In this study, the lack of IFNγ signaling impairs CAR T-driven ICAM-1 upregulation, a cell adhesion molecule involved in the immune synapse by the binding to LFA-1 in T cells (Ma et al., 2022). By overexpressing ICAM-1 in *IFNGR1* KO cells, these recovered the sensitivity to the CAR T treatment, and therefore, the authors suggest that this disrupted increase of ICAM-1 by IFNγ is the cause by which IFNγ deficient solid tumors become resistant to CAR T therapy (Larson et al., 2022). This result indicates that, apart from the antigen presentation and the apoptotic effect, IFNγ signaling is required to correctly adhere and engage to T cells in solid tumors. However, the study by Larson use CAR T cells, and no studies reported to date demonstrate if a disrupted immune synapse driven by IFNγ defective response is the cause of resistance in redirected lymphocytes via TCBs. Importantly, it is described that TCBs form a more “TCR-like”, a more organized immune synapse, than CAR T cells (Roda-Navarro et al., 2020), and therefore, interactions could differ. In order to address this question, we used our BT-R resistant model, with an IFNγ deficient signaling, and performed imaging experiments in coculture with the HER2-CAR and the HER2-TCB. Strikingly, with both treatments we observed a deficient immune synapse in resistant BT-R cells in comparison to sensitive BT474 cells, identified by a decreased contact area between the tumor cell and the T cell (**Figure 9, R3**). We additionally observed that intrinsic IFNγ response was the cause of this deficient immune synapse, as demonstrated in rescue experiment with JAK2 overexpression in BT-R cells, which not only recovered the sensitivity to IFNγ and redirected lymphocytes (**Figure 5a-e, R1**), but also the immune synapse disruption (**Figure 9, R3**). However, in our model, ICAM-1 is not the driver of this decreased binding between tumor and effector cell, as its expression is not disrupted in the resistant cells, and ICAM-1 gain of function in

BT-R cells did not recover sensitivity to T cell redirection (data not shown). Therefore, deeper insight into the tumor IFNγ response impact in immune synapse is essential for its understanding. Hence, these findings suggest that IFNγ deficient response may contribute to the resistance of T cell redirected therapies by both impeding the apoptosis process and compromising the interaction with the T cell.

Importantly, the IFNγ role in immunotherapy sensitivity has been mostly related with solid tumors. Despite that, the study by Liu shows that, by knocking down *JAK1* in an ALL and an acute myeloid leukemia (AML) cell lines, cells became resistant to a CD123-TCB (Liu et al., 2021). Contrarily, Larson and colleagues indicated that disruption of the IFNγ pathway by *IFNGR1* KO did not render any effect on hematological (leukemia, lymphoma, and myeloma) cell lines' response to CD19- and BCMA-CAR T cells, while it was crucial for solid tumors response (Larson et al., 2022). Therefore, it seems that the tumor cell intrinsic IFNγ role in immunotherapy response in hematological tumors could be different between TCBs and CAR T cells, and further studies should be performed in order to know the real role of IFNγ in hematological tumors.

Although important advances have been done in T cell redirection immunotherapy research, identifying the mechanisms of resistance still presents a challenge. The current models used in the field, as the ones used in this thesis (**Figure S6, R1**), fail to properly mimic the TME of a patient solid tumor. *In vitro* studies are based exclusively on the T cell-tumor cell interaction, avoiding the potential effect that the other components of the TME may exert on the cancer sensitivity to these therapies. Additionally, *in vivo* studies using humanized mice present the same limitation. Despite better than PBMC humanization, that induce GvHD and engraft mainly T cells, $CD34^+$ hematopoietic stem cell (HSC) mice humanization give rise to, after some months, mostly T cells and some B cells (Xu et al., 2022, Colas et al., 2023), lacking the myeloid compartment and consequently the MDSC and TAM role in the TME. Besides, these models do not phenocopy the complex dynamics between the tumor and the immune system described in the cancer immune cycle. In this regard, the use of syngeneic mice models would allow to better study the dynamics of the tumor evolution upon immunotherapy treatments in a physiologic TME. Nevertheless, these models

have a significant drawback, the data collected will apply to mouse cancer immune responses and involve therapies designed for mice. However, new strategies to improve mice models such as the NSG-SGM3 transgenic mice are being generated to increase the engraftment of myeloid lineages and regulatory T cells (Coughlan et al., 2016), which will allow for a more accurate assessment of the interaction between immune and tumor cells in a TME that mimics netter a real heterogeneous tumor and its interactions.

Additionally, the unavailability of pre and post-treatment tumor samples in T cell redirection clinical trials on solid tumors impedes to corroborate investigators' preclinical work in the clinical practice, which would allow to identify biomarkers of response to immunotherapy. Currently, the used biomarkers, particularly for ICIs, are the expression levels of PD-L1, the TMB state and the MSI tumor levels (Sankar et al., 2022). While tumors expressing high levels of PD-L1 may benefit from PD-1/PD-L1 blockade, a higher TMB and MSI is correlated with higher neoantigen expression. Despite that, although PD-L1 score is the most used biomarker of response to immunotherapy, a study of 45 FDA approvals of ICIs from 2011 to 2019 showed that PD-L1 was only predictive in 28.9% of cases (Davis & Patel, 2019). Consequently, there is an important clinical need to find a reliable biomarker of response to immunotherapy to better stratify those patients that can benefit, avoiding then important toxicities. We hypothesize that tumor intrinsic IFNγ response transcriptome is a good alternative as a biomarker of response. Through the application of scRNA-seq and an examination of tumor intrinsic IFNγ signaling genes, like *JAK1/2*, the responsiveness of patients to T cell-mediated attacks could be anticipated.

2. IFNγ dual role during tumor evolution

It becomes clear that IFNγ antitumoral effects are numerous and diverse, both by activating antitumoral immunity and by exerting direct and indirect tumor suppression effects on cancer cells. Despite that, IFNγ displays as well a "dark" side, with different protumoral effects. The most described T cell inhibitory effect by IFNγ is the upregulation of PD-L1 in tumor cells (Abiko et al., 2015) and other cells in the TME, mostly APCs (Peng et al., 2020). Morover, preclinical data indicates that IFNγ induces production of IDO in both tumor cells and APCs,

inhibiting T cell proliferation and antitumor activity (Jürgens et al., 2009); CXCL9/10, which promotes Treg and M2 macrophages recruitment to the tumor site (Russo et al., 2020); and iNOS in MDSC, suppressing $CD8^+$ T cell proliferation (Shime et al., 2018). In addition to these indirect T cell suppression effects, IFNγ can directly induce TIL apoptosis (Pai et al., 2019) and inhibit clonal diversity and proliferation of stem-like T cells (Mazet et al., 2023). However, when tumor cells become insensitive to IFNγ, the inhibitory effects typically induced by the IFNγ response are not expected to be induced. This was observed in our resistance models, where the PD-L1 induction upon T cell or IFNγ treatment was dramatically decreased in comparison to sensitive cells (data not shown).

The pro- and anti-inflammatory activities of IFNγ are probably sequential and the latter avoids deleterious effects when inflammation is no longer needed, which may happen when chronically exposed to IFNγ. Benci and colleagues hypothesize that initial IFNγ exposure recruits antitumoral immune cells such as APCs and T cells, and promotes antigen presentation, T cell activation and tumor cell killing. However, when chronically exposed to IFNγ, the epigenetic changes in the tumor drive immunosuppression and promote tumor scape (Benci et al., 2016). Interestingly, in this thesis, we generated models of resistance to IFNγ by chronically exposing cells to the cytokine, which became resistant not just to IFNγ, but to TCBs and CAR T cells (**Figure 6, Figure S7, R1; Figure S10, R2**). We hypothesize that while T cell-released IFNγ is vital for immunotherapy response, its prolonged exposure lead to resistance due to reduced sensitivity. In conclusion, IFNγ plays a central role in the control of antitumor inflammation, but depending on the tumor evolution stage, its role can shift to an immunosuppressive effect. Thus, studies measuring the IFNγ production and effect on the different compartments of the TME during tumor evolution is needed.

3. Interventions targeting IFNγ signaling

Given the pleiotropic effects of IFNγ on the immune compartment, and its direct antitumor effects, is not surprising that both activation and inhibition of IFNγ signaling has been tested in the clinic.

Activation of the IFNγ signaling. To activate IFNγ signaling, two strategies have been developed in clinical trials so far: direct administration of recombinant IFNγ or virus encoding IFNγ, or indirectly by the activation of the STING pathway, driving the production of type I IFNs and, as a consequence, IFNγ, boosting immune responses against tumors (Li et al., 2016).

The administration of IFNγ is approved for chronic granulomatous disease and severe malignant osteopetrosis, and has been tested in different tumors, including melanoma, lung adenocarcinoma, renal cell carcinoma, breast and ovarian carcinoma (Shen et al., 2018). Although some antitumor responses were observed, overall, these studies have not resulted positive and patients have suffered side effects such as fever, nausea or rash (Miller et al., 2009), probably due to IFNγ proinflammatory effect. These trials are based on systemic administration, but it has been described that IFNγ has a short half-life (Razaghi et al., 2016). Therefore, intratumoral induction of IFNγ expression in the TME has been also explored. In a phase II clinical trial in patients with cutaneous B cell lymphomas, the intratumoral delivery of an adenovirus encoding IFNγ showed beneficial responses in most patients, with 54% of patients exhibiting CR (Dreno et al., 2014), but due to unknown reasons further studies were discontinued. Additional interesting ways to deliver IFNγ to the tumor include oncolytic viruses expressing IFNγ, which had good preclinical results in mice models bearing solid tumors (Bourgeois-Daigneault et al., 2016).

Besides, there are 11 open clinical trials using different STING agonists ongoing, as single agents or in combination with checkpoint inhibitors. STING agonists activate the production of type I IFNs, which mount a proinflammatory effect, and additionally, activates IFNγ production by T cells (Ohkuri et al., 2014, Jing et al., 2019). So far, even though some toxicities arise, promising antitumor activities have been observed in these trials (Le Naour et al., 2020). However, we tested two different STING agonists in combination with the HER2-TCB and PBMCs and no effect was obtained in our resistant BT-R model (data not shown). We hypothesize that due to the lack of sensitivity to IFNγ in the tumor, even though it is described that T cells get more activated and produce more IFNγ, tumor cells are still unresponsive. For this reason, we believe delivering IFNγ direct or

indirectly is a good strategy to increase efficacy in tumors bearing other resistance mechanisms, but not in IFNγ deficient responsive cancers.

On the other side, a significant effort is being done to discover ways to recover an impaired IFNγ response, and thus, overcome resistance to immunotherapy. In this thesis, we aimed to find novel combinatorial strategies to recover IFNγ sensitivity. To do so, we performed a CRISPR screening in our BT474 and BT-R cells, with the aim to identify targetable genes whose inhibition allowed cells to recover IFNγ response. We identified SOCS1, a negative regulator of the pathway, whose genetic silencing recovered sensitivity to IFNγ and, strikingly, to the HER2-TCB both *in vitro* and *in vivo* (**Figure 10, R3**). Future studies will determine the druggability of SOCS1, but if directly inhibited in the tumor site, and therefore, avoiding systemic exacerbated response to IFNγ, it could be a good candidate to target. Additional targets identified recently to recover IFNγ signaling are the pathway negative regulators PTPN2 (Manguso et al., 2017) and STUB1 (Apriamashvili, 2022), and the RNA-editing enzyme ADAR1 (Ishizuka et al., 2019). Complimentary to the CRISPR screening, we also performed a drug screening of more than 300 compounds, many of them FDA approved, in the BT-R, to recover sensitivity to both HER2-TCB and IFNγ. A key advantage of using an FDA repurposing drug library is that candidates could be applied rapidly into the clinical practice. Our preliminary results indicate several candidates to exploit and validate as potential combinatorial strategies to overcome IFNγ mediated resistance to T cell redirection therapies, and further studies will determine their effectiveness and feasibility (**Figure 11, R3**).

Another strategy to recover therapy sensitivity in IFNγ unresponsive cancers is to surpass this deficiency independently of IFNγ. For instance, the BO-112, a nanoplexed version of polyisosinic-polycytidylic acid (poly I:C) that recovered the expression of MHC-I in murine melanoma B16-JAK1^{KO} cells via NFκB, independently of IFNγ signaling, and thus, restored the efficacy to TCRt T cells *in vivo* (Kalbasi et al., 2020). In an additional study, authors demonstrate in murine TNBC models, that by enhancing ligand-dependent corepressor (LCOR) expression through extracellular vesicle mRNA delivery, resistant tumors with IFNγ deficiency recovered APM genes expression independently of the IFNγ

pathway, and therefore, restored sensitivity to anti-PD-1 therapy *in vivo* (Perez-Nuñez et al., 2022).

Inhibition of the IFNγ signaling. On the contrary, the inhibition of IFNγ has been developed as precision therapy, as genetic activation of *JAK2* is considered a driver of various hematologic tumors (Roberts et al., 2017). This demonstrates that, in contrast to what happens in solid tumors, IFNγ impinge on lymphocyte cell proliferation and progression. Ruxolitinib, a JAK1/2 inhibitor, is approved for the treatment of some of these myeloproliferative neoplasms, demonstrating significant effectiveness. (Mascarenhas & Hoffman, 2012). As a consequence, clinical trials using JAK1/2 inhibitors in combination with ICIs have been performed in solid tumors, and the initial results of the combination with anti-PD-1 have not been positive, probably due to a reduced T cell activation (Kirkwood et al., 2018) and the deleterious effect that can have inhibiting IFNγ signaling in the tumor based on our results.

In summary, targeting the IFNγ pathway in the clinic is currently ongoing with different outcomes. If the disparate effects of IFNγ signaling in the tumor and immune compartment during different stages of tumor progression are confirmed, future effort should be focused in targeting separately these compartments.

4. The target antigen determines the mechanism of acquired resistance to T cell redirection therapies

In solid tumor treatment with CARs or TCBs, the major hurdles are the trafficking into the tumor, the immunosuppressive TME, the heterogeneity of tumor antigens and the antigen escape.

In this thesis, we generated independent acquired models of resistance to two different TCBs to elucidate if different mechanisms of resistance would arise depending on the targeted antigen. For this purpose, we used a TCB targeting HER2 and a TCB targeting CEACAM5, member of the carcinoembryonic antigen (CEA) family. Our main model for this study was the MKN45 gastric cancer cell line, due to the fact that express both antigens in the cell membrane. Strikingly, while the HER2-TCB resistant cell line maintained the HER2 antigen expression,

the CEACAM5-TCB resistant cell line exhibited a remarkable decrease in CEA expression after 6 months of treatment (**Figure 2A-D, R2**). This decrease in CEACAM5 expression was proven to be independent on the cancer type, as it was confirmed in a CRC PDX after generating acquired resistant tumors *in vivo* (**Figure 4, R2**). In addition to CEA, other solid tumor antigens have been described to be downmodulated after treatment pressure, leading to acquired resistance. In a study with 10 recurrent glioblastoma patients treated with a CAR T against EGFRvIII, 5 of 7 patients where biopsy could be taken exhibited antigen loss or downmodulation (O'Rourke et al., 2017). Furthermore, in a clinical trial a glioblastoma patient treated with a CAR against IL13Ra2, antigen downmodulation was observed in one patient (Brown et al., 2016). However, the mechanisms beyond this decrease in antigen expression has not been studied in solid tumors, in contrast to hematological malignancies. Treated patients with CD19 targeting TCBs or CAR T cells can exhibit relapse by CD19 antigen loss due to mutations on the target, alternative splicing and defects in antigen processing (Lemoine et al., 2021), or due to an expansion of antigen-negative pre-existing clones (Fischer et al., 2017). Having access to samples of solid tumor clinical trials, such as the clinical trial using cibisatamab (CEA-TCB) in CRC (NCT03866239), will be undoubtedly a useful strategy to confirm our preclinical results, or identify the mechanisms behind the antigen downmodulation in each antigen case.

As the regulation of each antigen is different, the understanding of its intrinsic biology is required, and preclinical studies are a useful way to study the regulation and the dynamics of the desired antigen, in order to understand its vulnerabilities to identify the mechanism of resistance that may arise. Currently, even though CEA is a common targeted antigen in T cell redirection therapies (Wu et al., 2021, Maher & Davies, 2023), and its heterogeneously expressed between patients, as previously observed by using CRC patient derived organoids (PDOs) (Gonzalez-Exposito et al., 2019), the mechanisms by which it is regulated remain unclear. Particularly, in this thesis we unveil that CEA was downregulated at the transcriptional level, and we hypothesize that the defects in its transcription could be due to inhibitory marks in its promoter. In order to identify the mechanism beyond this regulation, we performed a Methylated DNA Immunoprecipitation

(MeDIP), as well as a Chromatin Immunoprecipitation (ChIP) of two important histone marks (H3K27Ac and H3K27Me^3) in the promoter of *CEACAM5*. However, no differences were observed neither in the methylation nor in the histone regulation of the CEACAM5 promoter between the parental MKN45 and the resistant CEAR cell lines (**Figure S7A-B, R2**).

Regardless of the mechanisms behind antigen downmodulation, overcoming low antigen density is a need when this resistance arises in order to recover sensitivity to redirected T cell attack. In this thesis we demonstrate that the DNA demethylating agent 5-Azacytidine is able to increase tumor CEA expression and recover sensitivity to TCB *in vitro* and *in vivo* (**Figure 3, R2**). The mechanism by which 5-Azacytidine is able to upregulate CEACAM5 at the transcriptomic level remains to be elucidated, but it is likely that it is due to an indirect effect, given the fact that the CEACAM5 promoter is not methylated. We hypothesize that 5-Azacytidine demethylates the promoter of some transcription factor, therefore activating its transcription, which then can regulate *CEACAM5* transcription. A strategy to confirm this hypothesis would be to perform a methylation array in our resistant cells with and without 5-Aza treatment, in order to identify which regions of the genome have been demethylated. This approach can be combined with an RNA-Seq in the same samples, allowing us to identify transcription factors altered upon 5-Aza treatment, and by using transcription factor binding site prediction tools, determine the potential candidates to modulate *CEACAM5* expression. Other examples of antigen downmodulation that can be recovered include the folate receptor β (FRβ) and CD22, which recovered antigen levels and sensitivity to CAR T cells when treated with specific compounds (Lynn et al., 2015, Ramakrishna et al., 2019).

Interestingly, analysis of individual clones may point out the heterogeneity of the primary MKN45 cell line as the cause of CEA expression decrease, as some clones exhibited low levels of CEA expression (**Figure S3A, R2**), which could have been the ones selected after the chronic treatment. A strategy to determine whether these antigen-negative clones are the ones proliferating after treatment could involve lineage tracing. This would entail labeling the negative cells, generating new acquired resistance models to CEACAM5-TCB, and

subsequently examining if the selected clones were indeed the antigen-negative ones.

From our multiple models of HER2-TCB resistance generated in this thesis, both *in vitro* and *in vivo* (**Figure 1a-b, Figure S6, R1; Figure 1A-B, R2**), none of them exhibited HER2 downmodulation (**Figure 1i, Figure S6, R1; Figure 2A, R2**), probably meaning that these tumors require HER2 signaling, being an epidermal growth factor, in order to keep growing and replicating (**Figure 2E, R2**). Despite that, interestingly, the HER2-targetting TKi Neratinib has been described to induce HER2 downmodulation by its ubiquitylation and endocytic degradation in $HER2^+$ BC cells (Zhang et al., 2016), and another study claims that HER2 was downmodulated in a GBM cell line xenograft after treatment with a HER2-CAR T therapy (Hegde et al., 2016). These results contradict our initial hypothesis that HER2 is not feasible to be downmodulated by tumor cells in targeted therapies, but it could be therapy dependent, and it may depend on the addiction of tumor cells to HER2 expression.

To conclude, the targeted antigen is determinant on the mechanism of resistance that will arise when treated with T cell redirection therapies. Upcoming efforts should be directed to identify antigens that make good candidates to be targeted in T cell redirection therapies, to identify strategies to anticipate the antigen downmodulation, and, in cases where expression is disrupted, to identify combinatorial therapies to restore specific antigen expression and enhance therapy response, such as the combination of CEACAM5-TCB plus 5-Azacytadine presented in this thesis, which proved effective in CEA downmodulating tumors.

CONCLUSIONS

1. Tumor intrinsic IFNγ deficient response is a common cause of acquired resistance to T cell redirection therapies in solid tumors.

2. JAK2 downmodulation is a recurrent mechanism of IFNγ signaling disruption in acquired resistance to T cell-based therapies in solid tumors.

3. The tumor intrinsic mechanism of action of IFNγ in T cell redirection therapy response in solid tumors can be the apoptosis induction and the regulation of the immune synapse formation.

4. Tumor intrinsic IFNγ response and JAK2 expression levels have the potential to serve as surrogate biomarkers of response to immunotherapy.

5. Antigen downmodulation is a recurrent cause of resistance in T cell redirection therapies towards the antigen CEACAM5 in solid tumors.

6. The target antigen is determinant in the acquired mechanism of resistance that emerge to redirected lymphocytes. A better insight into the biology of the antigen will help to anticipate and design combinatorial treatments in order to anticipate resistances to cancer immunotherapies.

7. The CRISPR and drug screening results open the avenue for the use of new combinatorial therapies to overcome deficient IFNγ response and cancer immunotherapy resistance. We identified SOCS1 as a promising candidate to be targeted in IFNγ deficient tumors.

BIBLIOGRAPHY

Abiko, K., Matsumura, N., Hamanishi, J., Horikawa, N., Murakami, R., Yamaguchi, K., Yoshioka, Y., Baba, T., Konishi, I., & Mandai, M. (2015). IFN-γ from lymphocytes induces PD-L1 expression and promotes progression of ovarian cancer. *British Journal of Cancer*, *112*(9), 1501–1509. https://doi.org/10.1038/bjc.2015.101

Agarwal, P., Raghavan, A., Nandiwada, S. L., Curtsinger, J. M., Bohjanen, P. R., Mueller, D. L., & Mescher, M. F. (2009). Gene Regulation and Chromatin Remodeling by IL-12 and Type I IFN in Programming for CD8 T Cell Effector Function and Memory. *The Journal of Immunology*, *183*(3), 1695–1704. https://doi.org/10.4049/jimmunol.0900592

Alexandrov, L. B., Nik-Zainal, S., Wedge, D. C., Aparicio, S. A. J. R., Behjati, S., Biankin, A. V., Bignell, G. R., Bolli, N., Borg, A., Børresen-Dale, A.-L., Boyault, S., Burkhardt, B., Butler, A. P., Caldas, C., Davies, H. R., Desmedt, C., Eils, R., Eyfjörd, J. E., Foekens, J. A., … Stratton, M. R. (2013). Signatures of mutational processes in human cancer. *Nature*, *500*(7463), 415–421. https://doi.org/10.1038/nature12477

Almishri, W., Santodomingo-Garzon, T., Le, T., Stack, D., Mody, C. H., & Swain, M. G. (2016). TNFα Augments Cytokine-Induced NK Cell IFNγ Production through TNFR2. *Journal of Innate Immunity*, *8*(6), 617–629. https://doi.org/10.1159/000448077

Andtbacka, R. H. I., Kaufman, H. L., Collichio, F., Amatruda, T., Senzer, N., Chesney, J., Delman, K. A., Spitler, L. E., Puzanov, I., Agarwala, S. S., Milhem, M., Cranmer, L., Curti, B., Lewis, K., Ross, M., Guthrie, T., Linette, G. P., Daniels, G. A., Harrington, K., … Coffin, R. S. (2015). Talimogene Laherparepvec Improves Durable Response Rate in Patients With Advanced Melanoma. *Journal of Clinical Oncology : Official Journal of the American Society of Clinical Oncology*, *33*(25), 2780–2788. https://doi.org/10.1200/JCO.2014.58.3377

Ansell, S. M., Lesokhin, A. M., Borrello, I., Halwani, A., Scott, E. C., Gutierrez, M., Schuster, S. J., Millenson, M. M., Cattry, D., Freeman, G. J., Rodig, S. J., Chapuy, B., Ligon, A. H., Zhu, L., Grosso, J. F., Kim, S. Y., Timmerman, J. M., Shipp, M. A., & Armand, P. (2015). PD-1 Blockade with Nivolumab in Relapsed or Refractory Hodgkin's Lymphoma. *New England Journal of Medicine*, *372*(4), 311–319. https://doi.org/10.1056/NEJMoa1411087

Apriamashvili, G., Vredevoogd, D. W., Krijgsman, O., Bleijerveld, O. B., Ligtenberg, M. A., de Bruijn, B., Boshuizen, J., Traets, J. J. H., D'Empaire Altimari, D., van Vliet, A., Lin, C.-P., Visser, N. L., Londino, J. D., Sanchez-Hodge, R., Oswalt, L. E., Altinok, S., Schisler, J. C., Altelaar, M., & Peeper, D. S. (2022). Ubiquitin ligase STUB1 destabilizes IFNγ-receptor complex to suppress tumor IFNγ signaling. *Nature Communications*, *13*(1), 1923. https://doi.org/10.1038/s41467-022-29442-x

Ascierto, P. A., Kirkwood, J. M., Grob, J.-J., Simeone, E., Grimaldi, A. M., Maio, M., Palmieri, G., Testori, A., Marincola, F. M., & Mozzillo, N. (2012). The role of BRAF V600 mutation in melanoma. *Journal of Translational Medicine*, *10*(1), 85. https://doi.org/10.1186/1479-5876-10-85

Bai, R., Chen, N., Li, L., Du, N., Bai, L., Lv, Z., Tian, H., & Cui, J. (2020). Mechanisms of Cancer Resistance to Immunotherapy. *Frontiers in Oncology*, *10*(August), 1–12. https://doi.org/10.3389/fonc.2020.01290

Bai, X.-F., Liu, J., Li, O., Zheng, P., & Liu, Y. (2003). Antigenic drift as a mechanism for tumor evasion of destruction by cytolytic T lymphocytes. *Journal of Clinical Investigation*, *111*(10), 1487–1496. https://doi.org/10.1172/JCI17656

Balasubramanian, A., John, T., & Asselin-Labat, M.-L. (2022). Regulation of the antigen presentation machinery in cancer and its implication for immune surveillance. *Biochemical Society Transactions*, *50*(2), 825–837. https://doi.org/10.1042/BST20210961

Bancroft, C. C., Chen, Z., Dong, G., Sunwoo, J. B., Yeh, N., Park, C., & Van Waes, C. (2001). Coexpression of proangiogenic factors IL-8 and VEGF by human head and neck squamous cell carcinoma involves coactivation by MEK-MAPK and IKK-NF-kappaB signal pathways. *Clinical Cancer Research : An Official Journal of the American Association for Cancer Research*, *7*(2), 435–442. http://www.ncbi.nlm.nih.gov/pubmed/11234901

Baulu, E., Gardet, C., Chuvin, N., & Depil, S. (2023). TCR-engineered T cell therapy in solid tumors: State of the art and perspectives. *Science Advances*, *9*(7). https://doi.org/10.1126/sciadv.adf3700

Beano, A., Signorino, E., Evangelista, A., Brusa, D., Mistrangelo, M., Polimeni, M. A., Spadi, R., Donadio, M., Ciuffreda, L., & Matera, L. (2008). Correlation between NK function and response to trastuzumab in metastatic breast cancer patients. *Journal of Translational Medicine*, *6*, 25. https://doi.org/10.1186/1479-5876-6-25

Benci, J. L., Xu, B., Qiu, Y., Wu, T. J., Dada, H., Twyman-Saint Victor, C., Cucolo, L., Lee, D. S. M., Pauken, K. E., Huang, A. C., Gangadhar, T. C., Amaravadi, R. K., Schuchter, L. M., Feldman, M. D., Ishwaran, H., Vonderheide, R. H., Maity, A., Wherry, E. J., & Minn, A. J. (2016). Tumor Interferon Signaling Regulates a Multigenic Resistance Program to Immune Checkpoint Blockade. *Cell*, *167*(6), 1540-1554.e12. https://doi.org/10.1016/j.cell.2016.11.022

Besser, M. J., Shapira-Frommer, R., Itzhaki, O., Treves, A. J., Zippel, D. B., Levy, D., Kubi, A., Shoshani, N., Zikich, D., Ohayon, Y., Ohayon, D., Shalmon, B., Markel, G., Yerushalmi, R., Apter, S., Ben-Nun, A., Ben-Ami, E., Shimoni, A., Nagler, A., & Schachter, J. (2013). Adoptive Transfer of Tumor-Infiltrating Lymphocytes in Patients with Metastatic Melanoma: Intent-to-Treat Analysis and Efficacy after Failure to Prior Immunotherapies. *Clinical Cancer Research*, *19*(17), 4792–4800. https://doi.org/10.1158/1078-0432.CCR-13-0380

Beziaud, L., Young, C. M., Alonso, A. M., Norkin, M., Minafra, A. R., & Huelsken, J. (2023). IFNγ-induced stem-like state of cancer cells as a driver of metastatic progression following immunotherapy. *Cell Stem Cell*, *30*(6), 818-831.e6. https://doi.org/10.1016/j.stem.2023.05.007

Birdi, H. K., Jirovec, A., Cortés-Kaplan, S., Werier, J., Nessim, C., Diallo, J.-S., & Ardolino, M. (2021). Immunotherapy for sarcomas: new frontiers and unveiled opportunities. *Journal for ImmunoTherapy of Cancer*, *9*(2), e001580. https://doi.org/10.1136/jitc-2020-001580

Boon, T., Cerottini, J.-C., Van den Eynde, B., van der Bruggen, P., & Van Pel, A. (1994). Tumor Antigens Recognized by T Lymphocytes. *Annual Review of Immunology*, *12*(1), 337–365. https://doi.org/10.1146/annurev.iy.12.040194.002005

Botticelli, A., Cerbelli, B., Lionetto, L., Zizzari, I., Salati, M., Pisano, A., Federica, M., Simmaco, M., Nuti, M., & Marchetti, P. (2018). Can IDO activity predict primary resistance to anti-PD-1 treatment in NSCLC? *Journal of Translational Medicine*, *16*(1), 219. https://doi.org/10.1186/s12967-018-1595-3

Bourgeois-Daigneault, M.-C., Roy, D. G., Falls, T., Twumasi-Boateng, K., St-Germain, L. E., Marguerie, M., Garcia, V., Selman, M., Jennings, V. A., Pettigrew, J., Amos, S., Diallo, J.-S., Nelson, B., & Bell, J. C. (2016). Oncolytic vesicular stomatitis virus expressing interferon-σ has enhanced therapeutic activity. *Molecular Therapy - Oncolytics*, *3*, 16001. https://doi.org/10.1038/mto.2016.1

Bracci, L., Schiavoni, G., Sistigu, A., & Belardelli, F. (2014). Immune-based mechanisms of cytotoxic chemotherapy: implications for the design of novel and rationale-based combined treatments against cancer. *Cell Death and Differentiation*, *21*(1), 15–25. https://doi.org/10.1038/cdd.2013.67

Bradley, L. M., Dalton, D. K., & Croft, M. (1996). A direct role for IFN-gamma in regulation of Th1 cell development. *Journal of Immunology (Baltimore, Md.: 1950)*, *157*(4), 1350–1358. http://www.ncbi.nlm.nih.gov/pubmed/8759714

Braig, F., Brandt, A., Goebeler, M., Tony, H.-P., Kurze, A.-K., Nollau, P., Bumm, T., Böttcher, S., Bargou, R. C., & Binder, M. (2017). Resistance to anti-CD19/CD3 BiTE in acute lymphoblastic leukemia may be mediated by disrupted CD19 membrane trafficking. *Blood*, *129*(1), 100–104. https://doi.org/10.1182/blood-2016-05-718395

Brenner, E., Schörg, B. F., Ahmetlić, F., Wieder, T., Hilke, F. J., Simon, N., Schroeder, C., Demidov, G., Riedel, T., Fehrenbacher, B., Schaller, M., Forschner, A., Eigentler, T., Niessner, H., Sinnberg, T., Böhm, K. S., Hömberg, N., Braumüller, H., Dauch, D., … Röcken, M. (2020). Cancer immune control needs senescence induction by interferon-dependent cell cycle regulator pathways in tumours. *Nature Communications*, *11*(1), 1335. https://doi.org/10.1038/s41467-020-14987-6

Bromberg, J. F., Horvath, C. M., Wen, Z., Schreiber, R. D., & Darnell, J. E. (1996). Transcriptionally active Stat1 is required for the antiproliferative effects of both interferon alpha and interferon gamma. *Proceedings of the National Academy of Sciences*, *93*(15), 7673–7678. https://doi.org/10.1073/pnas.93.15.7673

Brown, C. E., Alizadeh, D., Starr, R., Weng, L., Wagner, J. R., Naranjo, A., Ostberg, J. R., Blanchard, M. S., Kilpatrick, J., Simpson, J., Kurien, A., Priceman, S. J., Wang, X., Harshbarger, T. L., D'Apuzzo, M., Ressler, J. A., Jensen, M. C., Barish, M. E., Chen, M., … Badie, B. (2016). Regression of Glioblastoma after Chimeric Antigen Receptor T-Cell Therapy. *New England Journal of Medicine*, *375*(26), 2561–2569. https://doi.org/10.1056/NEJMoa1610497

Burton, J., Siller-Farfán, J. A., Pettmann, J., Salzer, B., Kutuzov, M., van der Merwe, P. A., & Dushek, O. (2023). Inefficient exploitation of accessory receptors reduces the sensitivity of

chimeric antigen receptors. *Proceedings of the National Academy of Sciences*, *120*(2). https://doi.org/10.1073/pnas.2216352120

Cao, X., Leonard, K., Collins, L. I., Cai, S. F., Mayer, J. C., Payton, J. E., Walter, M. J., Piwnica-Worms, D., Schreiber, R. D., & Ley, T. J. (2009). Interleukin 12 Stimulates IFN-γ–Mediated Inhibition of Tumor-Induced Regulatory T-Cell Proliferation and Enhances Tumor Clearance. *Cancer Research*, *69*(22), 8700–8709. https://doi.org/10.1158/0008-5472.CAN-09-1145

Carrasco-Padilla, C., Hernaiz-Esteban, A., Álvarez-Vallina, L., Aguilar-Sopeña, O., & Roda-Navarro, P. (2022). Bispecific Antibody Format and the Organization of Immunological Synapses in T Cell-Redirecting Strategies for Cancer Immunotherapy. *Pharmaceutics*, *15*(1), 132. https://doi.org/10.3390/pharmaceutics15010132

Caruana, I., Savoldo, B., Hoyos, V., Weber, G., Liu, H., Kim, E. S., Ittmann, M. M., Marchetti, D., & Dotti, G. (2015). Heparanase promotes tumor infiltration and antitumor activity of CAR-redirected T lymphocytes. *Nature Medicine*, *21*(5), 524–529. https://doi.org/10.1038/nm.3833

Carvalho, H. de A., & Villar, R. C. (2018). Radiotherapy and immune response: the systemic effects of a local treatment. *Clinics (Sao Paulo, Brazil)*, *73*(suppl 1), e557s. https://doi.org/10.6061/clinics/2018/e557s

Casey, S. C., Tong, L., Li, Y., Do, R., Walz, S., Fitzgerald, K. N., Gouw, A. M., Baylot, V., Gütgemann, I., Eilers, M., & Felsher, D. W. (2016). MYC regulates the antitumor immune response through CD47 and PD-L1. *Science (New York, N.Y.)*, *352*(6282), 227–231. https://doi.org/10.1126/science.aac9935

Cha, J.-H., Chan, L.-C., Li, C.-W., Hsu, J. L., & Hung, M.-C. (2019). Mechanisms Controlling PD-L1 Expression in Cancer. *Molecular Cell*, *76*(3), 359–370. https://doi.org/10.1016/j.molcel.2019.09.030

Chang, C.-H., Hammer, J., Loh, J., Fodor, W., & Flavell, R. (1992). The activation of major histocompatibility complex class I genes by interferon regulatory factor-1 (IRF-1). *Immunogenetics*, *35*(6). https://doi.org/10.1007/BF00179793

Chau, B. N., Chen, T.-T., Wan, Y. Y., DeGregori, J., & Wang, J. Y. J. (2004). Tumor Necrosis Factor Alpha-Induced Apoptosis Requires p73 and c-ABL Activation Downstream of RB Degradation. *Molecular and Cellular Biology*, *24*(10), 4438–4447. https://doi.org/10.1128/MCB.24.10.4438-4447.2004

Chen, H., Chong, W., Teng, C., Yao, Y., Wang, X., & Li, X. (2019). The immune response-related mutational signatures and driver genes in non-small-cell lung cancer. *Cancer Science*, *110*(8), 2348–2356. https://doi.org/10.1111/cas.14113

Chen, J.-Y., Li, C.-F., Kuo, C.-C., Tsai, K. K., Hou, M.-F., & Hung, W.-C. (2014). Cancer/stroma interplay via cyclooxygenase-2 and indoleamine 2,3-dioxygenase promotes breast cancer progression. *Breast Cancer Research*, *16*(4), 410. https://doi.org/10.1186/s13058-014-0410-1

Chen, N., Fang, W., Zhan, J., Hong, S., Tang, Y., Kang, S., Zhang, Y., He, X., Zhou, T., Qin, T., Huang, Y., Yi, X., & Zhang, L. (2015). Upregulation of PD-L1 by EGFR Activation Mediates the Immune Escape in EGFR-Driven NSCLC: Implication for Optional Immune Targeted Therapy for NSCLC Patients with EGFR Mutation. *Journal of Thoracic Oncology*, *10*(6), 910–923. https://doi.org/10.1097/JTO.0000000000000500

Cheng, L., Wang, Y., & Du, J. (2020). Human Papillomavirus Vaccines: An Updated Review. *Vaccines*, *8*(3), 391. https://doi.org/10.3390/vaccines8030391

Chin, Y. E., Kitagawa, M., Su, W.-C. S., You, Z.-H., Iwamoto, Y., & Fu, X.-Y. (1996). Cell Growth Arrest and Induction of Cyclin-Dependent Kinase Inhibitor p21 WAF1/CIP1 Mediated by STAT1. *Science*, *272*(5262), 719–722. https://doi.org/10.1126/science.272.5262.719

Chinen, T., Kannan, A. K., Levine, A. G., Fan, X., Klein, U., Zheng, Y., Gasteiger, G., Feng, Y., Fontenot, J. D., & Rudensky, A. Y. (2016). An essential role for the IL-2 receptor in Treg cell function. *Nature Immunology*, *17*(11), 1322–1333. https://doi.org/10.1038/ni.3540

Cho, S. X., Vijayan, S., Yoo, J.-S., Watanabe, T., Ouda, R., An, N., & Kobayashi, K. S. (2021). MHC class I transactivator NLRC5 in host immunity, cancer and beyond. *Immunology*, *162*(3), 252–261. https://doi.org/10.1111/imm.13235

Choi, B. D., Yu, X., Castano, A. P., Bouffard, A. A., Schmidts, A., Larson, R. C., Bailey, S. R., Boroughs, A. C., Frigault, M. J., Leick, M. B., Scarfò, I., Cetrulo, C. L., Demehri, S., Nahed, B. V., Cahill, D. P., Wakimoto, H., Curry, W. T., Carter, B. S., & Maus, M. V. (2019). CAR-T cells secreting BiTEs circumvent antigen escape without detectable toxicity. *Nature Biotechnology*, *37*(9), 1049–1058. https://doi.org/10.1038/s41587-019-0192-1

Claus, C., Ferrara, C., Xu, W., Sam, J., Lang, S., Uhlenbrock, F., Albrecht, R., Herter, S., Schlenker, R., Hüsser, T., Diggelmann, S., Challier, J., Mössner, E., Hosse, R. J., Hofer, T., Brünker, P., Joseph, C., Benz, J., Ringler, P., … Umaña, P. (2019). Tumor-targeted 4-1BB agonists for combination with T cell bispecific antibodies as off-the-shelf therapy. *Science Translational Medicine*, *11*(496). https://doi.org/10.1126/scitranslmed.aav5989

Colas, C., Volodina, O., Béland, K., Pham, T. N. Q., Li, Y., Dallaire, F., Soulard, C., Lemieux, W., Colamartino, A. B. L., Tremblay-Laganière, C., Dicaire, R., Guimond, J., Vobecky, S., Poirier, N., Patey, N., Cohen, É. A., & Haddad, E. (2023). Generation of functional human T cell development in NOD/SCID/IL2rγnull humanized mice without using fetal tissue: Application as a model of HIV infection and persistence. *Stem Cell Reports*, *18*(2), 597–612. https://doi.org/10.1016/j.stemcr.2023.01.003

Coley, W. B. (1910). The Treatment of Inoperable Sarcoma by Bacterial Toxins (the Mixed Toxins of the Streptococcus erysipelas and the Bacillus prodigiosus). *Proceedings of the Royal Society of Medicine*, *3*(Surg Sect), 1–48. http://www.ncbi.nlm.nih.gov/pubmed/19974799

Condamine, T., Ramachandran, I., Youn, J.-I., & Gabrilovich, D. I. (2015). Regulation of tumor metastasis by myeloid-derived suppressor cells. *Annual Review of Medicine*, *66*, 97–110. https://doi.org/10.1146/annurev-med-051013-052304

Conforti, F., Pala, L., Bagnardi, V., De Pas, T., Martinetti, M., Viale, G., Gelber, R. D., & Goldhirsch, A. (2018). Cancer immunotherapy efficacy and patients' sex: a systematic review and meta-analysis. *The Lancet Oncology*, *19*(6), 737–746. https://doi.org/10.1016/S1470-2045(18)30261-4

Constant, S. L., & Bottomly, K. (1997). INDUCTION OF TH1 AND TH2 CD4 + T CELL RESPONSES:The Alternative Approaches. *Annual Review of Immunology*, *15*(1), 297–322. https://doi.org/10.1146/annurev.immunol.15.1.297

Corm, S., Berthon, C., Imbenotte, M., Biggio, V., Lhermitte, M., Dupont, C., Briche, I., & Quesnel, B. (2009). Indoleamine 2,3-dioxygenase activity of acute myeloid leukemia cells can be measured from patients' sera by HPLC and is inducible by IFN-gamma. *Leukemia Research*, *33*(3), 490–494. https://doi.org/10.1016/j.leukres.2008.06.014

Cortes, J., Rugo, H. S., Cescon, D. W., Im, S.-A., Yusof, M. M., Gallardo, C., Lipatov, O., Barrios, C. H., Perez-Garcia, J., Iwata, H., Masuda, N., Torregroza Otero, M., Gokmen, E., Loi, S., Guo, Z., Zhou, X., Karantza, V., Pan, W., & Schmid, P. (2022). Pembrolizumab plus Chemotherapy in Advanced Triple-Negative Breast Cancer. *New England Journal of Medicine*, *387*(3), 217–226. https://doi.org/10.1056/NEJMoa2202809

Coughlan, A. M., Harmon, C., Whelan, S., O'Brien, E. C., O'Reilly, V. P., Crotty, P., Kelly, P., Ryan, M., Hickey, F. B., O'Farrelly, C., & Little, M. A. (2016). Myeloid Engraftment in Humanized Mice: Impact of Granulocyte-Colony Stimulating Factor Treatment and Transgenic Mouse Strain. *Stem Cells and Development*, *25*(7), 530–541. https://doi.org/10.1089/scd.2015.0289

Creelan, B. C., Wang, C., Teer, J. K., Toloza, E. M., Yao, J., Kim, S., Landin, A. M., Mullinax, J. E., Saller, J. J., Saltos, A. N., Noyes, D. R., Montoya, L. B., Curry, W., Pilon-Thomas, S. A., Chiappori, A. A., Tanvetyanon, T., Kaye, F. J., Thompson, Z. J., Yoder, S. J., … Antonia, S. J. (2021). Tumor-infiltrating lymphocyte treatment for anti-PD-1-resistant metastatic lung cancer: a phase 1 trial. *Nature Medicine*, *27*(8), 1410–1418. https://doi.org/10.1038/s41591-021-01462-y

Cretella, Digiacomo, Giovannetti, & Cavazzoni. (2019). PTEN Alterations as a Potential Mechanism for Tumor Cell Escape from PD-1/PD-L1 Inhibition. *Cancers*, *11*(9), 1318. https://doi.org/10.3390/cancers11091318

Cullen, S. P., & Martin, S. J. (2015). Fas and TRAIL 'death receptors' as initiators of inflammation: Implications for cancer. *Seminars in Cell & Developmental Biology*, *39*, 26–34. https://doi.org/10.1016/j.semcdb.2015.01.012

Daei Sorkhabi, A., Mohamed Khosroshahi, L., Sarkesh, A., Mardi, A., Aghebati-Maleki, A., Aghebati-Maleki, L., & Baradaran, B. (2023). The current landscape of CAR T-cell therapy for solid tumors: Mechanisms, research progress, challenges, and counterstrategies. *Frontiers in Immunology*, *14*. https://doi.org/10.3389/fimmu.2023.1113882

Dagogo-Jack, I., & Shaw, A. T. (2018). Tumour heterogeneity and resistance to cancer therapies. *Nature Reviews Clinical Oncology*, *15*(2), 81–94. https://doi.org/10.1038/nrclinonc.2017.166

Davenport, A. J., Cross, R. S., Watson, K. A., Liao, Y., Shi, W., Prince, H. M., Beavis, P. A., Trapani, J. A., Kershaw, M. H., Ritchie, D. S., Darcy, P. K., Neeson, P. J., & Jenkins, M. R. (2018). Chimeric antigen receptor T cells form nonclassical and potent immune synapses

driving rapid cytotoxicity. *Proceedings of the National Academy of Sciences*, *115*(9). https://doi.org/10.1073/pnas.1716266115

Davis, A. A., & Patel, V. G. (2019). The role of PD-L1 expression as a predictive biomarker: an analysis of all US Food and Drug Administration (FDA) approvals of immune checkpoint inhibitors. *Journal for ImmunoTherapy of Cancer*, *7*(1), 278. https://doi.org/10.1186/s40425-019-0768-9

de Vries, T. J., Fourkour, A., Wobbes, T., Verkroost, G., Ruiter, D. J., & van Muijen, G. N. (1997). Heterogeneous expression of immunotherapy candidate proteins gp100, MART-1, and tyrosinase in human melanoma cell lines and in human melanocytic lesions. *Cancer Research*, *57*(15), 3223–3229. http://www.ncbi.nlm.nih.gov/pubmed/9242453

Debien, V., De Caluwé, A., Wang, X., Piccart-Gebhart, M., Tuohy, V. K., Romano, E., & Buisseret, L. (2023). Immunotherapy in breast cancer: an overview of current strategies and perspectives. *NPJ Breast Cancer*, *9*(1), 7. https://doi.org/10.1038/s41523-023-00508-3

Dedoni, S., Olianas, M. C., & Onali, P. (2010). Interferon-β induces apoptosis in human SH-SY5Y neuroblastoma cells through activation of JAK-STAT signaling and down-regulation of PI3K/Akt pathway. *Journal of Neurochemistry*, *115*(6), 1421–1433. https://doi.org/10.1111/j.1471-4159.2010.07046.x

Denko, N. C. (2008). Hypoxia, HIF1 and glucose metabolism in the solid tumour. *Nature Reviews Cancer*, *8*(9), 705–713. https://doi.org/10.1038/nrc2468

Deseke, M., & Prinz, I. (2020). Ligand recognition by the γδ TCR and discrimination between homeostasis and stress conditions. *Cellular & Molecular Immunology*, *17*(9), 914–924. https://doi.org/10.1038/s41423-020-0503-y

Dixon, S. J., Lemberg, K. M., Lamprecht, M. R., Skouta, R., Zaitsev, E. M., Gleason, C. E., Patel, D. N., Bauer, A. J., Cantley, A. M., Yang, W. S., Morrison, B., & Stockwell, B. R. (2012). Ferroptosis: An Iron-Dependent Form of Nonapoptotic Cell Death. *Cell*, *149*(5), 1060–1072. https://doi.org/10.1016/j.cell.2012.03.042

Donia, M., Harbst, K., van Buuren, M., Kvistborg, P., Lindberg, M. F., Andersen, R., Idorn, M., Munir Ahmad, S., Ellebæk, E., Mueller, A., Fagone, P., Nicoletti, F., Libra, M., Lauss, M., Hadrup, S. R., Schmidt, H., Andersen, M. H., thor Straten, P., Nilsson, J. A., … Svane, I. M. (2017). Acquired Immune Resistance Follows Complete Tumor Regression without Loss of Target Antigens or IFNγ Signaling. *Cancer Research*, *77*(17), 4562–4566. https://doi.org/10.1158/0008-5472.CAN-16-3172

Duan, Q., Zhang, H., Zheng, J., & Zhang, L. (2020). Turning Cold into Hot: Firing up the Tumor Microenvironment. *Trends in Cancer*, *6*(7), 605–618. https://doi.org/10.1016/j.trecan.2020.02.022

Dunn, G. P., Bruce, A. T., Ikeda, H., Old, L. J., & Schreiber, R. D. (2002). Cancer immunoediting: from immunosurveillance to tumor escape. *Nature Immunology*, *3*(11), 991–998. https://doi.org/10.1038/ni1102-991

Duperret, E. K., Trautz, A., Ammons, D., Perales-Puchalt, A., Wise, M. C., Yan, J., Reed, C., & Weiner, D. B. (2018). Alteration of the Tumor Stroma Using a Consensus DNA Vaccine Targeting Fibroblast Activation Protein (FAP) Synergizes with Antitumor Vaccine Therapy in Mice. *Clinical Cancer Research : An Official Journal of the American Association for Cancer Research*, *24*(5), 1190–1201. https://doi.org/10.1158/1078-0432.CCR-17-2033

Fischer, J., Paret, C., El Malki, K., Alt, F., Wingerter, A., Neu, M. A., Kron, B., Russo, A., Lehmann, N., Roth, L., Fehr, E.-M., Attig, S., Hohberger, A., Kindler, T., & Faber, J. (2017). CD19 Isoforms Enabling Resistance to CART-19 Immunotherapy Are Expressed in B-ALL Patients at Initial Diagnosis. *Journal of Immunotherapy (Hagerstown, Md. : 1997)*, *40*(5), 187–195. https://doi.org/10.1097/CJI.0000000000000169

Friedman, G. K., Johnston, J. M., Bag, A. K., Bernstock, J. D., Li, R., Aban, I., Kachurak, K., Nan, L., Kang, K.-D., Totsch, S., Schlappi, C., Martin, A. M., Pastakia, D., McNall-Knapp, R., Farouk Sait, S., Khakoo, Y., Karajannis, M. A., Woodling, K., Palmer, J. D., … Gillespie, G. Y. (2021). Oncolytic HSV-1 G207 Immunovirotherapy for Pediatric High-Grade Gliomas. *The New England Journal of Medicine*, *384*(17), 1613–1622. https://doi.org/10.1056/NEJMoa2024947

Gabrilovich, D. I. (2017). Myeloid-Derived Suppressor Cells. *Cancer Immunology Research*, *5*(1), 3–8. https://doi.org/10.1158/2326-6066.CIR-16-0297

Gaczynska, M., Rock, K. L., Spies, T., & Goldberg, A. L. (1994). Peptidase activities of proteasomes are differentially regulated by the major histocompatibility complex-encoded genes for LMP2 and LMP7. *Proceedings of the National Academy of Sciences*, *91*(20), 9213–9217. https://doi.org/10.1073/pnas.91.20.9213

Gao, J., Shi, L. Z., Zhao, H., Chen, J., Xiong, L., He, Q., Chen, T., Roszik, J., Bernatchez, C., Woodman, S. E., Chen, P. L., Hwu, P., Allison, J. P., Futreal, A., Wargo, J. A., & Sharma, P. (2016). Loss of IFN-γ Pathway Genes in Tumor Cells as a Mechanism of Resistance to Anti-CTLA-4 Therapy. *Cell*, *167*(2), 397-404.e9. https://doi.org/10.1016/j.cell.2016.08.069

Garcia-Diaz, A., Shin, D. S., Moreno, B. H., Saco, J., Escuin-Ordinas, H., Rodriguez, G. A., Zaretsky, J. M., Sun, L., Hugo, W., Wang, X., Parisi, G., Saus, C. P., Torrejon, D. Y., Graeber, T. G., Comin-Anduix, B., Hu-Lieskovan, S., Damoiseaux, R., Lo, R. S., & Ribas, A. (2017). Interferon Receptor Signaling Pathways Regulating PD-L1 and PD-L2 Expression. *Cell Reports*, *19*(6), 1189–1201. https://doi.org/10.1016/j.celrep.2017.04.031

Gardner, R. A., Finney, O., Annesley, C., Brakke, H., Summers, C., Leger, K., Bleakley, M., Brown, C., Mgebroff, S., Kelly-Spratt, K. S., Hoglund, V., Lindgren, C., Oron, A. P., Li, D., Riddell, S. R., Park, J. R., & Jensen, M. C. (2017). Intent-to-treat leukemia remission by CD19 CAR T cells of defined formulation and dose in children and young adults. *Blood*, *129*(25), 3322–3331. https://doi.org/10.1182/blood-2017-02-769208

Garris, C. S., Arlauckas, S. P., Kohler, R. H., Trefny, M. P., Garren, S., Piot, C., Engblom, C., Pfirschke, C., Siwicki, M., Gungabeesoon, J., Freeman, G. J., Warren, S. E., Ong, S., Browning, E., Twitty, C. G., Pierce, R. H., Le, M. H., Algazi, A. P., Daud, A. I., … Pittet, M. J. (2018). Successful Anti-PD-1 Cancer Immunotherapy Requires T Cell-Dendritic Cell Crosstalk Involving the Cytokines IFN-γ and IL-12. *Immunity*, *49*(6), 1148-1161.e7. https://doi.org/10.1016/j.immuni.2018.09.024

Germain, R. N. (2002). T-cell development and the CD4–CD8 lineage decision. *Nature Reviews Immunology*, *2*(5), 309–322. https://doi.org/10.1038/nri798

Gettinger, S., Choi, J., Hastings, K., Truini, A., Datar, I., Sowell, R., Wurtz, A., Dong, W., Cai, G., Melnick, M. A., Du, V. Y., Schlessinger, J., Goldberg, S. B., Chiang, A., Sanmamed, M. F., Melero, I., Agorreta, J., Montuenga, L. M., Lifton, R., … Politi, K. (2017). Impaired HLA Class I Antigen Processing and Presentation as a Mechanism of Acquired Resistance to Immune Checkpoint Inhibitors in Lung Cancer. *Cancer Discovery*, *7*(12), 1420–1435. https://doi.org/10.1158/2159-8290.CD-17-0593

Gocher, A. M., Workman, C. J., & Vignali, D. A. A. (2022). Interferon-γ: teammate or opponent in the tumour microenvironment? *Nature Reviews Immunology*, *22*(3), 158–172. https://doi.org/10.1038/s41577-021-00566-3

Gollob, J. A., Sciambi, C. J., Huang, Z., & Dressman, H. K. (2005). Gene Expression Changes and Signaling Events Associated with the Direct Antimelanoma Effect of IFN-γ. *Cancer Research*, *65*(19), 8869–8877. https://doi.org/10.1158/0008-5472.CAN-05-1387

Gonzalez-Exposito, R., Semiannikova, M., Griffiths, B., Khan, K., Barber, L. J., Woolston, A., Spain, G., von Loga, K., Challoner, B., Patel, R., Ranes, M., Swain, A., Thomas, J., Bryant, A., Saffery, C., Fotiadis, N., Guettler, S., Mansfield, D., Melcher, A., … Gerlinger, M. (2019). CEA expression heterogeneity and plasticity confer resistance to the CEA-targeting bispecific immunotherapy antibody cibisatamab (CEA-TCB) in patient-derived colorectal cancer organoids. *Journal for ImmunoTherapy of Cancer*, *7*(1), 101. https://doi.org/10.1186/s40425-019-0575-3

Grasso, C. S., Tsoi, J., Onyshchenko, M., Abril-Rodriguez, G., Ross-Macdonald, P., Wind-Rotolo, M., Champhekar, A., Medina, E., Torrejon, D. Y., Shin, D. S., Tran, P., Kim, Y. J., Puig-Saus, C., Campbell, K., Vega-Crespo, A., Quist, M., Martignier, C., Luke, J. J., Wolchok, J. D., … Ribas, A. (2020). Conserved Interferon-γ Signaling Drives Clinical Response to Immune Checkpoint Blockade Therapy in Melanoma. *Cancer Cell*, *38*(4), 500-515.e3. https://doi.org/10.1016/j.ccell.2020.08.005

Griffin, T. A., Nandi, D., Cruz, M., Fehling, H. J., Van Kaer, L., Monaco, J. J., & Colbert, R. A. (1998). Immunoproteasome assembly: Cooperative incorporation of interferon γ (IFN-γ)-inducible subunits. *Journal of Experimental Medicine*, *187*(1), 97–104. https://doi.org/10.1084/jem.187.1.97

Gross, G., Waks, T., & Eshhar, Z. (1989). Expression of immunoglobulin-T-cell receptor chimeric molecules as functional receptors with antibody-type specificity. *Proceedings of the National Academy of Sciences of the United States of America*, *86*(24), 10024–10028. https://doi.org/10.1073/pnas.86.24.10024

Grossman, W. J., Verbsky, J. W., Barchet, W., Colonna, M., Atkinson, J. P., & Ley, T. J. (2004). Human T Regulatory Cells Can Use the Perforin Pathway to Cause Autologous Target Cell Death. *Immunity*, *21*(4), 589–601. https://doi.org/10.1016/j.immuni.2004.09.002

Gschwandtner, M., Derler, R., & Midwood, K. S. (2019). More Than Just Attractive: How CCL2 Influences Myeloid Cell Behavior Beyond Chemotaxis. *Frontiers in Immunology*, *10*.

https://doi.org/10.3389/fimmu.2019.02759
Gubin, M. M., Zhang, X., Schuster, H., Caron, E., Ward, J. P., Noguchi, T., Ivanova, Y., Hundal, J., Arthur, C. D., Krebber, W.-J., Mulder, G. E., Toebes, M., Vesely, M. D., Lam, S. S. K., Korman, A. J., Allison, J. P., Freeman, G. J., Sharpe, A. H., Pearce, E. L., … Schreiber, R. D. (2014). Checkpoint blockade cancer immunotherapy targets tumour-specific mutant antigens. *Nature*, *515*(7528), 577–581. https://doi.org/10.1038/nature13988
Gutzmer, R., Stroyakovskiy, D., Gogas, H., Robert, C., Lewis, K., Protsenko, S., Pereira, R. P., Eigentler, T., Rutkowski, P., Demidov, L., Manikhas, G. M., Yan, Y., Huang, K.-C., Uyei, A., McNally, V., McArthur, G. A., & Ascierto, P. A. (2020). Atezolizumab, vemurafenib, and cobimetinib as first-line treatment for unresectable advanced BRAFV600 mutation-positive melanoma (IMspire150): primary analysis of the randomised, double-blind, placebo-controlled, phase 3 trial. *The Lancet*, *395*(10240), 1835–1844. https://doi.org/10.1016/S0140-6736(20)30934-X
Hanahan, D., & Weinberg, R. A. (2011). Hallmarks of Cancer: The Next Generation. *Cell*, *144*(5), 646–674. https://doi.org/10.1016/j.cell.2011.02.013
Hanley, C. J., & Thomas, G. J. (2020). T-cell tumour exclusion and immunotherapy resistance: a role for CAF targeting. *British Journal of Cancer*, *123*(9), 1353–1355. https://doi.org/10.1038/s41416-020-1020-6
Hao, Z., Li, R., Wang, Y., Li, S., Hong, Z., & Han, Z. (2021). Landscape of Myeloid-derived Suppressor Cell in Tumor Immunotherapy. *Biomarker Research*, *9*(1), 77. https://doi.org/10.1186/s40364-021-00333-5
Harrington, K. J., Brody, J., Ingham, M., Strauss, J., Cemerski, S., Wang, M., Tse, A., Khilnani, A., Marabelle, A., & Golan, T. (2018). Preliminary results of the first-in-human (FIH) study of MK-1454, an agonist of stimulator of interferon genes (STING), as monotherapy or in combination with pembrolizumab (pembro) in patients with advanced solid tumors or lymphomas. *Annals of Oncology*, *29*, viii712. https://doi.org/10.1093/annonc/mdy424.015
Hashimoto, G., Wright, P. F., & Karzon, D. T. (1983). Antibody-Dependent Cell-Mediated Cytotoxicity Against Influenza Virus-Infected Cells. *Journal of Infectious Diseases*, *148*(5), 785–794. https://doi.org/10.1093/infdis/148.5.785
Hazini, A., Fisher, K., & Seymour, L. (2021). Deregulation of HLA-I in cancer and its central importance for immunotherapy. *Journal for ImmunoTherapy of Cancer*, *9*(8), e002899. https://doi.org/10.1136/jitc-2021-002899
Hegde, M., Mukherjee, M., Grada, Z., Pignata, A., Landi, D., Navai, S. A., Wakefield, A., Fousek, K., Bielamowicz, K., Chow, K. K. H., Brawley, V. S., Byrd, T. T., Krebs, S., Gottschalk, S., Wels, W. S., Baker, M. L., Dotti, G., Mamonkin, M., Brenner, M. K., … Ahmed, N. (2016). Tandem CAR T cells targeting HER2 and IL13Rα2 mitigate tumor antigen escape. *Journal of Clinical Investigation*, *126*(8), 3036–3052. https://doi.org/10.1172/JCI83416
Hellmann, M. D., Nathanson, T., Rizvi, H., Creelan, B. C., Sanchez-Vega, F., Ahuja, A., Ni, A., Novik, J. B., Mangarin, L. M. B., Abu-Akeel, M., Liu, C., Sauter, J. L., Rekhtman, N., Chang, E., Callahan, M. K., Chaft, J. E., Voss, M. H., Tenet, M., Li, X.-M., … Wolchok, J. D. (2018). Genomic Features of Response to Combination Immunotherapy in Patients with Advanced Non-Small-Cell Lung Cancer. *Cancer Cell*, *33*(5), 843-852.e4. https://doi.org/10.1016/j.ccell.2018.03.018
Heusinkveld, M., & van der Burg, S. H. (2011). Identification and manipulation of tumor associated macrophages in human cancers. *Journal of Translational Medicine*, *9*(1), 216. https://doi.org/10.1186/1479-5876-9-216
Hilton, I. B., D'Ippolito, A. M., Vockley, C. M., Thakore, P. I., Crawford, G. E., Reddy, T. E., & Gersbach, C. A. (2015). Epigenome editing by a CRISPR-Cas9-based acetyltransferase activates genes from promoters and enhancers. *Nature Biotechnology*, *33*(5), 510–517. https://doi.org/10.1038/nbt.3199
Hirabayashi, K., Du, H., Xu, Y., Shou, P., Zhou, X., Fucá, G., Landoni, E., Sun, C., Chen, Y., Savoldo, B., & Dotti, G. (2021). Dual-targeting CAR-T cells with optimal co-stimulation and metabolic fitness enhance antitumor activity and prevent escape in solid tumors. *Nature Cancer*, *2*(9), 904–918. https://doi.org/10.1038/s43018-021-00244-2
Hirata, A., Hashimoto, H., Shibasaki, C., Narumi, K., & Aoki, K. (2019). Intratumoral IFN-α gene delivery reduces tumor-infiltrating regulatory T cells through the downregulation of tumor CCL17 expression. *Cancer Gene Therapy*, *26*(9–10), 334–343. https://doi.org/10.1038/s41417-018-0059-5
Hubbard, S. R. (2018). Mechanistic Insights into Regulation of JAK2 Tyrosine Kinase. *Frontiers in Endocrinology*, *8*. https://doi.org/10.3389/fendo.2017.00361

Hume, D. A. (2015). The Many Alternative Faces of Macrophage Activation. *Frontiers in Immunology*, *6*. https://doi.org/10.3389/fimmu.2015.00370

Hunt, J. S., & Wood, G. W. (1986). Interferon-gamma induces class I HLA and beta 2-microglobulin expression by human amnion cells. *The Journal of Immunology*, *136*(2).

Ikezawa, Y., Mizugaki, H., Morita, R., Tateishi, K., Yokoo, K., Sumi, T., Kikuchi, H., Kitamura, Y., Nakamura, A., Kobayashi, M., Aso, M., Kimura, N., Yoshiike, F., Furuta, M., Tanaka, H., Sekikawa, M., Hachiya, T., Nakamura, K., Shimokawa, M., & Oizumi, S. (2022). Current status of first-line treatment with pembrolizumab for non–small-cell lung cancer with high PD-L1 expression. *Cancer Science*, *113*(6), 2109–2117. https://doi.org/10.1111/cas.15361

Ishizuka, J. J., Manguso, R. T., Cheruiyot, C. K., Bi, K., Panda, A., Iracheta-Vellve, A., Miller, B. C., Du, P. P., Yates, K. B., Dubrot, J., Buchumenski, I., Comstock, D. E., Brown, F. D., Ayer, A., Kohnle, I. C., Pope, H. W., Zimmer, M. D., Sen, D. R., Lane-Reticker, S. K., … Haining, W. N. (2019). Loss of ADAR1 in tumours overcomes resistance to immune checkpoint blockade. *Nature*, *565*(7737), 43–48. https://doi.org/10.1038/s41586-018-0768-9

Janelle, V., Rulleau, C., Del Testa, S., Carli, C., & Delisle, J.-S. (2020). T-Cell Immunotherapies Targeting Histocompatibility and Tumor Antigens in Hematological Malignancies. *Frontiers in Immunology*, *11*. https://doi.org/10.3389/fimmu.2020.00276

Janku, F., de Vos, F., de Miguel, M., Forde, P., Ribas, A., Nagasaka, M., Argiles, G., Arance, A. M., Calvo, A., Giannakis, M., Melendez, M., Gong, J., Szpakowski, S., Kan, R., Moody, S. E., & De Jonge, M. (2020). Abstract CT034: Phase I study of WNT974 + spartalizumab in patients (pts) with advanced solid tumors. *Cancer Research*, *80*(16_Supplement), CT034–CT034. https://doi.org/10.1158/1538-7445.AM2020-CT034

Jayaprakash, P., Vignali, P. D. A., Delgoffe, G. M., & Curran, M. A. (2022). Hypoxia Reduction Sensitizes Refractory Cancers to Immunotherapy. *Annual Review of Medicine*, *73*(1), 251–265. https://doi.org/10.1146/annurev-med-060619-022830

Jennifer Rivett, A., Bose, S., Brooks, P., & Broadfoot, K. I. (2001). Regulation of proteasome complexes by γ-interferon and phosphorylation. *Biochimie*, *83*(3–4), 363–366. https://doi.org/10.1016/S0300-9084(01)01249-4

Jiang, T., Zhou, C., & Ren, S. (2016). Role of IL-2 in cancer immunotherapy. *OncoImmunology*, *5*(6), e1163462. https://doi.org/10.1080/2162402X.2016.1163462

Jing, W., McAllister, D., Vonderhaar, E. P., Palen, K., Riese, M. J., Gershan, J., Johnson, B. D., & Dwinell, M. B. (2019). STING agonist inflames the pancreatic cancer immune microenvironment and reduces tumor burden in mouse models. *Journal for ImmunoTherapy of Cancer*, *7*(1), 115. https://doi.org/10.1186/s40425-019-0573-5

Joshi, S., Kaur, S., Redig, A. J., Goldsborough, K., David, K., Ueda, T., Watanabe-Fukunaga, R., Baker, D. P., Fish, E. N., Fukunaga, R., & Platanias, L. C. (2009). Type I interferon (IFN)-dependent activation of Mnk1 and its role in the generation of growth inhibitory responses. *Proceedings of the National Academy of Sciences*, *106*(29), 12097–12102. https://doi.org/10.1073/pnas.0900562106

Joshi, S., Sharma, B., Kaur, S., Majchrzak, B., Ueda, T., Fukunaga, R., Verma, A. K., Fish, E. N., & Platanias, L. C. (2011). Essential role for Mnk kinases in type II interferon (IFNgamma) signaling and its suppressive effects on normal hematopoiesis. *The Journal of Biological Chemistry*, *286*(8), 6017–6026. https://doi.org/10.1074/jbc.M110.197921

Jürgens, B., Hainz, U., Fuchs, D., Felzmann, T., & Heitger, A. (2009). Interferon-γ–triggered indoleamine 2,3-dioxygenase competence in human monocyte-derived dendritic cells induces regulatory activity in allogeneic T cells. *Blood*, *114*(15), 3235–3243. https://doi.org/10.1182/blood-2008-12-195073

Kalbasi, A., Tariveranmoshabad, M., Hakimi, K., Kremer, S., Campbell, K. M., Funes, J. M., Vega-Crespo, A., Parisi, G., Champekar, A., Nguyen, C., Torrejon, D., Shin, D., Zaretsky, J. M., Damoiseaux, R. D., Speiser, D. E., Lopez-Casas, P. P., Quintero, M., & Ribas, A. (2020). Uncoupling interferon signaling and antigen presentation to overcome immunotherapy resistance due to JAK1 loss in melanoma. *Science Translational Medicine*, *12*(565). https://doi.org/10.1126/scitranslmed.abb0152

Kaur, S., Lal, L., Sassano, A., Majchrzak-Kita, B., Srikanth, M., Baker, D. P., Petroulakis, E., Hay, N., Sonenberg, N., Fish, E. N., & Platanias, L. C. (2007). Regulatory effects of mammalian target of rapamycin-activated pathways in type I and II interferon signaling. *The Journal of Biological Chemistry*, *282*(3), 1757–1768. https://doi.org/10.1074/jbc.M607365200

Kim, B.-G., Malek, E., Choi, S. H., Ignatz-Hoover, J. J., & Driscoll, J. J. (2021). Novel therapies emerging in oncology to target the TGF-β pathway. *Journal of Hematology & Oncology*, *14*(1), 55. https://doi.org/10.1186/s13045-021-01053-x

Kim, P. K. M., Armstrong, M., Liu, Y., Yan, P., Bucher, B., Zuckerbraun, B. S., Gambotto, A., Billiar, T. R., & Yim, J. H. (2004). IRF-1 expression induces apoptosis and inhibits tumor growth in mouse mammary cancer cells in vitro and in vivo. *Oncogene*, *23*(5), 1125–1135. https://doi.org/10.1038/sj.onc.1207023

Kirkwood, J. M., Iannotti, N., Cho, D., O'Day, S., Gibney, G., Hodi, F. S., Munster, P., Hoyle, P., Owens, S., Smith, M., & Mettu, N. (2018). Abstract CT176: Effect of JAK/STAT or PI3Kδ plus PD-1 inhibition on the tumor microenvironment: Biomarker results from a phase Ib study in patients with advanced solid tumors. *Cancer Research*, *78*(13_Supplement), CT176–CT176. https://doi.org/10.1158/1538-7445.AM2018-CT176

Klein, C., Schaefer, W., & Regula, J. T. (2016). The use of CrossMAb technology for the generation of bi- and multispecific antibodies. *MAbs*, *8*(6), 1010–1020. https://doi.org/10.1080/19420862.2016.1197457

Klempner, S. J., Bendell, J. C., Villaflor, V. M., Tenner, L. L., Stein, S., Naik, G. S., Sirard, C. A., Kagey, M., Chaney, M. F., & Strickler, J. H. (2020). DKN-01 in combination with pembrolizumab in patients with advanced gastroesophageal adenocarcinoma (GEA): Tumoral DKK1 expression as a predictor of response and survival. *Journal of Clinical Oncology*, *38*(4_suppl), 357–357. https://doi.org/10.1200/JCO.2020.38.4_suppl.357

Koneru, M., Purdon, T. J., Spriggs, D., Koneru, S., & Brentjens, R. J. (2015). IL-12 secreting tumor-targeted chimeric antigen receptor T cells eradicate ovarian tumors in vivo. *OncoImmunology*, *4*(3), e994446. https://doi.org/10.4161/2162402X.2014.994446

Kuemmel, S., Campone, M., Loirat, D., Lopez, R. L., Beck, J. T., De Laurentiis, M., Im, S.-A., Kim, S.-B., Kwong, A., Steger, G. G., Adelantado, E. Z., Duhoux, F. P., Greil, R., Kuter, I., Lu, Y.-S., Tibau, A., Özgüroğlu, M., Scholz, C. W., Singer, C. F., … Chan, A. (2022). A Randomized Phase II Study of Anti-CSF1 Monoclonal Antibody Lacnotuzumab (MCS110) Combined with Gemcitabine and Carboplatin in Advanced Triple-Negative Breast Cancer. *Clinical Cancer Research*, *28*(1), 106–115. https://doi.org/10.1158/1078-0432.CCR-20-3955

Lang, F., Schrörs, B., Löwer, M., Türeci, Ö., & Sahin, U. (2022). Identification of neoantigens for individualized therapeutic cancer vaccines. *Nature Reviews Drug Discovery*, *21*(4), 261–282. https://doi.org/10.1038/s41573-021-00387-y

Larkin, J., Chiarion-Sileni, V., Gonzalez, R., Grob, J.-J., Rutkowski, P., Lao, C. D., Cowey, C. L., Schadendorf, D., Wagstaff, J., Dummer, R., Ferrucci, P. F., Smylie, M., Hogg, D., Hill, A., Márquez-Rodas, I., Haanen, J., Guidoboni, M., Maio, M., Schöffski, P., … Wolchok, J. D. (2019). Five-Year Survival with Combined Nivolumab and Ipilimumab in Advanced Melanoma. *New England Journal of Medicine*, *381*(16), 1535–1546. https://doi.org/10.1056/NEJMoa1910836

Larson, R. C., Kann, M. C., Bailey, S. R., Haradhvala, N. J., Llopis, P. M., Bouffard, A. A., Scarfó, I., Leick, M. B., Grauwet, K., Berger, T. R., Stewart, K., Anekal, P. V., Jan, M., Joung, J., Schmidts, A., Ouspenskaia, T., Law, T., Regev, A., Getz, G., & Maus, M. V. (2022). CAR T cell killing requires the IFNγR pathway in solid but not liquid tumours. *Nature*, *604*(7906), 563–570. https://doi.org/10.1038/s41586-022-04585-5

Lattanzio, L., Denaro, N., Vivenza, D., Varamo, C., Strola, G., Fortunato, M., Chamorey, E., Comino, A., Monteverde, M., Lo Nigro, C., Milano, G., & Merlano, M. (2017). Elevated basal antibody-dependent cell-mediated cytotoxicity (ADCC) and high epidermal growth factor receptor (EGFR) expression predict favourable outcome in patients with locally advanced head and neck cancer treated with cetuximab and radiotherapy. *Cancer Immunology, Immunotherapy : CII*, *66*(5), 573–579. https://doi.org/10.1007/s00262-017-1960-8

Lauterbach, H., Bathke, B., Gilles, S., Traidl-Hoffmann, C., Luber, C. A., Fejer, G., Freudenberg, M. A., Davey, G. M., Vremec, D., Kallies, A., Wu, L., Shortman, K., Chaplin, P., Suter, M., O'Keeffe, M., & Hochrein, H. (2010). Mouse CD8α+ DCs and human BDCA3+ DCs are major producers of IFN-λ in response to poly IC. *Journal of Experimental Medicine*, *207*(12), 2703–2717. https://doi.org/10.1084/jem.20092720

Lawson, K. A., Sousa, C. M., Zhang, X., Kim, E., Akthar, R., Caumanns, J. J., Yao, Y., Mikolajewicz, N., Ross, C., Brown, K. R., Zid, A. A., Fan, Z. P., Hui, S., Krall, J. A., Simons, D. M., Slater, C. J., De Jesus, V., Tang, L., Singh, R., … Moffat, J. (2020). Functional genomic landscape of cancer-intrinsic evasion of killing by T cells. *Nature*, *586*(7827), 120–126. https://doi.org/10.1038/s41586-020-2746-2

Lazear, H. M., Nice, T. J., & Diamond, M. S. (2015). Interferon-λ: Immune Functions at Barrier Surfaces and Beyond. *Immunity*, *43*(1), 15–28. https://doi.org/10.1016/j.immuni.2015.07.001

Lazear, H. M., Schoggins, J. W., & Diamond, M. S. (2019). Shared and Distinct Functions of Type

I and Type III Interferons. *Immunity*, *50*(4), 907–923. https://doi.org/10.1016/j.immuni.2019.03.025
Le Naour, J., Zitvogel, L., Galluzzi, L., Vacchelli, E., & Kroemer, G. (2020). Trial watch: STING agonists in cancer therapy. *OncoImmunology*, *9*(1). https://doi.org/10.1080/2162402X.2020.1777624
Leach, D. R., Krummel, M. F., & Allison, J. P. (1996). Enhancement of Antitumor Immunity by CTLA-4 Blockade. *Science*, *271*(5256), 1734–1736. https://doi.org/10.1126/science.271.5256.1734
Lechner, M. G., Liebertz, D. J., & Epstein, A. L. (2010). Characterization of Cytokine-Induced Myeloid-Derived Suppressor Cells from Normal Human Peripheral Blood Mononuclear Cells. *The Journal of Immunology*, *185*(4), 2273–2284. https://doi.org/10.4049/jimmunol.1000901
Lemoine, J., Ruella, M., & Houot, R. (2021). Born to survive: how cancer cells resist CAR T cell therapy. *Journal of Hematology & Oncology*, *14*(1), 199. https://doi.org/10.1186/s13045-021-01209-9
Lhuillier, C., Rudqvist, N.-P., Yamazaki, T., Zhang, T., Charpentier, M., Galluzzi, L., Dephoure, N., Clement, C. C., Santambrogio, L., Zhou, X. K., Formenti, S. C., & Demaria, S. (2021). Radiotherapy-exposed CD8+ and CD4+ neoantigens enhance tumor control. *Journal of Clinical Investigation*, *131*(5). https://doi.org/10.1172/JCI138740
Li, F., Zhao, S., Wei, C., Hu, Y., Xu, T., Xin, X., Zhu, T., Shang, L., Ke, S., Zhou, J., Xu, X., Gao, Y., Zhao, A., & Gao, J. (2022). Development of Nectin4/FAP-targeted CAR-T cells secreting IL-7, CCL19, and IL-12 for malignant solid tumors. *Frontiers in Immunology*, *13*. https://doi.org/10.3389/fimmu.2022.958082
Li, J., Yang, Y., Inoue, H., Mori, M., & Akiyoshi, T. (1996). The expression of costimulatory molecules CD80 and CD86 in human carcinoma cell lines: its regulation by interferon γ and interleukin-10. *Cancer Immunology, Immunotherapy*, *43*(4), 213–219. https://doi.org/10.1007/s002620050324
Li, S., Gong, M., Zhao, F., Shao, J., Xie, Y., Zhang, Y., & Chang, H. (2018). Type I Interferons: Distinct Biological Activities and Current Applications for Viral Infection. *Cellular Physiology and Biochemistry*, *51*(5), 2377–2396. https://doi.org/10.1159/000495897
Li, T., Cheng, H., Yuan, H., Xu, Q., Shu, C., Zhang, Y., Xu, P., Tan, J., Rui, Y., Li, P., & Tan, X. (2016). Antitumor Activity of cGAMP via Stimulation of cGAS-cGAMP-STING-IRF3 Mediated Innate Immune Response. *Scientific Reports*, *6*(1), 19049. https://doi.org/10.1038/srep19049
Liau, N. P. D., Laktyushin, A., Lucet, I. S., Murphy, J. M., Yao, S., Whitlock, E., Callaghan, K., Nicola, N. A., Kershaw, N. J., & Babon, J. J. (2018). The molecular basis of JAK/STAT inhibition by SOCS1. *Nature Communications*, *9*(1), 1558. https://doi.org/10.1038/s41467-018-04013-1
Liu, B. L., Robinson, M., Han, Z.-Q., Branston, R. H., English, C., Reay, P., McGrath, Y., Thomas, S. K., Thornton, M., Bullock, P., Love, C. A., & Coffin, R. S. (2003). ICP34.5 deleted herpes simplex virus with enhanced oncolytic, immune stimulating, and anti-tumour properties. *Gene Therapy*, *10*(4), 292–303. https://doi.org/10.1038/sj.gt.3301885
Liu, J. K. H. (2014). The history of monoclonal antibody development - Progress, remaining challenges and future innovations. *Annals of Medicine and Surgery (2012)*, *3*(4), 113–116. https://doi.org/10.1016/j.amsu.2014.09.001
Liu, L., Mayes, P. A., Eastman, S., Shi, H., Yadavilli, S., Zhang, T., Yang, J., Seestaller-Wehr, L., Zhang, S.-Y., Hopson, C., Tsvetkov, L., Jing, J., Zhang, S., Smothers, J., & Hoos, A. (2015). The BRAF and MEK Inhibitors Dabrafenib and Trametinib: Effects on Immune Function and in Combination with Immunomodulatory Antibodies Targeting PD-1, PD-L1, and CTLA-4. *Clinical Cancer Research*, *21*(7), 1639–1651. https://doi.org/10.1158/1078-0432.CCR-14-2339
Liu, S.-Q., Grantham, A., Landry, C., Granda, B., Chopra, R., Chakravarthy, S., Deutsch, S., Vogel, M., Russo, K., Seiss, K., Tschantz, W. R., Rejtar, T., Ruddy, D. A., Hu, T., Aardalen, K., Wagner, J. P., Dranoff, G., & D'Alessio, J. A. (2021). A CRISPR Screen Reveals Resistance Mechanisms to CD3-Bispecific Antibody Therapy. *Cancer Immunology Research*, *9*(1), 34–49. https://doi.org/10.1158/2326-6066.CIR-20-0080
Liu, Y.-T., & Sun, Z.-J. (2021). Turning cold tumors into hot tumors by improving T-cell infiltration. *Theranostics*, *11*(11), 5365–5386. https://doi.org/10.7150/thno.58390
Liu, Y., Sun, Y., Wang, P., Li, S., Dong, Y., Zhou, M., Shi, B., Jiang, H., Sun, R., & Li, Z. (2023). FAP-targeted CAR-T suppresses MDSCs recruitment to improve the antitumor efficacy of

claudin18.2-targeted CAR-T against pancreatic cancer. *Journal of Translational Medicine*, *21*(1), 255. https://doi.org/10.1186/s12967-023-04080-z

Llosa, N. J., Cruise, M., Tam, A., Wicks, E. C., Hechenbleikner, E. M., Taube, J. M., Blosser, R. L., Fan, H., Wang, H., Luber, B. S., Zhang, M., Papadopoulos, N., Kinzler, K. W., Vogelstein, B., Sears, C. L., Anders, R. A., Pardoll, D. M., & Housseau, F. (2015). The vigorous immune microenvironment of microsatellite instable colon cancer is balanced by multiple counter-inhibitory checkpoints. *Cancer Discovery*, *5*(1), 43–51. https://doi.org/10.1158/2159-8290.CD-14-0863

Lo, A. A., Wallace, A., Oreper, D., Lounsbury, N., Havnar, C., Pechuan-Jorge, X., Wu, T. D., Bourgon, R., Jones, R., Krogh, K., Yang, G.-Y., & Zill, O. A. (2021). Indication-specific tumor evolution and its impact on neoantigen targeting and biomarkers for individualized cancer immunotherapies. *Journal for ImmunoTherapy of Cancer*, *9*(10), e003001. https://doi.org/10.1136/jitc-2021-003001

Lorentzen, C. L., Kjeldsen, J. W., Ehrnrooth, E., Andersen, M. H., & Marie Svane, I. (2023). Long-term follow-up of anti-PD-1 naïve patients with metastatic melanoma treated with IDO/PD-L1 targeting peptide vaccine and nivolumab. *Journal for ImmunoTherapy of Cancer*, *11*(5), e006755. https://doi.org/10.1136/jitc-2023-006755

Lowin, B., Hahne, M., Mattmann, C., & Tschopp, J. (1994). Cytolytic T-cell cytotoxicity is mediated through perforin and Fas lytic pathways. *Nature*, *370*(6491), 650–652. https://doi.org/10.1038/370650a0

Lu, C., Klement, J. D., Ibrahim, M. L., Xiao, W., Redd, P. S., Nayak-Kapoor, A., Zhou, G., & Liu, K. (2019). Type I interferon suppresses tumor growth through activating the STAT3-granzyme B pathway in tumor-infiltrating cytotoxic T lymphocytes. *Journal for ImmunoTherapy of Cancer*, *7*(1), 157. https://doi.org/10.1186/s40425-019-0635-8

Lu, Y.-C., Yao, X., Crystal, J. S., Li, Y. F., El-Gamil, M., Gross, C., Davis, L., Dudley, M. E., Yang, J. C., Samuels, Y., Rosenberg, S. A., & Robbins, P. F. (2014). Efficient Identification of Mutated Cancer Antigens Recognized by T Cells Associated with Durable Tumor Regressions. *Clinical Cancer Research*, *20*(13), 3401–3410. https://doi.org/10.1158/1078-0432.CCR-14-0433

Lusty, E., Poznanski, S. M., Kwofie, K., Mandur, T. S., Lee, D. A., Richards, C. D., & Ashkar, A. A. (2017). IL-18/IL-15/IL-12 synergy induces elevated and prolonged IFN-γ production by ex vivo expanded NK cells which is not due to enhanced STAT4 activation. *Molecular Immunology*, *88*, 138–147. https://doi.org/10.1016/j.molimm.2017.06.025

Lynn, R. C., Poussin, M., Kalota, A., Feng, Y., Low, P. S., Dimitrov, D. S., & Powell, D. J. (2015). Targeting of folate receptor β on acute myeloid leukemia blasts with chimeric antigen receptor–expressing T cells. *Blood*, *125*(22), 3466–3476. https://doi.org/10.1182/blood-2014-11-612721

Ma, K.-Y., Schonnesen, A. A., Brock, A., Van Den Berg, C., Eckhardt, S. G., Liu, Z., & Jiang, N. (2019). Single-cell RNA sequencing of lung adenocarcinoma reveals heterogeneity of immune response–related genes. *JCI Insight*, *4*(4). https://doi.org/10.1172/jci.insight.121387

Ma, V. P.-Y., Hu, Y., Kellner, A. V., Brockman, J. M., Velusamy, A., Blanchard, A. T., Evavold, B. D., Alon, R., & Salaita, K. (2022). The magnitude of LFA-1/ICAM-1 forces fine-tune TCR-triggered T cell activation. *Science Advances*, *8*(8). https://doi.org/10.1126/sciadv.abg4485

Maher, J., & Davies, D. M. (2023). CAR Based Immunotherapy of Solid Tumours—A Clinically Based Review of Target Antigens. *Biology*, *12*(2), 287. https://doi.org/10.3390/biology12020287

Majzner, R. G., Frank, M. J., Mount, C., Tousley, A., Kurtz, D. M., Sworder, B., Murphy, K. A., Manousopoulou, A., Kohler, K., Rotiroti, M. C., Spiegel, J. Y., Natkunam, Y., Younes, S. F., Sotillo, E., Duong, V., Macaulay, C., Good, Z., Xu, P., Labanieh, L., … Mackall, C. L. (2020). CD58 Aberrations Limit Durable Responses to CD19 CAR in Large B Cell Lymphoma Patients Treated with Axicabtagene Ciloleucel but Can be Overcome through Novel CAR Engineering. *Blood*, *136*(Supplement 1), 53–54. https://doi.org/10.1182/blood-2020-139605

Malmberg, K.-J., Carlsten, M., Björklund, A., Sohlberg, E., Bryceson, Y. T., & Ljunggren, H.-G. (2017). Natural killer cell-mediated immunosurveillance of human cancer. *Seminars in Immunology*, *31*, 20–29. https://doi.org/10.1016/j.smim.2017.08.002

Manguso, R. T., Pope, H. W., Zimmer, M. D., Brown, F. D., Yates, K. B., Miller, B. C., Collins, N. B., Bi, K., La Fleur, M. W., Juneja, V. R., Weiss, S. A., Lo, J., Fisher, D. E., Miao, D., Van Allen, E., Root, D. E., Sharpe, A. H., Doench, J. G., & Haining, W. N. (2017). In vivo CRISPR screening identifies Ptpn2 as a cancer immunotherapy target. *Nature*, *547*(7664), 413–418.

https://doi.org/10.1038/nature23270
Marabelle, Aurélien, Fakih, M., Lopez, J., Shah, M., Shapira-Frommer, R., Nakagawa, K., Chung, H. C., Kindler, H. L., Lopez-Martin, J. A., Miller, W. H., Italiano, A., Kao, S., Piha-Paul, S. A., Delord, J.-P., McWilliams, R. R., Fabrizio, D. A., Aurora-Garg, D., Xu, L., Jin, F., … Bang, Y.-J. (2020). Association of tumour mutational burden with outcomes in patients with advanced solid tumours treated with pembrolizumab: prospective biomarker analysis of the multicohort, open-label, phase 2 KEYNOTE-158 study. *The Lancet. Oncology*, *21*(10), 1353–1365. https://doi.org/10.1016/S1470-2045(20)30445-9
Marabelle, Aurelien, Le, D. T., Ascierto, P. A., Di Giacomo, A. M., De Jesus-Acosta, A., Delord, J.-P., Geva, R., Gottfried, M., Penel, N., Hansen, A. R., Piha-Paul, S. A., Doi, T., Gao, B., Chung, H. C., Lopez-Martin, J., Bang, Y.-J., Frommer, R. S., Shah, M., Ghori, R., … Diaz, L. A. (2020). Efficacy of Pembrolizumab in Patients With Noncolorectal High Microsatellite Instability/Mismatch Repair-Deficient Cancer: Results From the Phase II KEYNOTE-158 Study. *Journal of Clinical Oncology : Official Journal of the American Society of Clinical Oncology*, *38*(1), 1–10. https://doi.org/10.1200/JCO.19.02105
Marin-Acevedo, J. A., Dholaria, B., Soyano, A. E., Knutson, K. L., Chumsri, S., & Lou, Y. (2018). Next generation of immune checkpoint therapy in cancer: new developments and challenges. *Journal of Hematology & Oncology*, *11*(1), 39. https://doi.org/10.1186/s13045-018-0582-8
Martínez-Sabadell, A., Morancho, B., Rius Ruiz, I., Román Alonso, M., Ovejero Romero, P., Escorihuela, M., Chicote, I., Palmer, H. G., Nonell, L., Alemany-Chavarria, M., Klein, C., Bacac, M., Arribas, J., & Arenas, E. J. (2022). The target antigen determines the mechanism of acquired resistance to T cell-based therapies. *Cell Reports*, *41*(3), 111430. https://doi.org/10.1016/j.celrep.2022.111430
Mascarenhas, J., & Hoffman, R. (2012). Ruxolitinib: The First FDA Approved Therapy for the Treatment of Myelofibrosis. *Clinical Cancer Research*, *18*(11), 3008–3014. https://doi.org/10.1158/1078-0432.CCR-11-3145
Matsushita, H., Hosoi, A., Ueha, S., Abe, J., Fujieda, N., Tomura, M., Maekawa, R., Matsushima, K., Ohara, O., & Kakimi, K. (2015). Cytotoxic T lymphocytes block tumor growth both by lytic activity and IFNγ-Dependent Cell-cycle arrest. *Cancer Immunology Research*, *3*(1), 26–36. https://doi.org/10.1158/2326-6066.CIR-14-0098
Maude, S. L., Laetsch, T. W., Buechner, J., Rives, S., Boyer, M., Bittencourt, H., Bader, P., Verneris, M. R., Stefanski, H. E., Myers, G. D., Qayed, M., De Moerloose, B., Hiramatsu, H., Schlis, K., Davis, K. L., Martin, P. L., Nemecek, E. R., Yanik, G. A., Peters, C., … Grupp, S. A. (2018). Tisagenlecleucel in Children and Young Adults with B-Cell Lymphoblastic Leukemia. *The New England Journal of Medicine*, *378*(5), 439–448. https://doi.org/10.1056/NEJMoa1709866
Mazet, J. M., Mahale, J. N., Tong, O., Watson, R. A., Lechuga-Vieco, A. V., Pirgova, G., Lau, V. W. C., Attar, M., Koneva, L. A., Sansom, S. N., Fairfax, B. P., & Gérard, A. (2023). IFNγ signaling in cytotoxic T cells restricts anti-tumor responses by inhibiting the maintenance and diversity of intra-tumoral stem-like T cells. *Nature Communications*, *14*(1), 321. https://doi.org/10.1038/s41467-023-35948-9
Mejstríková, E., Hrusak, O., Borowitz, M. J., Whitlock, J. A., Brethon, B., Trippett, T. M., Zugmaier, G., Gore, L., von Stackelberg, A., & Locatelli, F. (2017). CD19-negative relapse of pediatric B-cell precursor acute lymphoblastic leukemia following blinatumomab treatment. *Blood Cancer Journal*, *7*(12), 659. https://doi.org/10.1038/s41408-017-0023-x
Meric-Bernstam, F., Sandhu, S. K., Hamid, O., Spreafico, A., Kasper, S., Dummer, R., Shimizu, T., Steeghs, N., Lewis, N., Talluto, C. C., Dolan, S., Bean, A., Brown, R., Trujillo, D., Nair, N., & Luke, J. J. (2019). Phase Ib study of MIW815 (ADU-S100) in combination with spartalizumab (PDR001) in patients (pts) with advanced/metastatic solid tumors or lymphomas. *Journal of Clinical Oncology*, *37*(15_suppl), 2507–2507. https://doi.org/10.1200/JCO.2019.37.15_suppl.2507
Miller, C. H. T., Maher, S. G., & Young, H. A. (2009). Clinical Use of Interferon-γ. *Annals of the New York Academy of Sciences*, *1182*(1), 69–79. https://doi.org/10.1111/j.1749-6632.2009.05069.x
Mirlekar, B., & Pylayeva-Gupta, Y. (2021). IL-12 Family Cytokines in Cancer and Immunotherapy. *Cancers*, *13*(2), 167. https://doi.org/10.3390/cancers13020167
Montoya, M., Schiavoni, G., Mattei, F., Gresser, I., Belardelli, F., Borrow, P., & Tough, D. F. (2002). Type I interferons produced by dendritic cells promote their phenotypic and functional activation. *Blood*, *99*(9), 3263–3271. https://doi.org/10.1182/blood.V99.9.3263

Müller, L., Aigner, P., & Stoiber, D. (2017). Type I Interferons and Natural Killer Cell Regulation in Cancer. *Frontiers in Immunology*, *8*. https://doi.org/10.3389/fimmu.2017.00304

Musella, M., Manic, G., De Maria, R., Vitale, I., & Sistigu, A. (2017). Type-I-interferons in infection and cancer: Unanticipated dynamics with therapeutic implications. *OncoImmunology*, *6*(5), e1314424. https://doi.org/10.1080/2162402X.2017.1314424

Nabors, L. B., Suswam, E., Huang, Y., Yang, X., Johnson, M. J., & King, P. H. (2003). Tumor necrosis factor alpha induces angiogenic factor up-regulation in malignant glioma cells: a role for RNA stabilization and HuR. *Cancer Research*, *63*(14), 4181–4187. http://www.ncbi.nlm.nih.gov/pubmed/12874024

Nagarsheth, N. B., Norberg, S. M., Sinkoe, A. L., Adhikary, S., Meyer, T. J., Lack, J. B., Warner, A. C., Schweitzer, C., Doran, S. L., Korrapati, S., Stevanović, S., Trimble, C. L., Kanakry, J. A., Bagheri, M. H., Ferraro, E., Astrow, S. H., Bot, A., Faquin, W. C., Stroncek, D., … Hinrichs, C. S. (2021). TCR-engineered T cells targeting E7 for patients with metastatic HPV-associated epithelial cancers. *Nature Medicine*, *27*(3), 419–425. https://doi.org/10.1038/s41591-020-01225-1

Nathan, P., Hassel, J. C., Rutkowski, P., Baurain, J.-F., Butler, M. O., Schlaak, M., Sullivan, R. J., Ochsenreither, S., Dummer, R., Kirkwood, J. M., Joshua, A. M., Sacco, J. J., Shoushtari, A. N., Orloff, M., Piulats, J. M., Milhem, M., Salama, A. K. S., Curti, B., Demidov, L., … Piperno-Neumann, S. (2021). Overall Survival Benefit with Tebentafusp in Metastatic Uveal Melanoma. *New England Journal of Medicine*, *385*(13), 1196–1206. https://doi.org/10.1056/NEJMoa2103485

Negishi, H., Taniguchi, T., & Yanai, H. (2018). The Interferon (IFN) Class of Cytokines and the IFN Regulatory Factor (IRF) Transcription Factor Family. *Cold Spring Harbor Perspectives in Biology*, *10*(11), a028423. https://doi.org/10.1101/cshperspect.a028423

Ni, J., Miller, M., Stojanovic, A., Garbi, N., & Cerwenka, A. (2012). Sustained effector function of IL-12/15/18-preactivated NK cells against established tumors. *The Journal of Experimental Medicine*, *209*(13), 2351–2365. https://doi.org/10.1084/jem.20120944

Niu, G.-J., Xu, J.-D., Yuan, W.-J., Sun, J.-J., Yang, M.-C., He, Z.-H., Zhao, X.-F., & Wang, J.-X. (2018). Protein Inhibitor of Activated STAT (PIAS) Negatively Regulates the JAK/STAT Pathway by Inhibiting STAT Phosphorylation and Translocation. *Frontiers in Immunology*, *9*. https://doi.org/10.3389/fimmu.2018.02392

O'Hara, M. H., Messersmith, W., Kindler, H., Zhang, W., Pitou, C., Szpurka, A. M., Wang, D., Peng, S.-B., Vangerow, B., Khan, A. A., Koneru, M., & Wang-Gillam, A. (2020). Safety and Pharmacokinetics of CXCR4 Peptide Antagonist, LY2510924, in Combination with Durvalumab in Advanced Refractory Solid Tumors. *Journal of Pancreatic Cancer*, *6*(1), 21–31. https://doi.org/10.1089/pancan.2019.0018

O'Hara, M. H., O'Reilly, E. M., Varadhachary, G., Wolff, R. A., Wainberg, Z. A., Ko, A. H., Fisher, G., Rahma, O., Lyman, J. P., Cabanski, C. R., Mick, R., Gherardini, P. F., Kitch, L. J., Xu, J., Samuel, T., Karakunnel, J., Fairchild, J., Bucktrout, S., LaVallee, T. M., … Vonderheide, R. H. (2021). CD40 agonistic monoclonal antibody APX005M (sotigalimab) and chemotherapy, with or without nivolumab, for the treatment of metastatic pancreatic adenocarcinoma: an open-label, multicentre, phase 1b study. *The Lancet Oncology*, *22*(1), 118–131. https://doi.org/10.1016/S1470-2045(20)30532-5

O'Rourke, D. M., Nasrallah, M. P., Desai, A., Melenhorst, J. J., Mansfield, K., Morrissette, J. J. D., Martinez-Lage, M., Brem, S., Maloney, E., Shen, A., Isaacs, R., Mohan, S., Plesa, G., Lacey, S. F., Navenot, J.-M., Zheng, Z., Levine, B. L., Okada, H., June, C. H., … Maus, M. V. (2017). A single dose of peripherally infused EGFRvIII-directed CAR T cells mediates antigen loss and induces adaptive resistance in patients with recurrent glioblastoma. *Science Translational Medicine*, *9*(399). https://doi.org/10.1126/scitranslmed.aaa0984

Ohkuri, T., Ghosh, A., Kosaka, A., Zhu, J., Ikeura, M., David, M., Watkins, S. C., Sarkar, S. N., & Okada, H. (2014). STING Contributes to Antiglioma Immunity via Triggering Type I IFN Signals in the Tumor Microenvironment. *Cancer Immunology Research*, *2*(12), 1199–1208. https://doi.org/10.1158/2326-6066.CIR-14-0099

Ohue, Y., & Nishikawa, H. (2019). Regulatory T (Treg) cells in cancer: Can Treg cells be a new therapeutic target? *Cancer Science*, *110*(7), 2080–2089. https://doi.org/10.1111/cas.14069

Oshima, M., Oshima, H., Matsunaga, A., & Taketo, M. M. (2005). Hyperplastic Gastric Tumors with Spasmolytic Polypeptide–Expressing Metaplasia Caused by Tumor Necrosis Factor-α–Dependent Inflammation in Cyclooxygenase-2/Microsomal Prostaglandin E Synthase-1 Transgenic Mice. *Cancer Research*, *65*(20), 9147–9151. https://doi.org/10.1158/0008-5472.CAN-05-1936

Overacre-Delgoffe, A. E., Chikina, M., Dadey, R. E., Yano, H., Brunazzi, E. A., Shayan, G., Horne, W., Moskovitz, J. M., Kolls, J. K., Sander, C., Shuai, Y., Normolle, D. P., Kirkwood, J. M., Ferris, R. L., Delgoffe, G. M., Bruno, T. C., Workman, C. J., & Vignali, D. A. A. (2017). Interferon-γ Drives Treg Fragility to Promote Anti-tumor Immunity. *Cell*, *169*(6), 1130-1141.e11. https://doi.org/10.1016/j.cell.2017.05.005

Pai, C.-C. S., Huang, J. T., Lu, X., Simons, D. M., Park, C., Chang, A., Tamaki, W., Liu, E., Roybal, K. T., Seagal, J., Chen, M., Hagihara, K., Wei, X. X., DuPage, M., Kwek, S. S., Oh, D. Y., Daud, A., Tsai, K. K., Wu, C., … Fong, L. (2019). Clonal Deletion of Tumor-Specific T Cells by Interferon-γ Confers Therapeutic Resistance to Combination Immune Checkpoint Blockade. *Immunity*, *50*(2), 477-492.e8. https://doi.org/10.1016/j.immuni.2019.01.006

Park, J. H., & Lee, H. K. (2021). Function of γδ T cells in tumor immunology and their application to cancer therapy. *Experimental & Molecular Medicine*, *53*(3), 318–327. https://doi.org/10.1038/s12276-021-00576-0

Park, S.-Y., Seol, J.-W., Lee, Y.-J., Cho, J.-H., Kang, H.-S., Kim, I.-S., Park, S.-H., Kim, T.-H., Yim, J. H., Kim, M., Billiar, T. R., & Seol, D.-W. (2004). IFN-γ enhances TRAIL-induced apoptosis through IRF-1. *European Journal of Biochemistry*, *271*(21), 4222–4228. https://doi.org/10.1111/j.1432-1033.2004.04362.x

Parlato, S., Santini, S. M., Lapenta, C., Di Pucchio, T., Logozzi, M., Spada, M., Giammarioli, A. M., Malorni, W., Fais, S., & Belardelli, F. (2001). Expression of CCR-7, MIP-3β, and Th-1 chemokines in type I IFN-induced monocyte-derived dendritic cells: importance for the rapid acquisition of potent migratory and functional activities. *Blood*, *98*(10), 3022–3029. https://doi.org/10.1182/blood.V98.10.3022

Pasetto, A., Gros, A., Robbins, P. F., Deniger, D. C., Prickett, T. D., Matus-Nicodemos, R., Douek, D. C., Howie, B., Robins, H., Parkhurst, M. R., Gartner, J., Trebska-McGowan, K., Crystal, J. S., & Rosenberg, S. A. (2016). Tumor- and Neoantigen-Reactive T-cell Receptors Can Be Identified Based on Their Frequency in Fresh Tumor. *Cancer Immunology Research*, *4*(9), 734–743. https://doi.org/10.1158/2326-6066.CIR-16-0001

Patel, S. J., Sanjana, N. E., Kishton, R. J., Eidizadeh, A., Vodnala, S. K., Cam, M., Gartner, J. J., Jia, L., Steinberg, S. M., Yamamoto, T. N., Merchant, A. S., Mehta, G. U., Chichura, A., Shalem, O., Tran, E., Eil, R., Sukumar, M., Guijarro, E. P., Day, C.-P., … Restifo, N. P. (2017). Identification of essential genes for cancer immunotherapy. *Nature*, *548*(7669), 537–542. https://doi.org/10.1038/nature23477

Pearce, E. L., Mullen, A. C., Martins, G. A., Krawczyk, C. M., Hutchins, A. S., Zediak, V. P., Banica, M., DiCioccio, C. B., Gross, D. A., Mao, C., Shen, H., Cereb, N., Yang, S. Y., Lindsten, T., Rossant, J., Hunter, C. A., & Reiner, S. L. (2003). Control of Effector CD8 + T Cell Function by the Transcription Factor Eomesodermin. *Science*, *302*(5647), 1041–1043. https://doi.org/10.1126/science.1090148

Peng, Q., Qiu, X., Zhang, Z., Zhang, S., Zhang, Y., Liang, Y., Guo, J., Peng, H., Chen, M., Fu, Y.-X., & Tang, H. (2020). PD-L1 on dendritic cells attenuates T cell activation and regulates response to immune checkpoint blockade. *Nature Communications*, *11*(1), 4835. https://doi.org/10.1038/s41467-020-18570-x

Peng, W., Chen, J. Q., Liu, C., Malu, S., Creasy, C., Tetzlaff, M. T., Xu, C., McKenzie, J. A., Zhang, C., Liang, X., Williams, L. J., Deng, W., Chen, G., Mbofung, R., Lazar, A. J., Torres-Cabala, C. A., Cooper, Z. A., Chen, P.-L., Tieu, T. N., … Hwu, P. (2016). Loss of PTEN Promotes Resistance to T Cell-Mediated Immunotherapy. *Cancer Discovery*, *6*(2), 202–216. https://doi.org/10.1158/2159-8290.CD-15-0283

Pérez-Núñez, I., Rozalén, C., Palomeque, J. Á., Sangrador, I., Dalmau, M., Comerma, L., Hernández-Prat, A., Casadevall, D., Menendez, S., Liu, D. D., Shen, M., Berenguer, J., Ruiz, I. R., Peña, R., Montañés, J. C., Albà, M. M., Bonnin, S., Ponomarenko, J., Gomis, R. R., … Celià-Terrassa, T. (2022). LCOR mediates interferon-independent tumor immunogenicity and responsiveness to immune-checkpoint blockade in triple-negative breast cancer. *Nature Cancer*, *3*(3), 355–370. https://doi.org/10.1038/s43018-022-00339-4

Petty, A. J., Owen, D. H., Yang, Y., & Huang, X. (2021). Targeting Tumor-Associated Macrophages in Cancer Immunotherapy. *Cancers*, *13*(21), 5318. https://doi.org/10.3390/cancers13215318

Pitt, J. M., Vétizou, M., Daillère, R., Roberti, M. P., Yamazaki, T., Routy, B., Lepage, P., Boneca, I. G., Chamaillard, M., Kroemer, G., & Zitvogel, L. (2016). Resistance Mechanisms to Immune-Checkpoint Blockade in Cancer: Tumor-Intrinsic and -Extrinsic Factors. *Immunity*, *44*(6), 1255–1269. https://doi.org/10.1016/j.immuni.2016.06.001

Platanias, L. C. (2005). Mechanisms of type-I- and type-II-interferon-mediated signalling. *Nature*

Reviews Immunology, *5*(5), 375–386. https://doi.org/10.1038/nri1604
Poorebrahim, M., Mohammadkhani, N., Mahmoudi, R., Gholizadeh, M., Fakhr, E., & Cid-Arregui, A. (2021). TCR-like CARs and TCR-CARs targeting neoepitopes: an emerging potential. *Cancer Gene Therapy*, *28*(6), 581–589. https://doi.org/10.1038/s41417-021-00307-7
Ramakrishna, S., Highfill, S. L., Walsh, Z., Nguyen, S. M., Lei, H., Shern, J. F., Qin, H., Kraft, I. L., Stetler-Stevenson, M., Yuan, C. M., Hwang, J. D., Feng, Y., Zhu, Z., Dimitrov, D., Shah, N. N., & Fry, T. J. (2019). Modulation of Target Antigen Density Improves CAR T-cell Functionality and Persistence. *Clinical Cancer Research*, *25*(17), 5329–5341. https://doi.org/10.1158/1078-0432.CCR-18-3784
Razaghi, A., Owens, L., & Heimann, K. (2016). Review of the recombinant human interferon gamma as an immunotherapeutic: Impacts of production platforms and glycosylation. *Journal of Biotechnology*, *240*, 48–60. https://doi.org/10.1016/j.jbiotec.2016.10.022
Reck, M., Rodríguez-Abreu, D., Robinson, A. G., Hui, R., Csőszi, T., Fülöp, A., Gottfried, M., Peled, N., Tafreshi, A., Cuffe, S., O'Brien, M., Rao, S., Hotta, K., Leal, T. A., Riess, J. W., Jensen, E., Zhao, B., Pietanza, M. C., & Brahmer, J. R. (2021). Five-Year Outcomes With Pembrolizumab Versus Chemotherapy for Metastatic Non–Small-Cell Lung Cancer With PD-L1 Tumor Proportion Score ≥ 50%. *Journal of Clinical Oncology*, *39*(21), 2339–2349. https://doi.org/10.1200/JCO.21.00174
Robert, C., Thomas, L., Bondarenko, I., O'Day, S., Weber, J., Garbe, C., Lebbe, C., Baurain, J.-F., Testori, A., Grob, J.-J., Davidson, N., Richards, J., Maio, M., Hauschild, A., Miller, W. H., Gascon, P., Lotem, M., Harmankaya, K., Ibrahim, R., … Wolchok, J. D. (2011). Ipilimumab plus dacarbazine for previously untreated metastatic melanoma. *The New England Journal of Medicine*, *364*(26), 2517–2526. https://doi.org/10.1056/NEJMoa1104621
Roberts, K. G., Gu, Z., Payne-Turner, D., McCastlain, K., Harvey, R. C., Chen, I.-M., Pei, D., Iacobucci, I., Valentine, M., Pounds, S. B., Shi, L., Li, Y., Zhang, J., Cheng, C., Rambaldi, A., Tosi, M., Spinelli, O., Radich, J. P., Minden, M. D., … Mullighan, C. G. (2017). High Frequency and Poor Outcome of Philadelphia Chromosome–Like Acute Lymphoblastic Leukemia in Adults. *Journal of Clinical Oncology*, *35*(4), 394–401. https://doi.org/10.1200/JCO.2016.69.0073
Rocha Pinheiro, S. L., Lemos, F. F. B., Marques, H. S., Silva Luz, M., de Oliveira Silva, L. G., Faria Souza Mendes dos Santos, C., da Costa Evangelista, K., Calmon, M. S., Sande Loureiro, M., & Freire de Melo, F. (2023). Immunotherapy in glioblastoma treatment: Current state and future prospects. *World Journal of Clinical Oncology*, *14*(4), 138–159. https://doi.org/10.5306/wjco.v14.i4.138
Roda-Navarro, P., & Álvarez-Vallina, L. (2020). Understanding the Spatial Topology of Artificial Immunological Synapses Assembled in T Cell-Redirecting Strategies: A Major Issue in Cancer Immunotherapy. *Frontiers in Cell and Developmental Biology*, *7*. https://doi.org/10.3389/fcell.2019.00370
Rodems, T. S., Heninger, E., Stahlfeld, C. N., Gilsdorf, C. S., Carlson, K. N., Kircher, M. R., Singh, A., Krueger, T. E. G., Beebe, D. J., Jarrard, D. F., McNeel, D. G., Haffner, M. C., & Lang, J. M. (2022). Reversible epigenetic alterations regulate class I HLA loss in prostate cancer. *Communications Biology*, *5*(1), 897. https://doi.org/10.1038/s42003-022-03843-6
Rodig, S. J., Gusenleitner, D., Jackson, D. G., Gjini, E., Giobbie-Hurder, A., Jin, C., Chang, H., Lovitch, S. B., Horak, C., Weber, J. S., Weirather, J. L., Wolchok, J. D., Postow, M. A., Pavlick, A. C., Chesney, J., & Hodi, F. S. (2018). MHC proteins confer differential sensitivity to CTLA-4 and PD-1 blockade in untreated metastatic melanoma. *Science Translational Medicine*, *10*(450). https://doi.org/10.1126/scitranslmed.aar3342
Roh, W., Chen, P.-L., Reuben, A., Spencer, C. N., Prieto, P. A., Miller, J. P., Gopalakrishnan, V., Wang, F., Cooper, Z. A., Reddy, S. M., Gumbs, C., Little, L., Chang, Q., Chen, W.-S., Wani, K., De Macedo, M. P., Chen, E., Austin-Breneman, J. L., Jiang, H., … Futreal, P. A. (2017). Integrated molecular analysis of tumor biopsies on sequential CTLA-4 and PD-1 blockade reveals markers of response and resistance. *Science Translational Medicine*, *9*(379). https://doi.org/10.1126/scitranslmed.aah3560
Rohaan, M. W., Borch, T. H., van den Berg, J. H., Met, Ö., Kessels, R., Geukes Foppen, M. H., Stoltenborg Granhøj, J., Nuijen, B., Nijenhuis, C., Jedema, I., van Zon, M., Scheij, S., Beijnen, J. H., Hansen, M., Voermans, C., Noringriis, I. M., Monberg, T. J., Holmstroem, R. B., Wever, L. D. V., … Haanen, J. B. A. G. (2022). Tumor-Infiltrating Lymphocyte Therapy or Ipilimumab in Advanced Melanoma. *New England Journal of Medicine*, *387*(23), 2113–2125. https://doi.org/10.1056/NEJMoa2210233
Romain, G., Strati, P., Rezvan, A., Fathi, M., Bandey, I. N., Adolacion, J. R. T., Heeke, D., Liadi,

I., Marques-Piubelli, M. L., Solis, L. M., Mahendra, A., Vega, F., Cooper, L. J., Singh, H., Mattie, M., Bot, A., Neelapu, S. S., & Varadarajan, N. (2022). Multidimensional single-cell analysis identifies a role for CD2-CD58 interactions in clinical antitumor T cell responses. *The Journal of Clinical Investigation*, *132*(17). https://doi.org/10.1172/JCI159402

Rooney, M. S., Shukla, S. A., Wu, C. J., Getz, G., & Hacohen, N. (2015). Molecular and Genetic Properties of Tumors Associated with Local Immune Cytolytic Activity. *Cell*, *160*(1–2), 48–61. https://doi.org/10.1016/j.cell.2014.12.033

Rosenberg, S. A., Packard, B. S., Aebersold, P. M., Solomon, D., Topalian, S. L., Toy, S. T., Simon, P., Lotze, M. T., Yang, J. C., Seipp, C. A., Simpson, C., Carter, C., Bock, S., Schwartzentruber, D., Wei, J. P., & White, D. E. (1988). Use of Tumor-Infiltrating Lymphocytes and Interleukin-2 in the Immunotherapy of Patients with Metastatic Melanoma. *New England Journal of Medicine*, *319*(25), 1676–1680. https://doi.org/10.1056/NEJM198812223192527

Rosenthal, R., Cadieux, E. L., Salgado, R., Bakir, M. Al, Moore, D. A., Hiley, C. T., Lund, T., Tanić, M., Reading, J. L., Joshi, K., Henry, J. Y., Ghorani, E., Wilson, G. A., Birkbak, N. J., Jamal-Hanjani, M., Veeriah, S., Szallasi, Z., Loi, S., Hellmann, M. D., … Swanton, C. (2019). Neoantigen-directed immune escape in lung cancer evolution. *Nature*, *567*(7749), 479–485. https://doi.org/10.1038/s41586-019-1032-7

Rosewicz, S., Detjen, K., Scholz, A., & von Marschall, Z. (2004). Interferon-α: Regulatory Effects on Cell Cycle and Angiogenesis. *Neuroendocrinology*, *80*(Suppl. 1), 85–93. https://doi.org/10.1159/000080748

Russo, E., Santoni, A., & Bernardini, G. (2020). Tumor inhibition or tumor promotion? The duplicity of CXCR3 in cancer. *Journal of Leukocyte Biology*, *108*(2), 673–685. https://doi.org/10.1002/JLB.5MR0320-205R

Sade-Feldman, M., Jiao, Y. J., Chen, J. H., Rooney, M. S., Barzily-Rokni, M., Eliane, J.-P., Bjorgaard, S. L., Hammond, M. R., Vitzthum, H., Blackmon, S. M., Frederick, D. T., Hazar-Rethinam, M., Nadres, B. A., Van Seventer, E. E., Shukla, S. A., Yizhak, K., Ray, J. P., Rosebrock, D., Livitz, D., … Hacohen, N. (2017). Resistance to checkpoint blockade therapy through inactivation of antigen presentation. *Nature Communications*, *8*(1), 1136. https://doi.org/10.1038/s41467-017-01062-w

Sahai, E., Astsaturov, I., Cukierman, E., DeNardo, D. G., Egeblad, M., Evans, R. M., Fearon, D., Greten, F. R., Hingorani, S. R., Hunter, T., Hynes, R. O., Jain, R. K., Janowitz, T., Jorgensen, C., Kimmelman, A. C., Kolonin, M. G., Maki, R. G., Powers, R. S., Puré, E., … Werb, Z. (2020). A framework for advancing our understanding of cancer-associated fibroblasts. *Nature Reviews. Cancer*, *20*(3), 174–186. https://doi.org/10.1038/s41568-019-0238-1

Salmon, H., Franciszkiewicz, K., Damotte, D., Dieu-Nosjean, M.-C., Validire, P., Trautmann, A., Mami-Chouaib, F., & Donnadieu, E. (2012). Matrix architecture defines the preferential localization and migration of T cells into the stroma of human lung tumors. *Journal of Clinical Investigation*, *122*(3), 899–910. https://doi.org/10.1172/JCI45817

Sankar, K., Ye, J. C., Li, Z., Zheng, L., Song, W., & Hu-Lieskovan, S. (2022). The role of biomarkers in personalized immunotherapy. *Biomarker Research*, *10*(1), 32. https://doi.org/10.1186/s40364-022-00378-0

Sarnaik, A. A., Hamid, O., Khushalani, N. I., Lewis, K. D., Medina, T., Kluger, H. M., Thomas, S. S., Domingo-Musibay, E., Pavlick, A. C., Whitman, E. D., Martin-Algarra, S., Corrie, P., Curti, B. D., Oláh, J., Lutzky, J., Weber, J. S., Larkin, J. M. G., Shi, W., Takamura, T., … Chesney, J. A. (2021). Lifileucel, a Tumor-Infiltrating Lymphocyte Therapy, in Metastatic Melanoma. *Journal of Clinical Oncology : Official Journal of the American Society of Clinical Oncology*, *39*(24), 2656–2666. https://doi.org/10.1200/JCO.21.00612

Saxena, M., van der Burg, S. H., Melief, C. J. M., & Bhardwaj, N. (2021). Therapeutic cancer vaccines. *Nature Reviews Cancer*, *21*(6), 360–378. https://doi.org/10.1038/s41568-021-00346-0

Scarzello, A. J., Romero-Weaver, A. L., Maher, S. G., Veenstra, T. D., Zhou, M., Qin, A., Donnelly, R. P., Sheikh, F., & Gamero, A. M. (2007). A Mutation in the SH2 Domain of STAT2 Prolongs Tyrosine Phosphorylation of STAT1 and Promotes Type I IFN-induced Apoptosis. *Molecular Biology of the Cell*, *18*(7), 2455–2462. https://doi.org/10.1091/mbc.e06-09-0843

Schoenborn, J. R., & Wilson, C. B. (2007). *Regulation of Interferon-γ During Innate and Adaptive Immune Responses* (pp. 41–101). https://doi.org/10.1016/S0065-2776(07)96002-2

Schreiber, R. D., Old, L. J., & Smyth, M. J. (2011). Cancer Immunoediting: Integrating Immunity's Roles in Cancer Suppression and Promotion. *Science*, *331*(6024), 1565–1570.

https://doi.org/10.1126/science.1203486
Schroder, K., Hertzog, P. J., Ravasi, T., & Hume, D. A. (2004). Interferon-γ: an overview of signals, mechanisms and functions. *Journal of Leukocyte Biology*, *75*(2), 163–189. https://doi.org/10.1189/jlb.0603252
Seliger, B., Hammers, S., Höhne, A., Zeidler, R., Knuth, A., Gerharz, C. D., & Huber, C. (1997). IFN-gamma-mediated coordinated transcriptional regulation of the human TAP-1 and LMP-2 genes in human renal cell carcinoma. *Clinical Cancer Research : An Official Journal of the American Association for Cancer Research*, *3*(4), 573–578. http://www.ncbi.nlm.nih.gov/pubmed/9815722
Shafer, P., Kelly, L. M., & Hoyos, V. (2022). Cancer Therapy With TCR-Engineered T Cells: Current Strategies, Challenges, and Prospects. *Frontiers in Immunology*, *13*. https://doi.org/10.3389/fimmu.2022.835762
Sharma, P., Hu-Lieskovan, S., Wargo, J. A., & Ribas, A. (2017). Primary, Adaptive, and Acquired Resistance to Cancer Immunotherapy. *Cell*, *168*(4), 707–723. https://doi.org/10.1016/j.cell.2017.01.017
Shen, J., Xiao, Z., Zhao, Q., Li, M., Wu, X., Zhang, L., Hu, W., & Cho, C. H. (2018). Anti-cancer therapy with TNFα and IFNγ: A comprehensive review. *Cell Proliferation*, *51*(4), e12441. https://doi.org/10.1111/cpr.12441
Shen, L., Huang, X., & Fan, C. (2018). Double-group particle swarm optimization and its application in remote sensing image segmentation. *Sensors (Switzerland)*, *18*(5), 1–13. https://doi.org/10.3390/s18051393
Shimabukuro-Vornhagen, A., Gödel, P., Subklewe, M., Stemmler, H. J., Schlößer, H. A., Schlaak, M., Kochanek, M., Böll, B., & von Bergwelt-Baildon, M. S. (2018). Cytokine release syndrome. *Journal for ImmunoTherapy of Cancer*, *6*(1), 56. https://doi.org/10.1186/s40425-018-0343-9
Shime, H., Maruyama, A., Yoshida, S., Takeda, Y., Matsumoto, M., & Seya, T. (2018). Toll-like receptor 2 ligand and interferon-γ suppress anti-tumor T cell responses by enhancing the immunosuppressive activity of monocytic myeloid-derived suppressor cells. *OncoImmunology*, *7*(1), e1373231. https://doi.org/10.1080/2162402X.2017.1373231
Shin, D. S., Zaretsky, J. M., Escuin-Ordinas, H., Garcia-Diaz, A., Hu-Lieskovan, S., Kalbasi, A., Grasso, C. S., Hugo, W., Sandoval, S., Torrejon, D. Y., Palaskas, N., Rodriguez, G. A., Parisi, G., Azhdam, A., Chmielowski, B., Cherry, G., Seja, E., Berent-Maoz, B., Shintaku, I. P., … Ribas, A. (2017). Primary Resistance to PD-1 Blockade Mediated by JAK1/2 Mutations. *Cancer Discovery*, *7*(2), 188–201. https://doi.org/10.1158/2159-8290.CD-16-1223
Shin, M. H., Kim, J., Lim, S. A., Kim, J., & Lee, K.-M. (2020). Current Insights into Combination Therapies with MAPK Inhibitors and Immune Checkpoint Blockade. *International Journal of Molecular Sciences*, *21*(7), 2531. https://doi.org/10.3390/ijms21072531
Sica, A., & Mantovani, A. (2012). Macrophage plasticity and polarization: in vivo veritas. *Journal of Clinical Investigation*, *122*(3), 787–795. https://doi.org/10.1172/JCI59643
Skov, V., Riley, C. H., Thomassen, M., Kjær, L., Stauffer Larsen, T., Bjerrum, O. W., Kruse, T. A., & Hasselbalch, H. C. (2017). The impact of interferon-alpha2 on HLA genes in patients with polycythemia vera and related neoplasms. *Leukemia & Lymphoma*, *58*(8), 1914–1921. https://doi.org/10.1080/10428194.2016.1262032
Song, J., Lan, J., Tang, J., & Luo, N. (2022). PTPN2 in the Immunity and Tumor Immunotherapy: A Concise Review. *International Journal of Molecular Sciences*, *23*(17), 10025. https://doi.org/10.3390/ijms231710025
Sotillo, E., Barrett, D. M., Black, K. L., Bagashev, A., Oldridge, D., Wu, G., Sussman, R., Lanauze, C., Ruella, M., Gazzara, M. R., Martinez, N. M., Harrington, C. T., Chung, E. Y., Perazzelli, J., Hofmann, T. J., Maude, S. L., Raman, P., Barrera, A., Gill, S., … Thomas-Tikhonenko, A. (2015). Convergence of Acquired Mutations and Alternative Splicing of CD19 Enables Resistance to CART-19 Immunotherapy. *Cancer Discovery*, *5*(12), 1282–1295. https://doi.org/10.1158/2159-8290.CD-15-1020
Speeckaert, R., Vermaelen, K., van Geel, N., Autier, P., Lambert, J., Haspeslagh, M., van Gele, M., Thielemans, K., Neyns, B., Roche, N., Verbeke, N., Deron, P., Speeckaert, M., & Brochez, L. (2012). Indoleamine 2,3-dioxygenase, a new prognostic marker in sentinel lymph nodes of melanoma patients. *European Journal of Cancer (Oxford, England : 1990)*, *48*(13), 2004–2011. https://doi.org/10.1016/j.ejca.2011.09.007
Spranger, S., Bao, R., & Gajewski, T. F. (2015). Melanoma-intrinsic β-catenin signalling prevents anti-tumour immunity. *Nature*, *523*(7559), 231–235. https://doi.org/10.1038/nature14404

Suarez, E. R., Chang, D.-K., Sun, J., Sui, J., Freeman, G. J., Signoretti, S., Zhu, Q., & Marasco, W. A. (2016). Chimeric antigen receptor T cells secreting anti-PD-L1 antibodies more effectively regress renal cell carcinoma in a humanized mouse model. *Oncotarget*, *7*(23), 34341–34355. https://doi.org/10.18632/oncotarget.9114

Sucker, A., Zhao, F., Pieper, N., Heeke, C., Maltaner, R., Stadtler, N., Real, B., Bielefeld, N., Howe, S., Weide, B., Gutzmer, R., Utikal, J., Loquai, C., Gogas, H., Klein-Hitpass, L., Zeschnigk, M., Westendorf, A. M., Trilling, M., Horn, S., … Paschen, A. (2017). Acquired IFNγ resistance impairs anti-tumor immunity and gives rise to T-cell-resistant melanoma lesions. *Nature Communications*, *8*(1), 15440. https://doi.org/10.1038/ncomms15440

Szabo, S. J., Sullivan, B. M., Stemmann, C., Satoskar, A. R., Sleckman, B. P., & Glimcher, L. H. (2002). Distinct Effects of T-bet in T H 1 Lineage Commitment and IFN-γ Production in CD4 and CD8 T Cells. *Science*, *295*(5553), 338–342. https://doi.org/10.1126/science.1065543

Takahashi, T., Kuniyasu, Y., Toda, M., Sakaguchi, N., Itoh, M., Iwata, M., Shimizu, J., & Sakaguchi, S. (1998). Immunologic self-tolerance maintained by CD25+CD4+ naturally anergic and suppressive T cells: induction of autoimmune disease by breaking their anergic/suppressive state. *International Immunology*, *10*(12), 1969–1980. https://doi.org/10.1093/intimm/10.12.1969

Tarhini, A. A., Gogas, H., & Kirkwood, J. M. (2012). IFN-α in the Treatment of Melanoma. *The Journal of Immunology*, *189*(8), 3789–3793. https://doi.org/10.4049/jimmunol.1290060

Tekguc, M., Wing, J. B., Osaki, M., Long, J., & Sakaguchi, S. (2021). Treg-expressed CTLA-4 depletes CD80/CD86 by trogocytosis, releasing free PD-L1 on antigen-presenting cells. *Proceedings of the National Academy of Sciences*, *118*(30). https://doi.org/10.1073/pnas.2023739118

Tella, S. H., Kommalapati, A., Mahipal, A., & Jin, Z. (2022). First-Line Targeted Therapy for Hepatocellular Carcinoma: Role of Atezolizumab/Bevacizumab Combination. *Biomedicines*, *10*(6), 1304. https://doi.org/10.3390/biomedicines10061304

Timmer, F. E. F., Geboers, B., Nieuwenhuizen, S., Dijkstra, M., Schouten, E. A. C., Puijk, R. S., de Vries, J. J. J., van den Tol, M. P., Bruynzeel, A. M. E., Streppel, M. M., Wilmink, J. W., van der Vliet, H. J., Meijerink, M. R., Scheffer, H. J., & de Gruijl, T. D. (2021). Pancreatic Cancer and Immunotherapy: A Clinical Overview. *Cancers*, *13*(16), 4138. https://doi.org/10.3390/cancers13164138

Togashi, Y., Shitara, K., & Nishikawa, H. (2019). Regulatory T cells in cancer immunosuppression — implications for anticancer therapy. *Nature Reviews Clinical Oncology*, *16*(6), 356–371. https://doi.org/10.1038/s41571-019-0175-7

Tomasik, J., Jasiński, M., & Basak, G. W. (2022). Next generations of CAR-T cells - new therapeutic opportunities in hematology? *Frontiers in Immunology*, *13*, 1034707. https://doi.org/10.3389/fimmu.2022.1034707

Topp, M. S., Gökbuget, N., Zugmaier, G., Klappers, P., Stelljes, M., Neumann, S., Viardot, A., Marks, R., Diedrich, H., Faul, C., Reichle, A., Horst, H.-A., Brüggemann, M., Wessiepe, D., Holland, C., Alekar, S., Mergen, N., Einsele, H., Hoelzer, D., & Bargou, R. C. (2014). Phase II Trial of the Anti-CD19 Bispecific T Cell–Engager Blinatumomab Shows Hematologic and Molecular Remissions in Patients With Relapsed or Refractory B-Precursor Acute Lymphoblastic Leukemia. *Journal of Clinical Oncology*, *32*(36), 4134–4140. https://doi.org/10.1200/JCO.2014.56.3247

Toulmonde, M., Penel, N., Adam, J., Chevreau, C., Blay, J.-Y., Le Cesne, A., Bompas, E., Piperno-Neumann, S., Cousin, S., Grellety, T., Ryckewaert, T., Bessede, A., Ghiringhelli, F., Pulido, M., & Italiano, A. (2018). Use of PD-1 Targeting, Macrophage Infiltration, and IDO Pathway Activation in Sarcomas. *JAMA Oncology*, *4*(1), 93. https://doi.org/10.1001/jamaoncol.2017.1617

Vetsika, E.-K., Koukos, A., & Kotsakis, A. (2019). Myeloid-Derived Suppressor Cells: Major Figures that Shape the Immunosuppressive and Angiogenic Network in Cancer. *Cells*, *8*(12), 1647. https://doi.org/10.3390/cells8121647

Vredevoogd, D. W., Kuilman, T., Ligtenberg, M. A., Boshuizen, J., Stecker, K. E., de Bruijn, B., Krijgsman, O., Huang, X., Kenski, J. C. N., Lacroix, R., Mezzadra, R., Gomez-Eerland, R., Yildiz, M., Dagidir, I., Apriamashvili, G., Zandhuis, N., van der Noort, V., Visser, N. L., Blank, C. U., … Peeper, D. S. (2019). Augmenting Immunotherapy Impact by Lowering Tumor TNF Cytotoxicity Threshold. *Cell*, *178*(3), 585-599.e15. https://doi.org/10.1016/j.cell.2019.06.014

Waldman, A. D., Fritz, J. M., & Lenardo, M. J. (2020). A guide to cancer immunotherapy: from T cell basic science to clinical practice. *Nature Reviews Immunology*, *20*(11), 651–668. https://doi.org/10.1038/s41577-020-0306-5

Wan, S., Pestka, S., Jubin, R. G., Lyu, Y. L., Tsai, Y.-C., & Liu, L. F. (2012). Chemotherapeutics and Radiation Stimulate MHC Class I Expression through Elevated Interferon-beta Signaling in Breast Cancer Cells. *PLoS ONE*, *7*(3), e32542. https://doi.org/10.1371/journal.pone.0032542

Wang, M., Munoz, J., Goy, A., Locke, F. L., Jacobson, C. A., Hill, B. T., Timmerman, J. M., Holmes, H., Jaglowski, S., Flinn, I. W., McSweeney, P. A., Miklos, D. B., Pagel, J. M., Kersten, M. J., Bouabdallah, K., Khanal, R., Topp, M. S., Houot, R., Beitinjaneh, A., … Reagan, P. M. (2023). Three-Year Follow-Up of KTE-X19 in Patients With Relapsed/Refractory Mantle Cell Lymphoma, Including High-Risk Subgroups, in the ZUMA-2 Study. *Journal of Clinical Oncology*, *41*(3), 555–567. https://doi.org/10.1200/JCO.21.02370

Wang, Q.-S., Shen, S.-Q., Sun, H.-W., Xing, Z.-X., & Yang, H.-L. (2018). Interferon-gamma induces autophagy-associated apoptosis through induction of cPLA2-dependent mitochondrial ROS generation in colorectal cancer cells. *Biochemical and Biophysical Research Communications*, *498*(4), 1058–1065. https://doi.org/10.1016/j.bbrc.2018.03.118

Wang, W., Green, M., Choi, J. E., Gijón, M., Kennedy, P. D., Johnson, J. K., Liao, P., Lang, X., Kryczek, I., Sell, A., Xia, H., Zhou, J., Li, G., Li, J., Li, W., Wei, S., Vatan, L., Zhang, H., Szeliga, W., … Zou, W. (2019). CD8+ T cells regulate tumour ferroptosis during cancer immunotherapy. *Nature*, *569*(7755), 270–274. https://doi.org/10.1038/s41586-019-1170-y

Wei, J., Yang, Y., Wang, G., & Liu, M. (2022). Current landscape and future directions of bispecific antibodies in cancer immunotherapy. *Frontiers in Immunology*, *13*. https://doi.org/10.3389/fimmu.2022.1035276

Wolf, P. R., & Ploegh, H. L. (1995). How MHC Class II Molecules Acquire Peptide Cargo: Biosynthesis and Trafficking through the Endocytic Pathway. *Annual Review of Cell and Developmental Biology*, *11*(1), 267–306. https://doi.org/10.1146/annurev.cb.11.110195.001411

Wu, Y., Yi, M., Zhu, S., Wang, H., & Wu, K. (2021). Recent advances and challenges of bispecific antibodies in solid tumors. *Experimental Hematology & Oncology*, *10*(1), 56. https://doi.org/10.1186/s40164-021-00250-1

Xiao, X., Cheng, Y., Zheng, X., Fang, Y., Zhang, Y., Sun, R., Tian, Z., & Sun, H. (2023). Bispecific NK-cell engager targeting BCMA elicits stronger antitumor effects and produces less proinflammatory cytokines than T-cell engager. *Frontiers in Immunology*, *14*. https://doi.org/10.3389/fimmu.2023.1113303

Xie, G., Dong, H., Liang, Y., Ham, J. D., Rizwan, R., & Chen, J. (2020). CAR-NK cells: A promising cellular immunotherapy for cancer. *EBioMedicine*, *59*, 102975. https://doi.org/10.1016/j.ebiom.2020.102975

Xiong, H., Xi, Y., Yuan, Z., Wang, B., Hu, S., Fang, C., Cai, Y., Fu, X., & Li, L. (2022). IFN-γ activates the tumor cell-intrinsic STING pathway through the induction of DNA damage and cytosolic dsDNA formation. *Oncoimmunology*, *11*(1), 2044103. https://doi.org/10.1080/2162402X.2022.2044103

Xu, X, Fu, X. Y., Plate, J., & Chong, A. S. (1998). IFN-gamma induces cell growth inhibition by Fas-mediated apoptosis: requirement of STAT1 protein for up-regulation of Fas and FasL expression. *Cancer Research*, *58*(13), 2832–2837. http://www.ncbi.nlm.nih.gov/pubmed/9661898

Xu, Xiongfei, Gu, H., Li, H., Gao, S., Shi, X., Shen, J., Li, B., Wang, H., Zheng, K., Shao, Z., Cheng, P., Cha, Z., Peng, S., Nie, Y., Li, Z., Guo, S., Qian, B., & Jin, G. (2022). Large-cohort humanized NPI mice reconstituted with CD34 + hematopoietic stem cells are feasible for evaluating preclinical cancer immunotherapy. *The FASEB Journal*, *36*(4). https://doi.org/10.1096/fj.202101548RR

Yang, L., Pang, Y., & Moses, H. L. (2010). TGF-β and immune cells: an important regulatory axis in the tumor microenvironment and progression. *Trends in Immunology*, *31*(6), 220–227. https://doi.org/10.1016/j.it.2010.04.002

Yang, R., Sun, L., Li, C.-F., Wang, Y.-H., Yao, J., Li, H., Yan, M., Chang, W.-C., Hsu, J.-M., Cha, J.-H., Hsu, J. L., Chou, C.-W., Sun, X., Deng, Y., Chou, C.-K., Yu, D., & Hung, M.-C. (2021). Galectin-9 interacts with PD-1 and TIM-3 to regulate T cell death and is a target for cancer immunotherapy. *Nature Communications*, *12*(1), 832. https://doi.org/10.1038/s41467-021-21099-2

Yeap, W. H., Wong, K. L., Shimasaki, N., Teo, E. C. Y., Quek, J. K. S., Yong, H. X., Diong, C. P., Bertoletti, A., Linn, Y. C., & Wong, S. C. (2016). CD16 is indispensable for antibody-dependent cellular cytotoxicity by human monocytes. *Scientific Reports*, *6*(1), 34310.

https://doi.org/10.1038/srep34310
Yi, M., Zheng, X., Niu, M., Zhu, S., Ge, H., & Wu, K. (2022). Combination strategies with PD-1/PD-L1 blockade: current advances and future directions. *Molecular Cancer*, *21*(1), 28. https://doi.org/10.1186/s12943-021-01489-2
Yoshie, O. (2021). CCR4 as a Therapeutic Target for Cancer Immunotherapy. *Cancers*, *13*(21), 5542. https://doi.org/10.3390/cancers13215542
Yoshimura, A., Suzuki, M., Sakaguchi, R., Hanada, T., & Yasukawa, H. (2012). SOCS, Inflammation, and Autoimmunity. *Frontiers in Immunology*, *3*. https://doi.org/10.3389/fimmu.2012.00020
Zacharakis, N., Chinnasamy, H., Black, M., Xu, H., Lu, Y.-C., Zheng, Z., Pasetto, A., Langhan, M., Shelton, T., Prickett, T., Gartner, J., Jia, L., Trebska-McGowan, K., Somerville, R. P., Robbins, P. F., Rosenberg, S. A., Goff, S. L., & Feldman, S. A. (2018). Immune recognition of somatic mutations leading to complete durable regression in metastatic breast cancer. *Nature Medicine*, *24*(6), 724–730. https://doi.org/10.1038/s41591-018-0040-8
Zappasodi, R., Serganova, I., Cohen, I. J., Maeda, M., Shindo, M., Senbabaoglu, Y., Watson, M. J., Leftin, A., Maniyar, R., Verma, S., Lubin, M., Ko, M., Mane, M. M., Zhong, H., Liu, C., Ghosh, A., Abu-Akeel, M., Ackerstaff, E., Koutcher, J. A., … Merghoub, T. (2021). CTLA-4 blockade drives loss of Treg stability in glycolysis-low tumours. *Nature*, *591*(7851), 652–658. https://doi.org/10.1038/s41586-021-03326-4
Zaretsky, J. M., Garcia-Diaz, A., Shin, D. S., Escuin-Ordinas, H., Hugo, W., Hu-Lieskovan, S., Torrejon, D. Y., Abril-Rodriguez, G., Sandoval, S., Barthly, L., Saco, J., Homet Moreno, B., Mezzadra, R., Chmielowski, B., Ruchalski, K., Shintaku, I. P., Sanchez, P. J., Puig-Saus, C., Cherry, G., … Ribas, A. (2016). Mutations Associated with Acquired Resistance to PD-1 Blockade in Melanoma. *New England Journal of Medicine*, *375*(9), 819–829. https://doi.org/10.1056/NEJMoa1604958
Zhai, L., Bell, A., Ladomersky, E., Lauing, K. L., Bollu, L., Sosman, J. A., Zhang, B., Wu, J. D., Miller, S. D., Meeks, J. J., Lukas, R. V., Wyatt, E., Doglio, L., Schiltz, G. E., McCusker, R. H., & Wainwright, D. A. (2020). Immunosuppressive IDO in Cancer: Mechanisms of Action, Animal Models, and Targeting Strategies. *Frontiers in Immunology*, *11*. https://doi.org/10.3389/fimmu.2020.01185
Zhang, R., Banik, N. L., & Ray, S. K. (2007). Combination of all-trans retinoic acid and interferon-gamma suppressed PI3K/Akt survival pathway in glioblastoma T98G cells whereas NF-κB survival signaling in glioblastoma U87MG cells for induction of apoptosis. *Neurochemical Research*, *32*(12), 2194–2202. https://doi.org/10.1007/s11064-007-9417-7
Zhang, T., Jou, T. H.-T., Hsin, J., Wang, Z., Huang, K., Ye, J., Yin, H., & Xing, Y. (2023). Talimogene Laherparepvec (T-VEC): A Review of the Recent Advances in Cancer Therapy. *Journal of Clinical Medicine*, *12*(3), 1098. https://doi.org/10.3390/jcm12031098
Zhang, Y., Zhang, J., Liu, C., Du, S., Feng, L., Luan, X., Zhang, Y., Shi, Y., Wang, T., Wu, Y., Cheng, W., Meng, S., Li, M., & Liu, H. (2016). Neratinib induces ErbB2 ubiquitylation and endocytic degradation via HSP90 dissociation in breast cancer cells. *Cancer Letters*, *382*(2), 176–185. https://doi.org/10.1016/j.canlet.2016.08.026
Zhao, L., Xie, F., Tong, X., Li, H., Chen, Y., Qian, W., Duan, S., Zheng, J., Zhao, Z., Li, B., Zhang, D., Zhao, J., Dai, J., Tong, X., Hou, S., & Guo, Y. (2014). Combating non-Hodgkin lymphoma by targeting both CD20 and HLA-DR through CD20–243 CrossMab. *MAbs*, *6*(3), 739–747. https://doi.org/10.4161/mabs.28613
Zhao, W., Beers, D. R., Thonhoff, J. R., Thome, A. D., Faridar, A., Wang, J., Wen, S., Ornelas, L., Sareen, D., Goodridge, H. S., Svendsen, C. N., & Appel, S. H. (2020). Immunosuppressive Functions of M2 Macrophages Derived from iPSCs of Patients with ALS and Healthy Controls. *IScience*, *23*(6), 101192. https://doi.org/10.1016/j.isci.2020.101192
Zhao, Y., Deng, J., Rao, S., Guo, S., Shen, J., Du, F., Wu, X., Chen, Y., Li, M., Chen, M., Li, X., Li, W., Gu, L., Sun, Y., Zhang, Z., Wen, Q., Xiao, Z., & Li, J. (2022). Tumor Infiltrating Lymphocyte (TIL) Therapy for Solid Tumor Treatment: Progressions and Challenges. *Cancers*, *14*(17). https://doi.org/10.3390/cancers14174160
Zou, W., Wolchok, J. D., & Chen, L. (2016). PD-L1 (B7-H1) and PD-1 pathway blockade for cancer therapy: Mechanisms, response biomarkers, and combinations. *Science Translational Medicine*, *8*(328). https://doi.org/10.1126/scitranslmed.aad7118